

**SYNTHESIS AND CHARACTERISATION OF NICKEL AND
PALLADIUM BIMETALLIC COMPLEXES AND THEIR CATALYTIC
APPLICATION IN OLIGOMERISATION OF 1-HEXENE**

By

ORANG'O DANIEL MOCHERE

**A THESIS SUBMITTED IN PARTIAL FULFILLMENT OF THE REQUIREMENTS
FOR THE DEGREE OF DOCTOR OF PHILOSOPHY IN INORGANIC CHEMISTRY
IN THE SCHOOL OF SCIENCE, UNIVERSITY OF ELDORET, KENYA.**

FEBRUARY, 2022

DECLARATION

Declaration by the candidate

This thesis is my original work and has not been submitted for any academic award in any other University or institution; and shall not be reproduced in part or full, or in any format without prior written permission from the author and/or the University of Eldoret. Sources of information used in this work have been properly acknowledged using appropriate referencing methods.

Orang'o Daniel Mochere Signature:.....Date:.....

SC/PhD/07/13

Declaration by supervisors

This thesis has been submitted with our approval as University Supervisors.

Prof. Samuel T. Lutta Signature.....Date.....

Department of Chemistry and Biochemistry, School of Science

University of Eldoret, Republic of Kenya

Prof. Paul K. Tarus Signature.....Date.....

Department of Chemistry and Biochemistry, School of Science

University of Eldoret, Republic of Kenya

Prof. Martin O. Onani Signature.....Date.....

Department of Chemistry, Faculty of Natural Sciences

University of the Western Cape, Republic of South Africa

DEDICATION

This work is dedicated to my lovely wife Carren Kerubo, daughter Sarange, son Orang'o, and daughter Mong'ina; they prayed and supported me to the end of the research work. My loving late mother Hellen Kong'ara and loving late father Isaiah Orang'o who always prayed and encouraged me. To my dear brothers and sisters for their support, and the Sirikwa Pentecostal Fellowship Church for praying with me.

ACKNOWLEDGEMENT

I am greatly indebted to a number of institutions and persons for their invaluable contributions to the realisation of this work. First, I thank the Almighty God through the Lord and Saviour Jesus Christ for giving me His grace and favour to carry on this work to its completion.

My appreciation goes to the University of Eldoret for the support, through the University of Eldoret Annual Research Grant which facilitated me to do research work in South Africa. Most sincere gratitude goes to the University of the Western Cape administration; thank you for admitting me as an affiliated student to do my research in your Chemistry labs.

My kind regards to the department of Chemistry staff at the University of the Western Cape headed by Prof Wilfred Mabusela. I am most thankful to my Supervisor Prof Martin Onani, who was a father to me in all aspects. He walked with me in every step of the research and ensured a great breakthrough. My other Supervisors Prof Samuel Lutta and Prof Paul Tarus for their selfless support and encouragement. Much appreciation goes to Prof Roger Lalancette of Rutgers State University New Jersey USA, for helping to solve the crystal structures of some of my compounds. Full recognition goes to Mrs Charney Anderson-Small of Stellenbosch University for a work well done on elemental analysis of my samples. I thank Prof Edith Beukes of the University of the Western Cape for her tireless work in NMR data for my samples. To the technical staff headed by Uncle Timothy Lesch who greatly assisted in the FT-IR, GC-MS and GC spectroscopic data. I appreciate Tim again for allowing me full access to the FTIR instrument to run my samples. I thank Dr Eunice Nyawade and Dr Asanda Busa for their guidance in some tricky lab experiments. I am grateful to all my colleagues in the Inorganic and

Organic Chemistry groups; Mbugua, Garvin, Diyoka, Masande, Masixole and Ndikho. You made me feel at home in South Africa.

I owe much gratitude to the University of Eldoret Chemistry department staff headed by Dr Vivian Twei for their support in my initial stages of the research.

“For with GOD nothing will be impossible” [Luke 1:37].

ABSTRACT

In this work, typical homobimetallic complexes derived from *N,O*-salicylaldimine ligands were investigated for their catalytic potential in oligomerisation of 1-hexene. Catalysts of monometallic nature, that is, those with one active metal centre have been used effectively in polymerisation for a long time. However, the few reports available have shown that catalysts of homobimetallic or heterobimetallic nature exhibited superior catalytic activity in comparison with their monometallic analogues. This work thus reports the synthesis of a series of new *N,O*-salicylaldimine Schiff base ligands from the condensation of substituted salicylaldehyde and primary amines. The ligands (propane-1,*x*-diylbis(azanylylidene))bis(methanylylidene))bis(*y*) [*x* = 3; *y* = 2-methylphenol, 4-methylphenol, 4-methoxyphenol, 2-bromo-4-chlorophenol, 4-bromophenol, and 4-chlorophenol for corresponding **SL1**, **SL2**, **SL3**, **SL4**, **SL5**, and **SL6**, respectively], (butane-1,*x*-diylbis(azanylylidene))bis(methanylylidene))bis(*y*) [*x* = 4; *y* = 2-methylphenol, 4-methylphenol, 4-methoxyphenol, 4-bromophenol, and 4-chlorophenol for **SL7** – **SL11**, respectively], (pentane-1,*x*-diylbis(azanylylidene))bis(methanylylidene))bis(*y*) [*x* = 5; *y* = 2-methylphenol, 4-methylphenol, 4-methoxyphenol, 2-bromo-4-chlorophenol, 4-bromophenol, and 4-chlorophenol corresponding to **SL12** – **SL17**, respectively] were prepared via condensation reaction of a primary diamine; 1,3-diaminopropane, 1,4-diaminobutane or 1,5-diaminopentane with 2 equivalents of an appropriate salicylaldehyde derivative, stirred at reflux for between 1 – 6 h. The ligands were obtained as yellow or bright yellow solids which were stable in both moisture and air and in appreciable yields ranging from 41 to 98 %. They were fully characterised using Fourier transform infrared spectroscopy (FTIR), nuclear magnetic resonance spectroscopy (NMR), elemental analysis (EA), mass spectroscopy (MS) and for some of them (**SL2**, **SL3**, **SL6**, and **SL9**) using single crystal X-ray diffraction (XRD). The ligands have their crystal structures reported for the first time. The *N,O*-salicylaldimine ligands were subsequently used to synthesize a series of new homobimetallic nickel(II) and palladium(II) complexes. To obtain palladium(II) complexes, ligands used included; **SL1** – **SL6**, **SL9**, **SL12** – **SL14**, whilst nickel(II) complexes were synthesized using **SL4**, **SL7**, **SL9**, **SL13**, and **SL15**. The ligands were reacted in a 1:2 mole ratio with PdCl₂(COD) and NiCl₂(DME) complex precursors stirred at room temperature which obtained light-yellow, yellow, orange or light-green complexes in appreciable yields ranging between 43 – 95 %. All the palladium(II) (**C1** – **C10**) and nickel(II) (**C11** – **C15**) complexes were observed to be both air and moisture stable. These complexes were characterised using FTIR, NMR and EA. They were reacted with 1-hexene to test their catalytic capability to polymerise 1-hexene. It was generally found that the nickel(II) complexes were highly active when activated with the cocatalyst, modified methyl aluminoxane (MMAO) compared with the palladium complexes. All the tested complexes were active for 1-hexene oligomerisation with **C14** showing the highest conversion. These catalysts were selective towards C₁₂ and to some extent C₁₈ and C₂₄.

PUBLICATION AND CONFERENCE CONTRIBUTIONS

1. Daniel M. Orang'o, Martin O. Onani, Paul K. Tarus, and Samuel T. Lutta
Synthesis, Characterisation and Crystallographic Studies of *N,O*-Salicylaldimine Ligands, 6TH International Interdisciplinary Conference (IIC6 2019), University of Eldoret, Kenya. 4 – 6TH September 2019, Oral Presentation.
2. Daniel M. Orang'o, Martin O. Onani, Paul K. Tarus, Samuel T. Lutta, and Roger A. Lalancette.
Crystal structure of 2,2'-(butane-1,4-diylbis(azanylylidene))bis(methanylylidene))bis(4-methoxyphenol), C₂₀H₂₄N₂O₄. *Zeitschrift für Kristallographie – New Crystal Structures*
Received July 6, 2021; accepted July 20, 2021; published online August 6, 2021
<https://doi.org/10.1515/ncrs-2021-0273>
3. Daniel M. Orang'o, Martin O. Onani, Paul K. Tarus, Samuel T. Lutta, and Roger A. Lalancette.
Crystal structure of 2,2'-(propane-1,3-dilylbis(azanylylidene))bis(methanylylidene))bis(4-methylphenol), C₁₉H₂₂N₂O₂. *Zeitschrift für Kristallographie – New Crystal Structures*
Received July 10, 2021; accepted July 25, 2021; published online August 30, 2021
<https://doi.org/10.1515/ncrs-2021-0279>
4. Daniel M. Orang'o, Martin O. Onani, Paul K. Tarus, Samuel T. Lutta, and Roger A. Lalancette.
Crystal structure of 2,2'-(propane-1,3-diylbis(azanylylidene))bis(methanylylidene))bis(4-methoxyphenol), C₁₉H₂₂N₂O₄. *Zeitschrift für Kristallographie – New Crystal Structures*
Received; accepted; published online
Manuscript number
5. Synthesis, Characterization and Catalytic Studies of *N,O*-salicylaldimine Ni(II) and Pd(II) Homobimetallic Complexes. *Synlett Journal*. Received.....; Accepted.....; Published online.....; Manuscript number.....

TABLE OF CONTENTS

DECLARATION	ii
DEDICATION	iii
ACKNOWLEDGEMENT	iv
ABSTRACT	vi
PUBLICATION AND CONFERENCE CONTRIBUTIONS	vii
TABLE OF CONTENTS	viii
LIST OF TABLES	xiii
LIST OF FIGURES	xiv
LIST OF SCHEMES	xvii
ABBREVIATIONS, ACRONYMS AND SYMBOLS	xviii
CHAPTER ONE	1
INTRODUCTION	1
1.1 Background	1
1.1.1 Homogeneous catalysts	1
1.1.2 Heterogeneous catalysts	3
1.1.3 Classes of organometallic complexes	4
1.1.4 Salicylaldimine ligands and their complexes	5
1.2 Problem identification	12
1.3 Research aims and objectives	14
1.3.1 General objective	14
1.3.2 Specific objectives	14
1.4 Justification of study	14
1.5 Structure of the thesis	15
CHAPTER TWO	16
LITERATURE REVIEW	16
2.1 Introduction	16
2.2 Hydrogenation	17
2.3 Hydroformylation	18

2.4 Alkene polymerisation	18
2.5 <i>N,O</i> -Salicylaldimine ligands	20
2.6 <i>N,O</i> -Salicylaldimine complexes	24
2.7 Catalytic oligomerisation/polymerisation	38
2.8 Future prospects	47
CHAPTER THREE	49
METHODOLOGY	49
3.1 Materials and methods	49
3.2 Instrumentation	50
3.3 Synthesis of salicylaldimine ligands	51
3.3.1 Preparation of 6,6'-(propane-1,3-diylbis(azanylylidene))bis(methanylylidene))bis(2-methylphenol) (SL1)	51
3.3.2 Preparation of 2,2'-(propane-1,3-diylbis(azanylylidene))bis(methanylylidene))bis(4-methylphenol) (SL2)	52
3.3.3 Preparation of 2,2'-(propane-1,3-diylbis(azanylylidene))bis(methanylylidene))bis(4-methoxyphenol) (SL3)	53
3.3.4 Preparation of 6,6'-(propane-1,3-diylbis(azanylylidene))bis(methanylylidene))bis(2-bromo-4-chlorophenol) (SL4)	54
3.3.5 Preparation of 2,2'-(propane-1,3-diylbis(azanylylidene))bis(methanylylidene))bis(4-bromophenol) (SL5)	55
3.3.6 Preparation of 2,2'-(propane-1,3-diylbis(azanylylidene))bis(methanylylidene))bis(4-chlorophenol) (SL6)	56
3.3.7 Preparation of 6,6'-(butane-1,4-diylbis(azanylylidene))bis(methanylylidene))bis(2-methylphenol) (SL7)	57
3.3.8 Preparation of 2,2'-(butane-1,4-diylbis(azanylylidene))bis(methanylylidene))bis(4-methylphenol) (SL8)	58
3.3.9 Preparation of 2,2'-(butane-1,4-diylbis(azanylylidene))bis(methanylylidene))bis(4-methoxyphenol) (SL9)	59
3.3.10 Preparation of 2,2'-(butane-1,4-diylbis(azanylylidene))bis(methanylylidene))bis(4-bromophenol) (SL10)	60

3.3.11 Preparation of 2,2'-(butane-1,4-diylbis(azanylylidene))bis(methanylylidene))bis(4-chlorophenol) (SL11)	61
3.3.12 Preparation of 6,6'-(pentane-1,5-diylbis(azanylylidene))bis(methanylylidene))bis(2-methylphenol) (SL12)	62
3.3.13 Preparation of 2,2'-(pentane-1,5-diylbis(azanylylidene))bis(methanylylidene))bis(4-methylphenol) (SL13)	63
3.3.14 Preparation of 2,2'-(pentane-1,5-diylbis(azanylylidene))bis(methanylylidene))bis(4-methoxyphenol) (SL14)	64
3.3.15 Preparation of 6,6'-(pentane-1,5-diylbis(azanylylidene))bis(methanylylidene))bis(2-bromo-4-chlorophenol) (SL15)	65
3.3.16 Preparation of 2,2'-(pentane-1,5-diylbis(azanylylidene))bis(methanylylidene))bis(4-bromophenol) (SL16)	66
3.3.17 Preparation of 2,2'-(pentane-1,5-diylbis(azanylylidene))bis(methanylylidene))bis(4-chlorophenol) (SL17)	67
3.4 Synthesis of Pd(II) and Ni(II) salicylaldimine complexes	68
3.4.1 Pd Complex C1	68
3.4.2 Pd Complex C2	69
3.4.3 Pd Complex C3	69
3.4.4 Pd Complex C4	70
3.4.5 Pd Complex C5	70
3.4.6 Pd Complex C6	71
3.4.7 Pd Complex C7	71
3.4.8 Pd Complex C8	71
3.4.9 Pd Complex C9	72
3.4.10 Pd Complex C10	72
3.4.11 Ni Complex C11	73
3.4.12 Ni Complex C12	74
3.4.13 Ni Complex C13	74
3.4.14 Ni Complex C14	75
3.4.15 Ni Complex C15	75

3.4.16 Procedure for hexene oligomerisation	75
CHAPTER FOUR.....	77
RESULTS AND DISCUSSION	77
4.1 Introduction	77
4.2 Results and discussion	77
4.2.1 Synthesis and characterisation of <i>N,O</i> -salicylaldimine ligands SL1 – SL17	77
4.2.2 Infrared spectroscopy of the <i>N,O</i> -salicylaldimine ligands SL1 – SL17	80
4.2.3 ¹ H and ¹³ C NMR for SL1 – SL17	83
4.2.4 Elemental Analysis and Mass Spectroscopy of SL1 – SL17	90
4.3 Single X-ray structure studies of the ligands	92
4.3.1 Crystal and molecular structures of salicylaldimine SL2, SL3, SL6 and SL9	92
4.4 Synthesis and characterisation of <i>N,O</i> -salicylaldimine Pd(II) complexes C1 – C10	103
4.4.1 Introduction	103
4.4.2 Infrared spectroscopy for Pd(II) complexes C1 – C10	105
4.4.3 ¹ H and ¹³ C NMR for Pd(II) complexes C1 – C10	107
4.5 Synthesis and characterisation of <i>N,O</i> -salicylaldimine Ni(II) complexes C11 – C15	110
4.5.1 Introduction	110
4.5.2 Infrared spectroscopy for Ni(II) complexes C11 – C15	111
4.5.3 ¹ H NMR for Ni(II) complexes C11 – C15	114
4.6 Catalytic application of the <i>N,O</i> -salicylaldimine complexes	116
4.6.1 Introduction	116
4.6.2 Hexene catalysis by palladium and nickel complexes	116
CHAPTER FIVE	125
CONCLUSION AND RECOMMENDATIONS	125
5.1 Conclusion	125
5.2 Recommendations	126
REFERENCES	127
APPENDICES	147
Appendix A. FTIR Graphs for Ligands	147

Appendix B. NMR Graphs for Ligands	155
Appendix C. FTIR Graphs for Complexes	171
Appendix D. NMR Graphs for Complexes	178
Appendix E. Tables	185
Appendix F. Turnitin Originality Report	219

LIST OF TABLES

Table 4.1: Yield and melting points for the ligands SL1 – SL17	79
Table 4.2: Infrared stretching frequencies (cm^{-1}) for the <i>N,O</i> -salicylaldimine ligands SL1 – SL17	82
Table 4.3: ^1H NMR spectral data (δ in ppm) for imine and phenolic protons in CDCl_3	85
Table 4.4: ^{13}C NMR spectral data (δ in ppm) for SL1 – SL8 in CDCl_3	88
Table 4.5: Crystal data structure refinement for ligands SL2, SL3, SL6 and SL9	94
Table 4.6: Selected bond angles ($^\circ$) for SL3	95
Table 4.7: Selected bond lengths (\AA) for SL3	95
Table 4.8: Selected bond angles ($^\circ$) for SL9	97
Table 4.9: Selected bond lengths (\AA) for SL9	98
Table 4.10: Selected bond angles ($^\circ$) for SL2	100
Table 4.11: Selected bond lengths (\AA) for SL2	100
Table 4.12: Selected bond angles ($^\circ$) for SL6	102
Table 4.13: Selected bond lengths (\AA) for SL6	103
Table 4.14: $\nu(\text{C}=\text{N})$ stretching frequencies in wavenumbers (cm^{-1}) for complexes C1 – C10 ..	107
Table 4.15: $\nu(\text{C}=\text{N})$ stretching frequencies in wavenumbers (cm^{-1}) for complexes C11 – C15	113
Table 4.16: ^1H NMR chemical shifts (δ in ppm) of imine protons for C11 – C15	115
Table 4.17: Percentage conversion of 1-hexene for Pd(II) salicylaldimine complexes C2, C3, C5 and C6	117
Table 4.18: Percentage conversion of 1-hexene for Ni(II) salicylaldimine complexes C11 – C15	119
Table 4.19: Comparison of catalytic activity between Pd(II) and Ni(II) complexes	122

LIST OF FIGURES

Figure 1.1: Structure of ferrocene	5
Figure 1.2: General structure for <i>N,O</i> -salicylaldimine bidentate ligand	6
Figure 3.1: Structure of SL1	51
Figure 3.2: Structure of SL2	52
Figure 3.3: Structure of SL3	53
Figure 3.4: Structure of SL4	54
Figure 3.5: Structure of SL5	55
Figure 3.6: Structure of SL6	56
Figure 3.7: Structure of SL7	57
Figure 3.8: Structure of SL8	58
Figure 3.9: Structure of SL9	59
Figure 3.10: Structure of SL10	60
Figure 3.11: Structure of SL11	61
Figure 3.12: Structure of SL12	62
Figure 3.13: Structure of SL13	63
Figure 3.14: Structure of SL14	64
Figure 3.15: Structure of SL15	65
Figure 3.16: Structure of SL16	66
Figure 3.17: Structure of SL17	67
Figure 4.1: FTIR spectrum for the salicylaldimine ligand SL1	80
Figure 4.2: ¹ H NMR for <i>N,O</i> -salicylaldimine ligand SL1 (^x solvent CDCl ₃ -d ₁)	84
Figure 4.3: ¹³ C NMR for <i>N,O</i> -salicylaldimine ligand SL1 (^x solvent CDCl ₃ -d ₁)	88
Figure 4.4: Chromatogram retention time for the molecular ion of SL2	91
Figure 4.5: Fragmentation peaks for the ligand SL2	91
Figure 4.6: ORTEP representation of molecular ligand SL3 . Thermal ellipsoids are drawn at the 50 % probability level	93
Figure 4.7: Crystal packing diagram for the ligand SL3	93

Figure 4.8: ORTEP representation of molecular ligand SL9 . Thermal ellipsoids are drawn at the 50 % probability level	96
Figure 4.9: Crystal packing diagram for the ligand SL9	97
Figure 4.10: ORTEP view of molecular ligand SL2	99
Figure 4.11: Crystal packing diagram for SL2	99
Figure 4.12: ORTEP representation of molecular ligand SL6 . Thermal ellipsoids are drawn at the 50 % probability level	101
Figure 4.13: Crystal packing diagram for the ligand SL6	102
Figure 4.14: Comparison of FTIR spectra for the ligand SL1 with its complex C1	106
Figure 4.15: ¹ H NMR spectrum for complex C2 (^x solvent DMSO-d ₆)	108
Figure 4.16: ¹³ C NMR spectrum for complex C2 (^x solvent DMSO-d ₆)	109
Figure 4.17: Comparison of FTIR spectra for the ligand SL1 with its complex C11	112
Figure 4.18: ¹ H NMR spectrum for C11	114
Figure 4.19: Catalytic conversion of hexene for palladium(II) complexes C2 , C3 , C5 and C6	119
Figure 4.20: Catalytic conversion of hexene for nickel(II) complexes C11 – C15	121
Figure 4.21: Comparison of catalytic activity between C3 and C12 having methoxy substituents	123
Figure 4.22: Comparison of catalytic activity between C5 and C14 having bromine substituents	123

LIST OF SCHEMES

Scheme 1.1: General Schiff base condensation reaction for the formation of salicylaldimine ligand.....	5
Scheme 2.1: General hydroformylation reaction.....	18
Scheme 2.2: Polymerisation of ethylene.....	38
Scheme 2.3: Proposed mechanism for ethylene polymerisation.....	39
Scheme 2.4: Heck coupling reaction of aryl bromide and styrene.....	45
Scheme 4.1: Synthesis of <i>N,O</i> -salicylaldimine ligands SL1 – SL17	77
Scheme 4.2: Possible tautomerism of the hydroxyimine (SL1 , left) to the keto-imine (right)....	83
Scheme 4.3: Possible fragmentation pattern for SL2	91
Scheme 4.4: Synthesis of <i>N,O</i> -salicylaldimine palladium(II) complexes C1 – C10	104
Scheme 4.5: Reaction mechanism for deprotonation of <i>N,O</i> -salicylaldimine ligand.....	105
Scheme 4.6: Synthesis of <i>N,O</i> -salicylaldimine nickel(II) complexes C11 – C15	111
Scheme 4.7: Hexene oligomerisation using nickel and palladium complexes.....	117

ABBREVIATIONS, ACRONYMS AND SYMBOLS

Å	Angstrom
ATR	Attenuated total reflectance
br	Broad
δ	Chemical shifts
COSY	Correlation spectroscopy
<i>J</i>	Coupling constant
COD	1,5-Cyclooctadiene
Cp	Cyclopentadienyl
°	Degrees
°C	Degrees Celsius
DCM	Dichloromethane
Et ₂ AlCl	Diethyl aluminium chloride
Et ₂ O	Diethyl ether
DMA	<i>N,N</i> -Dimethylacetamide
DME	1,2-Dimethoxyethane
DMF	Dimethylformamide
DMSO	Dimethylsulfoxide

CDCl_3-d_1	Deuterated chloroform
$\text{DMSO}-d_6$	Deuterated dimethylsulfoxide
d	Doublet
dd	Doublet of doublets
EDG	Electron donating group
EWG	Electron withdrawing group
ESI-MS	Electrospray ionisation mass spectrometry
EA	Elemental analysis
eq.	Equivalents
EtOH	Ethanol
EASC	Ethyl aluminium sesquichloride
FT-IR	Fourier-transform infrared
GC	Gas chromatography
GC-MS	Gas chromatography-mass spectrometry
g	Gram(s)
Hz	Hertz
HSQC	Heteronuclear single quantum coherence

h	Hour(s)
IR	Infrared
MS	Mass spectrometry
m/z	Mass to charge ratio
MHz	Mega hertz
MeOH	Methanol
Me	Methyl
MAO	Methylaluminoxane
μmol	Micromole
ml	Millilitre
mmol	Millimole
MMAO	Modified methylaluminoxane
M_w	Molecular weight(s)
m	Multiplet
NMR	Nuclear magnetic resonance
1D	One-dimensional
ppm	Parts per million

PE	Polyethylene
POM	Polyoxometalate
KBr	Potassium bromide
ROP	Ring opening process
r.t	Room temperature
s	Singlet
<i>t</i> -Bu	<i>Tert</i> -butyl group
THF	Tetrahydrofuran
TMS	Tetramethyl silane
Et ₃ N	Triethylamine
t	Triplet
TLS	Turnover limiting step
2D	Two-dimensional
XRD	X-ray diffraction
ZSM-5	Zeolite Socony Mobil-5 (aluminosilicate zeolite)

CHAPTER ONE

INTRODUCTION

1.1 Background

Catalysis is a very important component in many industrial chemical manufacturing processes. This arises from the fact that manufacturers need to maximize on production within a short period of time. This is achievable by use of catalytic materials which may alter the rate of production (Centi & Perathoner, 2003). Catalysts may be homogeneous in which they function in the same phase as the reactants, or heterogeneous in which they function in a different phase from reacting materials (Deutschmann *et al.*, 2012). Homogeneous catalysts are frequently used in highly selective organic transformation. However, in industry most catalytic processes use heterogeneous catalysts because of their ease of separation from the product stream (Hardy *et al.*, 2004). For homogeneous catalysts the separation is rather complicated. However, homogeneous catalysts can still be used in commercial application at very low concentrations, such as parts per million (ppm) level which will not require recovery of the catalyst from the production stream (Dijkstra *et al.*, 2002).

1.1.1 Homogeneous catalysts

Homogeneous catalysts are considered superior in terms of activity and selectivity and possess a higher atom efficiency. Typical examples of homogeneous catalysts applied commercially in the hydrogenation of functionalized ketones include; dimeric triethylamine ruthenium(II), dicarboxylate ruthenium(II) complexes and the complexes of the kind $\text{RuX}_2(\text{binap})$ which contains halogens (Kitamura *et al.*, 1988). The catalyst 2,2-*bis*(diphenylphosphino)-1,1-

binaphthyl ruthenium(II) complex have shown to be exceptionally effective for the asymmetric hydrogenation of functionalized ketones which brings about the large scale manufacture of synthetic intermediates of antibacterial levofloxacin and antibiotic carbapenems (Ohkuma *et al.*, 1995).

Furthermore, ruthenium catalysts are used commercially to catalyse enantioselective hydrogenation of phenylthio ketones to phenylthio alcohols which are interesting building blocks for natural product synthesis (Tranchier *et al.*, 1997). Besides functionalized ketones, a number of other substrates which acts as hydrogen acceptors include; α,β -unsaturated carbonyl compounds, α,β -unsaturated acids and esters, imines and nitro compounds have been successfully reduced for transfer of both heterogeneous and homogeneous catalysts. Other metal complex catalysts applied in reduction hydrogenation other than the ruthenium ones are those of iridium and rhodium (Saluzzo & Lemaire, 2002).

Catalysts which are used under homogeneous conditions may at times be separated by precipitation using diethyl ether and then recycled. For instance, a number of ruthenium catalysts have been precipitated and reused (Brunner *et al.*, 1997). Another method to obtain insoluble catalysts involves immobilising the catalyst on inorganic solid support through ion pair formation (Brunner *et al.*, 1997), covalent bond (Pugin, 1996) or by entrapment (Dioos *et al.*, 2006; Ogunwumi & Bein, 1997).

Nevertheless, the greatest disadvantage for all homogeneously catalysed reactions is that of separating the homogeneously dissolved catalyst. The difficulty of separating between the catalyst and the reaction products could only be overcome by expensive recycle processes. When

homogeneous catalysis is two-phase, the active catalyst for the reaction is always dissolved in water. Thus, the reactants and products which in many cases are organic in nature and to a great extent non-polar, can be separated off after the reaction by simply separating the second phase from the catalyst solution, making it possible to recycle the catalyst. The industrial details of this modern separation technique for aqueous homogeneous catalysis has been discussed extensively in published research reports (Cornils, 1998; Cornils & Kuntz, 1995).

The separation of some homogeneous catalysts is achievable by use of the modern method used by Ruhrchemie/Rhône-Poulenc which is called liquid-liquid biphasic system employed for hydroformylation of alkenes. By using this method, the reactants and products are absorbed and retained in the organic solvent system, while the water-soluble catalyst is retained in the aqueous phase. The catalyst can easily be recovered by separating the two solvent phases (*Kohlpaintner et al.*, 2001).

1.1.2 Heterogeneous catalysts

Heterogeneous catalysis can be defined as a type of catalysis in which the catalyst occupies a different phase from the reactants and products. This may refer to the physical phase – solid, liquid or gas – but also to immiscible fluids. These catalysts are very easy to separate from product stream and can be recycled efficiently. Hence, the quantity of catalyst needed is low and high turnover numbers are achieved, making heterogeneous catalyst rather cheap. Heterogeneous catalysis can be more easily recycled than the homogeneous one, but the major challenge is the characterisation of the catalyst and optimization of properties that can be more difficult to achieve.

One of the most important raw materials in industrial processes is ethylene, especially in making synthetic products. Ethylene is traditionally produced via cracking processes from petroleum which is getting depleted (Alvira *et al.*, 2010). In the dehydration of ethanol to produce ethylene via green chemistry, there is quite a number of heterogeneous catalysts applied. Among these catalysts we have zeolites particularly ZSM-5 or the modified ZSM-5 which is tuned to give higher activity (Zhou *et al.*, 2019). Other examples of heterogeneous catalysts for the dehydration of bioethanol to form ethylene applied in large scale include; microscale HZSM-5 zeolite, nanoscale HZSM-5 zeolite (Phillips & Datta, 1997), alumina (γ -Al₂O₃) (Roy *et al.*, 2012) and Polyoxometalate (POM) catalysts (Janik *et al.*, 2009). The nanosized Zn_xZr_yO_z mixed oxides catalyst is effectively applied in high-yield conversion of bioethanol to isobutene, a value-added intermediate useful for the synthesis of fuels and chemicals (Sun *et al.*, 2011).

1.1.3 Classes of organometallic complexes

Many of the homogeneous and heterogeneous catalyst are organometallic-based compounds and will be discussed in the subsequent sections. A lot of research has been done on organometallic complexes. This is strongly attributed to their use in biological studies as well as catalysis. All the typical classes of organometallics such as metallocenes, metal-based half-sandwich, metal carbenes, metal carbonyls or metal-based π -ligands are widely used for catalysis or biosensing (Gasser *et al.*, 2011). Metallocenes, for instance are compounds with two π -bonded cyclopentadienyl (Cp) ligands on a metal atom. A common example is ferrocene (bis-cyclopentadienyl iron, Cp₂Fe) as shown in Figure 1.1.

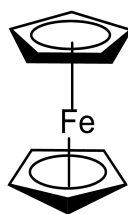
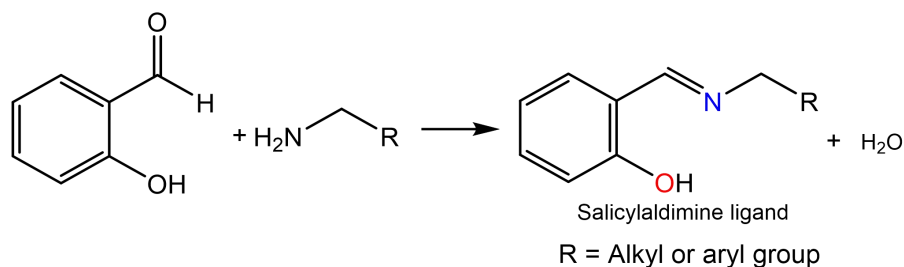


Figure 1.1: Structure of ferrocene

1.1.4 Salicylaldimine ligands and their complexes

Salicylaldimine ligands are synthesized through Schiff base condensation reaction of a salicylaldehyde derivative with a primary amine (Scheme 1.1). To form a bidentate complex compound, the salicylaldimine ligand binds to the metal atom using *N,O*-donor atoms. The *N,O*-salicylaldimine complexes are of great interest in catalysis since they are easy to synthesize and form stable complexes. It is also easy to manipulate the ligand structure and refine the catalytic properties by varying the electronic and steric bulkiness around the ligand backbone.

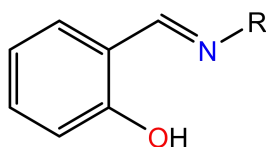


Scheme 1.1: General Schiff base condensation reaction for the formation of salicylaldimine ligand

Since the main focus of this work is homogeneous catalysis, and *N,O*-salicylaldimine complexes in particular, it is prudent to give an extensive background discussion on this subject matter. In recent years many studies have been conducted on the complexes of the late transition metals, such as nickel and palladium. One of the main reasons is that these metals have lower

oxophilicity (the tendency of certain chemical compounds to form oxides by hydrolysis or abstraction of an oxygen atom from another molecule usually organic compounds) and also allow copolymerisation of for example; ethylene, 1-hexene and other polar vinyl monomers than the early transition metals (Britovsek *et al.*, 1999; Gibson & Spitzmesser, 2003). Early transition metals exhibit high oxophilic properties.

Mononuclear and binuclear complexes have been studied for these particular metals. These studies have revealed that the bimetallic complexes for both palladium(II) and nickel(II) have better catalytic activity for over ethylene polymerisation compared to their monometallic counterparts (Guisado-Barrios *et al.*, 2013). This superior activity is closely attributed to the cooperative effect (Bahuleyan *et al.*, 2008). The postulation is that cooperative effects involving two or more metal centres in close proximity, might achieve more efficient chain propagation to yield novel polymeric architectures (Bahuleyan *et al.*, 2011). The active metal centres are brought into closeness to one another by preparing complexes using a suitable ligand system. For nickel(II) homobimetallic complexes, there are many types of ligand systems that have been shown to work well with it such as *N,N* (Salo & Guan, 2003) (for instance, α -diimines, β -diimines or iminopyridyls) and *N,O* (Speiser & Braunstein, 2004) (such as salicylaldimines) bidentate ligands (Figure 1.2), which have been widely investigated.



R = alkyl, aryl group or linker

Figure 1.2: General structure for *N,O*-salicylaldimine bidentate ligand

It has been reported that iminopyridine nickel(II) catalysts are quite effective polymerisation catalysts (Britovsek *et al.*, 2003; Laine *et al.*, 1999). This team of researchers conducted ethylene polymerisation experiments involving iminopyridyl Ni(II) homobimetallic catalyst and compared it to its monometallic analogue. The homobimetallic catalyst produced oligomers with higher molecular weights, $M_w = 8800$ while its monometallic Ni(II) analogue produced $M_w = 2000$. These results were attributed to the additional cooperative effect of the two active centres on the same catalyst such that the olefin produced by one centre are quickly taken up by the readily available nearby metal centre. Further, they investigated the cooperative effect using 1-hexene as a substrate for polymerisation. The result confirmed further this effect in that 35 % polyhexene was obtained using bimetallic Ni(II) catalyst while 11 % polyhexene with the monometallic analogue (Bahuleyan *et al.*, 2008). This is approximately three times the yield obtained by monometallic Ni(II) catalyst.

Considerable research effort has been devoted over the past few years to the design of new chelating *N,O*-ligands, and their nickel complexes. The results have shown very high catalytic activity for olefin polymerisation (Yang *et al.*, 2006; Zhang & Jin, 2006). A typical example is in the work reported by Younkin and his team (Younkin *et al.*, 2000). The Brookhart group also reported neutral single-component nickel(II) complexes based on anilinetropone ligand which was shown to be highly active ethylene polymerisation catalysts which produced high-molecular-weight polyethylene. Functionalized (addition of a functional group to a compound by chemical synthesis) olefins were also polymerised and required no cocatalyst (Hicks & Brookhart, 2001).

A group led by Zhang also synthesized neutral single-component binuclear nickel(II) complexes for olefin polymerisation similar to the one by Brookhart group (Zhang & Jin, 2003). The binuclear nickel(II) were catalytically active in ethylene polymerisation. The complexes with bulky substituted aryl group bound to anilino function exhibited uniquely greater activity than those with less bulky substituent (Zhang & Jin, 2003).

There are a number of significant factors that influence the catalytic activities as was demonstrated by another research team (Chen *et al.*, 2007). The study involved nickel complexes that possess *m*-arene-bridged *bis*-salicylaldimine chelate ligands. The ligands were synthesized via condensation reaction of *m*-phenylenediamine with 2 equiv. of salicylaldehyde then treated with 2 equiv. of *trans*-Ni(Ph)PPh₃)₂ in toluene to afford binuclear nickel(II) complexes. Upon testing catalytic activity of the binuclear nickel(II) complexes, it was revealed that the complexes exhibited high catalytic activities for ethylene polymerisation. Another factor that was investigated is the effect of varying the *ortho*-substituents on the phenol and *N*-aryl moieties of the ligands on ethylene polymerisation. It was found that small substituents at the *ortho* position of the phenolic ring are less active at room temperature. Further investigation revealed that complexes containing bulky *ortho*-substituents (*t*-Bu or Ph) obtained optimal activities at lower temperatures (at 25 or 50 °C) compared with those with smaller *ortho*-substituents. It was also revealed that complexes containing electron-withdrawing groups (EWG) like nitro (NO₂) group showed increased catalytic activities and generated polyethylene compounds with higher molecular weights (Chen *et al.*, 2007).

Polymerisation temperature was observed to have a considerable effect on the catalytic behaviour as well. The optimal polymerisation temperature for each particular catalytic system

depends immensely on the balance between propagation rate of the polymer and the thermal stability of the catalyst (Wang *et al.*, 1998; Zhang *et al.*, 2003). The polymerisation time is also of great consideration. It was established that catalytic activity decreases steadily when polymerisation time is prolonged. This decrease was as a result of the deactivation of the active metal centre or obstruction of part of the catalyst in the precipitated polymer product (Chen *et al.*, 2007). This indicates that, the type of substituent at the ligand backbone has great influence on the catalytic activity.

A study led by Ji and co-workers synthesized salicylaldimine ligands containing both aryl-naphthyl and dibenzhydryl moieties (Ji *et al.*, 2017). They further synthesized monometallic nickel(II) complexes with which ethylene polymerisation was investigated. In their findings, the complexes that bore most bulky *tert*-butyl (*t*-Bu) groups displayed highest activity and molecular weight. Consequently, the deactivation of the catalyst and chain transfer was considerably suppressed by the bulky ligands. Moreover, the complexes bearing electron-withdrawing groups (EWG) or substituents near the metal active centre exhibited higher activity and produced polyethylene with higher molecular weight than those bearing electron-donating groups (EDG) or substituents. The explanation behind this phenomenon is that, the EWG do reduce the electron density around the metal active centre, leading to better monomer coordination and faster chain propagation (Ji *et al.*, 2017). The main drawback for Ji and group, class of salicylaldimine nickel(II) complexes is that they showed very low thermal stability. Research findings have proved that substituents on the peripheral aromatic ring have a profound effect on the catalytic properties, their remoteness notwithstanding (Zuideveld *et al.*, 2004). Another crucial finding is that high molecular weight linear polyethylene or low molecular weight, highly branched

oligomers are generated depending on the substituent. Studies on a variety of different substituents in 2,4-position (for instance -OMe, CF₃, Me or *t*-Bu) in the phenolic ring have shown that the catalytic properties correspond to their electronic character (Bastero *et al.*, 2007; Göttker-Schnetmann *et al.*, 2007; Osichow *et al.*, 2013). Strong electron-donating substituents support branch formation and chain transfer which both occur through β -hydride elimination as the fundamental step in polymerisation process.

The Stephenson group approached the effect of remote substituent on polymerisation in a very interesting manner. The team introduced a spatially proximate but electronically remote “hard” sulfonyl, –SO₂–, groups in the vicinity of “soft” d^{10} catalytic centres which advances a new means to regulate single-site polymerisation process (Stephenson *et al.*, 2014). Further, it was reported that a Ni(II) phenoxyiminato catalyst with a remote ligand –SO₂– group displayed a markedly raised polymerisation activity and thermal stability which generated higher molecular weight (M_w) polyethylene compounds with distinctively high levels of chain branching (Wiedemann *et al.*, 2014).

Other systems whose metal complexes have been used in catalysis also include various *P,N* (Daugulis & Brookhart, 2002) and *P,P* (Dennett *et al.*, 2004) bidentate ligands. Most of these catalysts contain ligands based on hard-donor atoms (*N,N* or *N,O*) or mixed hard-soft donors (*P,O* or *P,N*) (Albers *et al.*, 2004). Owing to their bonding versatility, *P,N* ligands play an important role in the coordination chemistry of transition metals and in homogeneous catalysis (Speiser *et al.*, 2005). For palladium bimetallic complexes, the tetradentate-*bis*(dithiolene) and *bis*(phosphino) pyrazole ligand systems were established to be acceptable for catalysis.

Further still, the use of Pd-catalysts in Suzuki-Miyaura (Lai *et al.*, 2005; Oncel *et al.*, 2016; Shahnaz *et al.*, 2013; Tas *et al.*, 2009; Yundong *et al.*, 2009) and Heck-Mizoroki (Knowles & Whiting, 2007) cross-coupling reactions in aqueous media stems interest from a viewpoint of “green sustainable chemistry” (Biswas *et al.*, 2013). Salicylaldimine palladium complexes have been widely studied and applied for synthesis of pharmaceutical intermediates, natural products and polymers (Nicolaou *et al.*, 2005; Schomaker & Delia, 2001; Vaz *et al.*, 2001). A research team led by Cui reported the synthesis and characterisation of amino-salicylaldimine ligands 5-methyl-3-(R-1-ylmethyl)-salicylaldimine (R = morpholine, piperidine, pyrrolidine, 4-methylpiperazine, diisopropylamine) and their palladium(II) complexes (Cui *et al.*, 2010). The complexes were investigated for Suzuki and Heck reactions. In the Suzuki reaction, coupling of 4-chlorobenzaldehyde with phenylboronic acid in the presence of Dimethylformamide (DMF) was studied. It was observed that the solvent DMF gave better yield due to good solubility of the reagents and easier reduction of Pd⁺² to Pd(0). The activated electron-deficient aryl chloride, such as 4-chloroacetophenone, 4-chlorobenzaldehyde, and 4-chloronitrobenzene effectively coupled with phenylboronic acid to give high yields. The deactivated electron-rich substrates such as 4-chlorotoluene and 4-chlorophenol gave very low yields even with prolonged reaction time of up to 12 h (Cui *et al.*, 2010). All these results indicated that electronic effect of substituents on the aryl chlorides display great influence on the reaction and electron-withdrawing substituents were effective for coupling.

Solid-phase organotransition metal complexes having high activity and selectivity, particularly those based on palladium, offer several significant practical advantages in synthetic and

industrial chemistry; among these are; the ease of separation of the catalyst from the desired reaction products and the ease of recovery and re-use (green chemistry) of the catalyst are most important (Dawood, 2007).

Due to the success of the homobimetallic complexes as far as catalysis is concerned, salicylaldimine ligands provide convenient building blocks of supramolecules, partly because ligands with various functional groups can be obtained easily by simple condensation reactions of diamines and salicylaldehyde (2-hydroxybenzaldehyde) derivatives, forming a new C=N bond (Baran & Yaşar, 2013). These ligands were first synthesized via a Schiff-base condensation reaction using salicylaldehyde derivatives and a primary diamine in which the aliphatic carbon chain length of the diamine is varied. This created a bulky *N,O*-ligand system which is known to increase activity of nickel(II) catalysts (Arduengo *et al.*, 2005). The reason for using the late-transition metals nickel and palladium is that, one can vary the coordination geometry and not forgetting lower oxophilicity property as mentioned earlier (Kuwabara *et al.*, 2009). Indeed, the salicylaldimine-based nickel and palladium complexes serve as the active catalysts for olefin polymerisation (Chen *et al.*, 2007; Ji *et al.*, 2017; Soshnikov *et al.*, 2013; Takeuchi *et al.*, 2017). It is worth noting that nickel and palladium are found in group ten of the transition metal block of the periodic table. Nickel happens to be more reactive with air and other substances compared with palladium and their behaviour as catalytic complexes should be quite interesting to study.

1.2 Problem identification

Most reported palladium and nickel complex catalysts, based on Schiff base ligands, applied in C-C coupling reactions, especially ethylene polymerisation, Heck and Suzuki coupling are

monometallic in nature (Cao *et al.*, 2013; Domin *et al.*, 2005; Guo *et al.*, 2008; Liu *et al.*, 2010; Liu & Wang, 2009; Mao *et al.*, 2012; Tang *et al.*, 2013), and most of these catalyst precursors have been reported to show high activity. Little work has been reported on multinuclear catalysts (homobimetallic and heterobimetallic), but the very few published reports involving nickel and palladium catalysts have shown a much higher activity in comparison to their mononuclear counterparts, as already clearly pointed out in the in-depth discussion on background section. The bimetallic complexes should possess superior catalytic properties over monometallic counterparts because of the tandem effect.

Some of the possible challenges that were encountered included finding the optimum conditions for the syntheses of both the salicylaldimine ligands and their nickel and palladium complexes. However, after several trial experiments, the most favourable reaction conditions were established which gave the desired results. There was also the possibility of the nickel complex dimerizing due to competing β -hydride elimination with an alkene. It is a very crucial chain termination step in the polymerisation of olefins (Johnson *et al.*, 1995). Another possible difficulty was that nickel can sometimes undergo paramagnetism, especially when tetrahedral and octahedral nickel complexes are formed, and thus interferes with NMR analysis (Bahuleyan *et al.*, 2008). The choice of N and O donor atoms of the salicylaldimine ligands synthesized in this work ensured the formation of square planar complexes which are always diamagnetic which can be studied using NMR (Britovsek *et al.*, 2003). Therefore, the main questions this project sought to answer were:

- (1) Can nickel and palladium homobimetallic complexes based on substituted salicylaldimine ligands be synthesized and can they catalyse 1-hexene polymerization reactions?
- (2) Can these complexes be utilized in Heck coupling reactions?
- (3) How does the catalytic activity (if any) of these complexes compare to that of their monometallic counterparts?

1.3 Research aims and objectives

1.3.1 General objective

The aim of this study was to synthesize homobimetallic nickel and palladium complexes and test their potential as catalysts for 1-hexene polymerisation.

1.3.2 Specific objectives

The specific objectives in this thesis were as follows:

- (1) Synthesis and characterisation of substituted *N,O*-salicylaldimine ligands
- (2) Synthesis and characterisation of Ni and Pd homobimetallic complexes of substituted salicylaldimine ligands
- (3) Evaluation of the complexes synthesized in (2) for their catalytic potential in 1-hexene oligomerisation

1.4 Justification of study

The application of *N,O*-salicylaldimine complexes have grown over time (Jian *et al.*, 2017; Weberski *et al.*, 2012). The ease of synthesis of these Schiff base ligands via condensation

reaction is one of the reasons for this growth. The late transition metals, for instance nickel and palladium were found to easily coordinate with *N,O*-salicylaldimine ligands.

One area that has not been explored fully is the synthesis of complexes with two active metal centres (homobimetallic and heterobimetallic). There is a strong indication that these types of complexes will greatly transform the chemistry of catalysis, noting that there are few homo- and heterobimetallic catalysts that are known.

1.5 Structure of the thesis

The following chapters report on: work already done related to this one in literature review (Chapter 2); the syntheses of ligands and complexes, as well as the instrumental information (Chapter 3); syntheses, characterisation and catalysis in results and discussions (Chapter 4). Finally, the conclusion and recommendations for future research on this topic (Chapter 5).

CHAPTER TWO

LITERATURE REVIEW

2.1 Introduction

Organometallic compounds are metal complexes containing at least one direct, covalent metal-carbon (M-C) bond. They are kinetically stable, usually uncharged, and relatively lipophilic and their metal atom is in a low oxidation state. Because of these fundamental differences compared to classical coordination metal complexes, organometallic compounds offer ample opportunities in the design of novel classes of compounds, potentially with new metal-specific mode of action. Interestingly, all typical classes of organometallics such as metallocenes, metal half-sandwich, metal carbenes, metal carbonyls, or metal π -ligands (Figure 2.1) are widely used in catalysis and biosensing (Gasser *et al.*, 2011) as already discussed in chapter one in the introduction.

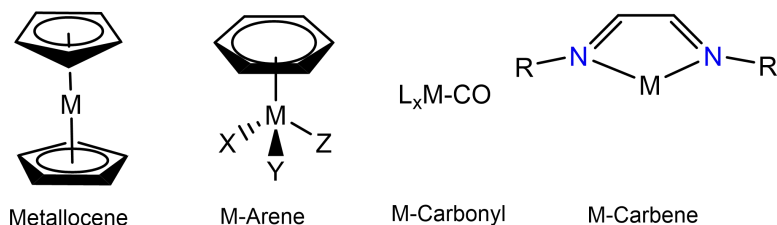


Figure 2.1: Structures of metallocene, M-arene, M-carbonyl and M-carbene

A number of heterobimetallic catalysts with two different active metal centres have been synthesized and are widely used. For example, the heterobimetallic complex containing an *N*-heterocyclic carbene-based multidentate ligand (Figure 2.2) (Mechler *et al.*, 2013).

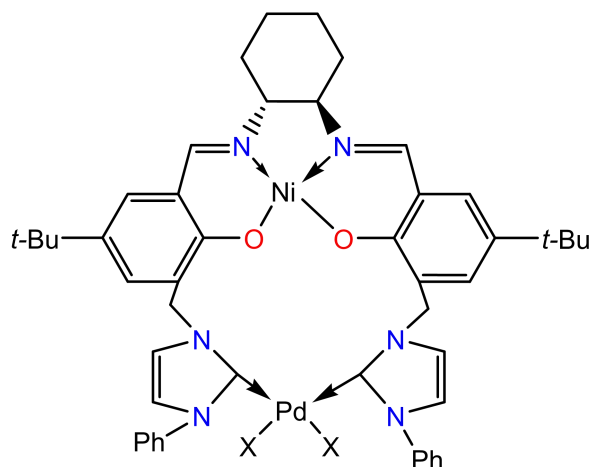


Figure 2.2: Heterobimetallic complex containing *N*-heterocyclic carbene

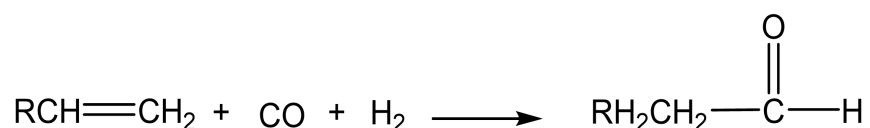
2.2 Hydrogenation

Catalytic hydrogenation of alkenes involves addition of molecular H_2 across the alkene double bond. The reactants, H_2 and ethylene (C_2H_4), enter the catalytic cycle by reaction with the Rh complex to produce in succession a hydrido complex and an alkene complex. In the final step, the hydrogenated product leaves the loop with the regeneration of the coordinatively unsaturated Rh complex to repeat the process (Bernales *et al.*, 2017). The cycle continues as long as hydrogen gas and ethylene are supplied. The rhodium complexes in solution serve as the catalyst compounds and are not used up in the reaction. Rhodium, which is more expensive than platinum, can be used even in catalytic processes where the products are inexpensive, because the rhodium complex catalyst is not consumed. Modifications of this type of catalyst are also employed in other applications like the production of pharmaceuticals such as levodopa (or L-

dopa) (Tolstikov *et al.*, 2001), which is used to treat Parkinson disease (Ledeti *et al.*, 2017; Lees *et al.*, 2017).

2.3 Hydroformylation

Hydroformylation involves the addition of carbon monoxide and hydrogen to an alkene to form an aldehyde containing one more carbon atom than the original alkene (Scheme 2.1).



Scheme 2.1: General hydroformylation reaction

This catalytic reaction which is employed in the petrochemical industry utilizes $\text{Co}_2(\text{CO})_8$ or various rhodium complex catalysts. The catalytic cycle proceeds through a series of organometallic intermediates. The aldehydes produced by hydroformylation are normally reduced to alcohols that are used as solvents, plasticizers, and in the synthesis of detergents (Botteghi *et al.*, 1994). The scale of production is enormous, amounting to millions of tonnes per year (Bantu *et al.*, 2007).

2.4 Alkene polymerisation

The polyalkenes, being the most common and useful class of synthetic polymers, are often prepared by use of organometallic catalysts, either in solution or supported (immobilised) on a solid surface. In the 1950s, the German chemist Karl Ziegler developed a catalyst for ethylene

polymerisation based on a catalyst formed by the reaction of TiCl_4 with $\text{Al}(\text{C}_2\text{H}_5)_3$. Soon thereafter, Italian chemist Giulio Natta made use of this type of catalyst for the polymerisation of propylene to produce polymers with highly regular structures (Younkin *et al.*, 2000). The details of the reactions of these commercial catalytic processes are not entirely understood, but there are strong indications from more easily studied soluble organometallic catalysts that alkenes coordinate to a metal centre and then insert into a hydrocarbon chain, producing a longer-chain hydrocarbon attached to the metal centre (Lin & Siegel, 2006).

Another closely related heterobimetallic complex, Fe-M, containing an Fe→Ni dative bond $[\text{Ni}(\text{S}_2\text{fc})\text{PMe}_2\text{Ph}]$ (**1**; $\text{S}_2\text{fc} = 1,1'$ -ferrocenedithiolato) or those without any direct metal-metal interactions $[\text{M}(\text{S}_2\text{fc})\text{dppe}]$ (**2**; $\text{M} = \text{Ni}, \text{Pd}$ and Pt ; $\text{dppe} = \text{Ph}_2\text{PCH}_2\text{PPh}_2$) were obtained from the reaction of the corresponding dichloro-*bis*(phosphine) complexes with 1,1'-ferrocenedithiolato in the presence of a base (Takemoto *et al.*, 1998). The reaction of $[\text{NiCl}_2(\text{PMe}_2\text{Ph}_2)]$ with $\text{fc}(\text{SH})_2$ ($\text{fc}(\text{SH})_2 = 1,1'$ -ferrocenedithiolato) afforded the Ni-Fe heterobimetallic complex containing an Fe→Ni dative bond $[\text{Ni}(\text{S}_2\text{fc})(\text{PMe}_2\text{Ph})]$ (**1**). Similar treatment of $[\text{MCl}_2(\text{dppe})]$ ($\text{M} = \text{Ni}, \text{Pd}, \text{Pt}$; $\text{dppe} = \text{Ph}_2\text{PCH}_2\text{CH}_2\text{PPh}_2$) gave a series of metal-ferrocenedithiolato complexes (**2**) without dative bonds (Figure 2.3) (Kohlpaintner *et al.*, 2001).

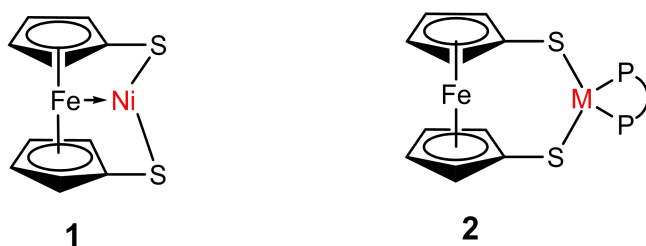


Figure 2.3: Heterobimetallic Fe-M (M = Ni, Pd, Pt) complexes containing 1,1'-ferrocenedithiolato

The presence of several metallic centres in one molecule of an organometallic complex creates favourable conditions for the appearance of new physicochemical characteristics. Bimetallic complexes are therefore currently attracting considerable attention from researchers (Alvira *et al.*, 2010).

2.5 *N,O*-Salicylaldimine ligands

Schiff base ligands (named after Hugo Schiff), also known as imines or azomethines are compounds with the general structure $R_1R_2C=NR_3$ (where R_3 is an alkyl or aryl group not a hydrogen, R_1 and R_2 may be hydrogens) (Qin *et al.*, 2013). They are synthesized via a condensation reaction between a primary amine and a carbonyl compound (aldehyde or ketone) (Holm & Everett, 1966; Vigato & Tamburini, 2004) by nucleophilic addition resulting in the formation of a hemi-amino functionality that is subsequently dehydrated in situ to produce an imine (Schiff, 1864; Schiff, 1866). They are considered a sub-class of imines being either aldimines or ketimines depending on their structure. Aldimines have R_1 as an alkyl or aryl group, and R_2 as a hydrogen atom whereas when both R_1 and R_2 are alkyls or aryl groups they are referred to as ketimines.

There are a number of subclasses of Schiff base ligands known with bidentate donor atoms which include; bidentate *N,N*-type ligands such as the imino-pyridine itself, which is synthesized by reacting pyridine derivatives with a primary amine. For instance, the condensation reaction between 4,4-methyl-*bis*(2,6-disubstituted aniline) and 2-pyridine carboxaldehyde (Jie *et al.*, 2005); diimine which can be synthesized by condensation of a substituted aniline derivative with a 1,2-diketone compound (Helldörfer *et al.*, 2003); imino-phenol is prepared for instance, by condensation of an appropriate aniline with 2-hydroxy-5-*tert*-butylisophthalaldehyde to afford a

2,6-*bis*(imino)phenoxy ligands (Wang *et al.*, 2002); 8-iminoquinoline ligand synthesized by condensation reaction of *o*-phenylenediamine with 2-acetylpyridine to achieve 2-(2-pyridyl)quinoxaline (Shao *et al.*, 2002). The salicylaldimine (Wang *et al.*, 1998; Younkin *et al.*, 2000); and anilinotropine (Hicks & Brookhart, 2001) which are in the *N,O*-ligand type are also synthesized by condensation reactions just like the aforementioned *N,N*-ligands. Some of the typical general examples of Schiff bases with bidentate and multidentate donor atoms are shown in Figure 2.4.

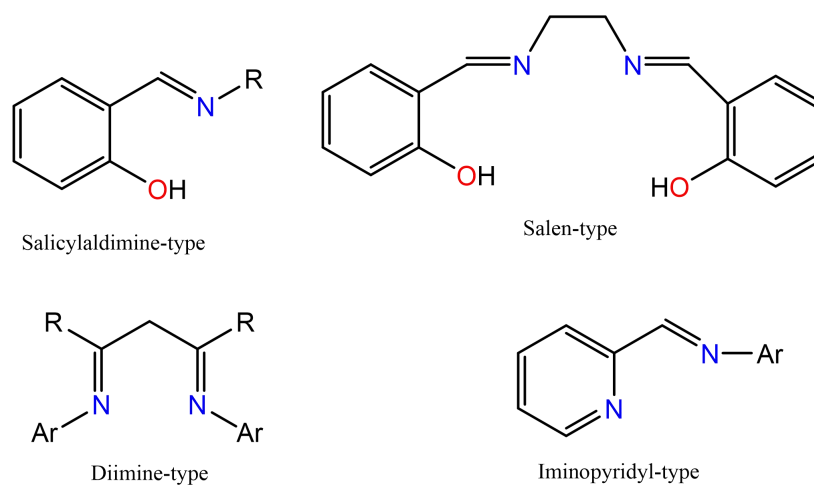


Figure 2.4: Some different subclasses of Schiff base ligands

This chapter focuses on the discussion of salicylaldimine ligands and their metal complexes, the extensive studies that have been conducted on them and specifically the applications of these salicylaldimine complexes. The salicylaldimine class of ligands are salicylaldehyde derivatives with the imine (C=N) functionality formed by condensation of salicylaldehyde with a primary amine. The *N,O*- donor atoms can bind metal ions in a bidentate fashion, forming either a square

planar, distorted square planar or distorted tetrahedral complex (Hu *et al.*, 2015; Oncel *et al.*, 2016; Zhang & Jin, 2006).

In the recent past, extensive research has been done on salicylaldimine ligand complexes for application as catalysts in polymerisation processes. The major reason has been to get an alternative to the traditional catalysts, that is, Ziegler-Natta and metallocenes. Both traditional catalysts for Ziegler-Natta polymerisation and cationic metallocenes suffer because heteroatoms (such as O, N, and S) poison these catalysts. The late-transition metals such as Ni and Pd have an advantage over the early transition metal complexes because they tolerate many functional groups in monomer substrates, and are capable of producing functionalized linear polyolefin materials. These late transition metals are also less oxophilic than early transition metals (Chen *et al.*, 2007; C. Wang *et al.*, 1998; Younkin *et al.*, 2000).

A research team led Connor reported on salicylaldimine neutral nickel catalysts which facilitates formation of high molecular weight, linear polyethylene in the presence of polar solvents such as ethers, esters, alcohols, amides and even water. These catalysts contain specifically tailored bulky salicylaldimine ligands which are capable of greatly increasing both the catalytic activity and their lifetime. The catalysts operate at low pressure of ethylene and work without cocatalyst additive. Further, these catalysts also allow incorporation of sensitive functionalities directly into the polyethylene (Connor *et al.*, 2002). These complexes (Figure 2.5) were greatly influenced by the structure around the ligand backbone. It was reported that the *ortho*-phenoxy substituents (R^1) bulkiness intensifies the catalytic activity of the metal complexes and branching in the polyolefin is also reduced. Further, the presence of EWG in the *para*-position (R^2) on the salicylaldiminato

ring was shown to greatly increase the catalytic activity of the metal complex (Wang *et al.*, 1998).

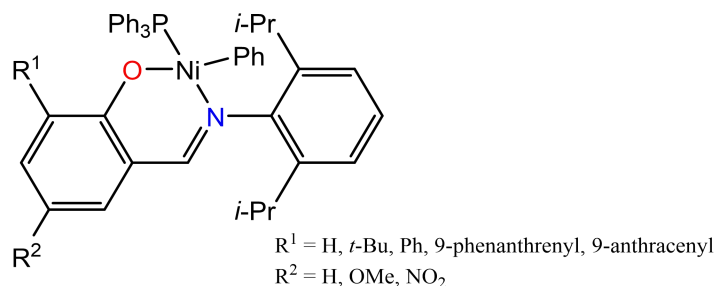


Figure 2.5: Neutral nickel(II) salicylaldiminato synthesized by Wang and co-workers (1998)

A salicylaldimine complex catalyst (Figure 2.6) similar to one synthesized by Wang, was prepared by Sun and co-workers which showed that complexes with more electron withdrawing chloro- substituent on the ligand segment showed a little higher catalytic activity on polymerisation of norbornene than the one with iodo- group. Also, the introduction of bigger naphthyl and more electron withdrawing substituents in the complexes exhibited the highest activities (Sun *et al.*, 2003).

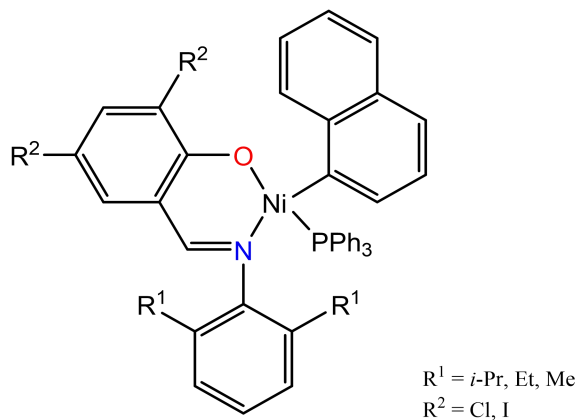


Figure 2.6: Neutral nickel(II) salicylaldiminato synthesized by Sun and co-workers (2003)

2.6 *N,O*-Salicylaldimine complexes

Salicylaldimine complex is formed when salicylaldimine ligand binds a metal in the central cavity in a bidentate fashion using nitrogen and oxygen donor atoms. The salicylaldimine ligand has the ability to coordinate metal atoms or ions using the hard oxygen and nitrogen donor atoms, which leads to better stabilisation of the metal complexes against reduction and eventually give good thermal stability (Li *et al.*, 2017).

Cui and Zhang designed a series of amino-salicylaldimine ligands, 5-*tert*-butyl-3-(*R*-1-ylmethyl)-salicylaldimine (*R* = morpholine, piperidine, pyrrolidine, 4-methylpiperazine). These ligands were prepared via condensation reaction in which case 1 equiv. of 2,6-diisopropylaniline was added to an equimolar of 5-*tert*-butyl-3-(*R*-1-ylmethyl)-salicylaldehyde in EtOH and heated to reflux for 4 h. Yellow solids were isolated in appreciable amounts. The ligands were then reacted with $[\text{CrCl}_3(\text{THF})_3]$ in a 1:1 mole ratio in tetrahydrofuran (THF) refluxed for 2 h to form Cr complexes isolated in high yields as stable green solids. The ligands were complexed by Cr metal in a tridentate fashion to form a mononuclear structure. In the presence of methylaluminoxane (MAO) as cocatalyst all the chromium complexes showed moderate ethylene polymerisation activities. The oligomers ranged from C_4 to C_{18} with good selectivity for α -olefins (Cui & Zhang, 2010).

As mentioned earlier in the introduction chapter, the early transition metal catalysts exhibit high oxophilicity. However, there is a lot of research that has been conducted on the phenoxyimine complexes of these metals and their application as catalysts in polymerisation reaction. For instance, the group 4 metals, titanium and zirconium. Despite their high oxophilic nature, many

of their complexes have been synthesized and tested. The binuclear (homobimetallic) titanium and zirconium exhibited significantly enhanced copolymerisation of ethylene versus their mononuclear analogues. The activity was observed to be up to five-fold in comparison with the mononuclear counterparts (Han *et al.*, 2012; Salata & Marks, 2008, 2009).

Complexes of zirconium metal, a group 4 transition metal were prepared by Matsui and his research team, which possessed two phenoxyimine chelate ligands. The aim was to investigate their catalytic performance for olefin polymerisation (Matsui *et al.*, 2001). To prepare the ligand, a phenol derivate was treated with paraformaldehyde in the presence of a base to produce an *ortho*-formylated phenol. The *ortho*-formylated phenol was subjected to a Schiff base condensation reaction with an appropriate primary amine to give a phenoxyimine ligand. The zirconium complex was achieved by reacting $ZrCl_4$ with the lithium salt of the phenoxyimine ligand in a 1:2 molar ratio. A zirconium complex was obtained with two 3-*tert*-butylsalicylideneaniline ligands, that is, *bis*[*N*-(3-*tert*-butylsalicylidene)anilinato]zirconium(IV) dichloride. When tested for catalytic activity in ethylene polymerisation, it showed an activity of 197 kg of polymer/mmol of catalyst, much higher than one displayed by Cp_2ZrCl_2 . The effect of temperature on catalytic activity of the catalysts with MAO as cocatalyst was also undertaken. The phenoxyimine zirconium complex showed 295 kg of polymer/mmol of catalyst at 0 °C. This activity was observed to increase to a maximum of 587 kg of polymer/mmol of catalyst at 40 °C. Above this temperature, the activity decreased (Matsui *et al.*, 2001).

Huang and his group synthesized salicylaldiminato cyclopentadienyl zirconium complexes. The ligand was prepared via condensation reaction of 3-(*tert*-butyl)-2-hydroxybenzaldehyde with cyclohexanamine then followed by the complexation with $BuC_5H_4ZrCl_3 \cdot DME$ to form zirconium

complex catalyst. A total of three complexes were synthesized. The desired mono(salicylaldiminato) cyclopentadienyl zirconium complexes were synthesized by the reaction of the lithium salt of the salicylaldimine with one equivalent of the corresponding $\text{CpZrCl}_3 \cdot \text{DME}$. Upon activation with MAO cocatalyst, these zirconium complexes were exhibited to be effective for ethylene polymerisation, but not for propylene when subjected to various reaction conditions. Temperature played a big role in the catalytic activity of these zirconium complexes. Some of them showed optimum activity temperature at 50 °C, while others had optimum activity at 70 °C (1.15×10^6 g PE/mol_{Zr} h) after which the catalytic activity started decreasing drastically. These zirconium complexes were also tested for ethylene/1-hexene copolymerisation which showed positive activity for all the prepared complexes (Huang *et al.*, 2010).

Another team of researchers led by Ivanchev prepared binuclear (homobimetallic) titanium halide complexes. This was achieved by reacting salicylic aldehydes with primary diamines to obtain *bis*-salicylaldimines. To achieve the desired titanium complexes, a 1:1 molar ratio of *bis*-salicylaldimine was reacted in absolute dichloromethane (DCM) with $\text{TiCl}_2(\text{OPr})_2$ in toluene. When the catalytic activities of these binuclear titanium complexes was investigated, it was reported that they showed quite high activities ranging from 10 to 70 kg(PE)/mmol(Ti)Mpa h at 30 °C with MAO as cocatalyst. In addition, when the catalytic activities of the binuclear phenoxyimine titanium complexes were compared with its corresponding mononuclear analogues, the former exhibited twice the activity of the latter. Besides, the binuclear titanium complexes were observed to show enhanced thermal stability in comparison with their corresponding mononuclear counterparts. This was attributed to the slower bimolecular

deactivation process for the binuclear complex than for its mononuclear analogue (Ivanchev *et al.*, 2012).

A research by Krasuska and co-workers synthesized some two group 4 and one group 5 metal complexes, that is, titanium, zirconium, and vanadium respectively, using a phenoxyimine ligand *bis*[*N*-(salicylidene)-1-naphthylaminato] (Krasuska *et al.*, 2011). This afforded the complexes; *bis*[*N*-(salicylidene)-1-naphthylaminato]titanium(IV) dichloride, *bis*[*N*-(salicylidene)-1-naphthylaminato]zirconium(IV) dichloride, and *bis*[*N*-(salicylidene)-1-naphthylaminato]vanadium(IV) dichloride. The complexes were prepared by reacting zirconium(IV) chloride, vanadium(IV) chloride and titanium(IV) chloride with 2 equivalents of the aforementioned phenoxyimine ligand. These complexes were immobilised on an inorganic support $\text{MgCl}_2(\text{THF})_2/\text{Et}_2\text{AlCl}$, and the product of this modification on catalytic performance was investigated. When vanadium complexes were tested, they exhibited remarkable catalytic activity with all the cocatalysts used in the work, that is, Et_3Al , Et_2AlCl , EtAlCl_2 , and MAO which varied from 14.3 to 488 kgPE/mol_v. Furthermore, it was found that just like in vanadium complexes, catalytic activity of zirconium complexes decreased with size of substituent at the phenoxyimine ligand backbone. The catalytic activity of a complex is also strongly influenced by the type of cocatalyst used. For instance, zirconium complexes were active with MAO as a cocatalyst exhibiting activity from 2.4 to 600 kg PE/mol_{Zr}. When zirconium complexes were activated with alkylaluminium cocatalyst (EtAlCl_2 or Et_2AlCl), it showed inactivity or gave traces of products. In this research a comparison was also made of the effects of the type of cocatalyst on catalytic activity of immobilised (supported) with that of non-immobilised (unsupported) complex catalyst. It was observed that immobilised (supported) catalysts,

regardless of the type of metal active centre, exhibited the highest activity with MAO at 3375.3 kg PE/mol and 4845.7 kg PE/mol. Temperature also played a significant role in catalytic activity. For example, the catalysts exhibited very low activity at 20 °C (47.6 kg PE/mol), which increased steadily with temperature up to 4800 kgPE/mol at 60 °C. All the other complexes, that is, the ones for zirconium and vanadium showed similar trends like those for titanium in terms of effects of temperature (Krasuska *et al.*, 2011).

The complexes of another group 4 metal, hafnium were synthesized and investigated for olefin (ethylene and propylene) polymerisation (Axenov *et al.*, 2007). The 3,5-dicumylphenoxyimines and *tert*-butylsalicylaldimines having CH₂Ph or C₆F₅ imino groups which were selected and used as ligand precursors. The ligands were deprotonated using NaH (sodium hydride) or *n*-BuLi in THF then followed by the reaction of the Li or Na salts with hafnium(IV) chloride (HfCl₄) in toluene which afforded the required hafnium *bis*(phenoxyimine) dichloride complexes in appreciable yields. Upon investigation of the catalytic activity, hafnium dichloro salicylaldimines exhibited remarkably very high activity for ethylene polymerisation with MAO as catalyst activator within very short time of 5 to 10 minutes. The activity ranged between 100 to 56,000 kg PE/mol_{Hf}. This is quite high when compared with its counterpart complexes of titanium and zirconium derivatives. Furthermore, the hafnium dichloro-salicylalimine catalysts showed increased activity with increase in polymerisation temperature from 30 to 80 °C.

Most hafnium salicylalimine catalysts showed optimum catalytic temperature of 60 °C, after which the activity was observed to decrease. In addition, the hafnium *bis*(phenoxyimino) dichloro complexes were tested for propylene polymerisation with MAO as cocatalyst which exhibited moderate activities. The maximum catalytic activities were observed at a low

temperature of 10 °C after which there was decrease in activity as temperature was increased (Axenov *et al.*, 2007).

Another research team synthesized *N,N'*-(1R,2R)-cyclohexylene *bis*(3,5-di-*tert*-butylsalicylideneimine) via a Schiff base condensation reaction of 3,5-di-*tert*-butyl-2-hydroxybenzaldehyde with (1R,2R)-cyclohexanediamine in methanol using formic acid as a catalyst (Cuomo *et al.*, 2004). The ligand was subsequently complexed with ZrBn₄ (tetrabenzylzirconium) in pentane to obtain zirconium benzyl complex [C₆H₁₀-{N=CH-(3,5-*t*-Bu₂C₆H₂-2-O)-κO}₂]Zr(CH₂Ph)₂. Another zirconium complex was also prepared using the same ligand which produced its chloride counterpart via metathesis of ZrCl₄(THF)₂. The two complexations were carried out at room temperature. The same group investigated the olefin polymerisation activity using MAO, perfluoroborane [B(C₆F₅)₃] and [CPh₃][B(C₆F₅)₄]. It was observed that perfluoroborane cocatalyst is less efficient when compared with MAO and trityl salt. Moreover, MAO cocatalyst was found to be about eight times more active than trityl activator, that is, 126 g PE/mmol_{Zr} h and 16 g PE/mmol_{Zr} h (Cuomo *et al.*, 2004).

Similar to Cuomo's work is a research report by Mazzeo and his team in which, a zirconium complex was prepared by stirring a solution of *N*-(3,5-dibromosalicylidene)-2,3,4,5,6-pentafluoroaniline in diethyl ether and *n*-butyllithium/*n*-hexane solution for 10 minutes at -78 °C and heating the content to room temperature for 2 h. The resulting solution was added dropwise to a solution of ZrCl₄.2THF followed by stirring at room temperature for 15 h. Yellow-brown crystals were obtained after purification process. The isolated complexes were tested for propylene polymerisation using MAO as an activator. It was observed that the polymerisation activity stretched from 100 to 408 kg PE/mol_{Zr} atm.h in a time of 30 minutes to 1 h which was

very high. However, on investigating the activity of this zirconium phenoxyimine catalyst on higher olefin (1-hexene) polymerisation using MAO as cocatalyst, it was found to be inactive. Further test was done for ethylene and 1-hexene copolymerisation which exhibited remarkable productivity of between 320 to 2560 kg polymer/mol_{Zr} h (Mazzeo *et al.*, 2009).

Vanadium, chromium and zirconium complexes containing modified phenoxyimine ligands with pendant imidazolium bromide moieties were also synthesized (Houghton *et al.*, 2008). The ligands used were *N*-heterocyclic carbenes synthesized from imidazolium salts. These *N*-heterocyclic carbene ligands were complexed with zirconium, vanadium, and chromium halides in tetrahydrofuran (THF) to yield the desired catalysts. All the complexes were tested for catalytic activity in the presence of MAO as activator and found to be active for ethylene polymerisation. The catalytic activity varied from 0.98 to 6.2 kg PE/mol catalyst h at a range of temperatures of 0 up to 75 °C. This is moderate activity compared with other similar complexes with the same active metal centre.

To further strengthen the idea of cooperative effect brought by the presence of two active metal centres in a complex catalyst, Marks and his research group investigated it using zirconium metal, to explore the possibility of enhancement of polyethylene chain branching in ethene homopolymerisation and α -olefin incorporation in ethene copolymerisation. Monometallic catalyst Zr₁ and bimetallic catalyst Zr₂ were synthesized for the investigation. In the ethylene polymerisation studies, it was observed that the molecular weights of the product polymers increased with increasing nuclearity of the catalyst. It showed that the bimetallic Zr₂ polymer product is ~ 2 times that of Zr₁ monometallic catalyst. Moreover, branching in polymer chain was significantly increased as nuclearity of catalyst also increased. The branches observed in the

polyethylene are ethyl branches. There were observed less butyl and branches with six or more carbons. Under the ethylene and α -olefin copolymerisation experiments, the catalyst derived from Zr_2 bimetallic complex incorporated greater than 3 times more butyl branches than the one derived from monometallic Zr_1 catalyst (Li *et al.*, 2002).

Binuclear phenoxyiminato-nickel catalysts have also been shown to exhibit enhanced stability, catalytic activity and monomer incorporation as well as greater tolerance for polar monomers in olefin polymerisation in comparison with their mononuclear analogues (Suo *et al.*, 2018). The enhanced catalytic activity was demonstrated effectively when the two metal centres are in close proximity to enhance the cooperative effect (Chen *et al.*, 2016). This research designed binuclear Ni(II) phenoxyiminato catalysts connected by inert and rigid naphthalene linkers, having *tert*-butyl groups *ortho* to the phenolate moieties. This rigid ligand backbone was able to force the two nickel centres into proportionately close proximity. Then, one of the nickel coordination planes sterically shields the sites axial to the other, hence hindering the rate of polymer chain transfer in comparison to chain propagation which results in high molecular weight polymer products (Chen *et al.*, 2016).

One of the advantages of the transition metal catalysts in the extreme right of the periodic table is the ability to modify or manipulate their properties. For instance, their steric and electronic properties can be adjusted or modified (Chen *et al.*, 2015; Dai *et al.*, 2015; Mu *et al.*, 2010; Rhinehart *et al.*, 2013; Zuideveld *et al.*, 2004). The bulky substituents in the ligand backbone are regarded to be essential for metal catalysts especially for neutral nickel catalysts to attain better activity and generate high molecular weight polymers (Song *et al.*, 2009). Furthermore, the

electronic effects of the ligand also exceedingly determine the performance of the catalysts. Modification of the bulky *N*-aryl moiety of their ligands demonstrated that electron-withdrawing and electron-donating substituents on the *N*-aryl groups of the ligands can control the catalytic activity of the neutral nickel complexes and microstructure of the generated polymer (Bastero *et al.*, 2006; Göttker-Schnetmann *et al.*, 2007; Guironnet *et al.*, 2009; Korthals *et al.*, 2007; Yu *et al.*, 2007). Typically, sterically bulky groups do promote polymer chain elongation over chain transfer by blocking the axial sites of especially square-planar nickel complexes (Johnson *et al.*, 1995). Binuclear nickel phenoxyiminato catalysts have been reported to have uniquely increased stability and catalytic activity, comonomer inclusion and polar monomer tolerance in olefin polymerisation in comparison with mononuclear catalysts owing to the property of metal-metal cooperativity (McInnis *et al.*, 2014). Besides, bulky steric substituents such as *tert*-butyl groups reduce the rate of catalyst deactivation by deterring the formation of *bis*(salicylaldiminato) complexes (Connor *et al.*, 2003).

The superior catalytic activity displayed by binuclear catalysts was further confirmed with the synthesis of a dinickel complex (Figure 2.7) (Rodriguez *et al.*, 2008). The binuclear nickel complex {[2-(*tert*-Butyl)-6-(2,6-diisopropylphenyl)-imino]phenolato}(*n*-butyl)(triphenylphosphine)Ni(II) was prepared by adding an appropriate salicylaldiminate sodium in toluene dropwise to a stirring solution of *trans*-[NiCl(PPh₃)₂] kept at -78 °C. The mixture was stirred for 4 h, then 2 equiv. of *n*-BuLi was added dropwise and allowed to continue to stir at -78 °C for another 4 h. The complex product was isolated and since it was thermally unstable, drying was done under vacuum at 0 °C. Due to its thermal instability, NMR probe was cooled to

– 80 °C before analysis. Upon testing the complex for ethylene polymerisation, the binuclear nickel complexes exhibited an estimated two-fold greater polymerisation activity together with increased methyl branch density. This is in comparison with the one displayed by corresponding mononuclear catalysts under similar reaction conditions. These catalysts exhibit cooperative effects shown by increased polymerisation activity, more methyl chain branching and increased polymer molecular weight (Rodriguez *et al.*, 2009; Weberski *et al.*, 2012).

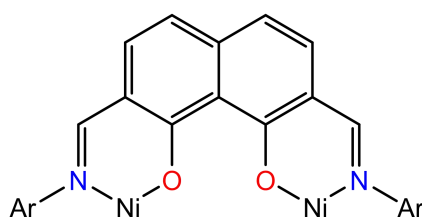


Figure 2.7: General core structure of binuclear phenoxyimine-nickel complexes

Moreover, a number of research teams have also independently synthesized and reported binuclear nickel and palladium phenoxyimine catalysts with a linker or spacer (Figure 2.8).

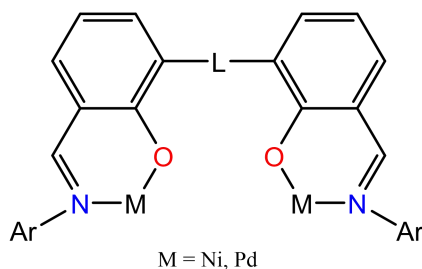


Figure 2.8: A general structure of binuclear phenoxyimine complex with a linker (spacer)

For instance, preparation of the appropriate ligand capable of binding to a metal atom in a binuclear fashion, in a two-step synthetic approach has been done (Hu *et al.*, 2005). First, the free ligand was synthesized via the condensation reaction of 2,2-dihydroxy-(1,1-biphenyl)-3,3-dicarbaldehyde with excess 2,6-diisopropylaniline. Then, the deprotonation of the free ligand readily proceeded with excess sodium hydride in anhydrous THF at room temperature. Ultimately, the isolated sodium salt was then reacted with 2 equiv. of *trans*-NiCl(Ph)(PPh₃)₂ for 14 h in benzene to yield the binuclear neutral nickel(II) catalyst. A similar procedure has also been used by another research group (Wang & Jin, 2006). The free ligands were prepared by condensation of 1,3-diaminopropane or *p*-diaminobenzene (which acted as linkers or spacers) and 2 equiv. of the substituted salicylaldehyde in suitable yields. Finally, the binuclear complexes were obtained by the reaction of 2 equiv. of *trans*-[NiClPh(PPh₃)₂] with sodium salts of the free ligands. These catalysts showed moderate to high catalytic activity in comparison with their mononuclear counterparts (Hu *et al.*, 2006; Hu *et al.*, 2005; Wang & Jin, 2006; Wehrmann & Mecking, 2008; Zhang & Jin, 2006).

The late-transition-metal catalysts continue to draw enormous interest from researchers since the breakthrough work in cationic Ni(II) and Pd(II) α -diimine catalysts by Brookhart (Johnson *et al.*, 1996; Johnson *et al.*, 1995) and neutral Ni(II) phenoxyimine catalysts by more research groups (Connor *et al.*, 2003; Waltman *et al.*, 2004; Wang *et al.*, 1998; Younkin *et al.*, 2000). One of such salicylaldimine nickel(II) catalysts copolymerises ethylene and olefins that possess functionality distant from the C=C double bonds. Nevertheless, attempts to copolymerise vinyl-functionalized monomers and ethylene using these nickel(II) salicylaldimine-based catalysts have led to catalyst deactivation. This is attributed to addition of a nonlabile chelate to the active

centre, thus associative addition of another olefin, which slows down the rate of polymerisation. As mentioned earlier, this has strongly been attributed to their greater tendency to tolerate polar monomers compared to the early-transition-metal catalysts. Moreover, the properties of the late-transition-metal catalysts can be modified by a number of ways including steric and electronic effects (Chen *et al.*, 2015; S. Dai *et al.*, 2015; Mu *et al.*, 2010; Rhinehart *et al.*, 2013; Zuideveld *et al.*, 2004). It has also been reported that for binuclear nickel catalyst (Figure 2.9) the polymer products showed reduced polymer branches and a higher catalytic activity due to close proximity of metal active centres producing metal-metal cooperative effect and the presence of bulky substituents at the backbone of the ligand moiety (Chen *et al.*, 2016).

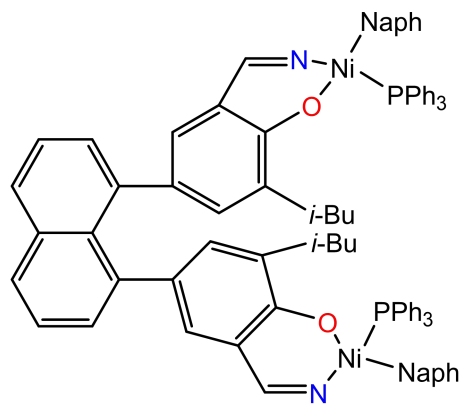


Figure 2.9: Binuclear phenoxyiminato nickel(II) complex by Chen and co-workers (2016)

As already indicated, nickel catalysts are capable of generating high molecular weight polyethylene (PE) with catalytic activity comparable to or even better than many early-transition metal catalysts, whilst palladium catalysts can copolymerise olefins with polar monomers like alkyl acrylates or methyl vinyl ketone (Killian *et al.*, 1996). There are two important types of chelating ligands used to support the metal centres namely; the phenoxyimine (*N,O*) and the α -

diimine (N,N), both of which have been adapted to be used as effective ligand moiety in binuclear nickel complexes. Moreover, a remarkable feature of the phenoxyimine nickel complexes is that they are neutrally charged in their activated forms and consequently considered to exhibit even greater tolerance toward polar functional groups than the α -diimine nickel complexes, which form cationic species upon activation (Makio *et al.*, 2011).

In another research, it was reported that all nickel(II) complexes bearing anilido-imine ligands and β -diimine ligands, nickel(II) and cobalt(II) complexes of β -ketoamine ligands exhibited characteristic vinyl polymerisation of norbornene (Li *et al.*, 2006). In this work, an N,N' and N,O' nickel(II) complexes bearing fluorinated β -diketimate backbone ligands were successfully synthesized. The β -diketimate ligands were synthesized via condensation of 1,1,1,5,5,5-hexafluoroacetylacetone with the corresponding aniline (Li *et al.*, 2006). Both complexes exhibited high activity for vinyl polymerisation of norbornene when activated by MAO (Wang *et al.*, 2007). All polynorbornenes obtained have high molecular weights and good solubility in ordinary solvents, such as cyclohexane, chlorobenzene, and *o*-dichlorobenzene.

In theory, the reactivity, selectivity and the ability to oligomerise or polymerise monomers is defined by the electronic, steric and geometric (chelate ring size) effects of the ligand. In the case of N,N or N,O -bidentate ligands (Alvira *et al.*, 2010; Chen *et al.*, 2007; Cornils & Kuntz, 1995; Ohkuma *et al.*, 1995; Zhang & Jin, 2003), the size of the aromatic substituents on the imine or imide and carboxamide nitrogens would influence ligand coordination mode (that is, N,N versus N,O) (Ji *et al.*, 2017; C. Wang *et al.*, 1998; Zhang *et al.*, 2003), the reactivity and the propagation and termination ratio, allowing access to a variety of new materials (Zuideveld *et al.*, 2004).

Studies by Budagumpi and his group on binuclear palladium catalysts demonstrated the effects on polymerisation activity by having sterically modulated *bis*-imine ligands with methylene spacer (Budagumpi *et al.*, 2011). Steric modulations in the methylene spacer bridged ligands affects ethylene polymerisation not only from the viewpoint of yield but also product distribution. It was also observed that the change from the original NMR active square-planar geometry to the NMR inactive tetrahedral geometry of binuclear palladium complexes under the polymerisation conditions is the major reason for the high activity of the binuclear complexes (Budagumpi *et al.*, 2011).

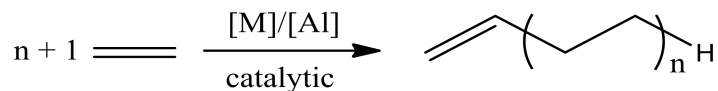
As is already pointed out in the objectives in chapter one, Heck-coupling reaction is one of the methods to be used to evaluate the activity of the new catalysts. The Heck coupling reaction has grown into one of the most prolific and efficient method of C–C coupling formation in the synthetic chemistry in industry and academia. Traditionally, phosphine-based complexes have been used as catalysts in Heck-coupling reactions. Nevertheless, phosphine-based complexes are difficult to prepare and rather expensive (Hollas *et al.*, 2011). For the phosphine ligands, a team of researchers synthesized some strong nitrogen-donor ligand complexes to study the Heck-coupling reactions (Motswainyana *et al.*, 2012). New nickel(II) complexes containing imino-pyridyl derived ligands were prepared. The complexes were evaluated as catalysts for Heck reactions of iodobenzene, bromobenzene and chlorobenzene with methyl acrylates. These nickel(II) complexes exhibited good catalytic activities under mild conditions (80 – 110 °C) towards iodobenzene and bromobenzene (Motswainyana *et al.*, 2012).

Multidentate ligands, for instance *N,N,N*- tridentate models have been developed (Adewuyi *et al.*, 2007) and are useful for the construction of early-late heterobimetallic (ELHB), although they

have to coordinate to two different metal atoms selectively. Heterobimetallic complexes containing titanium and palladium were prepared by a team of researchers from *O,N,O-N,N* multidentate ligand system (Suzuki *et al.*, 2015). Each ligand contained an *O,N,O*-tridentate di(pyridine-2-yl) part based on a 2,6-lutidine scaffold and an *N,N*-bidentate di(pyridine-2-yl) part. The *O,N,O*-moiety selectively coordinated to a titanium atom on treatment with titanium(tetraisopropoxide). It was also established that *N,N*-bidentate di(pyridine-2-yl) moiety coordinated to the palladium atom on treatment with *bis*(benzonitrile)palladium(II) chloride afforded a heterobimetallic complex (Suzuki *et al.*, 2015). Preliminary study on catalytic reactions especially the Mizoroki-Heck reaction between acrylic acid and iodobenzene afforded good yield of up to 81 % for cinnamic acid after the mixture had been stirred at 140 °C for 2 h.

2.7 Catalytic oligomerisation/polymerisation

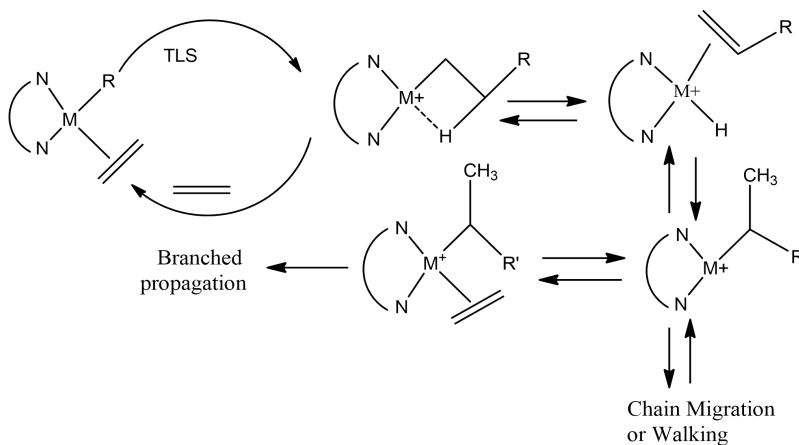
The α -olefins can be produced by four main processes that operate either by elimination reactions or by chain-growth reactions namely; (i) the cracking of paraffins, (ii) the dehydrogenation of paraffins (iii) the dehydration of alcohols and (iv) the polymerisation of ethylene. The main focus of this research was oligomerisation and polymerisation (Speiser *et al.*, 2005). For the ethylene oligomerisation or polymerisation systems require transition metals associated with aluminium cocatalysts (Scheme 2.2).



(Where $n = 2, 3\dots$)

Scheme 2.2: Polymerisation of ethylene

It is possible to monitor ethylene polymerisation, a process that can also be referred to as chain growth. This was reported in a research work as shown in Scheme 2.3 below (Ittel *et al.*, 2000).



TLS is "Turnover Limiting Step"

Scheme 2.3: Proposed mechanism for ethylene polymerisation

The process of testing of a new catalyst for possible catalytic activity requires a co-catalyst to be used. A co-catalyst (activator) is a substance that acts in tandem with another as a catalyst or a pair of cooperative catalysts that improve each other's catalytic activity. There are quite a number of co-catalysts that can be used in testing for the catalytic activity of newly synthesized complexes. For instance, there are ethylaluminium sesquichloride (EASC), methylaluminoxane (MAO), modified methylaluminoxane (MMAO), and diethyl aluminium chloride (Et₂AlCl). Moreover, the major considerations when one wants to design a catalyst include the electronic effect of the substituents near the metal active site. The substituents can either be electron-donating groups (EDG) or electron-withdrawing groups (EWG). This is likely to affect the catalytic activity. Another aspect is the steric bulkiness around the metal active centre. This

would greatly influence how branched or linear a polymer product will be. Besides electronic and steric effects, temperature also determines the functionality of a catalyst precursor.

When the electronic effect is considered, another research team, investigated the role of EWG remote substituents in neutral *N,O*-salicylaldimine Ni(II) complex. The complex has four nitro substituents on the *N*-terphenyl motif. When tested for ethylene polymerisation, the catalyst generated high molecular weight linear polyethylene (PE) with few branches. It was also reported that the degree of branching increased with temperature, while molecular weights decreased as a result of increased β -hydride elimination at high temperature. For instance, one of the nickel(II) catalysts generated PE with molecular weights $215 \times 10^3 \text{ g mol}^{-1}$ at $30 \text{ }^\circ\text{C}$ and $48 \times 10^3 \text{ g mol}^{-1}$ at $50 \text{ }^\circ\text{C}$, whilst another nickel(II) catalyst produced PE with $174 \times 10^3 \text{ g mol}^{-1}$ at $30 \text{ }^\circ\text{C}$ and $32 \times 10^3 \text{ g mol}^{-1}$ at $50 \text{ }^\circ\text{C}$ (Osichow *et al.*, 2013). This was a clear demonstration of the effect of temperature on catalytic activity. A bimetallic nickel(II) macrocyclic complexes were also studied. Three macrocyclic complexes obtained polymers with branches (32 – 56/1000 C) mostly methyl. The macrocyclic complex bearing a methyl substituent *para* to the phenolic oxygen exhibited significantly high molecular weights ($M_w = 37,000 - 38,000$) than those with hydrogen and fluorine substituents ($M_w = 6700 - 8700$). When polymerisation temperature was raised from 30 to $40 \text{ }^\circ\text{C}$, the activities reduced to approximately half. Further increase in temperature to $60 \text{ }^\circ\text{C}$, led to negligible activities being observed, which showed that the catalyst is thermally unstable (Na *et al.*, 2006).

Furthermore, another research group synthesized two phenoxyiminato Ni(II) catalysts to study electronic effect on ethylene polymerisation products. They investigated the influence of

introducing electron-withdrawing CF_3 group against electron-donating CH_3 group on the ethylene polymerisation. At room temperature, the CF_3 -substituted complex catalyst was found to be ~ 6.5 times more active than the CH_3 -substituted analogue (which was 250 against 38 kg of polymer $(\text{mol of Ni})^{-1} \text{ h}^{-1} \text{ atm}^{-1}$ respectively). Additionally, the obtained polyethylene M_w for CF_3 -substituted catalyst was remarkably greater at 92,000 against 1400 g mol^{-1} for CH_3 -substituted catalyst. The alkyl branching for CF_3 -substituted catalyst was far lower at 7 as opposed to 88 branches/1000 C for its CH_3 analogue (Weberski *et al.*, 2012). The CF_3 substituent was found to immensely intensify the polymerisation activity, thermal stability and product molecular weights and inhibit polyethylene branching as opposed to the corresponding CH_3 substituted catalyst.

Another team of researchers used methylene, benzyl and terphenyl $[\text{C}_6\text{H}_4(\text{C}_6\text{H}_4)_2]$ bridged salicylaldimine ligands to synthesize both mono- and bimetallic neutral-nickel(II) complexes where binuclear effects were studied in the ethylene homopolymerisation and ethylene/functionalized norbornene copolymerisation. A higher incorporation of polymer branches in binuclear complexes was observed, which was attributed to the cooperative effect between the two metal centres. Molecular weights of the polymers produced by the bimetallic complexes were slightly lower than those for polymers obtained by corresponding monometallic complexes (M_w , 52,000 and 54,000 respectively). Considerable effects of the binuclearity were observed in the ethylene/functionalized norbornene copolymerisation. The bimetallic complexes showed ~ 2 times higher activities than monometallic complexes ($80 \text{ kg } (\text{mol of Ni})^{-1} \text{ h}^{-1}$ and $41 \text{ kg } (\text{mol of Ni})^{-1} \text{ h}^{-1}$, respectively) under the same conditions in ethylene/2(methoxycarbonyl)norbornene copolymerisation (Sujith *et al.*, 2005).

Furthermore, another team of researchers also explored the cooperative enchainment effects in polymerisation using binuclear phenoxyiminato nickel(II) catalysts. The cooperativity in ethylene homopolymerisation and in ethylene copolymerisation with polar functionalized norbornene and acrylates were also studied. Room temperature ethylene homopolymerisation using Ni(COD)₂ as cocatalyst was done. It was observed that bimetallic nickel(II) catalyst afforded polyethylenes with molecular weights comparable to those obtained by the analogous monometallic nickel(II) catalyst, M_w 10100 – 11700. No explanation was given for this phenomenon. Nevertheless, bimetallic catalysts exhibited approximately two-fold greater polymerisation activity (7.1 kg (mol of Ni)⁻¹ h⁻¹ atm⁻¹ and 3.6 kg (mol of Ni)⁻¹ h⁻¹ atm⁻¹, respectively) together with increased methyl branch density (Rodriguez *et al.*, 2009). Ethylene/norbornene copolymerisation were investigated with mono- and bimetallic nickel(II) catalyst, using diverse norbornenes bearing polar substituents. It was reported that remarkable comonomer enchainment levels are obtained with monometallic nickel(II) catalyst, which is in agreement with results of similar reported mononuclear systems (Connor *et al.*, 2003). Ethylene/norbornene copolymerisation in the presence of binuclear nickel(II) proceeded with ~ 4 times greater activity (1.3 kg (mol of Ni)⁻¹ h⁻¹ atm⁻¹ and 0.3 kg (mol of Ni)⁻¹ h⁻¹ atm⁻¹, respectively) and also about 4 times greater selectivity comonomer enchainment than mononuclear catalyst under the same reaction conditions.

In view of polymerisation itself, it was reported in one article that the Ni(II) and Pd(II) α -diimine catalysts, for instance, are able to afford hyperbranched polymer from a feedstock of pure

ethylene, a monomer which, on its own, offers no predisposition toward branch formation (Guan & Popeney, 2008). Polymer branches result from metal migration along the chain due to the facile nature of late metals to perform β -hydride elimination and reinsertion reactions. Further, the ethylene polymers obtained with α -diimine Ni(II) and Pd(II) catalysts exhibit a branching-rich structure, and multiple branching types including short and long, even and odd were observed (Bastero *et al.*, 2007; Stephenson *et al.*, 2014; Wiedemann *et al.*, 2014). In α -diimine systems, especially in the α -diimine Pd(II) complex type, these branches are believed to be formed via “*chain walking*” mechanism rather than by generating from the incorporation of short-chain oligomers (Daugulis & Brookhart, 2002). In closely related work it was reported that the type and amount of branches formed in the polymerisation of ethylene promoted by typical α -diimine nickel pre-catalysts depends on reaction parameters such as the reaction temperature, ethylene pressure and ligand bulkiness or structure (Yuan *et al.*, 2011; Lin *et al.*, 2010; Wang *et al.*, 2014).

“Chain walking or chain running” is a mechanism that operates during some alkene polymerisation reactions. This reaction gives rise to the branched and hyperbranched hydrocarbon polymers. This process is also characterised by accurate control of polymer architecture and topology (Guan *et al.*, 1999). The position of branches on the polymer are controlled by the choice of a catalyst. The potential applications of polymers formed by this reaction are diverse, ranging from drug delivery to phase transfer agents, nanomaterials and catalysis (Guan, 2010).

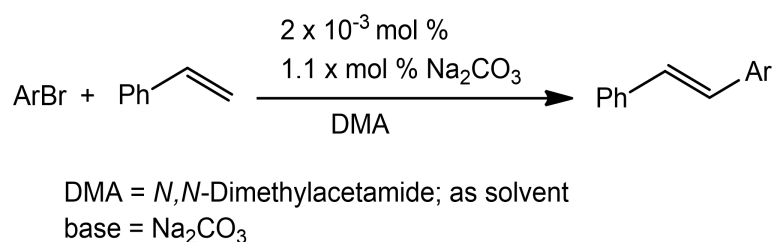
Catalysts that promote chain walking were discovered in the 1980 – 1990s. Nickel(II) and palladium(II) complexes of α -diimine were known to efficiently catalyse polymerisation of alkenes. Currently nickel and palladium complexes bearing α -diimine ligands are the most thoroughly described chain walking catalysts in scientific research literature (Domski *et al.*, 2007). Chain walking occurs after the polymer chain has grown somewhat on the metal catalyst. The precursor is a $16e^-$ complex with the general formula $[\text{Ni}(\text{diimine})(\text{C}_2\text{H}_4)(\text{chain})]^+$. The ethylene ligand (the monomer) dissociates to produce a highly unsaturated $14e^-$ cation which is stabilised by an agostic interaction. A β -hydride elimination then occurs to give a hydride-alkene complex. Subsequent reinsertion of the M-H into the C=C bond, but in the opposite sense gives a metal-alkyl complex. This process moves the metal from the end of a chain to a secondary carbon centre (Guan, 2010).

It is imperative to note that chain walking can be divided into three steps after catalytic initiation; (i) chain propagation (ii) chain transfer, and (iii) chain walking or isomerization. The first two are found to be common in most ethylene polymerisation. Nevertheless, chain walking process is rather rare for most early transition metal catalysts, but is a major route in α -diimine Pd(II) and Ni(II) catalysts for olefin polymerisation and copolymerisation reactions. In fact, chain walking is one of the most distinguishing features of these Pd(II) and Ni(II) catalysts (Guo *et al.*, 2016).

The carbon-carbon cross-coupling reactions has played a cardinal role on organic synthesis and has been applied in synthetic processes in pharmaceuticals and other useful materials like the natural products (Minto & Blacklock, 2008; Schrittwieser *et al.*, 2011). The Heck coupling reaction (Alonso *et al.*, 2008) is one that has drawn much attention from chemistry researchers

since its discovery in the early 1970s. When compared with palladium-activated reactions such as the Suzuki-Miyaura (Xi *et al.*, 2008; Yundong *et al.*, 2009) and the Sonogashira-Hagihara (Sonogashira, 2002), catalytic behaviour of palladium complexes in Heck reactions are greatly affected by the nature of ligands used as a result of the electronic and steric influences of substituents (Knowles & Whiting, 2007; Zhang *et al.*, 2011).

A monometallic palladium complexes ligated by 2,6-dibenzhydryl-*N*-(2-aryliminoacenaphthylenylidene)-4-chlorobenzenamines have been explored for their ethylene polymerisation but unfortunately, they showed relatively very low activity. Ban and fellow researchers broadened their study on the above palladium complex to involve catalytic activity on Heck coupling reactions (Ban *et al.*, 2012). The Heck reaction required an optimum activation temperature of 150 °C and the conversion greatly increased to 92 % as opposed to the trace product at 130 °C. It was also established that at a temperature of 250 °C the catalyst decomposed. The Heck reaction involved a typical coupling reaction between bromobenzene and styrene which afforded 1,2-diphenylethene (Scheme 2.4).



Scheme 2.4: Heck coupling reaction of aryl bromide and styrene

Early-transition metal catalysts suffer from one noteworthy disadvantage, that is, they generally cannot tolerate polar functional groups because of their highly electron-deficient nature as

reported in literature (Camacho & Guan, 2010). This limits their appropriateness to copolymerisation of polar olefins so as to create more significant polyolefin products. One significant feature of polymerisation catalyst-design is to make certain catalyst stability at the required polymerisation conditions. For commercially practical procedures, polymerisation should be kept running at increased temperature and regularly within the sight of a controlled measure of hydrogen gas for molecular weight control. One disadvantage of the Brookhart-type α -diimine catalyst is its expeditious deactivation in the presence of hydrogen gas (Neto *et al.*, 2001).

In addition to ethylene (commonly used as monomers), cyclic olefins (typically norbornene) are also used mainly as monomers or comonomers. Norbornene can be polymerised by two distinct mechanisms (i) ring opening process (ROP) metathesis and (ii) vinyl addition polymerisation (Gao *et al.*, 2009; Janiak & Lassahn, 2001). In a research report, the ROP of norbornene was studied and its copolymerisation with styrene. The investigation involved a Pd- and Ni-based novel bridged binuclear diimine complexes with MAO as cocatalyst. It was established that all the bridged diimine nickel(II) and palladium(II) complexes exhibited higher activities than the corresponding nickel complexes under the same conditions. All the systems catalysed by palladium-based complexes gave 100 % yield and were insoluble in cyclohexane, chloroform, benzene, chlorobenzene, 1,2-dichlorobenzene, 1,2,4-trichlorobenzene, and tetrachloroethane. However, polynorbornene formed with nickel-based complexes dissolved in all the above-mentioned solvents. In the copolymerisation of norbornene and styrene, the nickel-based bridged binuclear diimine complexes in MAO showed activity while palladium-based ones did not (Mi *et al.*, 2003).

Another research report explored addition polymerisation of functionalized norbornenes (Funk *et al.*, 2004). The research specifically focused on the effects of stereochemistry, size and ability of coordination of substituents. A palladium catalyst, (1,5-Cyclopentadiene)Pd(CH₃)Cl {(COD)Pd(CH₃)Cl} was synthesized as per the established procedures. In order to explore the effects of size, stereochemistry and coordinating ability of the substituted norbornenes, the research team used 5-Butyl-2-norbornene (Butyl-NB), 5-Ethylester-2-norbornene (EtEster-NB), 5-Methyl acetate-2-norbornene (MeOAc-NB), 5-Hexyl-2-norbornene (Hexyl-NB), and 5-Decyl-2-norbornene (Decyl-NB). In the research, MeOAc-NB, Butyl-NB, and EtEster-NB were subjected to homopolymerisation process. The polymers obtained had the following molecular weights (M_w); Butyl-NB: $M_w = 13,000$, EtEster-NB: $M_w = 4300$ while MeOAc-NB: $M_w = 4300$. Furthermore, homopolymerisation of Butyl-NB, Hexyl-NB and Decyl-NB was done in which case, after 1 h of reaction and quenching of catalyst, the results obtained were very interesting as shown; Hexyl-NB: $M_w = 200,000$ and Butyl-NB: $M_w = 260,000$. This team also tested the functionalized substituted norbornene for copolymerisation and obtained M_w for Butyl-NB/MeOAc-NB: $M_w = 3400$, while Butyl-NB/EtEster-NB gave $M_w = 5200$. It was generally observed that the rate of polymerisation of the substituted norbornenes increased in the order Decyl-NB < Hexyl-NB < Butyl-NB (Funk *et al.*, 2004). Therefore, it means that the bulkier the substituted norbornene monomer, the lower the M_w of the polymer obtained.

2.8 Future prospects

It is an undisputable fact that in the last few years, much work has been dedicated in the exploration of the late-transition metals complexes for catalytic activities in both oligomerisation and polymerisation reactions. The complex catalysts of monometallic nature have immeasurably

been investigated in comparison with the homobimetallic type. That notwithstanding, the homobimetallic compounds have been researched considerably. It has emerged clearly from the discussed literature work that complexes that have two metal centres as active sites exhibit superior catalytic activities in comparison with their monometallic analogues. This has been strongly attributed to the cooperative (tandem) effect quality brought about by the presence of two metals as active centres.

Furthermore, the *N,O*-salicylaldimine-ligand complexes have found immense applications in catalysis. The salicylaldimine ligands are easy to synthesize and characterise and they easily coordinate with late-transition metals especially nickel and palladium. Nonetheless, nickel complexes have some challenges, for instance, its paramagnetic nature which hinders its complexes from being characterised using NMR. But this drawback is easily overcome by designing and synthesizing square planar complexes which are diamagnetic in nature.

Despite the fact that worthwhile research has been carried out on monometallic complex catalysts, not much work has been reported on catalysts with two metals as active centres. This is whether they are homobimetallic or heterobimetallic complexes. It can therefore, be confidently stated that this research work is still lacking and is clearly worth pursuing. Moreover, there is no reported work on homobimetallic nickel and palladium *N,O*-salicylaldimine complexes and investigated for hexene catalytic activities.

Consequently, this current research work synthesized, characterised and investigated these salicylaldimine palladium(II) and nickel(II) complexes for olefin oligomerisation and polymerisation catalytic activities and reactions.

CHAPTER THREE

METHODOLOGY

3.1 Materials and methods

In this work, all reactions were carried out under nitrogen atmosphere using a dual vacuum/nitrogen line and standard Schlenk technique unless otherwise stated or explained. The method of heating to reflux under nitrogen atmosphere in the presence of suitable drying agents was used to purify the solvents before use. Methanol and ethanol were refluxed, distilled and dried over a mixture of Mg and I₂. Dichloromethane (DCM) was distilled and dried over calcium hydride, while hexane, diethyl ether, and toluene were distilled and dried over sodium wire/benzophenone under nitrogen. The palladium and nickel metal complex precursors, PdCl₂(COD) and NiCl₂(DME), respectively, were prepared following modified procedures with closer comparison to established protocols in the literature (Motswainyana *et al.*, 2011).

The compounds; 1,3-diaminopropane, 1,4-diaminobutane, 1,5-diaminopentane (Cadaverine), 2-hydroxy-3-methylbenzaldehyde, 2-hydroxy-5-methoxybenzaldehyde, 2-hydroxy-5-methylbenzaldehyde, 3-bromo-5-chlorosalicylaldehyde, 5-bromosalicylaldehyde, 5-chlorosalicylaldehyde, nickel(II) chloride hydrate, palladium(II) chloride, 1,5-cyclooctadiene (COD), triethylamine (Et₃N), 1,2-dimethoxyethane (DME), modified methylaluminoxane (MMAO), triethyl orthoformate (1,1,1-triethoxymethane), pentane, and 1-hexene were purchased from Sigma-Aldrich and used without any further purification, since they were of analytical grade.

3.2 Instrumentation

The ^1H and ^{13}C NMR spectra were recorded on Bruker Avance IIIHD Nanobay 400 MHz Spectrometer at room temperature (298 K) equipped with a 5 mm BBO probe, at the University of the Western Cape (400 MHz for ^1H and 100 MHz for ^{13}C). Standard 1D and 2D pulse programs were used to acquire the spectra. The ^1H NMR experiments were referenced internally using the residual CDCl_3 and reported relative to the internal standard tetramethyl silane (TMS). The ^1H and ^{13}C Chemical shift (δ) values were reported in ppm. The deuterated solvents used were CDCl_3-d_1 and $\text{DMSO}-d_6$ respectively and coupling constants (J) were given in Hertz (Hz).

Elemental analysis (EA) was performed on the Server 1112 Series Elemental analyser by the micro-analytical laboratory, Central Analytical Facilities (CAF) at the Stellenbosch University, Republic of South Africa.

The X-ray diffraction (XRD) analysis for some crystalline compounds were done and solved using Bruker HiStar System model at the Rutgers State University Newark, New Jersey, USA. The bond angle values were recorded in degrees ($^\circ$) while the bond lengths were reported in angstrom (\AA) unit.

GC-MS was carried out using Agilent 7820A GC with 5977E MSD fitted with flame ionization detector and HP5-MS column, 100 % dimethylpolysiloxane with dimensions of 30 m by 0.25 mm. The GC was carried out in Agilent 7890A with 7683B auto injector fitted with DB-225 column, both at the University of the Western Cape, Republic of South Africa.

The FT-IR spectra were recorded with Perkin-Elmer 100 Series FT-IR spectrometer using KBr pellets for solids and ATR-FTIR (Attenuated Total Reflectance-Fourier Transform Infrared) for

both solids and solutions/oils, Chemistry Department, University of the Western Cape, Republic of South Africa.

Melting points of the synthesized compounds were determined using open capillaries using SMP10 melting point apparatus and were reported as uncorrected, at the University of the Western Cape, Republic of South Africa.

3.3 Synthesis of salicyaldimine ligands

3.3.1 Preparation of 6,6'-(propane-1,3-diylbis(azanilylidene))bis(methanylylidene))bis(2-methylphenol) (SL1)

The structural formula for the ligand **SL1** is shown in Figure 3.1.

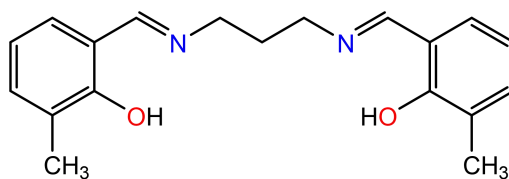


Figure 3.1: Structure of SL1

In a Schlenk tube filled with dry ethanol (10 ml) under nitrogen atmosphere, 2-hydroxy-3-methylbenzaldehyde (0.2723 g, 2 mmol) was added whilst stirring which continued rapidly for 2 min. Then a solution of 1,3-diaminopropane (0.0741 g, 1 mmol) was added dropwise while stirring giving a light-orange solution. The mixture was refluxed while stirring for 1 h and the resulting product cooled. The solvent was removed in vacuo in an inert environment to obtain a yellow solid. The solid product was re-dissolved in ethanol (5 ml), just enough to dissolve all the solid. The solution was cooled in hexane-liquid N₂ mixture for 1 h. Then the solution part (mother liquor) was filtered off and the solid dried in vacuo for a further 2 h to obtain a yellow

solid, air and moisture stable. [Yield = 0.5559 g (66 %)]. Melting point: 60 – 62 °C. IR (KBr cm^{-1}): $\nu(\text{C}=\text{N})$ 1623 cm^{-1} . ^1H NMR (400 MHz, CDCl_3): δ H (*phenolic*) 13.63 (s, 1H); H (*imine*) 8.36 (s, 1H); H (*aromatic*) 7.25 (s, 1H); 7.19 (d, $J = 7.60$ Hz, 2H); 7.09 (d, $J = 7.60$ Hz, 2H); 6.79 (s, 1H); H (*aliphatic*) 3.71 (t, $J = 6.40$ Hz, 3H); 2.11 (m, $J = 7.80$ Hz, 6H). ^{13}C NMR (100 MHz, CDCl_3): δ CH (*imine*) 159.41; CH (*aromatic*) 165.22; 138.18; 128.96; 125.74; 117.95; CH_2 (*aliphatic*) 56.44; 31.35; CH_3 (*aliphatic*) 15.40. Elemental analysis for $\text{C}_{19}\text{H}_{22}\text{N}_2\text{O}_2$ (310.39 g/mol), Calculated: C, 73.52 %; H, 7.10; N, 9.03. Found: C, 73.35 %; H, 7.20; N, 9.03. ESI-MS, m/z : 310{[M] + H}.

3.3.2 Preparation of 2,2'-(propane-1,3-diylbis(azanilylidene))bis(methanylylidene))bis(4-methylphenol) (SL2)

The structural formula for the ligand **SL2** is shown in Figure 3.2.

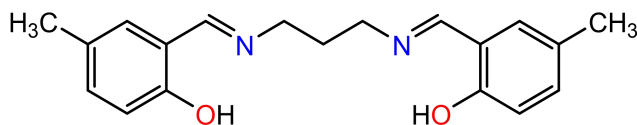


Figure 3.2: Structure of SL2

Dry methanol (10 ml) was transferred to a Schlenk tube saturated with N_2 to which 2-hydroxy-5-methylbenzaldehyde (0.2723 g, 2 mmol) was added then stirred for 2 min for complete dissolution. Then 1,3-diaminopropane (0.0741 g, 1 mmol) was added dropwise whilst stirring. The reaction was allowed to proceed with rapid stirring at reflux for 1 h. The resulting product solution was allowed to cool and the reaction solvent removed under inert reduced pressure (vacuum). The solid obtained was re-dissolved in minimum amount of methanol (5 ml), just

enough to dissolve the solid. The Schlenk tube and its content was then cooled in hexane-liquid N₂ mixture and the content allowed to precipitate for 1 h, after which the solution part (mother liquor) was filtered off. The solid was then dried in vacuo for 2 h. A yellow solid was obtained which was air and moisture stable. [Yield = 0.2757 g (89 %)]. Melting point: 62 – 63 °C. IR (KBr cm⁻¹); $\nu(\text{C}=\text{N})$ 1637 cm⁻¹. ¹H NMR (400 MHz, CDCl₃): δ H (*phenolic*) 13.12 (s, 1H); H (*imine*) 8.32 (s, 1H); H (*aromatic*) 7.26 (s, 1H); 7.13 (dd, $J = 2.00, 1.60$ Hz, 2H); 7.04 (d, $J = 1.60$ Hz, 2H); 6.88 (d, $J = 8.40$ Hz, 2H); H (*aliphatic*) 3.71 (t, $J = 6.40$ Hz, 3H); 2.29 (s, 3H); 2.13 (m, $J = 6.80$ Hz, 5H). ¹³C NMR (100 MHz, CDCl₃): δ CH (*imine*) 158.87; CH (*aromatic*) 165.52; 132.03; 131.30; 127.68; 118.31; 116.70; CH₂ (*aliphatic*) 56.05; 31.58; CH₃ (*aliphatic*) 20.20. Elemental analysis for C₁₉H₂₂N₂O₂ (310.39 g/mol), Calculated: C, 73.52 %; H, 7.14; N, 9.03. Found: C, 73.08 %; H, 7.66; N, 9.29. ESI-MS, m/z : 310 {[M] + H}.

3.3.3 Preparation of 2,2'-(propane-1,3-diylbis(azanylylidene))bis(methanylylidene))bis(4-methoxyphenol) (SL3)

The structural formula for the ligand **SL3** is shown in Figure 3.3.

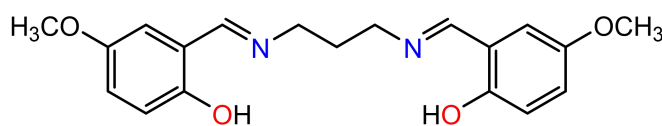


Figure 3.3: Structure of SL3

This compound was prepared following a procedure similar to that used in synthesizing **SL1**. The 2-hydroxy-5-methoxybenzaldehyde (0.3043 g, 2 mmol) and 1,3-diaminopropane (0.0741 g, 1 mmol) were used as starting materials. A yellow solid was obtained, both air and moisture

stable. [Yield = 0.3400 g (97 %)]. Melting point: 109 – 110 °C. IR (KBr cm^{-1}); $\nu(\text{C}=\text{N})$ 1635 cm^{-1} . ^1H NMR (400 MHz, CDCl_3): δ H (*phenolic*) 12.86 (s, 1H); H (*imine*) 8.33 (s, 1H); H (*aromatic*) 7.26 (s, 1H); 6.92 (dd, $J = 2.80, 2.00$ Hz, 2H); 6.76 (d, $J = 2.40$ Hz, 2H); H (*aliphatic*) 3.77 (s, 3H); 3.73 (t, $J = 6.80$ Hz, 3H); 2.15 (m, $J = 4.80$ Hz, 5H). ^{13}C NMR (100 MHz, CDCl_3): δ CH (*imine*) 165.17; CH (*aromatic*) 155.38; 152.23; 119.29; 118.37; 117.68; 114.81; CH_2 (*aliphatic*) 56.94; CH_3 (*methoxy*) 55.93; CH_2 (*aliphatic*) 31.66. Elemental analysis for $\text{C}_{19}\text{H}_{22}\text{N}_2\text{O}_4$ (342.39 g/mol), Calculated: C, 66.65 %; H, 6.48; N, 8.18. Found: C, 67.45 %; H, 6.74; N, 8.31. ESI-MS, m/z : 342 {[M] + H}.

3.3.4 Preparation of 6,6'-(propane-1,3-diylbis(azanylylidene))bis(methanylylidene))bis(2-bromo-4-chlorophenol) (SL4)

The structural formula for the ligand **SL4** is shown in Figure 3.4.

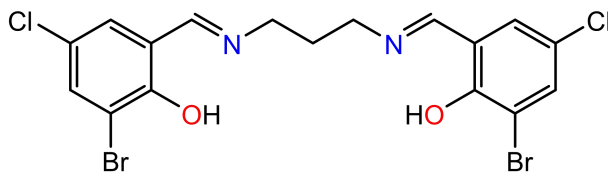


Figure 3.4: Structure of SL4

This compound was prepared following a procedure similar to that used in preparing **SL2**. The 3-bromo-5-chlorosalicylaldehyde (0.4709 g, 2 mmol) and 1,3-diaminopropane (0.0741 g, 1 mmol) in dry EtOH (10 ml) were used as starting materials. A yellow solid, both air and moisture stable was obtained. [Yield = 0.3325 g (67 %)], Melting point: 150 – 152 °C IR (KBr cm^{-1}); $\nu(\text{C}=\text{N})$ 1630 cm^{-1} . ^1H NMR (400 MHz, CDCl_3): δ H (*phenolic*) 14.41 (s, 1H); H (*imine*) 8.28 (s, 1H); H

(*aromatic*) 7.58 (d, $J = 2.40$ Hz, 1H); 7.26 (s, 1H); 7.20 (d, $J = 2.40$ Hz, 2H); H (*aliphatic*) 3.78 (t, $J = 6.40$ Hz, 3H); 2.14 (m, $J = 6.80$ Hz, 5H). ^{13}C NMR (100 MHz, CDCl_3): δ CH (*imine*) 157.61; CH (*aromatic*) 164.09; 135.22; 129.75; 123.18; 119.19; 112.04; CH_2 (*aliphatic*) 55.85; 31.20. Elemental analysis for $\text{C}_{17}\text{H}_{14}\text{Br}_2\text{Cl}_2\text{N}_2\text{O}_2$ (509.02 g/mol), Calculated: C, 40.11 %; H, 2.80; N, 5.50. Found: C, 40.11 %; H, 3.06; N, 5.65. ESI-MS, m/z : 509 $\{[\text{M}] + \text{H}\}$.

3.3.5 Preparation of 2,2'-(propane-1,3-diylbis(azanylylidene))bis(methanylylidene))bis(4-bromophenol) (**SL5**)

The structural formula for the ligand **SL5** is shown in Figure 3.5.

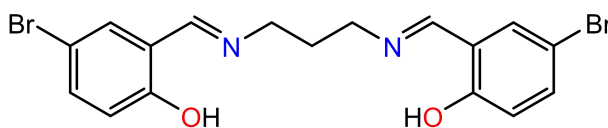


Figure 3.5: Structure of **SL5**

The ligand **SL5** was prepared following a procedure similar to the one used to prepare **SL2**. The starting materials were 5-bromosalicylaldehyde (0.4020 g, 2 mmol) and 1,3-diaminopropane (0.0741 g, 1 mmol) in dry EtOH (10 ml). The product obtained was a yellow solid, both air and moisture stable. [Yield = 0.4320 g (97 %)]. Melting point: 137 – 139 °C IR (KBr cm^{-1}); $\nu(\text{C}=\text{N})$ 1633 cm^{-1} . ^1H NMR (400 MHz, CDCl_3): δ H (*phenolic*) 13.38 (s, 1H); H (*imine*) 8.29 (s, 1H); H (*aromatic*) 7.39 (d, $J = 8.80$ Hz, 2H); 6.87 (d, $J = 8.80$ Hz, 2H); H (*aliphatic*) 3.72 (t, $J = 6.40$ Hz, 3H); 2.12 (m, $J = 6.40$ Hz, 5H). ^{13}C NMR (100 MHz, CDCl_3): δ CH (*imine*) 160.24; CH (*aromatic*) 164.28; 134.99; 133.38; 120.03; 119.02; 110.10; CH (*aliphatic*) 56.83; 31.49.

Elemental analysis for $C_{17}H_{16}Br_2N_2O_2$ (440.13 g/mol), Calculated: C, 46.39 %; H, 3.66; N, 6.36. Found: C, 46.47 %; H, 3.98; N, 6.59. ESI-MS, m/z : 440 {[M] + H}.

3.3.6 Preparation of 2,2'-(propane-1,3-diylbis(azanylylidene))bis(methanylylidene))bis(4-chlorophenol) (SL6)

The structural formula for the ligand **SL6** is shown in Figure 3.6.

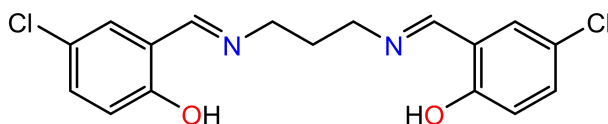


Figure 3.6: Structure of SL6

This ligand was prepared using a procedure similar to the one used to synthesize **SL2**. The reaction materials used were 5-chlorosalicylaldehyde (0.3131 g, 2 mmol) and 1,3-diaminopropane (0.0741 g, 1 mmol) in dry MeOH (10 ml) and stirred under reflux for 3 h. The yellow shiny solid product obtained was both air and moisture stable. [Yield = 0.2065 g (59 %)]. Melting point: 93 – 94 °C. IR (ATR cm^{-1}); $\nu(C=N)$ 1629 cm^{-1} . 1H NMR (400 MHz, $CDCl_3$): δ H (*phenolic*) 13.35 (s, 1H); H (*imine*) 8.31 (s, 1H); H (*aromatic*) 7.27 (dd, $J = 2.80, 2.40$ Hz, 2H); 7.22 (s, 1H); 6.92 (d, $J = 8.40$ Hz, 2H); H (*aliphatic*) 3.72 (t, $J = 6.80$ Hz, 3H); 2.13 (m, $J = 6.80$ Hz, 5H). ^{13}C NMR (100 MHz, $CDCl_3$): δ (*imine*) 159.68; CH (*aromatic*) 164.38; 132.19; 130.40; 123.26; 119.46; 118.57; CH_2 (*aliphatic*) 56.86; 31.51. Elemental analysis for $C_{17}H_{16}Cl_2N_2O_2$ (350.23 g/mol), Calculated: C, 58.13 %; H, 4.59; N, 7.98; Found: C, 58.00 %; H, 4.78; N, 8.27. ESI-MS, m/z : 350 {[M] + H}.

3.3.7 Preparation of 6,6'-(butane-1,4-diylbis(azanylylidene))bis(methanylylidene))bis(2-methylphenol) (SL7)

The structural formula for the ligand **SL7** is shown in Figure 3.7.

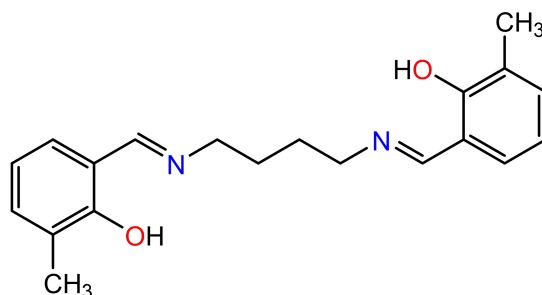


Figure 3.7: Structure of SL7

This compound was synthesized using a procedure similar to the one used to prepare **SL1**. The reaction materials used were 2-hydroxy-3-methylbenzaldehyde (0.1362 g, 1 mmol) and 1,4-diaminobutane (0.0441 g, 0.5 mmol) in dry EtOH (10 ml). A yellow solid was obtained which was both moisture and air stable. [Yield = 0.0820 g (51 %)]. Melting point: 113 – 114 °C. IR (KBr cm^{-1}); $\nu(\text{C}=\text{N})$ 1624 cm^{-1} . ^1H NMR (400 MHz, CDCl_3): δ H (*phenolic*) 13.83 (s, 1H); H (*imine*) 8.34 (s, 1H); H (*aromatic*) 7.18 (d, $J = 4.04$ Hz, 2H); 7.10 (d, $J = 8.00$ Hz, 2H); 6.80 (t, $J = 8.00$ Hz, 2H); H (*aliphatic*) 3.64 (s, 1H); 2.27 (s, 3H); 1.81 (s, 2H); 1.56 (m, $J = 1.00$ Hz, 5H). ^{13}C NMR (100 MHz, CDCl_3): δ COH (*aromatic*) 165.10; CH (*imine*) 159.54; CH (*aromatic*) 133.14; 128.85; 125.96; 118.02; 117.95; CH (*aliphatic*) 59.14; 28.56; 15.49. Elemental analysis for $\text{C}_{20}\text{H}_{24}\text{N}_2\text{O}_2$ (324.42 g/mol), Calculated: C, 74.04 %; H, 7.50; N, 8.64; Found: C, 73.79 %; H, 7.53; N, 8.43. ESI-MS, m/z : 324 $\{[\text{M}] + \text{H}\}$.

3.3.8 Preparation of 2,2'-(butane-1,4-diylbis(azanylylidene))bis(methanylylidene))bis(4-methylphenol) (SL8)

The structural formula for the ligand **SL8** is shown in Figure 3.8.

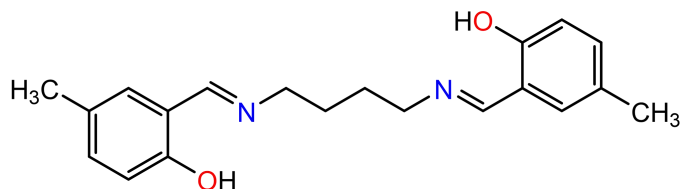


Figure 3.8: Structure of SL8

The compound **SL8** was synthesized following a similar procedure to the one used to prepare **SL2**. Condensation reaction involved 2-hydroxy-5-methylbenzaldehyde (0.1362 g, 1 mmol) and 1,4-diaminobutane (0.0441 g, 0.5 mmol) in dry MeOH (10 ml). The yellow solid obtained was both moisture and air stable. [Yield = 0.1607 g (98 %)]. Melting point: 130 – 132 °C. IR (KBr cm^{-1}); $\nu(\text{C}=\text{N})$ 1629 cm^{-1} . ^1H NMR (400 MHz, CDCl_3): δ H (*phenolic*) 13.25 (s, 1H); H (*imine*) 8.28 (s, 1H); H (*aromatic*) 7.11 (d, $J = 4.40$ Hz, 2H); 7.02 (s, 1H); 6.86 (d, $J = 9.40$ Hz, 2H); H (*aliphatic*) 3.62 (t, $J = 11.20$ Hz, 3H); 2.28 (s, 3H); 1.79 (m, $J = 2.80$ Hz, 5H). ^{13}C NMR (100 MHz, CDCl_3): δ COH (*aromatic*) 164.94; CH (*imine*) 158.98; CH (*aromatic*) 132.95; 131.27; 127.56; 118.52; 116.77; CH (*aliphatic*) 59.36; 28.59; 20.31. Elemental analysis for $\text{C}_{20}\text{H}_{24}\text{N}_2\text{O}_2$ (324.42 g/mol), Calculated: C, 74.05 %; H, 7.50; N, 8.63. Found: C, 73.71 % H, 6.70; N, 8.28. ESI-MS, m/z : 324 $\{[\text{M}] + \text{H}\}$.

3.3.9 Preparation of 2,2'-(butane-1,4-diylbis(azanylylidene))bis(methanylylidene))bis(4-methoxyphenol) (SL9)

The structural formula for the ligand **SL9** is shown in Figure 3.9.

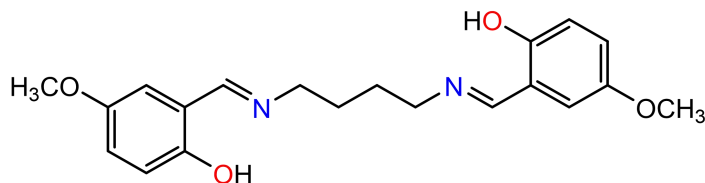


Figure 3.9: Structure of SL9

The synthesis of **SL9** was done following a similar procedure to the one for **SL1**. The starting reagents used were 2-hydroxy-5-methoxybenzaldehyde (0.1522 g, 1 mmol) and 1,4-diaminobutane (0.0441 g, 0.5 mmol) in dry EtOH (10 ml). The yellow solid obtained was moisture and air stable. [Yield = 0.1838 g (96 %)]. Melting point: 120 – 122 °C. IR (KBr cm^{-1}); $\nu(\text{C}=\text{N})$ 1633 cm^{-1} . ^1H NMR (400 MHz, CDCl_3): δ H (*phenolic*) 12.97 (s, 1H); H (*imine*) 8.30 (s, 1H); H (*aromatic*) 6.90 (d, $J = 12.00$ Hz, 2H); 6.87 (d, $J = 12.00$ Hz, 2H); 6.75 (s, 1H); H (*aliphatic*) 3.77 (s, 3H); 3.64 (t, $J = 3.70$ Hz, 3H); 1.80 (m, $J = 1.20$ Hz, 5H). ^{13}C NMR (100 MHz, CDCl_3): δ CH (*imine*) 164.63; CH (*aromatic*) 155.25; 151.98; 119.16; 118.41; 117.67; 114.80; CH (*aliphatic*) 59.42; 55.94; 28.53. Elemental analysis for $\text{C}_{20}\text{H}_{24}\text{N}_2\text{O}_4$ (356.42 g/mol), Calculated: C, 49.77 %; H, 5.64; N, 5.81; Found: C, 50.00 %; H, 5.72; N, 5.64. ESI-MS, m/z : 356 $\{[\text{M}] + \text{H}\}$.

3.3.10 Preparation of 2,2'-(butane-1,4-diylbis(azanylylidene))bis(methanylylidene))bis(4-bromophenol) (SL10)

The structural formula for the ligand **SL10** is shown in Figure 3.10.

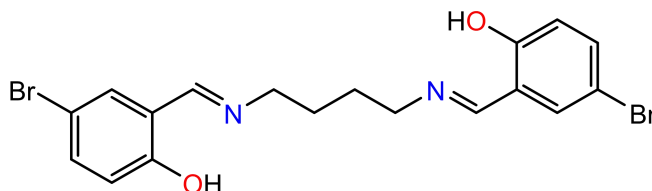


Figure 3.10: Structure of SL10

The compound **SL10** was synthesized following a similar procedure to the one used to prepare **SL1**. The reagents used for the reaction were 5-bromosalicylaldehyde (0.4020 g, 2 mmol) and 1,4-diaminobutane (0.0882 g, 1 mmol) in dry EtOH (10 ml). The yellow solid obtained was both air and moisture stable. [Yield = 0.4207 g (93 %)]. Melting point: 153 – 154 °C. IR (KBr cm^{-1}): $\nu(\text{C}=\text{N})$ 1631 cm^{-1} . ^1H NMR (400 MHz, CDCl_3): δ H (*phenolic*) 13.49 (s, 1H); H (*imine*) 8.27 (s, 1H); H (*aromatic*) 7.39 (d, $J = 2.40$ Hz, 1H); 7.35 (dd, $J = 2.40, 2.00$ Hz, 2H); 6.86 (s, 1H); 6.84 (s, 1H); H (*aliphatic*) 3.65 (t, $J = 1.20$ Hz, 3H); 1.80 (m, $J = 2.80$ Hz, 5H). ^{13}C NMR (100 MHz, CDCl_3): δ COH (*aromatic*) 163.77; CH (*imine*) 160.28; CH (*aromatic*) 134.87; 133.32; 120.06; 119.05; 109.98; CH (*aliphatic*) 59.20; 28.40. Elemental analysis for $\text{C}_{18}\text{H}_{18}\text{Br}_2\text{N}_2\text{O}_2$ (454.16 g/mol), Calculated: C, 47.60 %; H, 4.00; N, 6.17. Found: C, 47.66; H, 3.45; N, 5.93. ESI-MS, m/z : 454 $\{[\text{M}] + \text{H}\}$.

3.3.11 Preparation of 2,2'-(butane-1,4-diylbis(azanilylidene))bis(methanylylidene))bis(4-chlorophenol) (SL11)

The structural formula for the ligand **SL11** is shown in Figure 3.11.

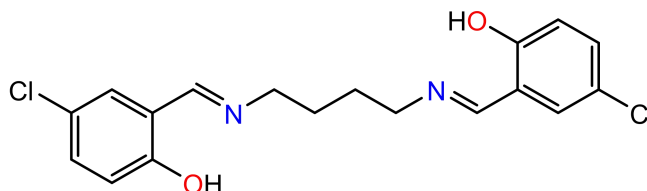


Figure 3.11: Structure of SL11

The compound **SL11** was synthesized following a similar procedure to the one used to prepare **SL1**. The reagents used as starting materials were 5-chlorosalicylaldehyde (0.3131 g, 2 mmol) and 1,4-diaminobutane (0.0882 g, 1 mmol) in dry EtOH (10 ml) at reflux for 3 h. A bright yellow solid was obtained, which was both moisture and air stable. [Yield = 0.3591 g (98 %)]. Melting point: 145 – 147 °C. IR (KBr cm^{-1}); $\nu(\text{C}=\text{N})$ 1631 cm^{-1} . ^1H NMR (400 MHz, CDCl_3): δ (*phenolic*) 13.45 (1s, 1H); H (*imine*) 8.28 (s, 1H); H (*aromatic*) 7.25 (d, $J = 2.80$ Hz, 1H); 7.23(dd, $J = 2.80$ Hz, 2H); 6.91 (s, 1H); 6.89 (s, 1H); H (*aliphatic*) 3.65 (t, $J = 1.80$ Hz, 5H); 1.80 (m, $J = 2.80$ Hz, 5H). ^{13}C NMR (100 MHz, CDCl_3): δ COH (*aromatic*) 163.85; CH (*imine*) 159.78; CH (*aromatic*) 132.05; 130.32; 123.12; 119.44; 118.58; CH (*aliphatic*) 59.23; 28.41. Elemental analysis for $\text{C}_{18}\text{H}_{18}\text{Cl}_2\text{N}_2\text{O}_2$ (365.25 g/mol), Calculated: C, 57.75 %; H, 4.97; N, 6.13. Found: C, 57.83 %; H, 4.92; N, 6.20. ESI-MS, m/z : 364 $\{[\text{M}] + \text{H}\}$.

3.3.12 Preparation of 6,6'-(pentane-1,5-diylbis(azanylylidene))bis(methanylylidene))bis(2-methylphenol) (SL12)

The structural formula for the ligand **SL12** is shown in Figure 3.12.

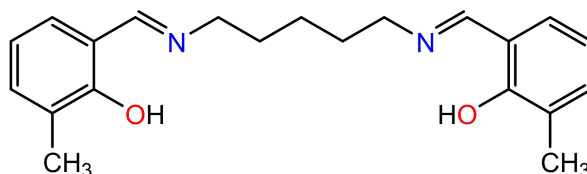


Figure 3.12: Structure of SL12

This compound was prepared using a procedure similar to the one used to prepare **SL1**. The reaction materials used were 2-hydroxy-3-methylbenzaldehyde (0.1702 g, 1.25 mmol) and 1,5-diaminopentane (0.639 g, 0.625 mmol) in dry EtOH (10 ml) at reflux for 1 h 45 min. A bright yellow solid obtained was both air and moisture stable. [Yield = 0.1942 g (92 %)]. Melting point: 76 – 77 °C. IR (KBr cm^{-1}); $\nu(\text{C}=\text{N})$ 1627 cm^{-1} . ^1H NMR (400 MHz, CDCl_3): δ H (*phenolic*) 13.87 (s, 1H); H (*imine*) 8.32 (s, 1H); H (*aromatic*) 7.18 (d, $J = 7.60$ Hz, 2H); 7.10 (d, $J = 7.60$ Hz, 2H); 6.77 (t, $J = 7.60$ Hz, 2H); H (*aliphatic*) 3.60 (t, $J = 6.40$ Hz, 3H); 2.27 (s, 3H); 1.75 (m, $J = 7.60$ Hz, 5H); 1.50 (m, $J = 8.00$ Hz, 5H). ^{13}C NMR (100 MHz, CDCl_3): δ COH (*aromatic*) 164.88; CH (*imine*) 159.63; CH (*aromatic*) 133.07; 128.81; 125.95; 117.95; CH (*aliphatic*) 59.22; 30.62; 24.76; 15.50. Elemental analysis for $\text{C}_{21}\text{H}_{26}\text{N}_2\text{O}_2$ (338.44 g/mol), Calculated: C, 74.53 %; H, 7.70; N, 8.28. Found: C, 74.56; H, 8.02; N, 8.73. ESI-MS, m/z : 338 $\{[\text{M}] + \text{H}\}$.

3.3.13 Preparation of 2,2'-(pentane-1,5-diylbis(azanylylidene))bis(methanylylidene))bis(4-methylphenol) (SL13)

The structural formula for the ligand **SL13** is shown in Figure 3.13.

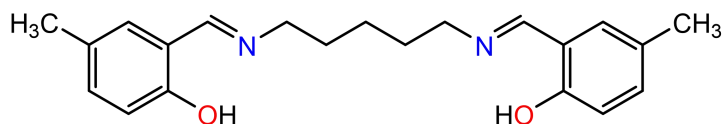


Figure 3.13: Structure of SL13

The ligand **SL13** was prepared using a procedure similar to the one used to prepare **SL2**. The starting reagents were 2-hydroxy-5-methylbenzaldehyde (0.1956 g, 1.4366 mmol) and 1,5-diaminopentane (0.0734 g, 0.7183 mmol) in dry MeOH (10 ml) at reflux for 2 h. The yellow solid obtained was both moisture and air stable. [Yield = 0.0990 g (41 %)]. Melting point: 98 – 99 °C. IR (KBr cm^{-1}); $\nu(\text{C}=\text{N})$ 1628 cm^{-1} . ^1H NMR (400 MHz, CDCl_3): δ H (*phenolic*) 14.75 (s, 1H); H (*imine*) 8.20 (s, 1H); H (*aromatic*) 7.57 (d, $J = 2.40$ Hz, 2H); 7.26 (s, 1H); 7.18 (d, $J = 2.40$ Hz, 2H); H (*aliphatic*) 3.65 (t, $J = 6.80$ Hz, 3H); 1.77 (m, $J = 8.00$ Hz, 5H); 1.50 (m, $J = 8.40$ Hz, 5H); 1.24 (t, $J = 7.20$ Hz, 3H). ^{13}C NMR (100 MHz, CDCl_3): δ COH (*aromatic*) 163.33; CH (*imine*) 158.86; CH (*aromatic*) 135.27; 129.64; 122.46; 118.73; 112.54; CH (*aliphatic*); 57.78; 30.13; 24.51. Elemental analysis for $\text{C}_{21}\text{H}_{26}\text{N}_2\text{O}_2$ (338.44 g/mol), Calculated: C, 74.53 %; H, 7.74.; N, 8.28. Found: C, 74.57 %; H, 7.76; N, 8.31. ESI-MS, m/z : 338 $\{[\text{M}] + \text{H}\}$.

3.3.14 Preparation of 2,2'-(pentane-1,5-diylbis(azanylylidene))bis(methanylylidene))bis(4-methoxyphenol) (SL14)

The structural formula for the ligand **SL14** is shown in Figure 3.14.

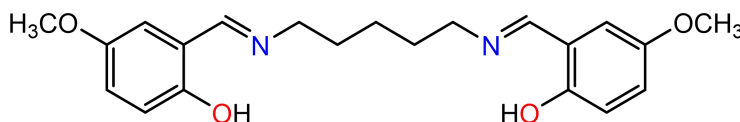


Figure 3.14: Structure of SL14

The ligand **SL14** was prepared using a procedure similar to the one used to synthesize **SL1**. The reagents for this reaction were 2-hydroxy-5-methoxybenzaldehyde (0.1902 g, 1.25 mmol) and 1,5-diaminopentane (0.0639 g, 0.625 mmol) in dry EtOH (10 ml) at reflux for 2 h. The bright yellow solid obtained was air and moisture stable. [Yield = 0.2543 g (96 %)]. Melting point: 89 – 91 °C. IR (KBr cm^{-1}): $\nu(\text{C}=\text{N})$ 1630 cm^{-1} . ^1H NMR (400 MHz, CDCl_3): δ H (*phenolic*) 13.05 (s, 1H); H (*imine*) 8.29 (s, 1H); H (*aromatic*) 7.26 (s, 1H); 6.91 (d, $J = 4.40$ Hz, 2H); 6.76 (d, $J = 2.40$ Hz, 2H); H (*aliphatic*) 3.77 (s, 3H); 3.60 (t, $J = 6.80$ Hz, 3H); 1.75 (m, $J = 7.20$ Hz, 5H); 1.48 (m, $J = 8.00$ Hz, 5H). ^{13}C NMR (100 MHz, CDCl_3): δ CH (*imine*) 164.39; CH (*aromatic*) 155.29; 151.93; 119.04; 118.44; 117.65; 114.76; CH (*aliphatic*) 59.54; CH (*methoxy*) 55.94; CH (*aliphatic*) 30.56; 24.78. Elemental analysis for $\text{C}_{21}\text{H}_{26}\text{N}_2\text{O}_4$ (370.44 g/mol), Calculated: C, 68.09 %; H, 7.10; N, 7.56 Found: C, 68.51 %; H, 7.21; N, 8.17. ESI-MS, m/z : 370 {[M] + H}.

3.3.15 Preparation of 6,6'-(pentane-1,5-diylbis(azanylylidene))bis(methanylylidene))bis(2-bromo-4-chlorophenol) (SL15)

The structural formula for the ligand **SL15** is shown in Figure 3.15.

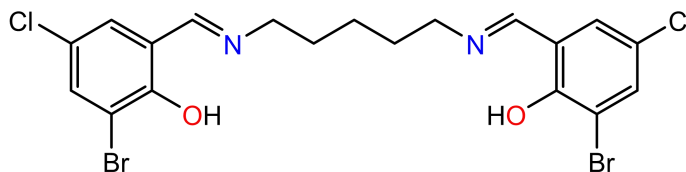


Figure 3.15: Structure of SL15

The compound **SL15** was prepared following a similar procedure to the one used to prepare **SL1**. The starting materials were 3-bromo-5-chlorosalicylaldehyde (0.4709 g, 2 mmol) and 1,5-diaminopentane (0.1022 g, 1 mmol) in dry EtOH (10 ml) refluxed for 2 h under nitrogen atmosphere. The yellow powder obtained was air and moisture stable. [Yield = 0.4173 g (78 %)]. Melting point: 167 – 168 °C. IR (KBr cm^{-1}); $\nu(\text{C}=\text{N})$ 1632 cm^{-1} . ^1H NMR (400 MHz, CDCl_3): δ H (*phenolic*) 14.77 (s, 1H); H (*imine*) 8.20 (s, 1H); H (*aromatic*) 7.57 (d, $J = 2.40$ Hz, 1H); 7.26 (s, 1H); 7.18 (d, $J = 1.60$ Hz, 1H); H (*aliphatic*) 3.65 (t, $J = 7.40$ Hz, 3H); 1.76 (m, $J = 8.00$ Hz, 5H); 1.50 (m, $J = 7.20$ Hz, 5H). ^{13}C NMR (100 MHz, CDCl_3): δ COH (*aromatic*) 163.33; CH (*imine*) 158.86; CH (*aromatic*) 135.26; 129.64; 122.45; 118.72; 112.53; CH (*aliphatic*) 57.77; 30.13; 24.50. Elemental analysis for $\text{C}_{19}\text{H}_{18}\text{Br}_2\text{Cl}_2\text{N}_2\text{O}_2$ (537.07 g/mol), Calculated: C, 39.80 %; H, 3.87; N, 4.89. Found: C, 39.48 %; H, 3.59; N, 4.59. ESI-MS, m/z : 537 $\{[\text{M}] + \text{H}\}$.

3.3.16 Preparation of 2,2'-(pentane-1,5-diylbis(azanylylidene))bis(methanylylidene)bis(4-bromophenol) (SL16)

The structural formula for the ligand **SL16** is shown in Figure 3.16.

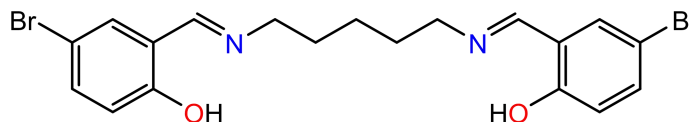


Figure 3.16: Structure of SL16

The synthesis of **SL16** was done following a procedure similar to the one used to prepare **SL1**. The reagents used were 5-bromosalicylaldehyde (0.4020 g, 2 mmol) and 1,5-diaminopentane (0.1022 g, 1 mmol) in dry EtOH (10 ml) stirred at reflux for 2 h in inert nitrogen atmosphere. The bright yellow solid obtained was both air and moisture stable. [Yield = 0.3965 g (85 %)]. Melting point: 99 – 100 °C. IR (KBr cm^{-1}); $\nu(\text{C}=\text{N})$ 1630 cm^{-1} . ^1H NMR (400 MHz, CDCl_3): δ H (*phenolic*) 13.59 (s, 1H); H (*imine*) 8.25 (s, 1H); H (*aromatic*) 7.38 (s, 1H); 7.35 (dd, $J = 2.40$ Hz, 2H); 6.86 (s, 1H); H (*aliphatic*) 3.61 (t, $J = 6.80$ Hz, 3H); 1.75 (m, $J = 8.00$ Hz, 5H); 1.47 (m, $J = 7.60$ Hz, 5H). ^{13}C NMR (100 MHz, CDCl_3): δ COH (*aromatic*) 163.54; CH (*imine*) 160.38; CH (*aromatic*) 134.80; 133.27; 120.08; 119.06; 109.89; CH (*aliphatic*) 59.26; 30.36; 24.64. Elemental analysis for $\text{C}_{19}\text{H}_{20}\text{Br}_2\text{N}_2\text{O}_2$ (468.18 g/mol), Calculated: C, 39.58 %; H, 4.30; N, 4.86. Found: 39.59 %; H, 4.02; N, 4.71. ESI-MS, m/z : 468 $\{[\text{M}] + \text{H}\}$.

3.3.17 Preparation of 2,2'-(pentane-1,5-diylbis(azanylylidene))bis(methanylylidene))bis(4-chlorophenol) (SL17)

The structural formula for the ligand **SL17** is shown in Figure 3.17.

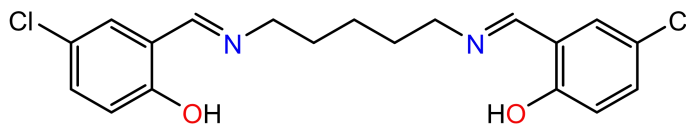


Figure 3.17: Structure of SL17

The ligand **SL17** was synthesized following a similar procedure to the one used for **SL2**. The starting reagents were 5-chlorosalicylaldehyde (0.3131 g, 2 mmol) and 1,5-diaminopentane (0.1022 g, 1 mmol) in dry MeOH (10 ml) which were stirred at reflux for 6 h in an inert nitrogen environment. During the reaction process, the mixture formed a wine-red colour which changed to yellow when the reaction solvent was removed. The yellow solid was both air and moisture stable. [Yield = 0.2567 g (68 %)]. Melting point: 78 – 80 °C. IR (ATR-FTIR cm^{-1}); $\nu(\text{C}=\text{N})$ 1626 cm^{-1} . ^1H NMR (400 MHz, CDCl_3): δ H (*phenolic*) 13.55 (s, 1H); H (*imine*) 8.28 (s, 1H); H (*aromatic*) 7.22 (d, $J = 2.80$ Hz, 2H); 7.20 (d, $J = 2.40$ Hz, 2H); 6.90 (d, $J = 8.80$ Hz, 2H); H (*aliphatic*) 3.61 (t, $J = 6.80$ Hz, 3H); 1.76 (m, $J = 7.60$ Hz, 5H); 1.47 (m, $J = 8.00$ Hz, 5H). ^{13}C NMR (100 MHz, CDCl_3): δ COH (*aromatic*) 163.63; CH (*imine*) 159.88; CH (*aromatic*) 131.98; 130.28; 123.04; 119.45; 118.58; CH (*aliphatic*) 59.28; 30.36; 24.64. Elemental analysis for $\text{C}_{19}\text{H}_{20}\text{Cl}_2\text{N}_2\text{O}_2$ (379.28 g/mol), Calculated: C, 42.13 %; H, 5.32; N, 5.18. Found: C, 42.96 %; H, 5.43; N, 5.24. ESI-MS, m/z : 379 $\{[\text{M}] + \text{H}\}$.

3.4 Synthesis of Pd(II) and Ni(II) Salicylaldimine Complexes

3.4.1 Pd Complex *CI*

(a) Preparation of palladium precursor complex [PdCl₂(COD)]

To PdCl₂ (1.7733 g, 0.01 mol) in a two-necked round bottomed flask fitted with a reflux condenser and a magnetic stir bar, concentrated HCl (15 ml) was added and the mixture stirred for 5 min under nitrogen until complete dissolution was achieved. An equimolar amount of 1,5-cyclooctadiene (COD) {1.0818 g, 0.01 mol} was added and the mixture stirred under reflux for a further 1 h. A yellow solid was formed. The solid was recovered by vacuum filtration and dried in vacuo at room temperature for 1 h to give a bright-yellow complex, PdCl₂(COD).

(b) Preparation of palladium complex *CI*

To a stirred solution of salicylaldimine ligand, **SL1** (0.0500 g, 0.1611 mmol) in dry DCM (10 ml) in a Schlenk tube saturated with N₂, was added dropwise triethylamine (Et₃N) {0.0326 g, 0.3222 mmol} in a 1:2 (ligand : base) mole ratio and the mixture stirred for 30 minutes. To this mixture, was added dropwise a solution of the precursor complex PdCl₂(COD) {0.0920 g, 0.3222 mmol} dissolved separately in dry DCM (10 ml). The reaction mixture was stirred overnight for 20 h. The mixture was concentrated in vacuo and diethyl ether added to precipitate a yellow solid. The precipitate was filtered and the light-yellow solid obtained dried in vacuo for 1 h.

Yield = 0.0410 g (43 %). Melting point: Decomposed at 138 °C. IR (KBr cm⁻¹); ν(C=N) 1611 cm⁻¹. ¹H NMR (400 MHz, DMSO): δ 7.69 (s, 1H); 7.26 (d, *J* = 12.0 Hz, 2H); 6.17 (s, 1H); 5.51 (s, 1H); 5.09 (d, *J* = 9.60 Hz, 2H); 3.53 (s, 3H); 2.51 (t, *J* = 37.80 Hz, 4H); 1.53 (m, *J* = 26.6, 5H).

Elemental analysis for $C_{19}H_{20}Cl_4N_2O_2Pd_2$ (663.02 g/mol), Calculated: C, 34.42 %; H, 3.04; N, 4.23. Found: C, 34.49 %; H, 3.08; N, 4.34.

3.4.2 Pd Complex C2

The complex **C2** was prepared using a similar procedure to the one for **C1**. The parent ligand **SL2** (0.0500 g, 0.1611 mmol) was reacted with triethylamine (Et_3N) {0.0326 g, 0.3222 mmol} then added $PdCl_2(COD)$ {0.0920 g, 0.3222 mmol} in dry DCM (20 ml) and stirred for a further 20 h. The reaction mixture turned wine-red then orange during the reaction. A light-yellow solid product was obtained. [Yield = 0.1913 g (95 %)]. Melting point: Decomposed at 137 °C. IR (KBr cm^{-1}); $\nu(C=N)$ 1622 cm^{-1} . 1H NMR (400 MHz, DMSO): δ 7.91 (s, 1H); 7.08 (d, $J = 8.40$ Hz, 2H); 6.70 (d, $J = 8.40$ Hz, 2H); 5.76 (s, 1H); 3.38 (s, 1H); 3.04 (m, $J = 7.20$ Hz, 5H); 1.18 (t, $J = 7.20$, 3H). ^{13}C NMR (100 MHz, DMSO): δ 163.59; 162.70; 136.79; 134.15; 122.84; 119.28; 60.06; 46.10; 20.22; 8.93. Elemental analysis for $C_{19}H_{20}Cl_4N_2O_2Pd_2$ (663.02 g/mol), Calculated: C, 34.42 %; H, 3.04; N, 4.23. Found: C, 34.59 %; H, 3.15; N, 4.31.

3.4.3 Pd Complex C3

Complex **C3** was synthesized following a similar procedure to the one for **C1**. The reaction materials were **SL3** (0.0800 g, 0.2337 mmol), triethylamine (Et_3N) {0.0473 g, 0.4673 mmol} and $PdCl_2(COD)$ {0.1334 g, 0.4673 mmol} in dry DCM (20 ml) stirred for 20 h. The reaction mixture turned dark-red during the reaction. The solid product obtained was orange. [Yield = 0.2282 g (90 %)]. Melting point: Decomposed at 155 °C. IR (KBr cm^{-1}); $\nu(C=N)$ 1618 cm^{-1} . 1H NMR (400 MHz, DMSO): δ 7.95 (s, 1H); 6.95 (d, $J = 3.40$ Hz, 2H); 6.84 (d, $J = 3.20$ Hz, 2H); 6.73 (s, 1H); 3.66 (s, 1H); 3.33 (s, 1H); 3.03 (m, $J = 6.60$ Hz, 5H); 1.78 (t, $J = 7.20$ Hz, 3H). ^{13}C NMR (100 MHz, DMSO): δ 163.60; 160.04; 148.73; 125.14; 120.27; 118.62; 115.05; 60.03;

45.87. Elemental analysis for $C_{19}H_{20}Cl_4N_2O_4Pd_2$ (695.02 g/mol), Calculated: C, 32.83 %; H, 2.90; N, 4.03. Found: C, 32.54 %; H, 2.90; N, 4.09.

3.4.4 Pd Complex C4

The experimental procedure similar to that for the synthesis of complex **C1** was followed. The reagents used included **SL4** (0.0800 g, 0.1818 mmol), triethylamine (Et_3N) {0.0368 g, 0.3635 mmol} and $PdCl_2(COD)$ {0.1038 g, 0.3635 mmol} in dry DCM (20 ml) stirred for 20 h. The reaction mixture turned orange. A yellow solid product was obtained. [Yield = 0.0740 g (51 %)]. Melting point: Decomposed at 146 °C. IR (KBr cm^{-1}); $\nu(C=N)$ 1620 cm^{-1} . 1H NMR (400 MHz, DMSO): δ 8.01 (s, 1H); 7.53 (d, $J = 2.40$ Hz, 2H); 7.35 (dd, $J = 2.80$ Hz, 2H); 6.76 (d, $J = 9.80$ Hz, 2H); 3.33 (s, 1H); 1.15 (t, $J = 6.80$ Hz, 3H). ^{13}C NMR (100 MHz, DMSO): δ 163.31; 137.45; 136.08; 128.63; 121.84; 104.75; 60.05; 46.10; 28.01. Elemental analysis for $C_{17}H_{12}Br_2Cl_6N_2O_2Pd_2$ (861.64 g/mol), Calculated: C, 23.70 %; H, 1.46; N, 3.25. Found: C, 24.00 %; H, 1.36; N, 3.39.

3.4.5 Pd Complex C5

The complex **C5** was synthesized in a similar procedure to the one for **C1**. The reaction materials were **SL5** (0.0600 g, 0.1708 mmol), triethylamine (Et_3N) {0.0346 g, 0.3417 mmol} and $PdCl_2(COD)$ {0.0975 g, 0.3417 mmol} in dry DCM (20 ml) stirred for 24 h. The reaction solution turned orange while the product isolated was a yellow solid. [Yield = 0.0716 g (60 %)]. Melting point: Decomposed at 141 °C. IR (KBr cm^{-1}); $\nu(C=N)$ 1620 cm^{-1} . 1H NMR (400 MHz, DMSO): δ 8.02 (s, 1H); 7.98 (s, 1H); 7.41 (d, $J = 2.60$ Hz, 2H); 7.37 (d, $J = 2.80$ Hz, 2H); 3.33 (s, 1H); 1.14 (t, $J = 6.80$ Hz, 3H). Elemental analysis for $C_{17}H_{14}Br_2Cl_4N_2O_2Pd_2$ (792.76 g/mol), Calculated: C, 25.76 %; H, 1.80; N, 3.53. Found: C, 25.66 %; H, 1.92; N, 3.50.

3.4.6 Pd Complex C6

A similar procedure to the one used for **C1** was followed. The reagents were **SL6** (0.0262 g, 0.0808 mmol), triethylamine (Et₃N) {0.0163 g, 0.1615 mmol} and PdCl₂(COD) {0.0461 g, 0.01615 mmol} in dry DCM (10 ml) stirred for 24 h. The reaction mixture turned wine-red, while the colour of the solid complex **C6** was light-yellow. [Yield = 0.0887 g (90 %)]. Melting point: Decomposed at 144 °C. IR (KBr cm⁻¹); $\nu(\text{C}=\text{N})$ 1619 cm⁻¹. ¹H NMR (400 MHz, CDCl₃): δ 7.28 (s, 1H); 7.03 (d, $J = 8.40$ Hz, 2H); 6.90 (d, $J = 9.20$ Hz, 2H); 5.59 (s, 1H); 3.11 (m, $J = 7.20$ Hz, 4H); 1.43 (t, $J = 7.20$ Hz, 3H). Elemental analysis for C₁₇H₁₄Cl₆N₂O₂Pd₂ (703.72 g/mol), Calculated: C, 29.01 %; H, 2.00; N, 3.98. Found: C, 28.86 %; H, 2.25; N, 3.94.

3.4.7 Pd Complex C7

The complex **C7** was prepared using a similar procedure to the one used to prepare **C1**. The reaction materials were **SL9** (0.0400 g, 0.1122 mmol), triethylamine (Et₃N) {0.0227 g, 0.2244 mmol} and PdCl₂(COD) {0.0641 g, 0.2244 mmol} in dry DCM (15 ml) stirred for 24 h. Reaction mixture turned wine-red but the isolated solid product was orange. [Yield = 0.0873 g (95 %)]. Melting point: Decomposed at 159 °C. IR (KBr cm⁻¹); $\nu(\text{C}=\text{N})$ 1620 cm⁻¹. ¹H NMR (400 MHz, CDCl₃): δ 7.28 (s, 1H); 6.58 (d, $J = 3.20$ Hz, 2H); 6.40 (d, $J = 2.40$ Hz, 2H); 5.31 (s, 1H); 3.12 (m, $J = 7.60$ Hz, 3H); 1.42 (t, $J = 7.20$ Hz, 3H). Elemental analysis for C₂₀H₂₂Cl₄N₂O₄Pd₂ (709.05 g/mol), Calculated: C, 33.88 %; H, 3.10; N, 3.95. Found: C, 33.94 %; H, 3.21; N, 3.40.

3.4.8 Pd Complex C8

The complex was prepared following a similar procedure used to synthesize **C1**. Reagents used were **SL12** (0.0800 g, 0.2364 mmol), triethylamine (Et₃N) {0.0478 g, 0.4728 mmol} and PdCl₂(COD) {0.1350 g, 0.4478 mmol} in dry DCM (20 ml) stirred for 24 h. Reaction mixture

turned wine-red but the product obtained was a light-yellow solid. [Yield = 0.0769 g (47 %)]. Melting point: Decomposed at 143 °C. IR (KBr cm^{-1}); $\nu(\text{C}=\text{N})$ 1621 cm^{-1} . ^1H NMR (400 MHz, CDCl_3): δ 7.26 (s, 1H); 6.49 (d, $J = 10.40$ Hz, 2H); 5.95 (d, $J = 9.60$ Hz, 2H); 3.13 (m, $J = 7.20$ Hz, 3H); 1.42 (t, $J = 6.60$ Hz, 3H). Elemental analysis for $\text{C}_{21}\text{H}_{24}\text{Cl}_4\text{N}_2\text{O}_2\text{Pd}_2$ (691.08 g/mol), Calculated C, 36.50 %; H, 3.50; N, 4.05. Found: C, 36.62 %; H, 3.45; N, 4.18.

3.4.9 Pd Complex C9

A similar protocol to the one used for complex C1 was followed. The starting reagents, SL13 (0.026 g, 0.0768 mmol), triethylamine (Et_3N) {0.01555 g, 0.1536 mmol} and $\text{PdCl}_2(\text{COD})$ {0.0439 g, 0.1536 mmol} in dry DCM (10 ml) stirred for 24 h. The isolated complex was a yellow solid. [Yield = 0.0559 g (95 %)]. Melting point: Decomposed at 129 °C. IR (ATR cm^{-1}); $\nu(\text{C}=\text{N})$ 1621 cm^{-1} . ^1H NMR (400 MHz, CDCl_3): δ 7.28 (s, 1H); 7.01 (d, $J = 4.00$ Hz, 2H); 6.86 (d, $J = 6.00$ Hz, 2H); 5.61 (s, 1H); 5.30 (s, 1H); 3.63 (m, $J = 10.20$ Hz, 3H); 3.14 (m, $J = 7.60$ Hz, 3H); 2.21 (m, $J = 2.80$ Hz, 5H); 1.43 (t, $J = 7.20$ Hz, 3H). Elemental analysis for $\text{C}_{21}\text{H}_{24}\text{Cl}_4\text{N}_2\text{O}_2\text{Pd}_2$ (691.08 g/mol), Calculated: C, 33.88 %; H, 3.13; N, 3.95. Found: 33.94 %; H, 2.93; N, 3.96.

3.4.10 Pd Complex C10

A similar methodology to the one for C1 was used. Reagents were SL14 (0.0700 g, 0.1900 mmol), triethylamine (Et_3N) {0.0382 g, 0.3779 mmol} and $\text{PdCl}_2(\text{COD})$ {0.1079 g, 0.3779 mmol} in dry DCM (10 ml) stirred for 24 h. The recovered solid complex was orange. [Yield = 0.1300 g (94 %)]. Melting point: Decomposed at 160 °C. IR (ATR cm^{-1}); $\nu(\text{C}=\text{N})$ 1618 cm^{-1} . ^1H NMR (400 MHz, CDCl_3): δ 7.29 (s, 1H); 6.88 (s, 1H); 6.60 (d, $J = 18.8$ Hz, 2H); 6.48 (d, $J = 4.00$ Hz, 2H); 5.56 (s, 1H); 5.30 (s, 1H); 3.71 (m, $J = 5.20$ Hz, 3H); 3.14 (m, $J = 7.60$ Hz, 5H); 1.43 (t, $J = 7.20$ Hz, 3H).

Elemental analysis for $C_{21}H_{24}Cl_4N_2O_4Pd_2$ (723.07 g/mol), Calculated: C, 26.80 %; H, 2.00; N, 3.47. Found: C, 26.83 %; H, 2.05; N, 3.08.

3.4.11 Ni Complex **C11**

(a) Preparation of nickel precursor complex [NiCl₂(DME)]

A two-necked round bottomed flask (100 ml) fitted with a reflux condenser and magnetic stir bar was charged with pulverized nickel(II) chloride hydrate (2.5920 g, 20 mmol). A solution of 1,2-dimethoxyethane (1.8024 g, 20 mmol) and triethyl orthoformate (15 ml, 4 moles) were added. The slurry was stirred rapidly and heated under reflux in a nitrogen atmosphere for 2 h. The completed reaction slurry was cooled, and the orange granular solid collected under N₂ atmosphere on Schlenk frit, rinsed successively with 1,2-dimethoxyethane and then followed by pentane. It was then dried in vacuo in a nitrogen environment at room temperature for a further 1 h.

(b) Preparation of nickel complex **C11**

The complex **C11** was synthesized using a similar procedure used to prepare **C1** but with nickel precursor complex, NiCl₂(DME) in place of PdCl₂(COD) for all the nickel(II) complexes (**C11** to **C15**). The starting materials were, **SL4** (0.0840 g, 0.2706 mmol), triethylamine (Et₃N) {0.0548 g, 0.5413 mmol} and NiCl₂(DME) {0.1189 g, 0.5413 mmol} in dry DCM (15 ml). The reaction mixture formed a brown solution which yielded a light-yellow solid complex. [Yield = 0.2073 g (90 %)]. Melting point: 142 °C. IR (KBr cm⁻¹); $\nu(C=N)$ 1608 cm⁻¹. ¹H NMR (400 MHz, CDCl₃): δ 7.06 (d, $J = 6.40$ Hz, 2H); 6.91 d, $J = 7.60$ Hz, 2H); 6.44 (t, $J = 7.60$ Hz, 2H); 3.12 (m, $J = 7.20$ Hz, 5H);

2.19 (s, 1H); 1.42 (t, $J = 7.20$ Hz, 3H). Elemental analysis for $C_{19}H_{20}Cl_4N_2O_2Ni_2$ (567.57 g/mol), Calculated: C, 40.21 %; H, 3.55; N, 4.94. Found: C, 40.30 %; H, 3.58; N, 4.52.

3.4.12 Ni Complex C12

A procedure similar to the one used to synthesize **C1** was followed. Reagents used were, **SL7** (0.0805 g, 0.2351 mmol), triethylamine (Et_3N) {0.0476 g, 0.4702 mmol} and $NiCl_2(DME)$ {0.1033 g, 0.4702 mmol} in dry DCM (20 ml). The reaction mixture formed a brown solution which yielded a yellow solid complex. [Yield = 0.1985 g (95 %)]. Melting point: 153 °C. IR (KBr cm^{-1}); $\nu(C=N)$ 1627 cm^{-1} . 1H NMR (400 MHz, $CDCl_3$): δ 7.28 (s, 1H); 6.93 (d, $J = 22.40$ Hz, 2H); 6.48 (s, 1H); 6.06 (d, $J = 47.20$ Hz, 2H); 3.71 (s, 1H); 3.06 (m, $J = 6.80$ Hz, 5H); 1.37 (s, 3H). Elemental analysis for $C_{19}H_{20}Cl_4N_2O_4Ni_2$ (599.57 g/mol), Calculated: C, 38.06 %; H, 3.36; N, 4.67. Found: C, 38.17 %; H, 3.42; N, 4.76.

3.4.13 Ni Complex C13

The complex was synthesized using a procedure similar to the one used to prepare **C1**. Reagents used were, **SL9** (0.0865 g, 0.1965 mmol), triethylamine (Et_3N) {0.0398 g, 0.3931 mmol} and $NiCl_2(DME)$ {0.0864 g, 0.3931 mmol} in dry DCM (20 ml). The reaction mixture formed a brown solution which yielded a light-yellow solid complex. [Yield = 0.1040 g (76 %)]. Melting point: 144 °C. IR (KBr cm^{-1}); $\nu(C=N)$ 1627 cm^{-1} . 1H NMR (400 MHz, $CDCl_3$): δ 10.70 (s, 1H); 7.53 (s, 1H); 7.26 (d, $J = 18.00$ Hz, 2H); 6.87 (s, 1H); 3.70 (t, $J = 9.60$ Hz, 3H); 1.14 (m, $J = 41.20$ Hz, 5H). Elemental analysis for $C_{20}H_{22}Cl_4N_2O_4Ni_2$ (613.59 g/mol), Calculated: C, 39.15 %; H, 3.61; N, 4.57. Found: C, 39.25 %; H, 3.71; N, 4.61.

3.4.14 Ni Complex C14

This complex was synthesized using a similar procedure to the one used to synthesize C1. Reagents used were, **SL15** (0.0335 g, 0.0940 mmol), triethylamine (Et₃N) {0.0190 g, 0.1880 mmol} and NiCl₂(DME) {0.0413 g, 0.1880 mmol} in dry DCM (10 ml). The reaction mixture formed an orange solution which yielded a light-green solid complex. [Yield = 0.0450 g (78 %)]. Melting point: 148 °C. IR (KBr cm⁻¹); $\nu(\text{C}=\text{N})$ 1623 cm⁻¹. ¹H NMR (400 MHz, DMSO): δ 10.24 (s, 1H); 7.13(d, $J = 11.20$ Hz, 2H); 6.99 (d, $J = 8.80$ Hz, 2H); 5.76 (s, 1H); 5.32 (s, 1H); 3.36 (s, 3H); 3.01 (d, $J = 7.20$ Hz, 2H); 1.17 (t, $J = 7.20$ Hz, 3H). Elemental analysis for C₁₇H₁₄Br₂Cl₄N₂O₂Ni₂ (697.31 g/mol), Calculated: C, 29.28 %; H, 2.02; N, 4.02. Found: C, 29.37 %; H, 2.11; N, 4.12.

3.4.15 Ni Complex C15

The complex C15 was synthesized using a similar procedure to the one used to synthesize C1. Reagents used were, **SL13** (0.0228 g, 0.0703 mmol), triethylamine (Et₃N) {0.0142 g, 0.1406 mmol} and NiCl₂(DME) {0.0309 g, 0.1406 mmol} in dry DCM (10 ml). The reaction mixture formed a light-orange solution which yielded a light-green solid complex. [Yield = 0.0368 g, (90 %)]. Melting point: 165 °C. IR (KBr cm⁻¹); $\nu(\text{C}=\text{N})$ 1603 cm⁻¹. ¹H NMR (400 MHz, DMSO): δ 10.08 (s, 1H); 8.10 (s, 1H); 7.77 (d, $J = 6.80$ Hz, 2H); 7.09 (d, $J = 9.60$ Hz, 2H); 5.95 (t, $J = 6.80$ Hz, 3H); 4.75 (s, 3H). Elemental analysis for C₂₀H₂₂Cl₄N₂O₂Ni₂ (581.59 g/mol), Calculated: C, 41.30 %; H, 3.81; N, 4.82. Found: C, 41.44 %; H, 3.92; N, 4.76.

3.4.16 Procedure for hexene oligomerisation

Oligomerisation of 1-hexene was carried out in 100 ml two-neck round-bottomed flask equipped with a magnetic stirrer. The reactor system was re-degassed five times and saturated with N₂ atmosphere, then toluene was added (10 ml) to the reactor. Hexene (0.372 ml, 4.42 μ mol) and

modified methyl aluminoxane (MMAO) measured in the glovebox under argon atmosphere, was added via a syringe (catalyst : MMAO = 1:400 eq.) to the toluene kept at polymerisation temperature (varying it from r.t to 50 °C). Polymerisation was started by addition of the catalyst solution (10 μ mol) in toluene and run from between 4 – 24 h with sampling (using a syringe) at various time intervals of 4, 8, 18 and 24 h. Approximately 1 ml of each sample was filtered using microfilter and taken for GC analysis.

CHAPTER FOUR

RESULTS AND DISCUSSION

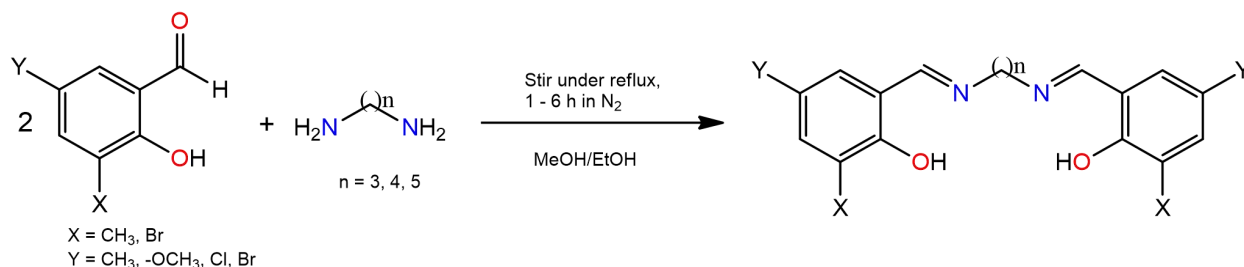
4.1 Introduction

Even though complexes of the *N,O*-salicylaldehyde ligands have been widely studied for polymerisation, few research groups have reported synthesis of bimetallic complexes of the aforementioned ligands. In this thesis a report is given on the synthesis and characterisation of *N,O*-salicylaldehyde ligands which upon coordination to binuclear nickel and palladium metal centres formed stable complexes for 1-hexene oligomerisation.

4.2 Results and discussion

4.2.1 Synthesis and characterisation of *N,O*-salicylaldehyde ligands *SL1* – *SL17*

The new salicylaldehyde ligands *SL1* – *SL17* were prepared by modifications of the reported methodology (Fonseca *et al.*, 2010; Xue *et al.*, 2013). This was achieved by reacting a substituted 3 and/or 5-salicylaldehyde with a primary diamine via Schiff base condensation reaction (Scheme 4.1). The progressive formation of the expected imine ($C=N_{imine}$) functionality was monitored and confirmed by infrared spectroscopy.



Scheme 4.1: Synthesis of *N,O*-salicylaldehyde ligands *SL1* – *SL17*

The ligands were separated either from a methanolic or ethanolic solution after a time ranging from 1 to 6 h depending on their solubility and formation. The ligands were separated by removing the reaction solvent in vacuo. They were subsequently re-dissolved in minimum amount of reaction solvent and cooled in hexane-nitrogen mixture to crystallize off and separate unreacted starting materials. The ligands were isolated as light-yellow, yellow or bright-yellow solids in appreciable yields ranging from 41 – 98 % (Table 4.1). All the ligands were soluble in DCM and chloroform. Therefore, a small portion of each were dissolved in DCM and overlaid with hexane and set for crystal growth for over 2 – 4 weeks, in which four of all the ligands formed crystals.

Table 4.1: Yield and melting points for the ligands SL1 – SL17

Ligand	X	Y	n (linker)	% Yield	M. point (°C)
SL1	-CH ₃	H	3	66	60-62
SL2	H	-CH ₃	3	89	62-63
SL3	H	-OCH ₃	3	97	109-110
SL4	Br	Cl	3	67	150-152
SL5	H	Br	3	97	137-139
SL6	H	Cl	3	59	93-94
SL7	-CH ₃	H	4	51	113-114
SL8	H	-CH ₃	4	98	130-132
SL9	H	-OCH ₃	4	96	120-122
SL10	H	Br	4	93	153-154
SL11	H	Cl	4	98	145-147
SL12	-CH ₃	H	5	92	76-77
SL13	H	-CH ₃	5	41	98-99
SL14	H	-OCH ₃	5	96	89-91
SL15	Br	Cl	5	78	167-168
SL16	H	Br	5	85	99-100
SL17	H	Cl	5	68	78-80

The melting points of the ligands varied from 60 to 168 °C as summarised in Table 4.1. All the ligands were reported to be air and moisture stable. Spectroscopic (FTIR, ¹H and ¹³C NMR) and

analytical data (elemental analysis and mass spectrometry) techniques were employed to confirm the proposed structural formulation.

4.2.2 Infrared spectroscopy of the *N,O*-salicylaldimine ligands **SL1** – **SL17**

Formation of Schiff bases was monitored by studying the C=N, C=C, and OH functional groups stretching frequencies using FTIR spectroscopy. The FTIR spectra for these ligands were recorded using KBr pellets or diamond ATR as backgrounds. The IR spectrum for **SL1** in Figure 4.1 is a typical example of the spectrum obtained for all ligands. The other FTIR spectra for the ligands are shown in Appendix A.

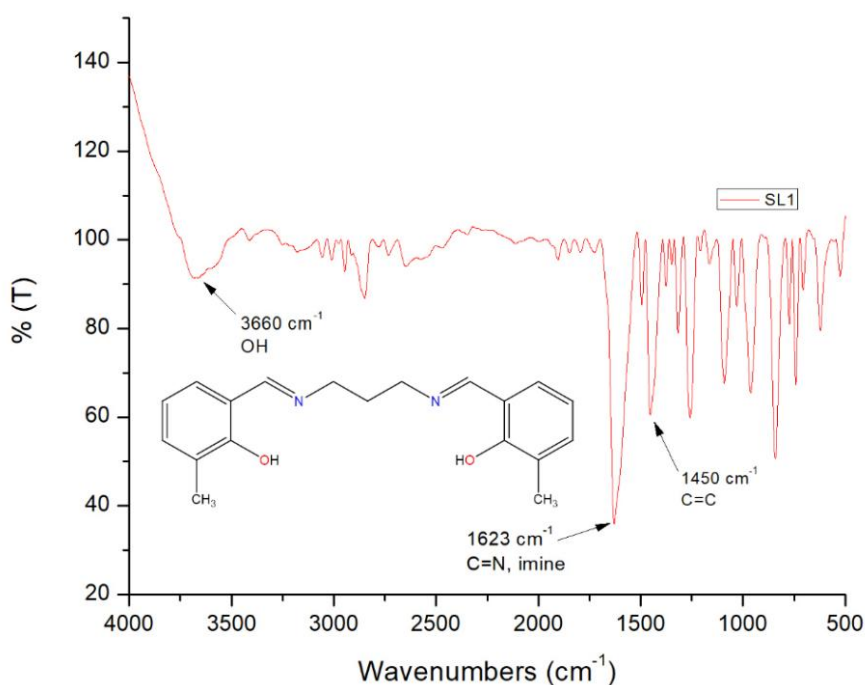


Figure 4.1: FTIR spectrum for the salicylaldimine ligand **SL1**

The stretching vibrational frequencies characteristic of the phenolic hydroxyl groups for **SL1** – **SL17** were observed in the region 3100 – 3600 cm⁻¹ as broad bands (br) for all the synthesized

Schiff base ligands in this work. The broadness of these bands is due to the formation of intramolecular hydrogen bonding of OH to N of C=N chromophore similar and close to those reported in literature which appeared between 3200 – 3427 cm^{-1} (El-Sonbati, 1991; Xue *et al.*, 2013). The appearance of a strong stretching frequencies at 1623, 1624...1637 cm^{-1} (Table 4.2) for **SL1** to **SL17** suggests successful condensation reaction of the carbonyl and the amine functionalities and were attributed to the imine $\nu(\text{C}=\text{N})$ stretching frequencies for all the ligands. These stretching frequencies are in agreement with other salicylaldimine ligands previously reported in literature, one appearing at 1627 cm^{-1} , another one in the range 1645 to 1651 cm^{-1} , also at 1610 – 1640 cm^{-1} , another research got 1623 cm^{-1} , further report showed at 1612 – 1623 cm^{-1} while yet another group reported 1623 cm^{-1} (Hille & Gust, 2010; Naeimi & Moradian, 2013; Sheng *et al.*, 2015; Zhang, 2016; Zhou *et al.*, 2018; Zhou *et al.*, 1999). In this work, there was insignificant difference in $\nu(\text{C}=\text{N})$ stretching vibrational frequencies when the linker between imine and the phenolic ring was only varied by one carbon with observed stretching frequencies of 1623 cm^{-1} , 1624 cm^{-1} and 1627 cm^{-1} for propylene (**SL1**), butylene (**SL7**) and pentylene (**SL12**), respectively. This phenomenon was also observed in **SL5**, **SL10** and **SL16**, where the $\nu(\text{C}=\text{N})$ stretching frequencies were observed at 1633, 1631 and 1630 cm^{-1} for the three ligands, respectively. The presence of homocyclic rings in the ligands was also supported by the observed bands in the region 1442 – 1495 cm^{-1} , that are characteristic for a $\nu(\text{C}=\text{C})$ stretching frequencies of homocyclic rings especially benzyl which appear between 1468 – 1497 cm^{-1} as reported in researched work (Donmez *et al.*, 2007). A summary of the infrared stretching vibrational frequencies (cm^{-1}) of the main functional groups for the *N,O*-salicylaldimine ligands **SL1** – **SL17** are given in Table 4.2 below.

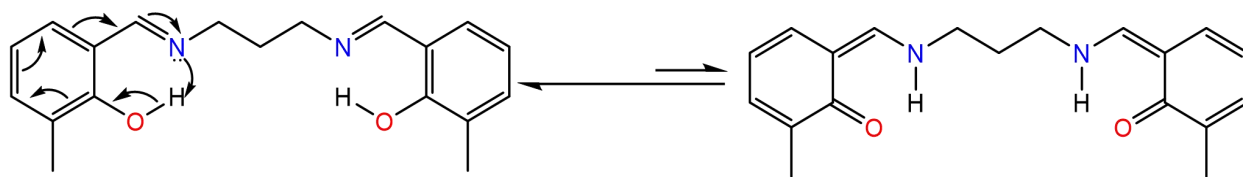
Table 4.2: Infrared stretching frequencies (cm⁻¹) for the *N,O*-salicylaldimine ligands SL1 – SL17

Ligand	$\nu(\text{C}=\text{N})$	$\nu(\text{OH})$	$\nu(\text{C}=\text{C})$
SL1	1623	3660	1450
SL2	1637	3438	1491
SL3	1635	3075	1493
SL4	1630	3420	1448
SL5	1633	3432	1479
SL6	1629	3136	1480
SL7	1624	3590	1442
SL8	1629	3436	1493
SL9	1633	3503	1493
SL10	1631	3259	1480
SL11	1631	3142	1481
SL12	1627	3158	1458
SL13	1628	3406	1495
SL14	1636	3436	1495
SL15	1632	3150	1462
SL16	1630	3375	1480
SL17	1626	3250	1478

The observed lower imine $\nu(\text{C}=\text{N})$ stretching vibrational frequencies at around 1623 cm⁻¹ for **SL1** can be attributed to the decreased electron density around the azomethine nitrogen. On the other hand, the highest stretching frequencies exhibited by **SL2** at around 1637 cm⁻¹ can be

attributed to the increased electron density around the imine nitrogen, as was also observed by other researchers (Lopez-Garriga *et al.*, 1986; Wang & Poirier, 1997).

The *N,O*-salicylaldimine ligands are capable of exhibiting tautomeric properties. Tautomerism is the ability of certain organic compounds to exist in a mixture of two interconvertible constitutional isomers in equilibrium. These compounds differ from each other in the position of a hydrogen atom or a double bond. The possibility of whether tautomerism occurred or not between the hydroxyimine and keto-imine structures as shown in Scheme 4.2 was carefully studied by looking at the infrared stretching vibrational frequencies of the carbonyl which occurs at around 1700 cm^{-1} and the amine that absorbs at approximately 3300 cm^{-1} . It was found that these characteristic peaks were absent, hence the hydroxyimine was favoured. The data obtained for the ligands **SL1** – **SL17** was in accordance with the observation of similar $\text{NH}\cdots\text{O}$ and $\text{OH}\cdots\text{N}$ system that pointed to the favourable formation of a hydroxyimine than the keto-imine.



Scheme 4.2: Possible tautomerism of the hydroxyimine (SL1, left) to the keto-imine (right)

4.2.3 ^1H and ^{13}C NMR for **SL1** – **SL17**

All the ^1H and ^{13}C NMR spectra for the synthesized *N,O*-salicylaldimine ligands, **SL1** – **SL17**, were recorded in deuterated chloroform (CDCl_3) in order to study and establish their structural

formulations. The reference solvent used was TMS whose chemical shift was 0.00 ppm, and was consistent for all the ligands and complexes in this work.

The ^1H NMR spectra for all the ligands, exhibited a characteristic azomethine ($\text{HC}=\text{N}$) resonances appearing between 8.20 – 8.38 ppm (Table 4.3). A typical ^1H NMR spectrum for salicylaldehyde ligands and assignment of ^1H chemical shifts is shown in Figure 4.2, with the imine proton singlet peak appearing at 8.36 ppm with integration ratio of 2 for proton number 7 and 13 in Figure 4.3. The appearance of the singlet peaks for all the ligands in this work observed within the range of 8.20 – 8.38 ppm (Table 4.3), was thus attributed to the presence of an azomethine functionality and the successful Schiff base condensation reaction.

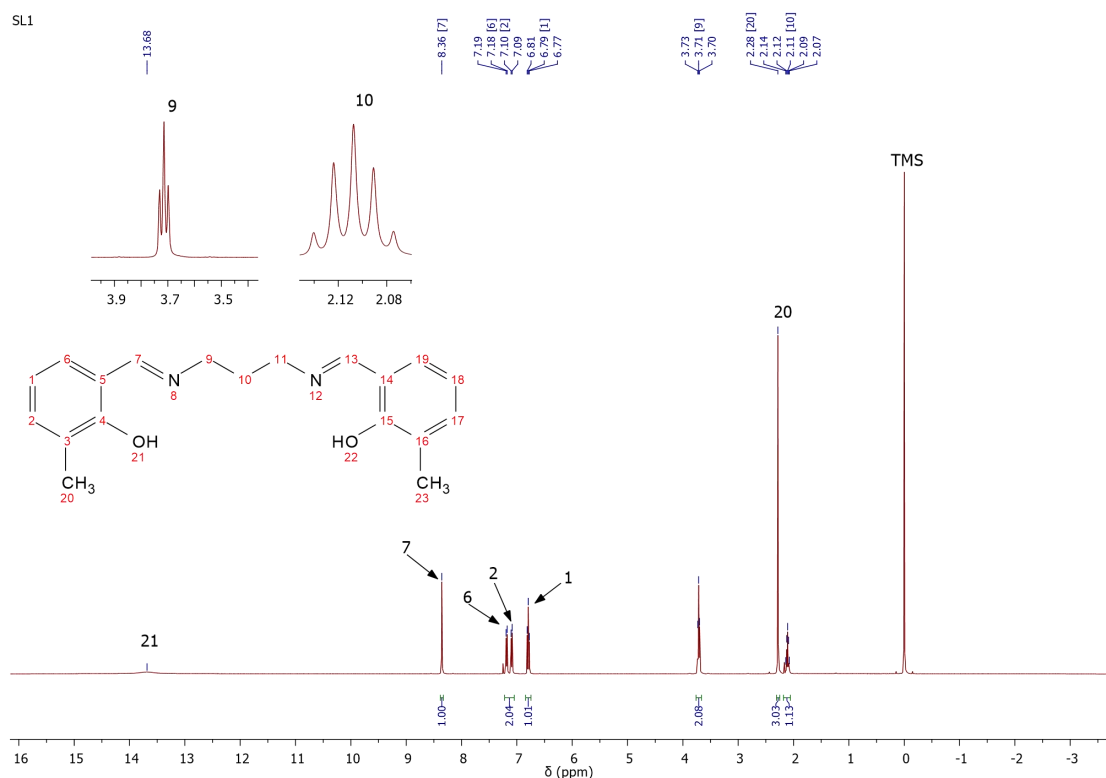


Figure 4.2: ^1H NMR for *N,O*-salicylaldehyde ligand SL1 (α solvent $\text{CDCl}_3\text{-d}_1$)

Table 4.3: ^1H NMR spectral data (δ in ppm) for imine and phenolic protons in CDCl_3

Ligand	$\delta(\text{HC}=\text{N})$	$\delta(\text{O}-\text{H})$
SL1	8.36	13.68
SL2	8.32	13.12
SL3	8.33	12.86
SL4	8.28	14.44
SL5	8.29	13.35
SL6	8.31	13.35
SL7	8.38	13.82
SL8	8.28	13.25
SL9	8.30	12.97
SL10	8.27	13.49
SL11	8.28	13.45
SL12	8.32	13.87
SL13	8.20	14.74
SL14	8.29	13.05
SL15	8.20	14.77
SL16	8.25	13.59
SL17	8.26	13.55

The formation of the azomethine ($\text{C}=\text{N}$) bond resulted in the increase in electron density between the C and N atoms, thus causing an upfield shift in the resonance of the protons of the azomethine ($\text{HC}=\text{N}$) moiety as compared with the aldehyde proton that normally appears downfield at approximately 10 ppm. These chemical shift values are close to the ones reported by other research groups. For instance, one group reported the signals for azomethine protons between 8.27 – 8.63, another research team observed this signal at 8.30 – 8.60 while yet another team observed it at 8.90 ppm for similar salicylaldimine ligands (Mohebbi & Abdi, 2008; Naeimi & Moradian, 2010; Nejo *et al.*, 2011).

The hydroxyl ($\text{HO}-$) protons were observed downfield in the range 12.86 – 14.77 ppm for all the *N,O*-salicylaldimine ligands, synthesized and used in this work. This can be attributed to the intramolecular hydrogen bonding ($\text{HO}\cdots\text{N}$) that was observed in these and other related ligands in

reported work (Naeimi & Moradian, 2010). The peaks for the aromatic (phenolic ring) protons appeared in the range 6.62 – 8.39 ppm for all the ligands. This is consistent with one by a research group which was reported in the range 7.25 to 7.45 ppm and another team recorded between 6.80 – 7.63 ppm (Schulz *et al.*, 2011; Tas *et al.*, 2008).

The chemical shifts for the phenolic (*O-H*) proton of **SL3** was observed at 12.86 ppm, while that for **SL15** (Table 4.3) was observed further downfield at 14.77 ppm (Table 4.3). These two extreme absorption peaks in this work can be accounted for using the chemical environments in which the protons are found. The ligand **SL3** (Appendix B Figure B.2) has a methoxy (-OCH₃) substituent *para* to the phenolic proton. The methoxy group is a good electron donating group (EDG), which adds electron density to the phenyl ring. The extra electron density shields the phenolic proton from the external magnetic field, hence the absorption peak observed upfield in comparison with the other ligands in this work. On the other hand, the ligand **SL15** (Appendix B Figure B.14) has two electron-withdrawing groups (EWG), Br and Cl, which are *ortho* and *para*, respectively to the phenolic proton. The phenolic proton in this ligand resonates at 14.77 ppm downfield because it is deshielded from external magnetic field.

The chemical shifts for the protons of the aliphatic spacers (linkers), that is, propylene, butylene and pentylene (=N-(CH₂)_n-N=) appeared as triplets and multiplets for all *N,O*-salicylaldimine ligands at 1.47 – 3.74 ppm (Figure 4.3) compared to unreacted diamines at about 4.05 ppm, an upfield shift upon successful Schiff base condensation reaction. The triplet and multiplet peaks indicate that these protons are coupled differently to their neighbouring protons. The absorption proton signals for the linkers are also in close agreement with those reported earlier at 1.78 – 3.62 ppm (Hisham *et al.*, 2012). The intense singlet peak characteristically observed at about

2.28 ppm was due to the protons of the methyl substituent on the *N,O*-salicylaldimine phenolic ring. Other singlet peaks attributed to the protons of methyl substituents on the phenolic ring for **SL2**, **SL7**, **SL8**, **SL12**, and **SL13** (Appendix B) were observed at 2.29, 2.32, 2.28, 2.27, and 3.65 ppm, respectively which are in agreement with what others have reported (Binder *et al.*, 2007). Moreover, another intense singlet peak observed at 3.77 ppm for salicylaldimine ligands **SL3**, **SL9** and **SL14** (Appendix B) was attributed to the protons of methoxy (-OCH₃) substituent on the phenolic ring. Singlet peaks for methoxy substituents ranging between 3.87 and 4.05 ppm were also reported by other researchers with similar ligands (Mohebbi & Abdi, 2008).

In the ¹³C NMR spectrum for the **SL1** ligand, the imine carbon peak was observed at 159.41 ppm as shown in Figure 4.3. Generally in this work, the characteristic signals for the imine carbons appeared between 157.61 and 165.17 ppm (Table 4.4) and these signals are within the range of other reported work (Fonseca *et al.*, 2010; Naeimi & Moradian, 2013) for similar salicylaldimine ligands.

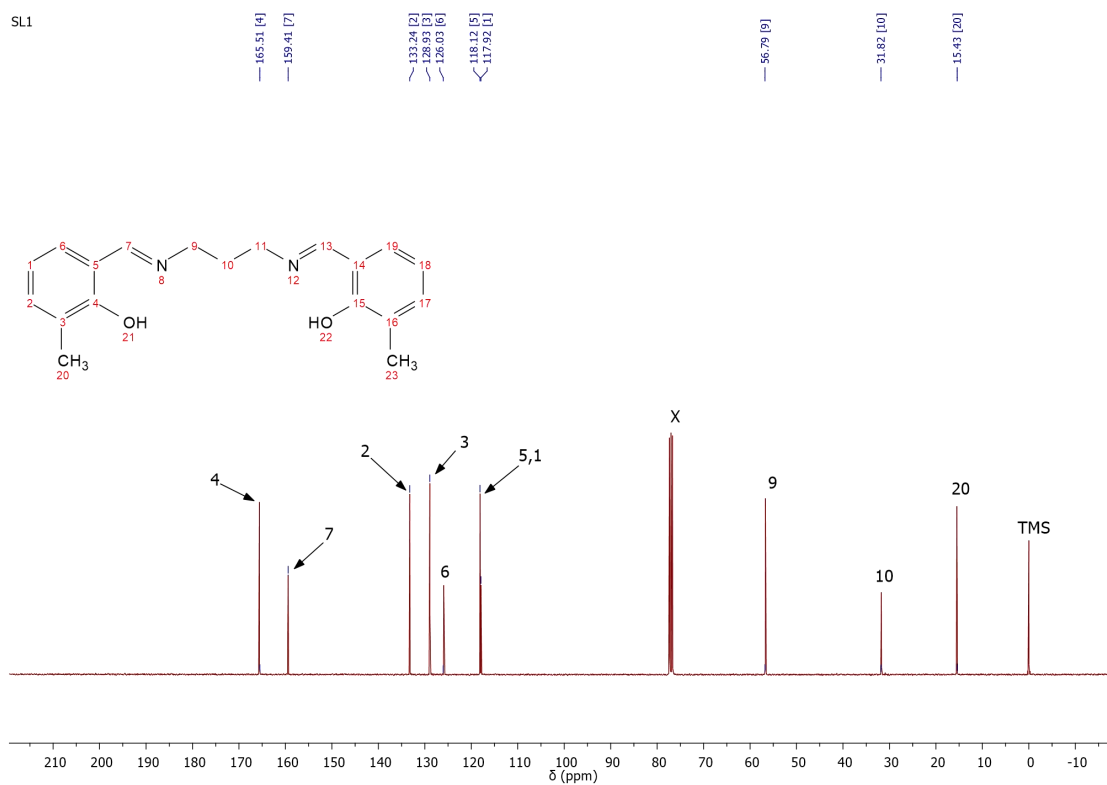


Figure 4.3: ^{13}C NMR for *N,O*-salicylaldimine ligand SL1 (\times solvent $\text{CDCl}_3\text{-d}_1$)

Table 4.4: ^{13}C NMR spectral data (δ in ppm) for SL1 – SL8 in CDCl_3

Ligand	$\delta(\text{HC=N})$	$\delta(\text{C-OH})$
SL1	159.41	165.51
SL2	158.87	165.52
SL3	165.17	155.38
SL4	157.61	164.09
SL5	160.24	164.28
SL6	159.68	164.38
SL7	159.54	165.10
SL8	158.98	164.94

The signals for the significant imine carbons (C=N) exhibited an upfield shift in comparison with the corresponding aldehyde carbons as expected because it experienced an increase in electron density, clearly confirming the successful synthesis of the salicylaldimine ligands. The carbon signals for the salicylaldimine phenolic ring for **SL1** appeared between 117.92 to 133.24 ppm while generally for all the ligands in this work were observed in the range 109.89 – 151.98 ppm in close comparison with reported work (Ananthi *et al.*, 2010; Naeimi & Rabiei, 2007; Naeimi *et al.*, 2007). In all the ligands, the peaks that appeared in the chemical shift range of 155.16 – 176.21 ppm are attributed to the aromatic carbon bound to the phenolic oxygen. The carbon chemical shift signal for the propylene linker exhibited at 31.82 and 56.79 ppm are characteristic of aliphatic carbons, while the carbon signal for methyl substituent on the ring appeared at 15.43 ppm (Figure 4.3). The propylene, butylene and pentylene linkers (spacers) to the imine nitrogen exhibited peaks in the range 15.42 – 59.42 ppm for all the ligands synthesized in this work which is consistent with similar compounds reported in literature (Borhade & Waghmode, 2008).

There were observed similarities in the chemical shifts of the phenolic carbon for some ligands in this work. For instance, the chemical shifts for the phenolic carbon of **SL1** and **SL2** appeared at 165.51 and 165.52 ppm (Table 4.4), respectively. This can be attributed to the presence of the methyl (-CH₃) substituent on the phenolic ring, though at different positions, that is, at *ortho* and *para* to the hydroxyl group. The ligands **SL3**, **SL9** and **SL14** had their absorption peaks for phenolic carbon were close at 155.38, 151.98, and 151.93 ppm, respectively. All the three ligands; **SL3**, **SL9** and **SL14** have a methoxy (-OCH₃) substituent, *para* to the phenolic carbon. The methoxy substituent – being an electron donating group – is likely to have increased electron density on the ring, shielding the phenolic carbon and therefore causing an upfield chemical shift

for these ligands. Other ligands with close chemical shifts are; **SL4**, **SL5** and **SL6** with the phenolic carbon at approximately 164 ppm deshielded downfield. This is likely caused by the presence of Cl and Br on the ring, which are strong electron withdrawing groups (EWG). The ^1H and ^{13}C chemical shifts (δ) in ppm for all the ligands are summarised in section 3.3 chapter three of this work.

4.2.4 Elemental Analysis and Mass Spectroscopy of SL1 – SL17

The elemental analysis for all the *N,O*-salicylaldimine ligands in this work were found to be in agreement with the formulation of the compounds. No solvent inclusion was observed due to thorough recrystallization of the ligands before microanalysis. The elemental analysis data for all the compounds are summarised in section 3.3 of chapter three of this thesis.

Electrospray ionisation mass spectrometry (ESI-MS) further confirmed the successful synthesis of the ligands as the molecular parent ions $[\text{M}]^+$ were observed for the respective ligands. Figures 4.4 and 4.5 shows a typical mass spectrum for **SL2** that exhibits a clear molecular ion parent peak for the ligand at $m/z = 310$. Possible fragmentation pattern of the ligand is shown in Scheme 4.3, with first fragmentation of a hydroxyl ion appended to the benzene ring resulting to $m/z = 293$ ion peak. This is followed by the loss of $-\text{C}_9\text{H}_9\text{N}$ showing an ion peak attributed at $m/z = 162$. Further fragmentation resulted in the loss of $-\text{C}_2\text{H}_2$ which leaves an ion peak at $m/z = 134$.

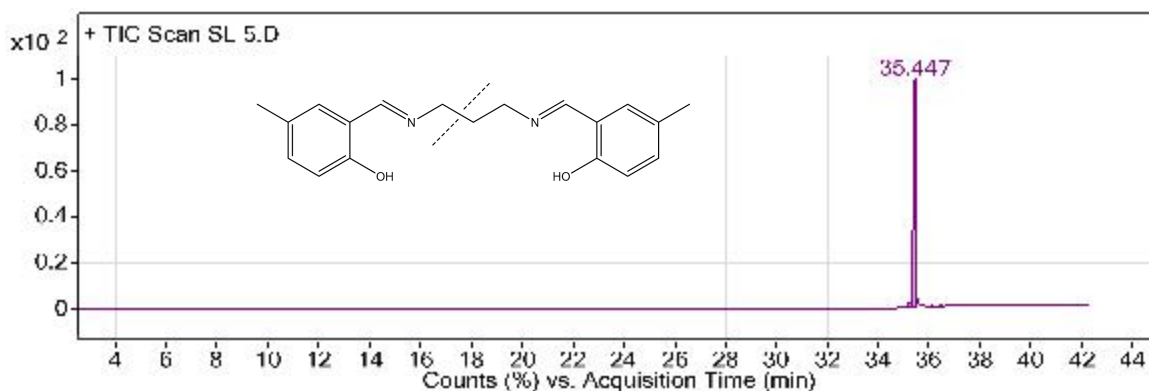


Figure 4.4: Chromatogram retention time for the molecular ion of SL2

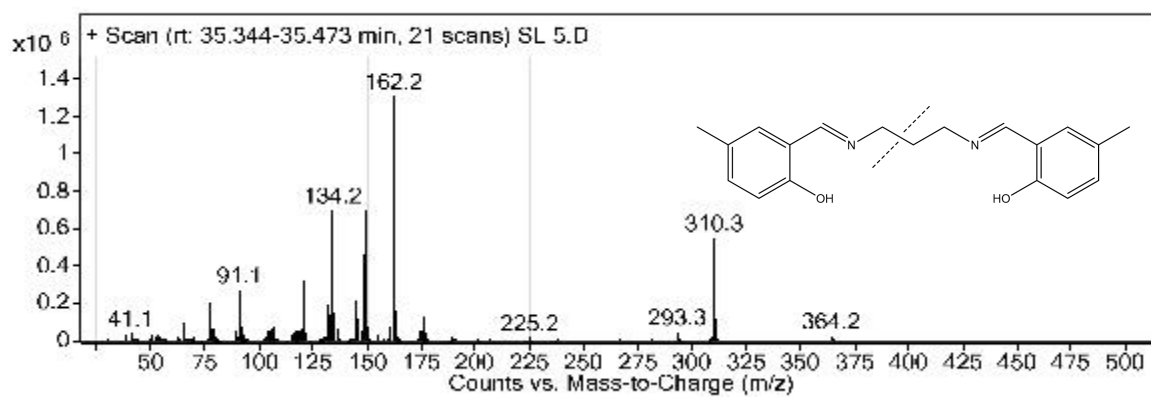
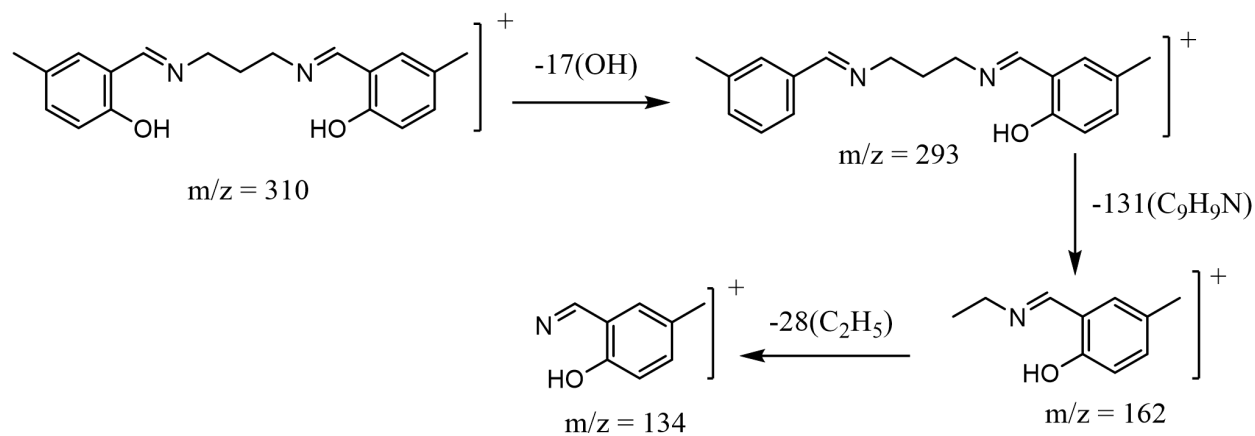


Figure 4.5: Fragmentation peaks for the ligand SL2



Scheme 4.3: Possible fragmentation pattern for SL2

The ESI-MS molecular weight ion peaks for the ligands **SL1**, **SL3** – **SL17** were observed at $m/z = 310$, 342, 509, 440, 350, 324, 324, 356, 454, 364, 338, 338, 370, 537, 468, and 379 $[M + H]^+$, respectively.

4.3 Single X-ray structure studies of the ligands

4.3.1 Crystal and molecular structures of salicylaldimine **SL2**, **SL3**, **SL6** and **SL9**

Single crystals suitable for single X-ray diffraction (XRD) studies for **SL2**, **SL3**, **SL6** and **SL9** were obtained after two to four weeks by slow diffusion and evaporation of hexane into a concentrated solution of the ligands in DCM.

The single-crystal structures of the salicylaldimine **SL2**, **SL3**, **SL6** and **SL9** authenticated the molecular composition of these Schiff bases. The complete data for the salicylaldimine ligands can be found in the Appendix E of this thesis.

The salicylaldimine ligand **SL3** crystallized in the triclinic crystal system with cell angles; $\alpha = 73.941(1)$, $\beta = 86.172(1)$ and $\gamma = 89.419(1)^\circ$, whilst cell dimensions were; $a = 9.3671(1)$, $b = 10.3955(1)$ and $c = 18.7666(2) \text{ \AA}$ and space group $P\bar{1}(2)$ with four molecules per unit cell. From the structural formula, the molecule is symmetrical. However, there was an observed kind of distortion around one of the C=N, imine bond angles. Both halves of the molecule are expected to be identical and on the same plane of symmetry. Nevertheless, to minimize energy during crystal formation half of the molecule had to orientate on a rather different plane as depicted in the ORTEP structure in Figure 4.7. The C(8)–N(1)_{imine}–C(9) and C(11)–N(2)_{imine}–C(12) bond angles were found to be $119.6(1)$ and $118.7(1)^\circ$, respectively. Further, the C(8)–N(1)_{imine} and C(12)–N(2) bond lengths, $1.279(2)$ and $1.276(2) \text{ \AA}$, respectively for **SL3**, were reported to be within the expected limit comparable to $1.290(2)$ and $1.459(3)$ in reported literature (Nazir *et al.*,

2006). The presence of the salicyl-*OH* functionality in the ligand was confirmed by the observed intramolecular hydrogen bond N1...OH, 2.583(1) and N2...OH, 2.599(1) Å between the salicyl-*OH* and the imine nitrogen, similar to what is reported in literature (Ha, 2012; Xue *et al.*, 2013). The molecular structures are depicted below in Figure 4.6.

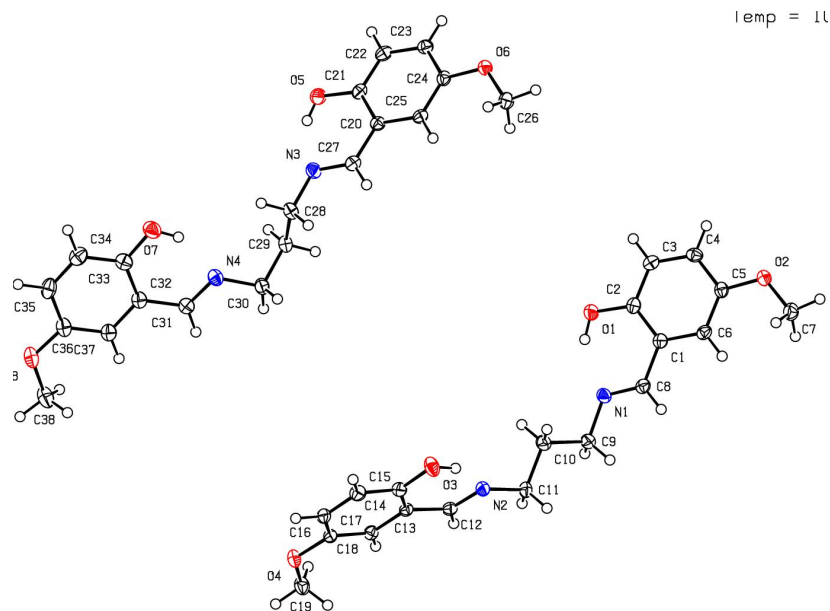


Figure 4.6: ORTEP representation of molecular ligand SL3. Thermal ellipsoids are drawn at the 50 % probability level.

The crystal packing diagram for *N,O*-salicylaldimine **SL3** is shown in Figure 4.7.

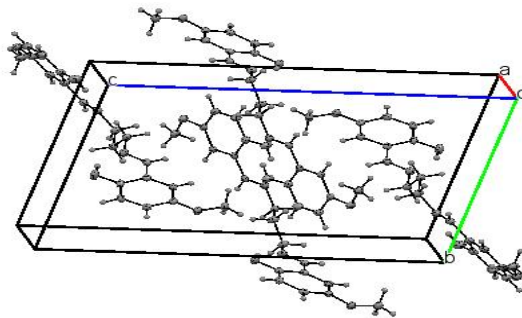


Figure 4.7: Crystal packing diagram for the ligand SL3

The summary of the crystallographic data collection and structure refinement residuals for **SL2**, **SL3**, **SL6** and **SL9** are given in Table 4.5.

Table 4.5: Crystal data structure refinement for ligands SL2, SL3, SL6 and SL9

	SL2	SL3	SL6	SL9
Bond precision C-C,	0.0020,	0.0018,	0.0028,	0.0030,
Wavelength	1.54178	1.54178	1.54178	1.54178
Formula	C ₁₉ H ₂₂ N ₂ O ₂	C ₁₉ H ₂₂ N ₂ O ₄	C ₁₇ H ₁₆ Cl ₂ N ₂ O ₂	C ₂₀ H ₂₄ N ₂ O ₄
Formula weight	310.38	342.39	351.22	365.41
Crystal system,	Monoclinic,	Triclinic,	Monoclinic,	Monoclinic,
Space group	<i>P</i> 2 ₁ / <i>c</i>	<i>P</i> Γ(2)	<i>P</i> 2 ₁ / <i>n</i>	<i>P</i> 2/1
Cell dimensions (<i>a</i> ,	19.3063(4),	9.3671(1),	11.2485 (5),	11.0474(3),
<i>b</i> ,	5.8320(1),	10.3955(1),	8.8712 (4), 16.6121	6.0853(2),
<i>c</i>) [Å]	14.7996(3)	18.7666(2)	(8)	13.9881(4)
Cell angles (α ,	90,	73.941(1),	90,	90,
β , γ)	92.715(1), 90	86.172(1), 89.419(1)	95.117(3), 90	104.271(2), 90
F 000	664.0	728.0	728.0	380.0
F 000'	665.91	730.29	732.71	381.18
<i>h</i> , <i>k</i> , <i>l</i>	22, 6, 17	11, 12, 22	13, 10, 19	13, 7, 16
V/Å ³	1664.48(6)	1752.12	1651.08 (13)	911.36 (5)
<i>Z</i>	4	4	4	2
Temperature (K)	100	100	100	100
D _x (g cm ⁻³)	1.239	1.298	1.413	1.299
μ (mm ⁻¹)	0.643	0.750	3.627	0.741
Theta, θ range for data collection (deg.)	66.811	69.281	66.634	66.629
no. of refinement meads	2818	6276	2907	2698
no. of reflections used (<i>R</i> _{int})	213	460	210	241
no. of params observed data $R [I >$ $2\sigma(I)]$				
<i>R</i> ₁ (reflections)	0.0423 (2575)	0.0339 (5384)	0.0366 (2488)	0.0290 (2539)
w <i>R</i> ₂ (reflections)	0.1102 (2818)	0.0894 (6276)	0.103 (2907)	0.0727 (2698)
Min. Max. Resd.	0.772, 0.875	0.757, 0.862	0.274, 0.686	0.835, 0.961
Dens. [e/Å ³]				

The data for selected bond angles for the *N,O*-salicylaldimine ligand **SL3** are summarised in Table 4.6 while the bond lengths are shown in Table 4.7, respectively.

Table 4.6: Selected bond angles (°) for SL3

SL3	Bond angles (°)
C12 – N2 _{imine} – C11	118.7(1)
C9 – N1 _{imine} – C8	119.6(1)
H19A – O4 – C17	104.62
C14 – O3 – H3	109.5
C17 – C18 – C13	120.4(1)
C17 – C16 – C15	120.5(1)
C14 – C15 – C16	120.6(1)

Table 4.7: Selected bond lengths (Å) for SL3

SL3	Bond lengths (Å)
C12 – N2 _{imine}	1.276(2)
C11 – N2 _{imine}	1.461(1)
C9 – N1	1.456(2)
C8 – N1 _{imine}	1.279(2)
O3 – N2 _{imine} (H...N)	2.599 (1)
O1 – N1 _{imine} (H...N)	2.583(1)
C17 – C16	1.398(2)
C16 – C15	1.379(2)
C15 – C14	1.394(2)

The compound **SL9** shown in Figure 4.8 was observed to be in the monoclinic crystal system with cell dimensions, $a = 11.0474(3)$, $b = 6.085(2)$ and $c = 13.9881(4)$ Å, while angles $\alpha = \gamma = 90^\circ$ and $\beta = 104.271(2)^\circ$. The compound crystallized in the space group $P2_1/1$ (Table 4.5). From

the crystal structure (Figure 4.8) **SL9** is non-centrosymmetric, as was also observed by other researchers (Ashwell, 1999; Ledoux *et al.*, 1990; Spek & Van Der Sluis, 1990) which means that it is an enantiomer. Similar to **SL3**, the **SL9** exhibited intramolecular H-bonding N1...OH, 2.584(2) and N2...OH, 2.595(2) Å between the salicyl-OH and the imine nitrogen which is within the range of those reported in literature (Steiner, 2002). The imine nitrogen bond angles C8 – N1 – C9 and C13 – N2 – C12 were found to be 118.2(2) and 117.6(2) °, respectively. Furthermore, the C5 – C4 – C3, C5 – C6 – C1 bond angles on the benzene ring were 121.0(2) and 120.2(2) °, respectively. The carbon bond angles on the butylene linkers, C9 – C10 – C11 and C10 – C11 – C12 were found to be 111.7(2) and 111.6(2) °, respectively, which are close to those in reported work (Fonseca *et al.*, 2010). Moreover, bond angles of the methoxy oxygen with neighbouring carbons, C18 – O4 – C2 and C5 – O2 – C7 were 117.2(2) and 117.1(2) °, respectively. The complete data for bond angles and bond distances are shown in Appendix E of this thesis.

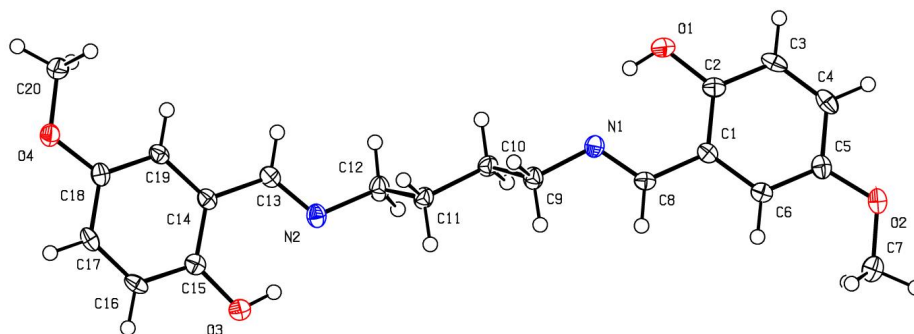


Figure 4.8: ORTEP representation of molecular ligand SL9. Thermal ellipsoids are drawn at the 50 % probability level

The packing diagram for the *N,O*-salicylaldimine ligand **SL9** is shown in Figure 4.9 while selected bond angles and bond lengths are displayed in Tables 4.8 and 4.9, respectively.

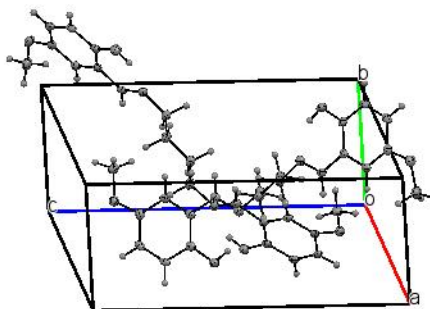


Figure 4.9: Crystal packing diagram for the ligand **SL9**

Table 4.8: Selected bond angles (°) for **SL9**

SL9	Bond angles (°)
C7 – O2 – C5	117.1(2)
C5 – C4 – C3	121.0(2)
C5 – C6 – C1	120.2(2)
O1 – C2 – C1	121.9(2)
C8 – N1 – C9	118.2(2)
C10 – C11 – C12	111.6(2)
C13 – N2 – C12	117.6(2)
H20C – O4 – C18	99
C14 – C15 – O3	122.3(2)

Table 4.9: Selected bond lengths (Å) for SL9

SL9	Bond lengths (Å)
O2 – C5	1.374(3)
O1 – N1	2.584(2)
C4 – C3	1.378(3)
C6 – C1	1.405(3)
N1 – C8	1.283(3)
C13 – N2	1.283(3)
O1 – C2	1.356(3)
C9 – C10	1.515(3)
C11 – C12	1.521(3)
O4 – C18	1.377(3)

The molecular ligand **SL2** in Figure 4.10 crystallized in the space group $P 2_1/c$ and is in the monoclinic crystal system (Table 4.5) in which case $\alpha = \gamma = 90^\circ$ while $\beta = 92.715(1)^\circ$ with cell dimensions, $a = 19.3063(4)$, $b = 5.8320(1)$ and $c = 14.7996(3)$ Å. From Figure 4.10, the bond angles for $C8 - (N1)_{\text{imine}} - C9$ and $C11 - (N2)_{\text{imine}} - C12$ were observed to be $118.8(1)$ and $119.0(1)^\circ$, respectively. The aromatic carbons bond angles $C2 - C3 - C4$ and $C4 - C6 - C7$ were observed at $121.9(1)$ and $122.6(1)^\circ$. The variation between these bond angles is attributed to the resonance properties exhibited by the benzene ring being an aromatic molecule with the appended imine, $-C=N$, group, which was also observed by other researchers in similar ligands (Bohm & Exner, 2004; Campanelli *et al.*, 2006; Campanelli *et al.*, 2008). Bond distances for $C12 - N2$ and $O2 - C14$ were found to be $1.274(2)$ and $1.352(2)$ Å, respectively. Moreover, **SL2**

exhibited H-bonding as well between the phenolic oxygen and the imine nitrogen, HO1...N1 and HO2...N2 at 2.593(2) and 2.599(2) Å, respectively, which was similar to an observation made by another research report (Steiner, 2002).

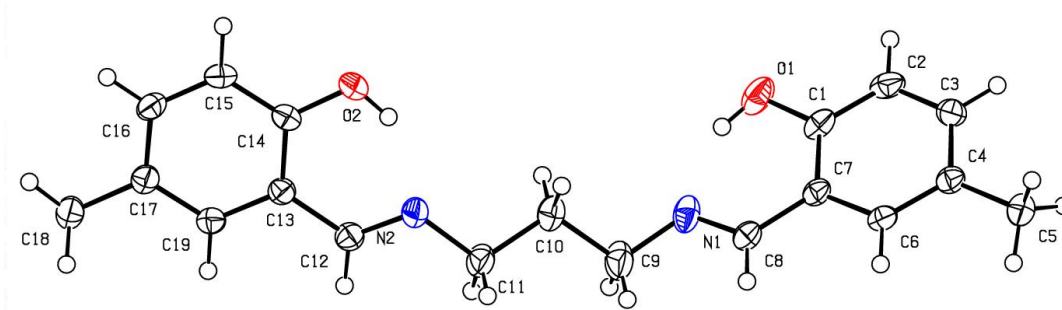


Figure 4.10: ORTEP view of molecular ligand SL2

The crystal packing diagram for *N,O*-salicylaldehyde ligand **SL2**, Figure 4.11 indicates four molecules per cell unit, as also observed in reported research for a similar compound (Xue *et al.*, 2013).

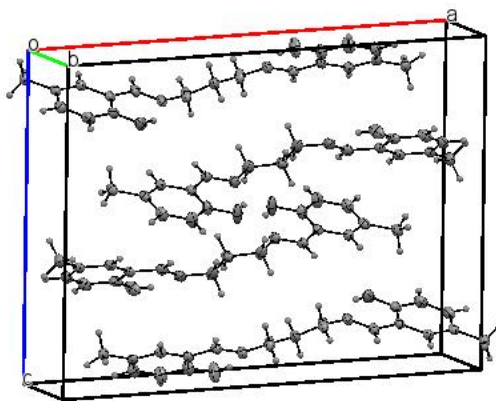


Figure 4.11: Crystal packing diagram for SL2

A summary of the selected bond angles and bond distances for *N,O*-salicylaldimine ligand **SL2** are depicted in Tables 4.10 and 4.11, respectively.

Table 4.10: Selected bond angles (°) for SL2

SL2	Bond angles (°)
C8 – N1 – C9	118.8(1)
C11 – N2 – C12	119.0(1)
C9 – C10 – C11	112.2(1)
O1 – C1 – C7	121.5(1)
C4 – C6 – C7	122.6(1)
C2 – C3 – C4	121.9(1)
C5 – C4 – C6	121.6(1)
O2 – C14 – C13	121.4(1)
O1 – N1 – C8	89.0(1)

Table 4.11: Selected bond lengths (Å) for SL2

SL2	Bond lengths (Å)
O2 – C14	1.352(2)
C14 – C13	1.407(2)
C16 – C17	1.392(2)
C13 – C19	1.395(2)
C12 – N2	1.274(2)
O10 – C11	1.516(2)
O1 – N1	2.593(2)
C12 – C13	1.458(2)
O1 – H1	0.840
C17 – C18	1.503(2)
O2 – N2	2.599(2)

The salicylaldimine ligand **SL6** in Figure 4.12 with chlorine substituent at the *para* position to the hydroxyl group on the phenolic ring, was also reported in the monoclinic crystal system (Table 4.5) with cell dimensions $a = 11.2485(5)$, $b = 8.8712(4)$ and $c = 16.6121(8)$ Å. Whilst the cell angles were $\alpha = \gamma = 90^\circ$ and $\beta = 95.117(3)^\circ$. The compound crystallized in the space group $P 2_1/n$ (Table 4.5). This ligand exhibited both intramolecular H-bonding N1...OH, 2.91(2) and intermolecular H-bonds Cl1...OH, 3.110(1) Å, comparable to those in reported research work (Ha, 2012; Nazir *et al.*, 2006; Xue *et al.*, 2013). The bond angles around the imine nitrogen, C7 – N1 – C6 and C10 – N2 – C9 were 118.4(2) and 119.2(2) °, respectively. The bond angles in the phenolic ring carbons, C2 – C3 – C4 and C2 – C1 – C5 were found to be 120.8(2) and 120.0(2) ° in that order, and are in close comparison to other researched work (Bilge *et al.*, 2009). The bond angles involving chlorine substituents *para* to the hydroxyl group on the benzene ring, C12 – C15 – C16 and C12 – C15 – C14 were 119.7(1) and 119.1(1) ° in that respect.

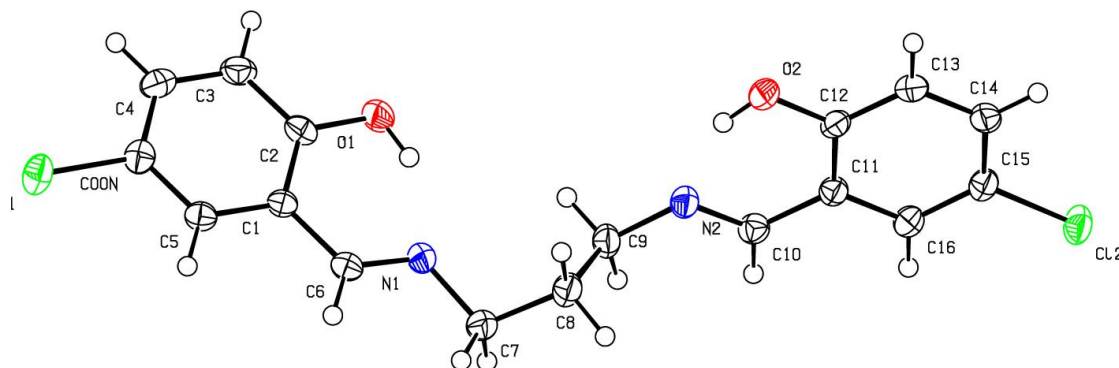


Figure 4.12: ORTEP representation of molecular ligand SL6. Thermal ellipsoids are drawn at the 50 % probability level

The *N,O*-salicylaldimine ligand **SL6** contains four molecules per unit cell as shown in Figure 4.13 packing diagram which is comparable to the ones reported in literature (Xue *et al.*, 2013).

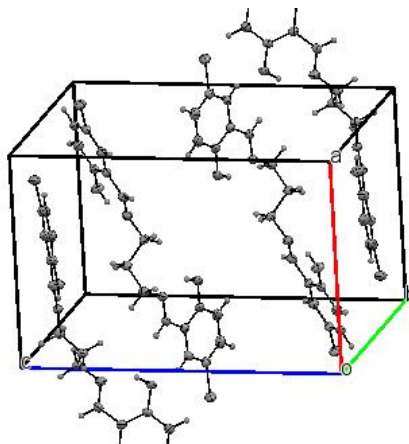


Figure 4.13: Crystal packing diagram for the ligand SL6

Some selected bond angles are shown in Table 4.12 while bond distances are displayed in Table 4.13.

Table 4.12: Selected bond angles (°) for SL6

SL6	Bond angles (°)
C12 – C15 – C14	119.1(1)
C15 – C16 – C11	119.9(2)
C14 – C13 – C12	120.0(2)
O2 – C12 – C11	120.7(2)
C10 – N2 – C9	119.2(2)
C9 – C8 – C7	112.3(2)
C7 – N1 – C6	118.4(2)
C11 – C00N – C5	119.5(1)
O1 – C2 – C3	118.9(2)
C6 – C1 – C2	120.7(2)

Table 4.13: Selected bond lengths (Å) for SL6

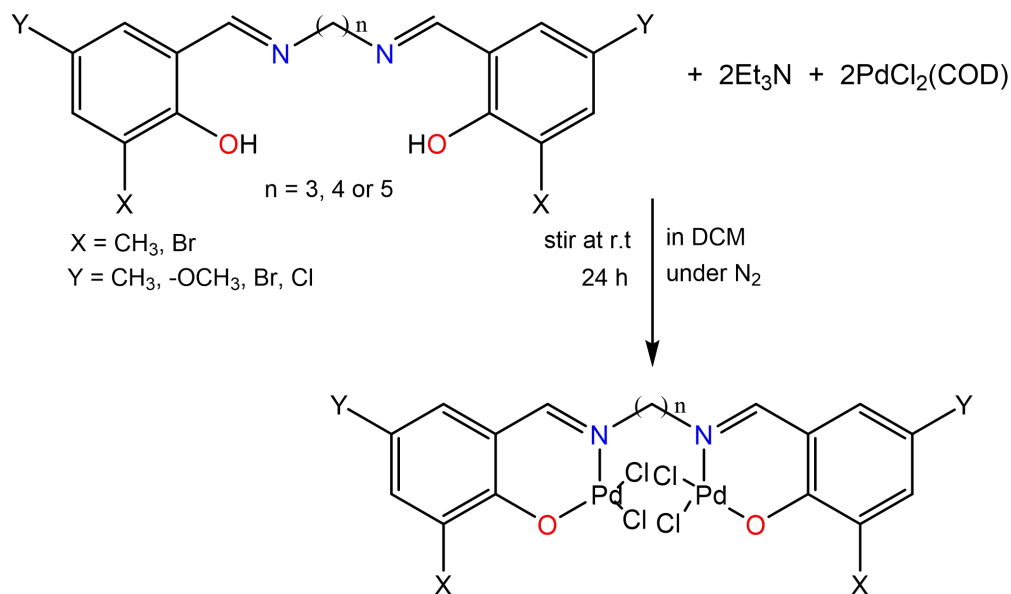
SL6	Bond distances (Å)
C11 – C00N	1.747(2)
C5 – C00N	1.381(3)
C5 – C1	1.394(3)
C2 – O1	1.347(2)
C6 – N1	1.270(2)
C1 – C6	1.461(2)
C7 – C8	1.518(3)
N2 – C10	1.277(2)
C9 – N2	1.458(2)
C12 – C15	1.747(2)
O2 – C12	1.352(2)
C11 – C16	1.395(3)

4.4 Synthesis and characterisation of *N,O*-salicylaldimine Pd(II) complexes C1 – C10

4.4.1 Introduction

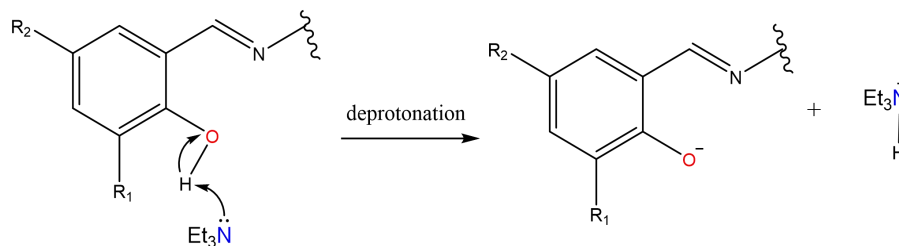
The synthesis of the title complexes began with synthesis of the suitable metal precursor complex PdCl₂(COD) following modified protocols from reported literature (Motswainyana *et al.*, 2011). The metal precursor complexes were subsequently reacted with the respective ligands.

The general procedure for synthesizing palladium complexes is as shown in Scheme 4.4.



Scheme 4.4: Synthesis of *N,O*-salicylaldimine palladium(II) complexes C1 – C10

As depicted in the reaction Scheme 4.4, the use of the weak base triethylamine (Et_3N) was intended to deprotonate (Scheme 4.5) the ligand, to create a coordinatively unsaturated position where the palladium metal ion will coordinate when introduced during the reaction. The complexes were isolated as solids with light-yellow, yellow or orange colours in yields ranging between 43 to 95%, as already mentioned in chapter three of this work. The low yields exhibited by complexes **C1**, **C4** and **C8** occurred during the process of purifying via recrystallization method. These complexes decomposed at temperatures between 129 and 160 °C. One of the notable challenges with the synthesized palladium complexes in this work was solubility. Some complexes were insoluble in all the common solvents like chloroform, DCM, and DMSO. Therefore, they could not be analysed using NMR spectroscopy. The formation of the Pd(II) complexes were confirmed by infrared (FTIR), ^1H , and ^{13}C NMR spectroscopy.



Scheme 4.5: Reaction mechanism for deprotonation of *N,O*-salicylaldimine ligand

4.4.2 Infrared spectroscopy for Pd(II) complexes **C1** – **C10**

The FTIR stretching frequencies were studied to give in-depth understanding of the complexes and help confirm coordination of palladium metal with the ligands. This was done by monitoring the stretching vibrational frequencies of the significant functional groups that are proposed to be involved in the chelation to the metal atom/ion centres. The characteristic $\nu(\text{C}=\text{N})$ IR stretching frequencies for the Pd(II) complex **C1** showed a blue shift of 12 cm^{-1} from 1623 cm^{-1} for the ligand **SL1** to 1611 cm^{-1} (Figure 4.15) upon coordination to the metal centre, an observation similar the one in reported research (Bourque *et al.*, 2005; Bowes *et al.*, 2011). The coordination of Pd(II) to the ligands was confirmed by a shift in the stretching frequencies of the imine $\nu(\text{C}=\text{N})$ moiety of the free ligands at $1623 - 1637\text{ cm}^{-1}$ to a lower stretching frequencies in the range of $1611 - 1622\text{ cm}^{-1}$. All the Pd(II) complexes **C1** to **C10** exhibited blue shifts of $\sim 6 - 18\text{ cm}^{-1}$ in agreement with observations made by a research team in similar compounds (Motswainyana *et al.*, 2011). The blue shift of $\nu(\text{C}=\text{N})$ absorption in the IR spectra can be attributed to the inactive $\nu(\text{C}=\text{N})$ stretching vibrational frequencies in the Pd(II) complexes as a result of coordination of the ligand to the metal centre. Additionally, reduction in electron density around the azomethine stretch $\nu(\text{C}=\text{N})$ arising from electron density being pulled away by the metal centre can be

ascribed to the negative shift, which is in agreement with a similar article in literature (Lutta & Kagwanja, 2000).

The absence of the broad hydroxyl (*OH*) band in the region 3100 to 3600 cm^{-1} of the IR of the metal complexes confirmed the deprotonation of the ligands and formation of the σ -bond with the metal ions in the coordination sphere as depicted in Figure 4.14. The imine $\nu(\text{C}=\text{N})$ stretching frequencies for the complexes **C1** – **C10** are summarised in Table 4.14.

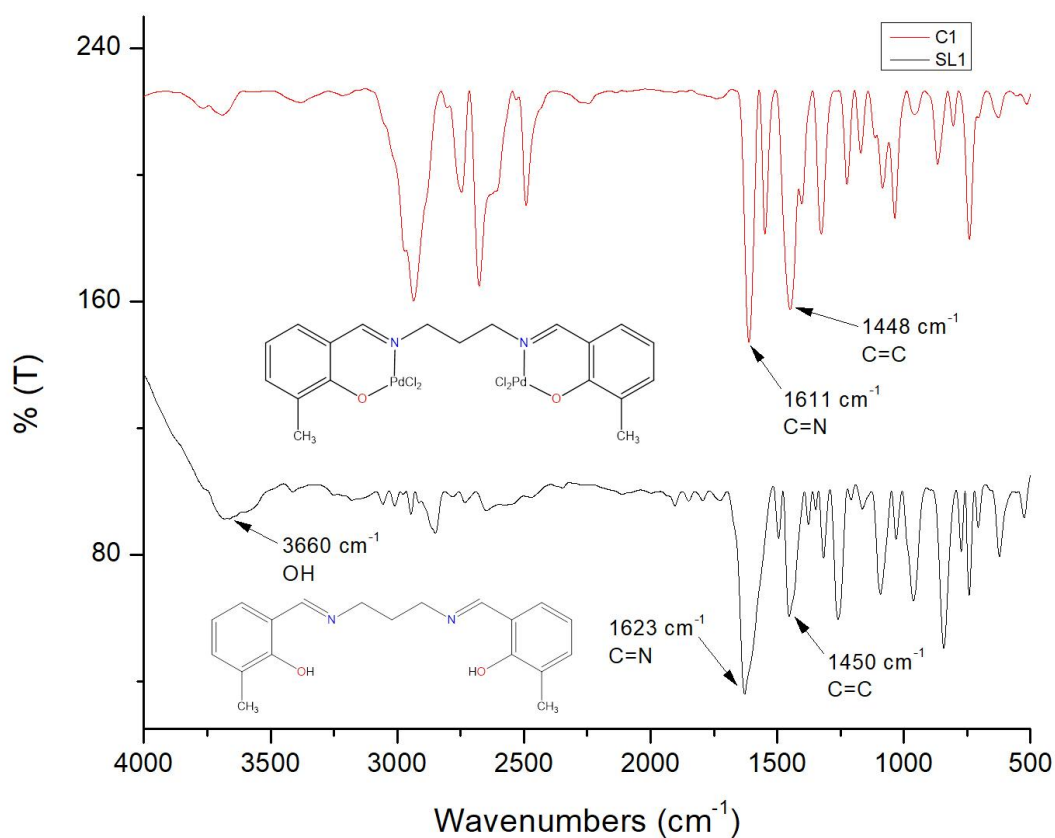


Figure 4.14: Comparison of FTIR spectra for the ligand SL1 with its complex C1

Table 4.14: $\nu(\text{C}=\text{N})$ stretching frequencies in wavenumbers (cm^{-1}) for complexes C1 – C10

Complex	% Yield	M. Point ($^{\circ}\text{C}$)	$\nu(\text{C}=\text{N})$
C1	43	138	1611
C2	95	137	1622
C3	90	155	1618
C4	51	146	1620
C5	60	141	1620
C6	90	144	1619
C7	95	159	1620
C8	47	143	1621
C9	95	129	1621
C10	94	160	1618

4.4.3 ^1H and ^{13}C NMR for Pd(II) complexes C1 – C10

The ^1H NMR for all the Pd(II) complexes exhibited the absence of hydroxyl (OH) proton peak at around 12.86 – 14.77 ppm, a confirmation of deprotonation and indicative of the successful participation of the phenolic O- atom in the coordination to the Pd(II) ion. A significant upfield shift in the ^1H NMR was observed for the methine proton of the salicylaldimine ligand from 8.32

ppm to 7.91 ppm upon coordination to the metal centre in **C2**, in agreement with the observation made for similar compounds as reported in some research work (Bowes *et al.*, 2011). This is depicted for **C2** in Figure 4.15. The methine proton in all palladium complexes exhibited an upfield shift from just above 8 ppm for the ligands to below 7.9 ppm for the complexes. There was a general upfield shift in the range of 1.15 – 2.60 ppm observed in all the complexes for the protons, in the propylene, butylene, and pentylene linkers adjacent to the imine functionality, in comparison with absorptions observed in the corresponding ligands. This can be attributed to the influence caused by the presence of the metal ion in the coordination sphere.

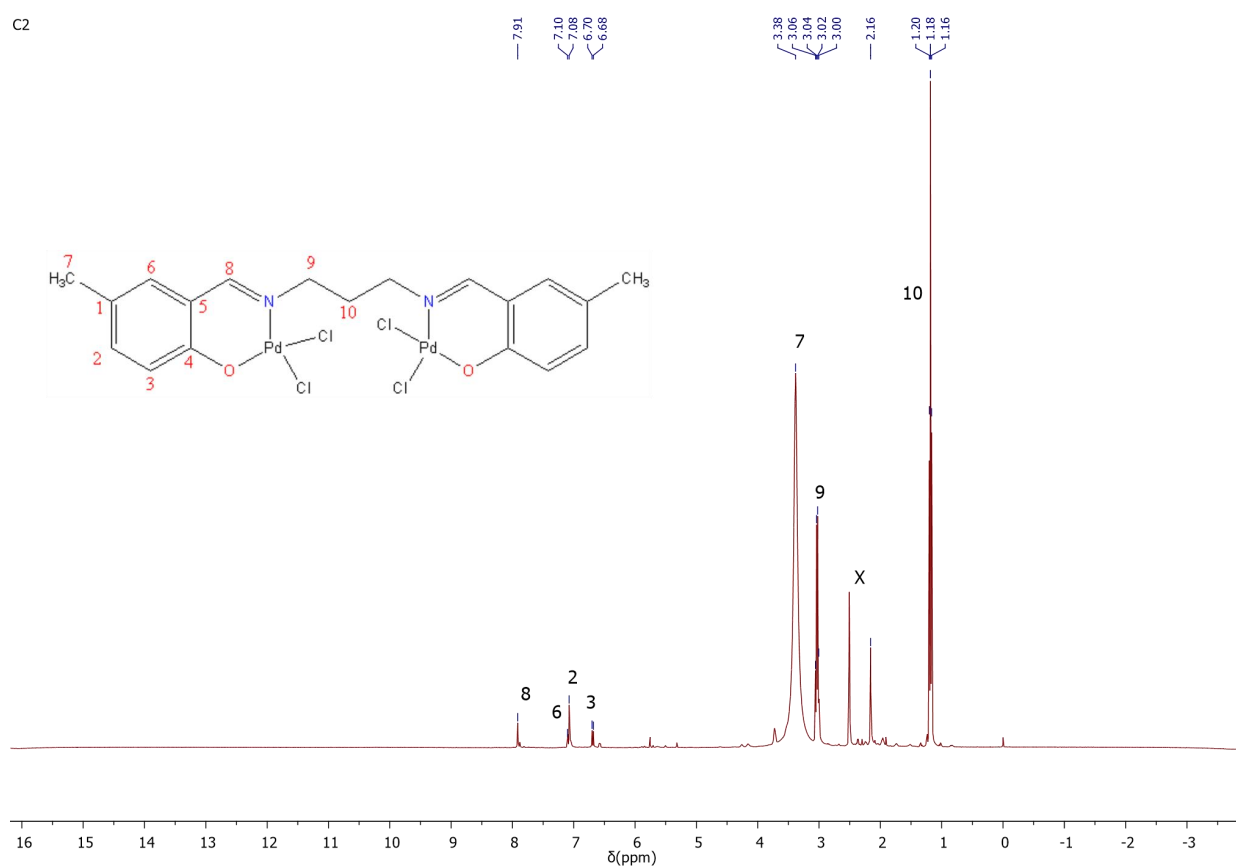


Figure 4.15: ^1H NMR spectrum for complex **C2** (x solvent DMSO- d_6)

In the ^{13}C NMR spectrum, the imine carbon signal for **C2** underwent a downfield shift from its corresponding ligand **SL2** with a shift from 158.87 ppm to 163.59 ppm (Figure 4.16). This shift is consistent with coordination of palladium(II) metal ion to the salicylaldimine ligand and this can be confirmed by comparing it to a research report, where the downfield shift occurred from 160.00 ppm to 164.60 ppm for a complex similar to **C2** (Tardiff *et al.*, 2007). A significant upfield shift was observed on the C-O phenolic carbon which shifted from 165.57 ppm to 162.70 ppm upon coordination to the Pd(II) metal ion. The propylene carbons exhibited an upfield shift from the range 31.86 – 56.97 ppm to 20.22 – 46.10 ppm in the complex. There was also an upfield shift for the methyl substituent on the phenolic ring from 20.42 ppm in the ligand to 8.93 ppm in the Pd(II) complex.

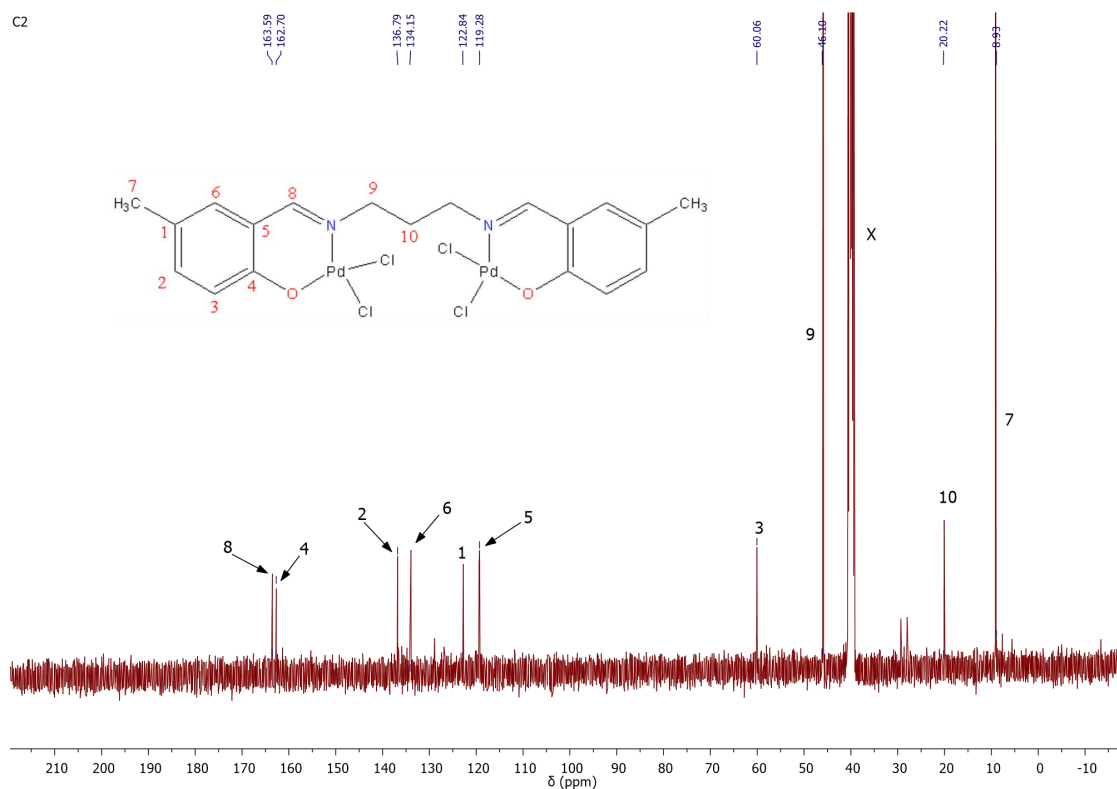


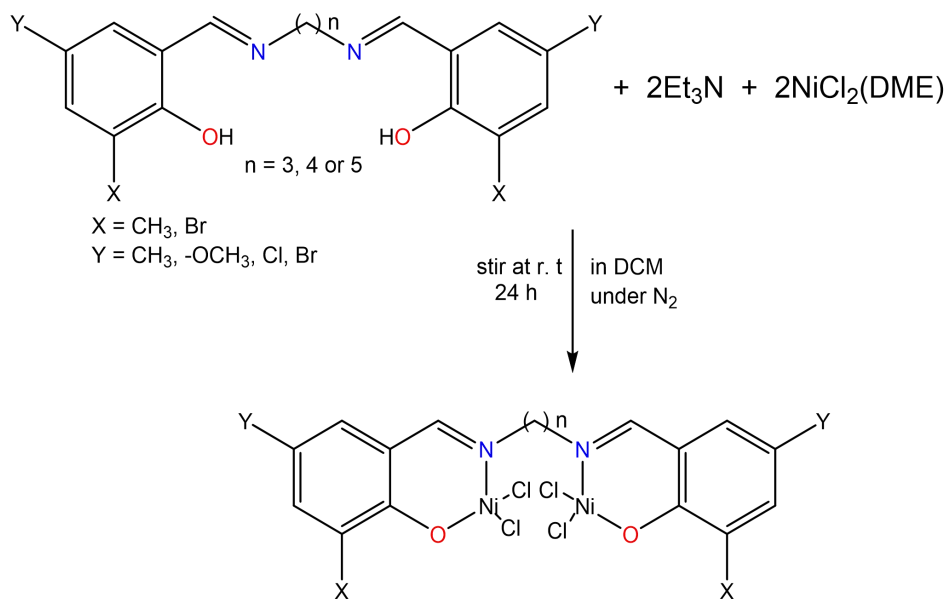
Figure 4.16: ^{13}C NMR spectrum for complex **C2** (x solvent $\text{DMSO-}d_6$)

Furthermore, ^{13}C NMR spectra for the *N,O*-salicylaldimine complexes **C1** – **C10**, showed the aromatic carbons in the region 104 – 148 ppm. The observed upfield chemical shifts of the imine carbons, phenolic carbons and the aromatic carbons were attributed to the influence caused by the chelation of the imine nitrogen and phenolic oxygen to the metal ions. In addition, the imine carbons were generally observed at approximately 163 ppm, while the propylene, butylene and pentylene linkers (spacers) carbons appeared in the range 20 – 60 ppm (Figure 4.16) in all the palladium complexes in this work.

4.5 Synthesis and characterisation of *N,O*-salicylaldimine Ni(II) complexes C11 – C15

4.5.1 Introduction

The nickel complexes were prepared first by synthesis of the precursor nickel metal complex $\text{NiCl}_2(\text{DME})$, following the protocol as reported earlier in the experimental section 3.4.11 of chapter three of this thesis. The nickel metal complexes were reacted with appropriate ligands following the procedure developed for synthesis of palladium complexes as explained in chapter 3. The general procedure for the synthesis of *N,O*-salicylaldimine nickel(II) complexes is depicted in Scheme 4.6. Nevertheless, it should be noted that, not all the ligands synthesized in this work were used for complexation of the Pd(II) and Ni(II) ions. The reason being the challenge of insufficient yield for some of the ligands.



Scheme 4.6: Synthesis of *N,O*-salicylaldehyde nickel(II) complexes C11 – C15

The complexes were isolated in good yields ranging from 76 to 95 %. Their melting (decomposing) temperatures were in the range 142 – 165 °C. Most of the nickel complexes exhibited a green colour while a few were light-yellow and were confirmed to be stable in both air and moisture. Like their palladium counterparts, some of the nickel complexes were not soluble in common solvents and could not therefore be characterized by NMR.

4.5.2 Infrared spectroscopy for Ni(II) complexes C11 – C15

The infrared spectroscopy was used to monitor coordination of nickel to the salicylaldehyde ligands. The stretching frequencies of the selected functional groups were used as indicators for coordination of nickel. The IR stretching frequencies of azomethine $\nu(\text{C}=\text{N})$ for **C11** exhibited a blue shift of 15 cm^{-1} , from 1623 for the free ligand **SL1** to 1608 cm^{-1} for the Ni(II) complex as

depicted in Figure 4.17. The stretching vibrational frequency shift for $\nu(\text{C}=\text{N})$ in the complex can be attributed to the movement of the electron density from the ligand to the metal coordination sphere and a change in the bond order around the azomethine $\text{C}=\text{N}$ group, in agreement with the observations made in reported research work (Lutta & Kagwanja, 2001).

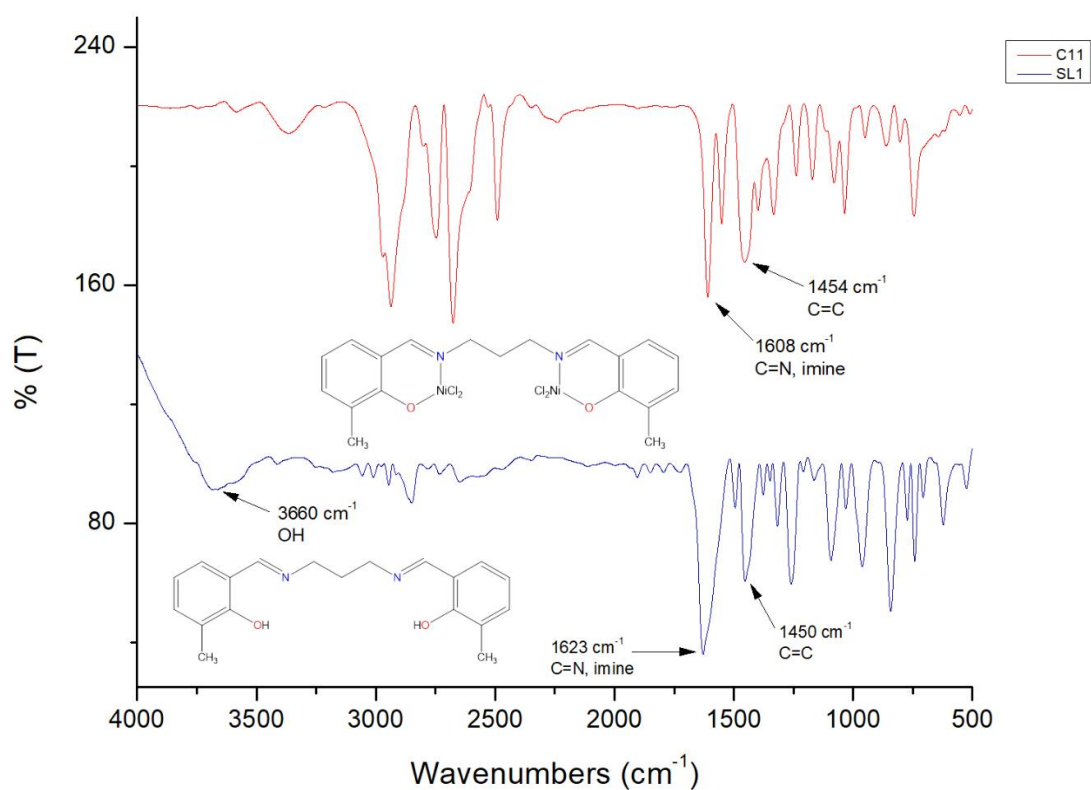


Figure 4.17: Comparison of FTIR spectra for the ligand SL1 with its complex C11

There was a clear shift of the stretching frequencies of the imine $\nu(\text{C}=\text{N})$ functionality to lower stretching vibrational frequencies which occurred in the range 1603 – 1627 cm^{-1} for all the nickel(II) complexes in this work. Generally, for all the Ni(II) complexes **C11** to **C15**, the

stretching frequencies showed a blue shift of between ~ 6 and 30 cm^{-1} upon coordination with the metal ion, in agreement with the observation made in reported research work (Kılınç *et al.*, 2018; Nejati & Rezvani, 2003). This confirmed the successful coordination of the ligands to the nickel metal atom. The complex **C13** showed a stretching frequency at 1627 cm^{-1} because of the presence of bromine, a good EWG at the ligand backbone, while **C15** exhibited a lower stretching vibrational frequencies at 1603 cm^{-1} due to the presence of methoxy ($-\text{OCH}_3$), a good EDG, in comparison with the other nickel complexes in this work. Figure 4.17 shows a typical FTIR spectrum of **C11**.

It is notable that the absence of the hydroxyl group stretching frequency at around the region 3100 to 3600 cm^{-1} of the ligand established the successful deprotonation of the hydroxyl functional group and subsequent chelation of the ligands to the nickel metal centre, in agreement with the observations made in reported literature (Naresh & Ramesh, 2005). The imine stretching frequencies for the *N,O*-salicylaldimine nickel(II) complexes **C11** – **C15** are summarised in Table 4.15.

Table 4.15: $\nu(\text{C}=\text{N})$ stretching frequencies in wavenumbers (cm^{-1}) for complexes **C11** – **C15**

Complex	% Yield	M. Point ($^{\circ}\text{C}$)	$\nu(\text{C}=\text{N})$
C11	90	142	1608
C12	95	153	1627
C13	76	144	1627
C14	78	148	1623
C15	90	165	1603

4.5.3 ^1H NMR for Ni(II) complexes **C11** – **C15**

The ^1H NMR spectra obtained for nickel(II) complexes exhibited similar chemical shifts in comparison with their palladium counterparts discussed in section 4.4.2. For instance, the hydroxyl (*OH*) proton peaks observed at 12.86 – 14.77 ppm in the salicylaldehyde ligands were remarkably absent from the peaks in nickel complexes. This evidently confirmed the deprotonation of the hydroxyl proton and participation of the phenolic oxygen in the coordination with the nickel metal atom. The imine proton (*H-C=N*) in complex **C11** characteristically absorbed at 7.26 ppm (Figure 4.18), an upfield shift from 8.26 ppm for the parent ligand **SL1**.

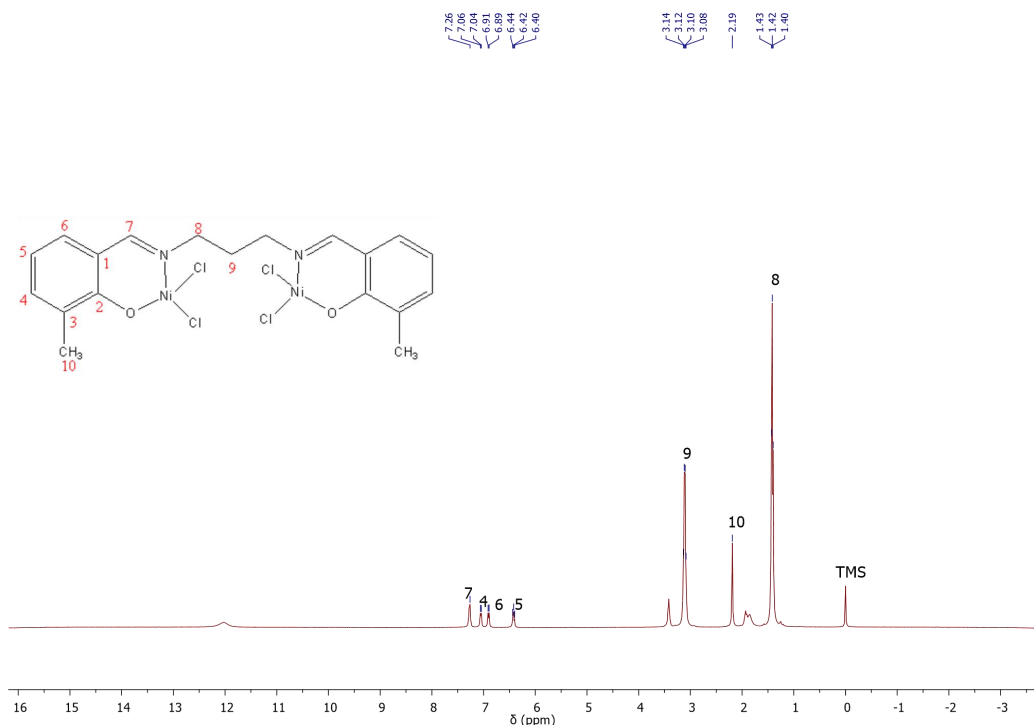


Figure 4.18: ^1H NMR spectrum for **C11**

The ^1H NMR spectra for the other nickel(II) complexes are shown in Appendix D.

All the complexes that were characterised in this work, also displayed a characteristic upfield shift for $H\text{-C=N}$ imine proton from slightly above 8 ppm in the parent ligand to below 7.52 ppm (Table 4.16), which can be attributed to the presence of nickel(II) ion in the coordination sphere with the imine nitrogen. Similarly, there was a general upfield chemical shift for the protons of the propylene, butylene and pentylene spacers in the range 1.17 – 3.70 ppm due to the influence of the nickel metal ion in the coordination sphere, in comparison with those for the corresponding ligands.

Table 4.16: ^1H NMR chemical shifts (δ in ppm) of imine protons for C11 – C15

Complex	$\delta(HC=N)$
C11	7.26
C12	7.28
C13	7.15
C14	7.52
C15	7.06

4.6 Catalytic application of the *N,O*-salicylaldimine complexes

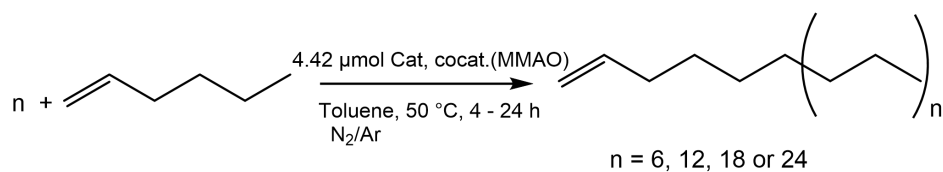
4.6.1 Introduction

Catalysis is a process by which a substance known as a catalyst speeds up a chemical reaction by lowering the activation energy of the process. The catalyst is not consumed or altered in the process. Catalysis has played an important role in the large-scale production of substances like liquid fuels and other synthetic products. The biggest percentage of catalysts in use today are made of organometallic compounds. Homogeneous catalysis – which is the focus in this work – has become increasingly popular in reactions such as oligomerisation. The end products in this work are known as oligohexenes ($C_{12} - C_{24}$) and polyhexenes ($C_{>24}$).

4.6.2 Hexene catalysis by palladium and nickel complexes

Of the fifteen nickel and palladium complexes synthesized, five nickel and four palladium complexes were tested in the 1-hexene oligomerisation reactions. Other complexes could not be tested because of low yields.

A trial reaction to establish the right temperature and time was done using palladium complexes (**C1** and **C5**) and nickel complex, **C11** at r.t and a time of 2 h. Later the temperature was adjusted progressively to 30 up to 50 °C, whilst the time was increased to between 4 and 24 h. During this period, reaction progress was monitored by sampling at a 4 – 6 h interval and ran a GC for the sampled product. The GC instrument compared the polymer products with its data base, and identified the presence of oligomers with C_{12} up to C_{24} as depicted in Scheme 4.7.



Scheme 4.7: Hexene oligomerisation using nickel and palladium complexes

The hexene-oligomer catalytic conversion for both nickel and palladium catalysts at room temperature and a time of 2 h was observed to be negligible, when sampled products were run on GC. However, raising the temperature to between 40 and 50 °C, and increasing the reaction time from 4 to 24 h, significant conversion of hexene monomer to hexene oligomers was observed as summarised in Tables 4.17 and 4.18.

With regard to palladium(II) complexes, **C2**, **C3**, **C5** and **C6**, the GC data for percentage conversion of 1-hexene to other oligomer products are shown in Table 4.17. All the palladium(II) complexes tested for 1-hexene oligomerisation showed some positive catalytic activity. The percent conversion of hexene to oligomers ranged between 11 – 73 % for a time range between 4 and 24 h. The percent conversions were calculated using the oligomer product amounts from GC together with the polymerisation reaction substrate amount.

Table 4.17: Percentage conversion of 1-hexene for Pd(II) salicylaldimine complexes C2, C3, C5 and C6

Catalyst	0 h (% conversion)	4 h	8 h	18 h	24 h
C2	0	26	15	47	56
C3	0	11	21	36	48
C5	0	44	46	51	54

C6	0	31	38	44	73
-----------	---	----	----	----	----

At 4 h, the palladium(II) catalyst **C3** showed the least catalytic activity at 11 % conversion, whilst **C5** was most active with 44 % conversion. After 24 h, **C6** exhibited the highest conversion at 73 %, while the least active catalyst was **C3** at 48 %.

A summary of the comparison for all palladium(II) complexes tested for 1-hexene oligomerisation activity is displayed in Figure 4.19. The catalytic activity of all the palladium(II) complexes tested increased in the order **C3** < **C2** < **C5** < **C6**. Generally, among the palladium(II) complexes tested in this work, **C3** showed the least activity in percent oligomer conversion (Figure 4.19). This can be attributed to the presence of a methoxy (-OCH₃), an electron donating group (EDG) at the ligand backbone, similar to observations made in reported work (Hu *et al.*, 2015). The EDG deactivates the metal active centre by releasing the electron density to the

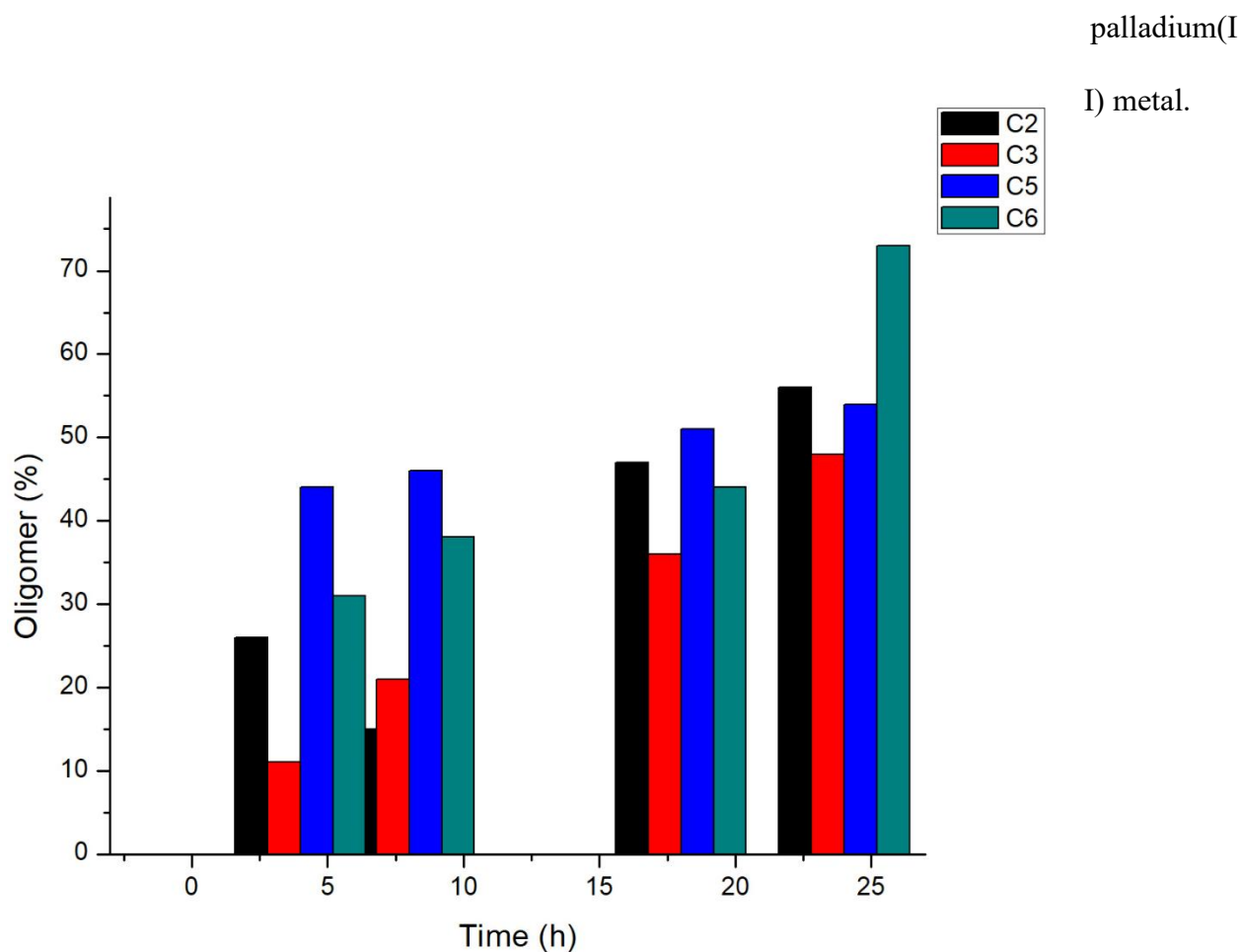


Figure 4.19: Catalytic conversion of hexene for palladium(II) complexes C2, C3, C5 and C6

The palladium(II) complex, C6 exhibited the highest catalytic conversion (Figure 4.19). This can be attributed to the presence of chlorine substituent *para* to the phenolic oxygen at the ligand backbone. The chlorine substituent is an EWG, in which case it withdraws or reduces the electron density from the metal active centre (Hu *et al.*, 2015), which in turn makes the metal centre more active towards hexene oligomerisation via a possible β -hydride elimination also reported in literature (Guo *et al.*, 2002; Svejda & Brookhart, 1999).

Even though both C5 and C6 have EWGs, the palladium(II) complex C5 has bromine substituent which is a weaker EWG than chlorine substituent on complex C6. This can be the possible reason why C5 showed less catalytic conversion activity in comparison with C6.

The oligomer percent conversion was obtained from the GC chromatogram amounts compared with the hexene substrate amounts used in the reaction. The GC data for percentage conversion of hexene – with nickel(II) complexes as catalyst – to other oligomer products are summarised in Table 4.18. The GC data obtained in Table 4.18 were from the established reaction temperature range and time.

Table 4.18: Percentage conversion of 1-hexene for Ni(II) salicylaldimine complexes C11 – C15

Catalyst	0 h (% conversion)	4 h	8 h	18 h	24 h
C11	0	27	39	36	61
C12	0	40	40	40	44
C13	0	38	49	60	68
C14	0	59	63	60	99
C15	0	30	31	33	51

Salicylaldimine nickel(II) complex, **C14** remarkably exhibited the highest catalytic conversion at 99 %, while **C12** was observed to be the least 44 % after 24 h. The catalytic activity for all the nickel(II) complexes tested in this work increased in the order **C12** < **C15** < **C11** < **C13** < **C14**. The comparison in catalytic conversion of 1-hexene using *N,O*-salicylaldimine nickel(II) complexes, **C11** – **C15**, in this thesis is displayed in Figure 4.20.

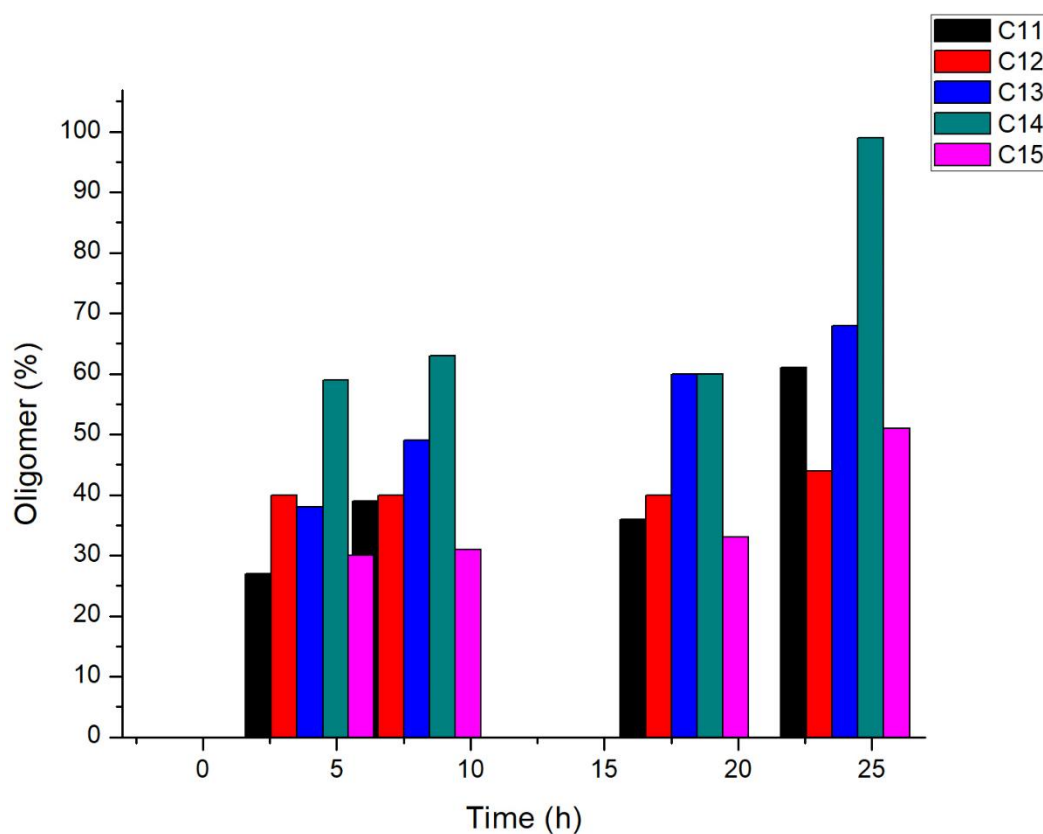


Figure 4.20: Catalytic conversion of hexene for nickel(II) complexes C11 – C15

The highest catalytic conversion displayed by **C14** can be attributed to the presence of bromine substituent on the phenolic ring at the ligand backbone, which is an EWG, a similar observation was made in reported work (Carlini *et al.*, 2004). The bromine substituent being strongly electronegative, withdraws electron density from the active metal centre, hence making it more active towards hexene oligomerisation possibly via β -hydride elimination as observed in reported work (Antonov *et al.*, 2016). Nickel(II) complex **C12**, on the other hand showed the least catalytic conversion of hexene which can be attributed to the presence of methoxy (-OCH₃) group, an electron donating group. These EDGs decrease the catalytic activity by increasing the electron density around the metal active centre. Additionally, the presence of EWD and EDGs which are less bulky at the ligand *N*-aryl moiety, for instance bromine, chlorine, methyl, and methoxy, respectively generated mainly oligomer products, in agreement with observations made in reported work (Schröder *et al.*, 2002), as it has also been observed strongly in this work. Conversely, the presence of bulkier substituents at the ligand backbone results in high molecular weight polymers and gives room for branched polymer materials, as it has been observed and reported by a number of research groups (Chandran *et al.*, 2012; Irrgang *et al.*, 2007).

A remarkable difference in the catalytic activity was observed when palladium(II) and nickel(II) complexes with similar substituents on the ligand backbone were compared as displayed in the Table 4.19.

Table 4.19: Comparison of catalytic activity between Pd(II) and Ni(II) complexes

Catalyst	Substituent	0 h (% conversion)	4 h	8 h	18 h	24 h
Pd (C3)	methoxy	0	11	21	36	48
Ni (C12)	methoxy	0	40	40	40	44
Pd (C5)	bromine	0	44	46	51	54
Ni (C14)	bromine	0	59	63	60	99

The catalytic conversion for palladium(II), **C3** was observed at 11 %, while that for nickel(II), **C12** was 40 % after 4 h of reaction. Generally, throughout the reaction period, nickel(II) complex, **C12** exhibited a higher catalytic activity in comparison with that of palladium(II) **C3** as shown in Figure 4.21.

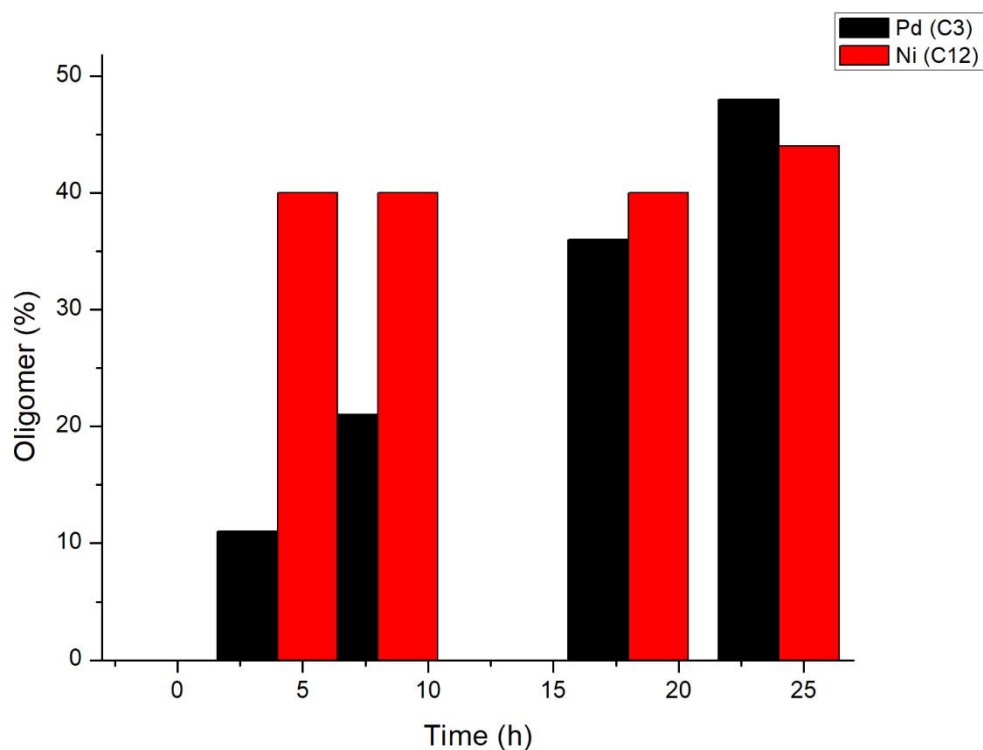


Figure 4.21: Comparison of catalytic activity between C3 and C12 having methoxy substituents

Furthermore, the nickel(II) complex **C14** showed much higher catalytic activity in comparison with its palladium(II) complex analogue, **C5** as clearly displayed in Figure 4.22. This is in agreement with observations made in similar research reports (Johnson *et al.*, 1995; Merna *et al.*, 2005; Noël *et al.*, 2006).

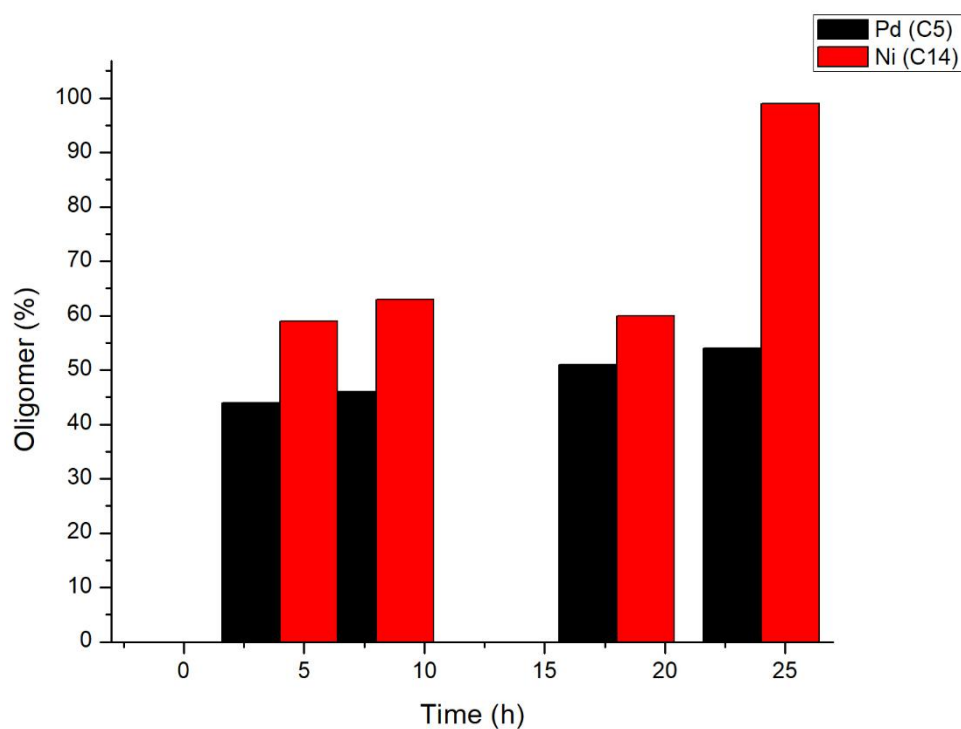


Figure 4.22: Comparison of catalytic activity between C5 and C14 having bromine substituents

Generally, in this work all the nickel(II) complexes exhibited a notably higher catalytic activity in comparison with their palladium(II) complex analogues. This can possibly be attributed to the fact that nickel metal is more reactive with other substances like air, moisture and ligands in comparison with palladium. Therefore, we can undoubtedly report that nickel can be designed into complexes to make better catalysts in comparison to palladium metal, as was also observed and reported by a number of researchers (Merna *et al.*, 2005; Noël *et al.*, 2006).

CHAPTER FIVE

CONCLUSION AND RECOMMENDATIONS

5.1 Conclusion

In this thesis, seventeen *N,O*-salicylaldimine ligands **SL1** – **SL17** with propylene, butylene and pentylene spacers (linkers), having bromide, chloride, methyl, methoxy substituents on the phenyl ring appended on the *ortho*- and/or *para*- to the phenoxy oxygen were successfully synthesized. The ligands were obtained as light-yellow, yellow or bright-yellow solids in appreciable yields between 41 – 98 % and were observed to be both air and moisture stable. The ligands were characterised by spectroscopic and analytical techniques (FT-IR, ¹H and ¹³C, GC-MS, XRD, and elemental analyser). The molecular structures of **SL2**, **SL3**, **SL6** and **SL9** have been solved by single X-ray diffraction (XRD) studies and their respective geometry and space orientation confirmed again for the first time. The ligands were then reacted with two molar equivalents of complex precursors, PdCl₂(COD) and NiCl₂(DME) to form palladium(II) and nickel(II) homobimetallic complexes **C1** – **C15**. All the synthesized complexes were obtained with varied colours from yellow, orange or green in moderate to high yields between 43 – 95 % and were also observed to be both air and moisture stable. Characterisation using the aforementioned techniques was done to confirm the structural formulation and geometry of the complexes.

Finally, evaluation of the potential catalytic activity of the complexes over 1-hexene oligomerisation generated new catalysts. Although the complexes exhibited positive catalytic activity, their effects were low compared to other similar complexes reported in literature.

However, the nickel complexes exhibited a higher catalytic activity in comparison to the corresponding palladium complexes. This is in agreement with many other established research findings. These differences were attributed to the fact that naturally nickel is more reactive than palladium, both of which are found in group 10 of the periodic table of elements.

5.2 Recommendations

Nickel(II) and palladium(II) *N,O*-salicylaldimine homobimetallic complexes were synthesized and characterised by various spectroscopic and analytical techniques. Some of the complexes were tested for 1-hexene oligomerisation reactions and exhibited high activity to become 1-hexene oligomerisation reaction catalysts. Nevertheless, the following future work on this project were recommended:

1. Synthesis of heterobimetallic Pd/Ni to replace Ni/Ni and Pd/Pd as an extension of the current study, probably this will enhance the catalytic activity
2. Change one half of the ligand to be five-membered ring and the other to be six-membered with more bulky substituents to the ligand backbone, maybe it will improve activity and quality of catalytic products
3. Change one half of the ligand to be ring and the other one to be aliphatic, possibly it will improve the quality of the catalytic products
4. Test the catalytic activity of the synthesized heterobimetallic Pd/Ni complexes

The recommended changes are expected to design catalysts that are possibly more active in polymerisation and copolymerisation of alkenes, Suzuki and Heck coupling reactions.

REFERENCES

- Adewuyi, S., Li, G., Zhang, S., Wang, W., Hao, P., Sun, W. H., Tang, N., and Yi, J. (2007). Nickel(II) complexes chelated by 2-quinoxaliny-6-iminopyridines: Synthesis, crystal structures and ethylene oligomerization. *Journal of Organometallic Chemistry*, **692**, 3532–3541. <https://doi.org/10.1016/j.jorganchem.2007.04.036>
- Albers, I., Álvarez, E., Cámpora, J., Maya, C. M., Palma, P., Sánchez, L. J., and Passaglia, E. (2004). Cationic η^3 -benzyl nickel compounds with diphosphine ligands as catalyst precursors for ethylene oligomerization/ polymerization: Influence of the diphosphine bite angle. *Journal of Organometallic Chemistry*, **689**(4), 833–839. <https://doi.org/10.1016/j.jorganchem.2003.12.007>
- Alonso, F., Beletskaya, I. P., and Yus, M. (2008). Non-conventional methodologies for transition-metal catalysed carbon-carbon coupling: a critical overview. Part 1: The Heck reaction. *Tetrahedron*, **61**, 11771–11835. <https://doi.org/10.1016/j.tet.2007.12.036>
- Alvira, P., Tomás-Pejó, E., Ballesteros, M., and Negro, M. J. (2010). Pretreatment technologies for an efficient bioethanol production process based on enzymatic hydrolysis: A review. *Bioresource Technology*, **101**(13), 4851–4861. <https://doi.org/10.1016/j.biortech.2009.11.093>
- Ananthi, N., Balakrishnan, U., and Velmathi, S. (2010). Salicylaldimine based copper (II) complex: A potential catalyst for the asymmetric Henry reaction. *Arkivoc*, **2010**(11), 370–379.
- Antonov, A. A., Semikolenova, N. V., Talsi, E. P., Matsko, M. A., Zakharov, V. A., and Bryliakov, K. P. (2016). 2-iminopyridine nickel(II) complexes bearing electron-withdrawing groups in the ligand core: Synthesis, characterization, ethylene oligo- and polymerization behavior. *Journal of Organometallic Chemistry*, **822**, 241–249. <https://doi.org/10.1016/j.jorganchem.2016.08.031>
- Arduengo, A. J., Tapu, D., and Marshall, W. J. (2005). A bimetallic complex containing a cyclopentadienyl-annulated imidazol-2-ylidene. *Journal of the American Chemical Society*, **127**(47), 16400–16401. <https://doi.org/10.1021/ja055565f>
- Ashwell, J. G. (1999). Langmuir–Blodgett films: molecular engineering of non-centrosymmetric structures for second-order nonlinear optical applications. *Journal of Material Chemistry*, **9**, 1991–2003.
- Axenov, K. V., Klinga, M., Lehtonen, O., Koskela, H. T., Leskelä, M., and Repo, T. (2007). Hafnium bis(phenoxyimino) Dibenzyl Complexes and Their Activation toward Olefin Polymerization. *Organometallics*, **26**(6), 1444–1460. <https://doi.org/10.1021/om060753f>
- Bahuleyan, B. K., Lee, K. J., Lee, S. H., Liu, Y., Zhou, W., and Kim, I. (2011). Trinuclear Fe(II)/Ni(II) complexes as catalysts for ethylene polymerizations. *Catalysis Today*, **164**(1), 80–87. <https://doi.org/10.1016/j.cattod.2010.10.084>
- Bahuleyan, B. K., Lee, U., Ha, C.-S., and Kim, I. (2008). Ethylene oligomerization/polymerization over a series of iminopyridyl Ni(II) bimetallic catalysts modulated electronically and sterically. *Applied Catalysis A: General*, **351**(1), 36–44.

<https://doi.org/10.1016/j.apcata.2008.08.026>

- Ban, Q., Zhang, J., Liang, T., Redshaw, C., and Sun, W. H. (2012). 2,6-Dibenzhydryl-N-(2-aryliminoacenaaphthylenylidene)-4-chlorobenzenamino- palladium dichlorides: Synthesis, characterization, and use as catalysts in the Heck-reaction. *Journal of Organometallic Chemistry*, **713**, 151–156. <https://doi.org/10.1016/j.jorganchem.2012.05.015>
- Bantu, B., Wurst, K., and Buchmeiser, M. R. (2007). N-Acetyl-N,N-dipyrid-2-yl (cyclooctadiene) rhodium (I) and iridium (I) complexes: Synthesis, X-ray structures, their use in hydroformylation and carbonyl hydrosilylation reactions and in the polymerization of diazocompounds. *Journal of Organometallic Chemistry*, **692**, 5272–5278. <https://doi.org/10.1016/j.jorganchem.2007.08.009>
- Bastero, A., Franciò, G., Leitner, W., and Mecking, S. (2006). Catalytic Ethylene Polymerisation in Carbon Dioxide as a Reaction Medium with Soluble Nickel(II) Catalysts. *Chemistry - A European Journal*, **12**(23), 6110–6116. <https://doi.org/10.1002/chem.200600499>
- Bastero, A., Göttker-Schnetmann, I., Röhr, C., and Mecking, S. (2007). Polymer Microstructure Control in Catalytic Polymerization Exclusively by Electronic Effects of Remote Substituents. *Advanced Synthesis and Catalysis*, **349**(14), 2307–2316. <https://doi.org/10.1002/adsc.200700127>
- Bernales, V., Yang, D., Yu, J., Gümüşlü, G., Cramer, C. J., Gates, B. C., and Gagliardi, L. (2017). Molecular Rhodium Complexes Supported on the Metal-Oxide-Like Nodes of Metal Organic Frameworks and on Zeolite HY: Catalysts for Ethylene Hydrogenation and Dimerization. *Applied Materials & Interfaces*, A-J. <https://doi.org/10.1021/acsami.7b03858>
- Bilge, S., Kiliç, Z., Hayvali, Z., Hökelek, T., and Safran, S. (2009). Intramolecular hydrogen bonding and tautomerism in Schiff bases: Part VI. Syntheses and structural investigation of salicylaldimine and naphthaldimine derivatives. *Journal of Chemical Sciences*, **121**(6), 989–1001. <https://doi.org/10.1007/s12039-009-0128-2>
- Binder, J. B., Guzei, I. A., and Raines, R. T. (2007). Salicylaldimine Ruthenium Alkylidene Complexes: Metathesis Catalysts Tuned for Protic Solvents. *Advanced Synthesis and Catalysis*, **349**, 395–404. <https://doi.org/10.1002/adsc.200600264>
- Biswas, C., Zhu, M., Lu, L., Kaity, S., Das, M., Samanta, A., and Prakash, J. (2013). A palladium (II) complex: Synthesis, structure, characterization, electrochemical behavior, thermal aspects, BVS calculation and antimicrobial activity. *Polyhedron*, **56**, 211–220. <https://doi.org/10.1016/j.poly.2013.03.064>
- Bohm, S., and Exner, O. (2004). Geometry at the aliphatic tertiary carbon atom: computational and experimental test of the Walsh rule. *Acta Crystallographica Section B*, **B60**, 103–107. <https://doi.org/10.1107/S010876810302826X>
- Borhade, S. R., and Waghmode, S. B. (2008). Phosphine-free Pd-salen complexes as efficient and inexpensive catalysts for Heck and Suzuki reactions under aerobic conditions. *Tetrahedron Letters*, **49**(21), 3423–3429. <https://doi.org/10.1016/j.tetlet.2008.03.109>
- Botteghi, C., Paganelli, S., Bigini, L., and Marchetti, M. (1994). Hydroformylation of 1-aryl-1-(2-pyridyl) ethenes catalyzed by rhodium complexes. *Journal of Molecular Catalysis*, **93**,

279–287.

- Bourque, T. A., Nelles, M. E., Gullon, T. J., Garon, C. N., Ringer, M. K., Leger, L. J., Mason, J. W., Wheaton, S. L., Baerlocher, F. J., Vogels, C. M., Decken, A., and Westcott, S. A. (2005). Late metal salicylaldimine complexes derived from 5-aminosalicylic acid - Molecular structure of a zwitterionic mono Schiff base zinc complex. *Canadian Journal of Chemistry*, **83**(8), 1063–1070. <https://doi.org/10.1139/v05-091>
- Bowes, E. G., Lee, G. M., Vogels, C. M., Decken, A., and Westcott, S. A. (2011). Palladium salicylaldimine complexes derived from 2,3-dihydroxybenzaldehyde. *Inorganica Chimica Acta*, **377**(1), 84–90. <https://doi.org/10.1016/j.ica.2011.07.051>
- Britovsek, G. J. P., Baugh, S. P. D., Hoarau, O., Gibson, V. C., Wass, D. F., White, A. J. P., and Williams, D. J. (2003). The role of bulky substituents in the polymerization of ethylene using late transition metal catalysts: a comparative study of nickel and iron catalyst systems. *Inorganica Chimica Acta*, **345**, 279–291. [https://doi.org/10.1016/S0020-1693\(02\)01293-8](https://doi.org/10.1016/S0020-1693(02)01293-8)
- Britovsek, G. J. P., Bruce, M., Gibson, V. C., Kimberley, B. S., Maddox, P. J., Mastroianni, S., McTavish, S. J., Redshaw, C., Solan, G. A., Strömberg, S., White, A. J. P., and Williams, D. J. (1999). Iron and Cobalt Ethylene Polymerization Catalysts Bearing 2,6-Bis(Imino)Pyridyl Ligands: Synthesis, Structures, and Polymerization Studies. *Journal of the American Chemical Society*, **121**(38), 8728–8740. <https://doi.org/10.1021/ja990449w>
- Brunner, H., Bublak, P., and Helget, M. (1997). Stereoselective Hydrogenation of Folic Acid with Immobilized Optically Active Rhodium(I)/Diphosphane Catalysts. *Chemische Berichte*, **130**(1), 55–62. <https://doi.org/10.1002/cber.19971300109>
- Budagumpi, S., Liu, Y., Suh, H., and Kim, I. (2011). Synthesis of and ethylene oligomerization with binuclear palladium catalysts having sterically modulated bis-imine ligands with methylene spacer. *Journal of Organometallic Chemistry*, **696**(9), 1887–1894. <https://doi.org/10.1016/j.jorganchem.2011.03.003>
- Camacho, D. H., and Guan, Z. (2010). Designing late-transition metal catalysts for olefin insertion polymerization and copolymerization. *Chemical Communications*, **46**, 7879–7893. <https://doi.org/10.1039/c0cc01535k>
- Campanelli, A. R., Arcadi, A., Domenicano, A., and Ramondo, F. (2006). Molecular Structure and Benzene Ring Deformation of Three Ethynylbenzenes from Gas-Phase Electron Diffraction and Quantum Chemical Calculations. *J. Phys. Chem. A*, **110**, 2045–2052.
- Campanelli, A. R., Domenicano, A., and Ramondo, F. (2008). Molecular Structure and Benzene Ring Deformation of Three Cyanobenzenes from Gas-Phase Electron Diffraction and Quantum Chemical Calculations. *Journal of Physics and Chemistry A*, **112**, 10998–11008.
- Cao, G., Yang, H.-Q., Luo, B.-T., and Liu, F.-S. (2013). Synthesis, characterization, and catalytic activity of palladium complexes with α -iminoamidate ligands. *Journal of Organometallic Chemistry*, **745–746**, 158–165. <https://doi.org/10.1016/j.poly.2012.06.010>
- Carlini, C., Macinai, A., Masi, F., Raspolli Galletti, A. M., Santi, R., Sbrana, G., and Sommazzi, A. (2004). Ethylene Polymerization by Bis(salicylaldiminate)nickel(II)/Aluminoxane Catalysts. *Journal of Polymer Science, Part A: Polymer Chemistry*, **42**(10), 2534–2542.

<https://doi.org/10.1002/pola.20102>

- Centi, G., and Perathoner, S. (2003). Catalysis and sustainable (green) chemistry. *Catalysis Today*, **77**(4), 287–297. [https://doi.org/10.1016/S0920-5861\(02\)00374-7](https://doi.org/10.1016/S0920-5861(02)00374-7)
- Chandran, D., Lee, K. M., Chang, H. C., Song, G. Y., Lee, J. E., Suh, H., and Kim, I. (2012). Ni(II) complexes with ligands derived from phenylpyridine, active for selective dimerization and trimerization of ethylene. *Journal of Organometallic Chemistry*, **718**, 8–13. <https://doi.org/10.1016/j.jorganchem.2012.08.005>
- Chen, Q., Yu, J., and Huang, J. (2007). Arene-bridged salicylaldimine-based binuclear neutral nickel(II) complexes; synthesis and ethylene polymerization activities. *Organometallics*, **26**(3), 617–625. <https://doi.org/10.1021/om060778e>
- Chen, Zhongtao, Yao, E., Wang, J., Gong, X., and Ma, Y. (2016). Ethylene (Co)polymerization by Binuclear Nickel Phenoximinato Catalysts with Cofacial Orientation. *Macromolecules*, **49**(23), 8848–8854. <https://doi.org/10.1021/acs.macromol.6b02078>
- Chen, Zhou, Mesgar, M., White, P. S., Daugulis, O., and Brookhart, M. (2015). Synthesis of Branched Ultrahigh-Molecular-Weight Polyethylene Using Highly Active Neutral, Single-Component Ni(II) Catalysts. *ACS Catalysis*, **5**(2), 631–636. <https://doi.org/10.1021/cs501948d>
- Connor, E. F., Younkin, T. R., Henderson, J. I., Hwang, S., Grubbs, R. H., Roberts, W. P., and Litzau, J. J. (2002). Linear functionalized polyethylene prepared with highly active neutral Ni(II) complexes. *Journal of Polymer Science, Part A: Polymer Chemistry*, **40**(16), 2842–2854. <https://doi.org/10.1002/pola.10370>
- Connor, E. F., Younkin, T. R., Henderson, J. I., Waltman, A. W., and Grubbs, R. H. (2003). Synthesis of neutral nickel catalysts for ethylene polymerization - the influence of ligand size on catalyst stability. *Chemical Communications*, **2003**, 2272–2273. <https://doi.org/10.1039/b306701g>
- Cornils, B. (1998). Industrial Aqueous Biphasic Catalysis: Status and Directions. *Organic Process Research and Development*, **2**(2), 121–127. <https://doi.org/10.1021/op970057e>
- Cornils, B., and Kuntz, E. G. (1995). Introducing TPPTS and related ligands for industrial biphasic processes. *Journal of Organometallic Chemistry*, **502**(1–2), 177–186. [https://doi.org/10.1016/0022-328X\(95\)05820-F](https://doi.org/10.1016/0022-328X(95)05820-F)
- Cui, J., and Zhang, M. (2010). Chromium complexes ligated by amino-salicylaldimine ligands: synthesis, structures and ethylene oligomerisation behaviour. *Journal of Chemical Research*, (1), 41–43. <https://doi.org/10.3184/030823410x12628736648105>
- Cui, Jin, Zhang, M., and Zhang, Y. (2010). Amino-salicylaldimine-palladium(II) complexes: New and efficient catalysts for Suzuki and Heck reactions. *Inorganic Chemistry Communications*, **13**(1), 81–85. <https://doi.org/10.1016/j.inoche.2009.10.023>
- Cuomo, C., Strianese, M., Cuenca, T., Sanz, M., and Grassi, A. (2004). Olefin Polymerization Promoted by a Stereorigid Bridged Diiminobis(phenolate) Zirconium Complex. *Macromolecules*, **37**(20), 7469–7476. <https://doi.org/10.1021/ma0492115>
- Dai, S., Sui, X., and Chen, C. (2015). Highly Robust Palladium(II) α -Diimine Catalysts for

- Slow-Chain-Walking Polymerization of Ethylene and Copolymerization with Methyl Acrylate. *Angewandte Chemie - International Edition*, **54**(34), 9948–9953. <https://doi.org/10.1002/anie.201503708>
- Daugulis, O., and Brookhart, M. (2002). Polymerization of ethylene with cationic palladium and nickel catalysts containing bulky nonenolizable imine-phosphine ligands. *Organometallics*, **21**(26), 5926–5934. <https://doi.org/10.1021/om0206305>
- Dawood, K. M. (2007). Microwave-assisted Suzuki-Miyaura and Heck-Mizoroki cross-coupling reactions of aryl chlorides and bromides in water using stable benzothiazole-based palladium(II) precatalysts. *Tetrahedron*, **63**(39), 9642–9651. <https://doi.org/10.1016/j.tet.2007.07.029>
- Dennett, J. N. L., Gillon, A. L., Heslop, K., Hyett, D. J., Fleming, J. S., Emma, L., C., Guy O. A., Pringle, P. G., Wass, D. F., Scutt, J. N., and Weatherhead, R. H. (2004). Diphosphine complexes of Nickel(II) are efficient catalysts for the polymerization and oligomerization of ethylene: Steric activation and ligand backbone effects. *Organometallics*, **23**(26), 6077–6079. <https://doi.org/10.1021/om0494014>
- Deutschmann, O., Knozinger, H., Kochloefl, K., and Turek, T. (2012). Heterogenous Catalysis and Solid Catalysts, 1. Fundamentals. *Ullmann's Encyclopedia of Industrial Chemistry*, 457–482. <https://doi.org/10.1002/14356007.a05>
- Dijkstra, Harm P. van Koten, G., and van Klink, G. P. M. (2002). The Use of Ultra- and Nanofiltration Techniques in Homogeneous Catalytic Recycling. *Accounts of Chemical Research*, **35**(9), 798–810. <https://doi.org/10.1021/ar0100778>
- Dioos, B. M. L., Vankelecom, I. F. J., and Jacobs, P. A. (2006). Aspects of immobilisation of catalysts on polymeric supports. *Advanced Synthesis and Catalysis*, **348**, 1413–1446. <https://doi.org/10.1002/adsc.200606202>
- Domin, D., Benito-Garagorri, D., Mereiter, K., Fröhlich, J., and Kirchner, K. (2005). Synthesis and reactivity of palladium and nickel β -diimine complexes: Application as catalysts for Heck, Suzuki, and Hiyama coupling reactions. *Organometallics*, **24**(16), 3957–3965. <https://doi.org/10.1021/om050201h>
- Domski, G. J., Rose, J. M., Coates, G. W., Bolig, A. D., and Brookhart, M. (2007). Living alkene polymerization: New methods for the precision synthesis of polyolefins. *Progress in Polymer Science*, **32**(1), 30–92. <https://doi.org/10.1016/j.progpolymsci.2006.11.001>
- Donmez, E., Kara, H., Karakaş, A., Ünver, H., and Elmali, A. (2007). Synthesis, molecular structure, spectroscopic studies and second-order nonlinear optical behaviour of N,N'-(2-hydroxy-propane-1,3-diyl)-bis(5-nitrosalicylaldiminato-N,O)-copper(II). *Spectrochimica Acta - Part A: Molecular and Biomolecular Spectroscopy*, **66**(4–5), 1141–1146. <https://doi.org/10.1016/j.saa.2006.05.027>
- El-Sonbati, A. Z. (1991). Polymer complexes, XVII. Thermal stability of poly(5-vinyl salicylidene)-2-aminophenol homopolymer and polymer complexes of 5-vinyl salicylidene-2-aminophenol with transition metal acetates. *Transition Metal Chemistry*, **16**(1), 45–47. <https://doi.org/10.1007/BF01127869>

- Fonseca, J., Martinez, J., Cunha-Silva, L., Magalhães, A. L., Duarte, M. T., and Freire, C. (2010). Insights into electronic and structural properties of novel Pd(II) salen-type complexes. *Inorganica Chimica Acta*, **363**(14), 4096–4107. <https://doi.org/10.1016/j.ica.2010.08.023>
- Funk, J. K., Andes, C. E., and Sen, A. (2004). Addition Polymerization of Functionalized Norbornenes: The Effect of Size, Stereochemistry, and Coordinating Ability of the Substituent. *Organometallics*, **23**(8), 1680–1683. <https://doi.org/10.1021/om0499431>
- Gao, A. H., Yao, W., Mu, Y., Gao, W., Sun, M. T., and Su, Q. (2009). Heterobimetallic aluminium and zinc complex with N-arylanilido-imine ligand: Synthesis, structure and catalytic property for ring-opening polymerization of ϵ -caprolactone. *Polyhedron*, **28**, 2605–2610. <https://doi.org/10.1016/j.poly.2009.05.037>
- Gasser, G., Ott, I., and Metzler-Nolte, N. (2011). Organometallic anticancer compounds. *Journal of Medicinal Chemistry*, **54**(1), 3–25. <https://doi.org/10.1021/jm100020w>
- Gibson, V. C., and Spitzmesser, S. K. (2003). Advances in non-metallocene olefin polymerization catalysis. *Chemical Reviews*, **103**(1), 283–315. <https://doi.org/10.1021/cr980461r>
- Göttker-Schnetmann, I., Wehrmann, P., Röhr, C., and Mecking, S. (2007). Substituent Effects in (κ^2 -N,O)-Salicylaldiminato nickel(II)-Methyl Pyridine Polymerization Catalysts: Terphenyls Controlling Polyethylene Microstructures. *Organometallics*, **26**(9), 2348–2362. <https://doi.org/10.1021/om0611498>
- Guan, Z., Cotts, P. M., McCord, E. F., and McLain, S. J. (1999). Chain Walking: A New Strategy to Control Polymer Topology. *Science*, **283**, 2059–2062. <https://doi.org/10.1126/science.283.5410.2059>
- Guan, Z. (2010). Recent progress of catalytic polymerization for controlling polymer Topology. *Chemistry - An Asian Journal*, **5**(5), 1058–1070. <https://doi.org/10.1002/asia.200900749>
- Guan, Z., and Popeney, C. S. (2008). Recent Progress in Late Transition Metal α -Diimine Catalysts for Olefin Polymerization. *Top Organometallic Chemistry*, 1–42. <https://doi.org/10.1007/3418>
- Guironnet, D., Göttker-Schnetmann, I., and Mecking, S. (2009). Catalytic Polymerization in Dense CO₂ to Controlled Microstructure Polyethylenes. *Macromolecules*, **42**(21), 8157–8164. <https://doi.org/10.1021/ma901397q>
- Guisado-Barrios, G., Hiller, J., and Peris, E. (2013). Pyracene-Linked bis-Imidazolylidene Complexes of Palladium and Some Catalytic Benefits Produced by Bimetallic Catalysts. *Chemistry - A European Journal*, **19**, 10405–10411. <https://doi.org/10.1002/chem.201300486>
- Guo, D., Han, L., Zhang, T., Sun, W.-H., Li, T., and Yang, X. (2002). Temperature Dependence of the Activity of a Late Transition Metal Catalyst by Molecular Modeling. *Macromolecular Theory and Simulations*, **11**(9), 1006–1012. [https://doi.org/10.1002/1521-3919\(200211\)11:9<1006::AID-MATS1006>3.0.CO;2-7](https://doi.org/10.1002/1521-3919(200211)11:9<1006::AID-MATS1006>3.0.CO;2-7)
- Guo, L., Dai, S., Sui, X., and Chen, C. (2016). Palladium and Nickel Catalyzed Chain Walking Olefin Polymerization and Copolymerization. *ACS Catalysis*, **6**(1), 428–441.

<https://doi.org/10.1021/acscatal.5b02426>

- Guo, X., Zhou, J., Li, X., and Sun, H. (2008). Synthesis and catalytic applications of sulfonate β -ketoimine and β -diimine in the Suzuki reaction in aqueous phase. *Journal of Organometallic Chemistry*, **693**(25), 3692–3696. <https://doi.org/10.1016/j.jorganchem.2008.08.038>
- Ha, K. (2012). 4,4'-Dinitro-2,2'-[propane-1,3-diylbis(iminiumylmethanylylidene)]diphenolate. *Acta Crystallographica Section E Structure Reports Online*, **68**(5), o1399–o1399. <https://doi.org/10.1107/S1600536812015504>
- Han, S., Yao, E., Qin, W., Zhang, S., and Ma, Y. (2012). Binuclear Heteroligated Titanium Catalyst Based on Phenoxyimine Ligands: Synthesis, Characterization, and Ethylene (Co)polymerization. *Macromolecules*, **45**(10), 4054–4059. <https://doi.org/10.1021/ma300384w>
- Hardy, J. J. E., Hubert, S., Macquarrie, D. J., and Wilson, A. J. (2004). Chitosan-based heterogeneous catalysts for Suzuki and Heck reactions. *Green Chemistry*, **6**(1), 53–56. <https://doi.org/10.1039/b312145n>
- Helldörfer, M., Backhaus, J., Milius, W., and Alt, H. G. (2003). (α -diimine)nickel(II) complexes containing chloro substituted ligands as catalyst precursors for the oligomerization and polymerization of ethylene. *Journal of Molecular Catalysis A: Chemical*, **193**(1–2), 59–70. [https://doi.org/10.1016/S1381-1169\(02\)00468-5](https://doi.org/10.1016/S1381-1169(02)00468-5)
- Hicks, F. A., and Brookhart, M. S. (2001). A Highly Active Anilinetropone-Based Neutral Nickel(II) Catalyst for Ethylene Polymerization. *Organometallics*, **20**(15), 3217–3219. <https://doi.org/10.1021/om010211s>
- Hille, A., and Gust, R. (2010). Influence of methoxy groups on the antiproliferative effects of [Fe III(salophene-OMe)Cl] complexes. *European Journal of Medicinal Chemistry*, **45**(11), 5486–5492. <https://doi.org/10.1016/j.ejmech.2010.08.037>
- Hisham, N. A. I., Khaledi, H., Mohd Ali, H., and Hadi, H. A. (2012). Coordination modes of two flexidentate salicylaldehyde ligands derived from N-(3-aminopropyl)morpholine toward zinc and copper. *Journal of Coordination Chemistry*, **65**(17), 2992–3006. <https://doi.org/10.1080/00958972.2012.708412>
- Hollas, A. M., Gu, W., Bhuvanesh, N., and Ozerov, O. V. (2011). Synthesis and characterization of Pd complexes of a carbazolyl/bis(Imine) NNN pincer ligand. *Inorganic Chemistry*, **50**, 3673–3679. <https://doi.org/10.1021/ic200026p>
- Holm, R., H., and Everett, G. W. (1966). Metal Complexes of Schiff Bases and β -Ketoamines. *Progress in Inorganic Chemistry*, **7**, 83–132.
- Houghton, J., Simonovic, S., Whitwood, A. C., Douthwaite, R. E., Carabineiro, S. A., Yuan, J. C., Marques, M. M., and Gomes, P. T. (2008). Transition-metal complexes of phenoxyimine ligands modified with pendant imidazolium salts: Synthesis, characterisation and testing as ethylene polymerisation catalysts. *Journal of Organometallic Chemistry*, **693**(4), 717–724. <https://doi.org/10.1016/j.jorganchem.2007.11.060>
- Hu, T., Li, Y. G., Li, Y. S., and Hu, N. H. (2006). Novel highly active binuclear neutral nickel

- and palladium complexes as precatalysts for norbornene polymerization. *Journal of Molecular Catalysis A: Chemical*, **253**(1–2), 155–164.
<https://doi.org/10.1016/j.molcata.2006.03.008>
- Hu, T., Tang, L. M., Li, X. F., Li, Y. S., and Hu, N. H. (2005). Synthesis and Ethylene Polymerization Activity of a Novel, Highly Active Single-Component Binuclear Neutral Nickel(II) Catalyst. *Organometallics*, **24**(11), 2628–2632.
<https://doi.org/10.1021/om049223e>
- Hu, X., Dai, S., and Chen, C. (2015). Ethylene polymerization by salicylaldimine nickel(II) complexes containing a dibenzhydryl moiety. *Dalton Transactions*, **45**(4), 1496–1503.
<https://doi.org/10.1039/c5dt04408a>
- Huang, W., Sun, X., Ma, H., and Huang, J. (2010). Ethylene homopolymerization and ethylene/1-hexene copolymerization catalysed by mixed salicylaldiminato cyclopentadienyl zirconium complexes. *Inorganica Chimica Acta*, **363**(9), 2009–2015.
<https://doi.org/10.1016/j.ica.2009.06.010>
- Irrgang, T., Keller, S., Maisel, H., Kretschmer, W., and Kempe, R. (2007). Sterically Demanding Iminopyridine Ligands. *European Journal of Inorganic Chemistry*, (26), 4221–4228.
<https://doi.org/10.1002/ejic.200700322>
- Ittel, S. D., Johnson, L. K., and Brookhart, M. (2000). Late-Metal Catalysts for Ethylene Homo- and Copolymerization. *Chemical Reviews*, **100**(4), 1169–1203.
- Ivanchev, S. S., Yakimansky, A. V., Ivancheva, N. I., Oleinik, I. I., and Tolstikov, G. A. (2012). Ethylene polymerization using catalysts based on binuclear phenoxyimine titanium halide complexes. *European Polymer Journal*, **48**(1), 191–199.
<https://doi.org/10.1016/j.eurpolymj.2011.10.020>
- Janiak, C., and Lassahn, P. G. (2001). The vinyl homopolymerization of norbornene. *Macromolecular Rapid Communications*, **22**(7), 479–492. [https://doi.org/10.1002/1521-3927\(20010401\)22:7<479::AID-MARC479>3.0.CO;2-C](https://doi.org/10.1002/1521-3927(20010401)22:7<479::AID-MARC479>3.0.CO;2-C)
- Janik, M. J., Macht, J., Iglesia, E., and Neurock, M. (2009). Correlating Acid Properties and Catalytic Function: A First-Principles Analysis of Alcohol Dehydration Pathways on Polyoxometalates. *Journal of Physical Chemistry C*, **113**(5), 1872–1885.
<https://doi.org/10.1021/jp8078748>
- Ji, P., Guo, L., Hu, X., and Li, W. (2017). Ethylene polymerization by salicylaldimine Nickel(II) complexes derived from aryl naphthylamine. *Journal of Polymer Research*, **24**(2), 1–9.
<https://doi.org/10.1007/s10965-017-1190-y>
- Jian, L. J., Zhang, D. D., Zhou, X. B., Lin, M. J., Li, H. P., Chen, J. X., and Zhang, Z. C. (2017). Nickel(II) Complex Bearing a Salicylaldimine Ligand: Synthesis, Crystal Structure and Application in Norbornene Polymerization. *Journal of Structural Chemistry*, **36**(9), 1511–1517. <https://doi.org/10.14102/j.cnki.0254-5861.2011-1556>
- Jie, S., Zhang, D., Zhang, T., Sun, W. H., Chen, J., Ren, Q., Liu, D., Zheng, G., and Chen, W. (2005). Bridged bis-pyridinylimino dinickel(II) complexes: Syntheses, characterization, ethylene oligomerization and polymerization. *Journal of Organometallic Chemistry*, **690**,

- 1739–1749. <https://doi.org/10.1016/j.jorganchem.2005.01.029>
- Johnson, L.K., Mecking, S., and Brookhart, M. (1996). Copolymerization of Ethylene and Propylene with Functionalized Vinyl Monomers by Palladium(II) Catalysts. *Journal of the American Chemical Society*, **118**(1), 267–268. <https://doi.org/10.1021/ja953247i>
- Johnson, L. K., Killian, C. M., and Brookhart, M. (1995). New Pd(II)-and Ni(II)-Based Catalysts for Polymerization of Ethylene and α -Olefins. *Journal of the American Chemical Society*, **117**(23), 6414–6415. <https://doi.org/10.1021/ja00128a054>
- Killian, C. M., Tempel, D. J., Johnson, L. K., and Brookhart, M. (1996). Living Polymerization of α -Olefins Using Ni(II)- α -Diimine Catalysts. Synthesis of New Block Polymers Based on α -Olefins. *Journal of the American Chemical Society*, **118**(46), 11664–11665. <https://doi.org/10.1021/ja962516h>
- Kitamura, M., Ohkuma, T., Inoue, S., Sayo, N., Kumobayashi, H., Akutagawa, S., Ohta, T., Takaya, H., and Noyori, R. (1988). Homogeneous Asymmetric Hydrogenation of Functionalized Ketones. *Journal of the American Chemical Society*, **110**, 629–631.
- Kılınç, D., Şahin, Ö., and Saka, C. (2018). Salicylaldimine-Ni complex supported on Al₂O₃: Highly efficient catalyst for hydrogen production from hydrolysis of sodium borohydride. *International Journal of Hydrogen Energy*, **43**(1), 251–261. <https://doi.org/10.1016/j.ijhydene.2017.10.151>
- Knowles, J. P., and Whiting, A. (2007). The Heck-Mizoroki cross-coupling reaction: A mechanistic perspective. *Organic and Biomolecular Chemistry*, **5**(1), 31–44. <https://doi.org/10.1039/b611547k>
- Kohlpaintner, C. W., Fischer, R. W., and Cornils, B. (2001). Aqueous biphasic catalysis: Ruhrchemie/Rhône-Poulenc oxo process Christian. *Applied Catalysis A: General*, **221**, 219–225. <https://doi.org/10.1007/s00221-006-0471-1>
- Korthals, B., Göttker-Schnetmann, I., and Mecking, S. (2007). Nickel(II)-Methyl Complexes with Water-Soluble Ligands L [(salicylaldiminato- κ 2N,O)NiMe(L)] and Their Catalytic Properties in Disperse Aqueous Systems. *Organometallics*, **26**(6), 1311–1316. <https://doi.org/10.1021/om0607191>
- Köse Baran, E., and Bağdat Yaşar, S. (2013). Synthesis, spectral studies and complexation properties of N,N'-bis(5-bromo-salicylidene)-2-hydroxy-1,3-propanediamine (BSHP) and iron extraction with BSHP from oils. *Journal of Analytical Chemistry*, **68**(9), 788–793. <https://doi.org/10.1134/S1061934813090074>
- Krasuska, A., BiaŁek, M., and Czaja, K. (2011). Ethylene Polymerization with FI Complexes Having Novel Phenoxy-imine Ligands: Effect of Metal Type and Complex Immobilization. *Journal of Polymer Science, Part A: Polymer Chemistry*, **49**(7), 1644–1654. <https://doi.org/10.1002/pola.24589>
- Kumar N., K., and Ramesh, R. (2005). Synthesis, luminescent, redox and catalytic properties of Ru(II) carbonyl complexes containing 2N2O donors. *Polyhedron*, **24**(14), 1885–1892. <https://doi.org/10.1016/j.poly.2005.05.020>
- Kuwabara, J., Takeuchi, D., and Osakada, K. (2009). Structures of Co, Pd and Ni complexes

- with iminopyridine ligands having an hydroxymethyl or acrylate pendant group. *Polyhedron*, **28**(12), 2459–2465. <https://doi.org/10.1016/j.poly.2009.04.050>
- Lai, Y. C., Chen, H. Y., Hung, W. C., Lin, C. C., and Hong, F. E. (2005). Palladium catalyzed Suzuki cross-coupling reactions using N,O-bidentate ligands. *Tetrahedron*, **61**(40), 9484–9489. <https://doi.org/10.1016/j.tet.2005.08.005>
- Laine, T. V., Klinga, M., and Leskelä, M. (1999). Synthesis and X-ray Structures of New Mononuclear and Dinuclear Diimine Complexes of Late Transition Metals. *European Journal of Inorganic Chemistry*, 959–964. [https://doi.org/10.1002/\(sici\)1099-0682\(199906\)1999:6<959::aid-ejic959>3.3.co;2-q](https://doi.org/10.1002/(sici)1099-0682(199906)1999:6<959::aid-ejic959>3.3.co;2-q)
- Ledeti, I., Bolintineanu, S., Vlase, G., Circioban, D., Ledeti, A., Vlase, T., Suta, L. M., Caunii, A., and Murariu, M. (2017). Compatibility study between antiparkinsonian drug Levodopa and excipients by FTIR spectroscopy, X-ray diffraction and thermal analysis. *Journal of Thermal Analysis and Calorimetry*, 1–9. <https://doi.org/10.1007/s10973-017-6393-2>
- Ledoux, I., Zyss, J., Siegel, J. S. L., Brienne, J., and Lehn, J. (1990). Second-harmonic generation from non-dipolar non-centrosymmetric aromatic charge-transfer molecules. *Chemical Physical Letters*, **172**(6), 440–444.
- Lees, A. J., Ferreira, J., Rascol, O., Reichmann, H., Stocchi, F., Tolosa, E., and Poewe, W. (2017). Opicapone for the management of end-of-dose motor fluctuations in patients with Parkinson's disease treated with L-DOPA. *Expert Review of Neurotherapeutics*, 1–11. <https://doi.org/10.1080/14737175.2017.1336086>
- Li, C. Q., Wang, F. F., Gao, R., Sun, P., Zhang, N., and Wang, J. (2017). Bidentate iron complexes based on hyperbranched salicylaldimine ligands and their catalytic behavior toward ethylene oligomerization. *Transition Metal Chemistry*, **42**(4), 339–346. <https://doi.org/10.1007/s11243-017-0137-9>
- Li, L., Metz, M. V., Li, H., Chen, M., Marks, T. J., Liable-sands, L., and Rheingold, A. L. (2002). Catalyst/Cocatalyst Nuclearity Effects in Single-Site Polymerization. Enhanced Polyethylene Branching and α -Olefin Comonomer Enchainment in Polymerizations Mediated by Binuclear Catalysts and Cocatalysts via a New Enchainment Pathway. *Journal of American Chemical Society*, **124**(43), 12725–12741. <https://doi.org/10.1021/ja0201698> CCC
- Li, Y., Jiang, L., Wang, L., Gao, H., Zhu, F., and Wu, Q. (2006). Nickel (II) complexes supported by a fluorinated β -diketiminato backbone ligand: Synthesis, catalytic activity toward norbornene polymerization, and the oxygenated species. *Applied Organometallic Chemistry*, **20**(3), 181–186. <https://doi.org/10.1002/aoc.1042>
- Lin, R. S., Li, M. R., Liu, Y. H., Peng, S. M., and Liu, S. T. (2010). Bimetallic complexes of porphyrinphenanthroline: Preparation and catalytic activities. *Inorganica Chimica Acta*, **363**, 3523–3529. <https://doi.org/10.1016/j.ica.2010.07.008>
- Lin, S.-T., and Siegel, S. (2006). Stereochemistry and the use of H₂/D₂ mixtures as probes into the mechanism of hydrogenations catalyzed by cationic rhodium(DIPHOS) complexes. *Kinetics and Catalysis*, **47**(1), 83–92. <https://doi.org/10.1134/S0023158406010137>

- Liu, P., Yan, M., and He, R. (2010). Bis(imino)pyridine palladium(II) complexes as efficient catalysts for the Suzuki-Miyaura reaction in water. *Applied Organometallic Chemistry*, **24**, 131–134. <https://doi.org/10.1002/aoc.1591>
- Liu, Y., and Wang, J. (2009). Synthesis of 4-substituted styrene compounds via palladium catalyzed Suzuki-Miyaura reaction using bidentate Schiff base ligands. *Applied Organometallic Chemistry*, **23**(11), 476–480. <https://doi.org/10.1002/aoc.1548>
- Lopez-Garriga, J. J., Babcock, G. T., and Harrison, J. F. (1986). Factors Influencing the C=N Stretching Frequency in Neutral and Protonated Schiff's Bases. *Journal of American Chemical Society*, **108**, 7241–7251.
- Lutta, S. T., and Kagwanja, S. M. (2000). Synthesis and electrochemical studies of heterobinuclear complexes containing copper and molybdenum nitrosyl groups linked by Schiff base ligands. *Transition Metal Chemistry*, **25**, 415–420. <https://doi.org/10.1023/A:1011067205029>
- Lutta, S. T., and Kagwanja, S. M. (2001). Synthesis and electrochemical studies of heterobinuclear zinc and molybdenum mononitrosyl complexes linked by Schiff base ligands. *Transition Metal Chemistry*, **26**(4–5), 523–527. <https://doi.org/10.1023/A:1011067205029>
- Makio, H., Terao, H., Iwashita, A., and Fujita, T. (2011). FI Catalysts for Olefin Polymerization—A Comprehensive Treatment. *Chemical Reviews*, **111**(3), 2363–2449. <https://doi.org/10.1021/cr100294r>
- Mao, P., Yang, L., Xiao, Y., Yuan, J., Liu, X., and Song, M. (2012). Suzuki cross-coupling catalyzed by palladium (II) complexes bearing 1-aryl-3,4,5,6-tetrahydropyrimidine ligands. *Journal of Organometallic Chemistry*, **705**, 39–43. <https://doi.org/10.1016/j.jorganchem.2012.01.015>
- Matsui, S., Mitani, M., Saito, J., Tohi, Y., Makio, H., Matsukawa, N., Takagi, Y., Tsuru, K., Nitabar, M., Nakano, T., Tanaka, H., Kashiwa, N., and Fujita, T. (2001). A Family of Zirconium Complexes Having Two Phenoxy - imine Chelate Ligands for Olefin Polymerization. *Journal of the American Chemical Society*, **123**(28), 6847–6856. <https://doi.org/10.1021/ja0032780>
- Mazzeo, M., Lamberti, M., Pappalardo, D., Annunziata, L., and Pellecchia, C. (2009). Polymerization of α -olefins promoted by zirconium complexes bearing bis(phenoxy-imine) ligands with ortho-phenoxy halogen substituents. *Journal of Molecular Catalysis A: Chemical*, **297**(1–2), 9–17. <https://doi.org/10.1016/j.molcata.2008.09.002>
- McInnis, J. P., Delferro, M., and Marks, T. J. (2014). Multinuclear Group 4 Catalysis: Olefin Polymerization Pathways Modified by Strong Metal-Metal Cooperative Effects. *Accounts of Chemical Research*, **47**(8), 2545–2557. <https://doi.org/10.1021/ar5001633>
- Mechler, M., Latendorf, K., Frey, W., and Peters, R. (2013). Homo- and Heterobimetallic Pd⁺, Ag⁺, and Ni⁺ Hybrid Salen– Bis-NHC Complexes. *Organometallics*, **32**, 112–130.
- Merna, J., Cihlar, J., Kucera, M., Deffieux, A., and Cramail, H. (2005). Polymerization of hex-1-ene initiated by diimine complexes of nickel and palladium. *European Polymer Journal*,

- 41(2), 303–312. <https://doi.org/10.1016/j.eurpolymj.2004.09.013>
- Mi, X., Ma, Z., Wang, L., Ke, Y., and Hu, Y. (2003). Homo- and Copolymerization of Norbornene and Styrene with Pd- and Ni-Based Novel Bridged Dinuclear Diimine Complexes and MAO. *Macromolecular Chemistry and Physics*, **204**(5/6), 868–876. <https://doi.org/10.1002/macp.200390057>
- Minto, R. E., and Blacklock, B. J. (2008). Biosynthesis and function of polyacetylenes and allied natural products. *Progress in Lipid Research*, **47**, 233–306. <https://doi.org/10.1016/j.plipres.2008.02.002>
- Mohebbi, S., and Abdi, M. (2008). Unsymmetrical mononuclear and insoluble polynuclear oxovanadium(IV) Schiff-base complexes. *Journal of Coordination Chemistry*, **61**(21), 3410–3419. <https://doi.org/10.1080/00958970802056479>
- Motswainyana, W. M., Ojwach, S. O., Onani, M. O., Iwuoha, E. I., and Darkwa, J. (2011). Novel hemi-labile pyridyl-imine palladium complexes: Synthesis, molecular structures and reactions with ethylene. *Polyhedron*, **30**(15), 2574–2580. <https://doi.org/10.1016/j.poly.2011.07.004>
- Motswainyana, W. M., Onani, M. O., Ojwach, S. O., and Omondi, B. (2012). New imino-pyridyl nickel(II) complexes: Synthesis, molecular structures and application as Heck coupling catalysts. *Inorganica Chimica Acta*, **391**, 93–97. <https://doi.org/10.1016/j.ica.2012.04.037>
- Mu, H. L., Ye, W. P., Song, D. P., and Li, Y. S. (2010). Highly active Single-Component Neutral Nickel Ethylene Polymerization Catalysts: The Influence of Electronic Effects and Spectator Ligands. *Organometallics*, **29**(23), 6282–6290. <https://doi.org/10.1021/om100658j>
- Na, S. J., Joe, D. J., Sujith, S., Han, W. S., Kang, S. O., and Lee, B. Y. (2006). Bimetallic nickel complexes of macrocyclic tetraaminodiphenols and their ethylene polymerization. *Journal of Organometallic Chemistry*, **691**(4), 611–620. <https://doi.org/10.1016/j.jorganchem.2005.09.032>
- Naeimi, H., and Moradian, M. (2010). Synthesis and characterization of nitro-Schiff bases derived from 5-nitro-salicylaldehyde and various diamines and their complexes of Co(II). *Journal of Coordination Chemistry*, **63**(1), 156–162. <https://doi.org/10.1080/00958970903225866>
- Naeimi, H., and Moradian, M. (2013). Efficient Synthesis and Characterization of Some Novel Nitro-Schiff Bases and Their Complexes of Nickel (II) and Copper (II). *Journal of Chemistry*, **2013**, 1–9.
- Naeimi, H., and Rabiei, K. (2007). Convenient, Mild and One-Pot Synthesis of Double Schiff Bases from Three Component Reaction of Salicylaldehyde, Ammonium Acetate and Aliphatic Aldehydes Accelerated by NEt₃ as a Base. *Journal of the Chinese Chemical Society*, **54**(5), 1293–1298. <https://doi.org/10.1002/jccs.200700182>
- Naeimi, H., Safari, J., and Heidarneshad, A. (2007). Synthesis of Schiff base ligands derived from condensation of salicylaldehyde derivatives and synthetic diamine. *Dyes and Pigments*, **73**(2), 251–253. <https://doi.org/10.1016/j.dyepig.2005.12.009>

- Nazir, H., Arici, C., Emregül, K. C., and Atakol, O. (2006). A crystallographic and spectroscopic study on the imine-amine tautomerism of 2-hydroxyaldimine compounds. *Zeitschrift Fur Kristallographie*, **221**(10), 699–704. <https://doi.org/10.1524/zkri.2006.221.10.699>
- Nejati, K., and Rezvani, Z. (2003). Syntheses, characterization and mesomorphic properties of new bis(alkoxyphenylazo)-substituted N,N' salicylidene diiminato Ni(II), Cu(II) and VO(IV) complexes. *New Journal of Chemistry*, **27**(11), 1665–1669. <https://doi.org/10.1039/b305278h>
- Nejo, A. A., Kolawole, G. A., Nejo, A. O., Segapelo, T. V., and Muller, C. J. (2011). Synthesis, structural, and insulin-enhancing studies of oxovanadium(IV) complexes. *Australian Journal of Chemistry*, **64**(12), 1574–1579. <https://doi.org/10.1071/CH11291>
- Neto, O. I. R., Mauler, R. S., and de Souza, R. F. (2001). Influence of Hydrogen on the Polymerization of Ethylene with Nickel- α -diimine Catalyst. *Macromolecular Chemistry and Physics*, **202**(17), 3432–3436. [https://doi.org/10.1002/1521-3935\(20011101\)202:17<3432::AID-MACP3432>3.0.CO;2-A](https://doi.org/10.1002/1521-3935(20011101)202:17<3432::AID-MACP3432>3.0.CO;2-A)
- Nicolaou, K. C., Bulger, P. G., and Sarlah, D. (2005). Palladium-Catalyzed Cross-Coupling Reactions in Total Synthesis. *Angewandte Chemie - International Edition*, **44**(29), 4442–4489. <https://doi.org/10.1002/anie.200500368>
- Noël, G., Röder, J. C., Dechert, S., Pritzkow, H., Bolk, L., Mecking, S., and Meyer, F. (2006). Pyrazolate-Based Dinuclear α -Diimine-Type Palladium(II) and Nickel(II) Complexes - a Bimetallic Approach in Olefin Polymerisation. *Advanced Synthesis and Catalysis*, **348**(7–8), 887–897. <https://doi.org/10.1002/adsc.200505457>
- Ogunwumi, S. B., and Bein, T. (1997). Intrazeolite assembly of a chiral manganese salen epoxidation catalyst. *Chemical Communications*, (9), 901–902. <https://doi.org/10.1039/a607879f>
- Ohkuma, T., Ooka, H., Hashiguchi, S., Ikariya, T., and Noyori, R. (1995). Practical Enantioselective Hydrogenation of Aromatic Ketones. *Journal of the American Chemical Society*, **117**(9), 2675–2676. <https://doi.org/10.1021/ja00114a043>
- Oncel, N., Kasumov, V. T., Sahin, E., and Ulusoy, M. (2016). Synthesis, characterization and catalytic activity of new bis(N-2,6-diphenylphenol-R-salicylaldiminato)Pd(II) complexes in Suzuki-Miyaura and CO₂ fixation reactions. *Journal of Organometallic Chemistry*, **811**, 81–90. <https://doi.org/10.1016/j.jorganchem.2016.03.024>
- Osichow, A., Göttker-Schnetmann, I., and Mecking, S. (2013). Role of Electron-Withdrawing Remote Substituents in Neutral Nickel(II) Polymerization Catalysts. *Organometallics*, **32**(18), 5239–5242. <https://doi.org/10.1021/om400757f>
- Osichow, A., Rabe, C., Vogtt, K., Narayanan, T., Harnau, L., Drechsler, M., Ballauff, M., and Mecking, S. (2013). Ideal Polyethylene Nanocrystals. *Journal of the American Chemical Society*, **135**(31), 11645–11650. <https://doi.org/10.1021/ja4052334>
- Phillips, C. B., and Datta, R. (1997). Production of Ethylene from Hydrous Ethanol on H-ZSM-5 under Mild Conditions. *Industrial and Engineering Chemistry Research*, **36**(11), 4466–4475. <https://doi.org/10.1021/ie9702542>

- Pugin, B. (1996). Immobilized catalysts for enantioselective hydrogenation: The effect of site-isolation. *Journal of Molecular Catalysis A: Chemical*, **107**, 273–279. [https://doi.org/10.1016/1381-1169\(95\)00174-3](https://doi.org/10.1016/1381-1169(95)00174-3)
- Qin, W., Long, S., Panunzio, M., and Biondi, S. (2013). Schiff Bases: A Short Survey on an Evergreen Chemistry Tool. *Molecules*, **18**(10), 12264–12289. <https://doi.org/10.3390/molecules181012264>
- Rhinehart, J. L., Brown, L. A., and Long, B. K. (2013). A Robust Ni(II) α -Diimine Catalyst for High Temperature Ethylene Polymerization. *Journal of American Chemical Society*, **135**, 16316–16319. <https://doi.org/10.1021/ja408905t>
- Rodriguez, B. A., Delferro, M., and Marks, T. J. (2008). Neutral Bimetallic Nickel(II) Phenoxyiminato Catalysts for Highly Branched Polyethylenes and Ethylene-Norbornene Copolymerizations. *Organometallics*, **27**, 2166–2168.
- Rodriguez, B. A., Delferro, M., and Marks, T. J. (2009). Bimetallic effects for enhanced polar comonomer enchainment selectivity in catalytic ethylene polymerization. *Journal of the American Chemical Society*, **131**(16), 5902–5919. <https://doi.org/10.1021/ja900257k>
- Roy, S., Mpourmpakis, G., Hong, D.-Y., Vlachos, D. G., Bhan, A., and Gorte, R. J. (2012). Mechanistic Study of Alcohol Dehydration on γ -Al₂O₃. *ACS Catalysis*, **2**, 1846–1853. <https://doi.org/10.1021/acs.energyfuels.5b01294>
- Salata, M. R., and Marks, T. J. (2008). Synthesis, Characterization, and Marked Polymerization Selectivity Characteristics of Binuclear Phenoxyiminato Organozirconium Catalysts. *Journal of the American Chemical Society*, **130**(1), 12–13. <https://doi.org/10.1021/ja076857e>
- Salata, M. R., and Marks, T. J. (2009). Catalyst Nuclearity Effects in Olefin Polymerization. Enhanced Activity and Comonomer Enchainment in Ethylene + Olefin Copolymerizations Mediated by Bimetallic group 4 Phenoxyiminato Catalysts. *Macromolecules*, **42**(6), 1920–1933. <https://doi.org/10.1021/ma8020745>
- Salo, E. V., and Guan, Z. (2003). Late-Transition-Metal Complexes with Bisazaferrocene Ligands for Ethylene Oligomerization. *Organometallics*, **22**(24), 5033–5046. <https://doi.org/10.1021/om034051r>
- Saluzzo, C., and Lemaire, M. (2002). Homogeneous-Supported Catalysts for Enantioselective Hydrogenation and Hydrogen Transfer Reduction. *Advanced Synthesis and Catalysis*, **344**(10), 915–928. [https://doi.org/10.1002/1615-4169\(200210\)344:9<915::AID-ADSC915>3.0.CO;2-I](https://doi.org/10.1002/1615-4169(200210)344:9<915::AID-ADSC915>3.0.CO;2-I)
- Schiff, H. (1864). Eine neue Reihe organischer Basen. *Justus Liebigs Ann. Chem*, **131**, 118–119.
- Schiff, Hugo. (1866). Eine neue Reihe organischer Diamine; *Justus Liebigs Annalen Der Chemie*, **140**(1), 92–137. <https://doi.org/10.1002/jlac.18661400106>
- Schomaker, J. M., and Delia, T. J. (2001). Arylation of Halogenated Pyrimidines via a Suzuki Coupling Reaction. *Journal of Organic Chemistry*, **66**(21), 7125–7128. <https://doi.org/10.1021/jo010573+>
- Schrittwieser, J. H., Resch, V., Sattler, J. H., Lienhart, W. D., Durchschein, K., Winkler, A.,

- Gruber, K., MacHeroux, P., and Kroutil, W. (2011). Biocatalytic enantioselective oxidative C-C coupling by aerobic C-H activation. *Angewandte Chemie - International Edition*, **50**, 1068–1071. <https://doi.org/10.1002/anie.201006268>
- Schröder, D. L., Keim, W., Zuideveld, M. A., and Mecking, S. (2002). Ethylene Polymerization by Novel, Easily Accessible Catalysts Based on Nickel(II) Diazene Complexes. *Macromolecules*, **35**(16), 6071–6073. <https://doi.org/10.1021/ma012171+>
- Schulz, M., Debel, R., Görls, H., Plass, W., and Westerhausen, M. (2011). Synthesis and characterization of a N-salicylaldimine ligand and its vanadium(V) complex. *Inorganica Chimica Acta*, **365**(1), 349–355. <https://doi.org/10.1016/j.ica.2010.09.052>
- Shahnaz, N., Banik, B., and Das, P. (2013). A highly efficient Schiff-base derived palladium catalyst for the Suzuki-Miyaura reactions of aryl chlorides. *Tetrahedron Letters*, **54**(22), 2886–2889. <https://doi.org/10.1016/j.tetlet.2013.03.115>
- Shao, C., Sun, W., Li, Z., Hu, Y., and Han, L. (2002). Ethylene oligomerization promoted by group 8 metal complexes containing 2-(2-pyridyl) quinoxaline ligands. *Catalysis Communications*, **3**, 405–410. [https://doi.org/10.1016/S1566-7367\(02\)00158-9](https://doi.org/10.1016/S1566-7367(02)00158-9)
- Sheng, G. H., Cheng, X. S., You, Z. L., and Zhu, H. L. (2015). Characterization and crystal structure of a novel tetranuclear zinc(II) complex derived from N,N'-bis(2-hydroxy-5-methoxybenzylidene)propane-1,3-diamine. *Journal of Structural Chemistry*, **56**(1), 197–201. <https://doi.org/10.1134/S0022476615010291>
- Song, D. P., Ye, W. P., Wang, Y. X., Liu, J. Y., and Li, Y. S. (2009). Highly Active Neutral Nickel(II) Catalysts for Ethylene Polymerization Bearing Modified β -Ketoiminato Ligands. *Organometallics*, **28**(19), 5697–5704. <https://doi.org/10.1021/om900477k>
- Sonogashira, K. (2002). Development of Pd-Cu catalyzed cross-coupling of terminal acetylenes with sp^2 -carbon halides. *Journal of Organometallic Chemistry*, **653**, 46–49. [https://doi.org/10.1016/S0022-328X\(02\)01158-0](https://doi.org/10.1016/S0022-328X(02)01158-0)
- Soshnikov, I. E., Semikolenova, N. V., Zakharov, V. A., Möller, H. M., Ölscher, F., Osichow, A., Göttker-Schnetmann, I., Mecking, S., Talsi, E. P., and Bryliakov, K. P. (2013). Formation and evolution of chain-propagating species upon ethylene polymerization with neutral salicylaldiminato nickel(II) catalysts. *Chemistry - A European Journal*, **19**(34), 11409–11417. <https://doi.org/10.1002/chem.201301037>
- Speiser, F., and Braunstein, P. (2004). Dinuclear Nickel Complexes with Bidentate N,O Ligands: Synthesis, Structure, and Catalytic Oligomerization of Ethylene. *Inorganic Chemistry*, **43**(14), 4234–4240. <https://doi.org/10.1021/om034197q>
- Speiser, F., Braunstein, P., and Saussine, L. (2005). Catalytic Ethylene Dimerization and Oligomerization: Recent Developments with Nickel Complexes Containing P,N-Chelating Ligands. *Accounts of Chemical Research*, **38**(10), 784–793. <https://doi.org/10.1021/ar050040d>
- Spek, A. L., and Van Der Sluis, P. (1990). Structure of 1,2,5,6-tetramethyltricyclohexane-3,4-dione. *Acta Crystallographica*, **46**, 1357–1358. <https://doi.org/10.1107/S0108270190001433>

- Steiner, T. (2002). The Hydrogen Bond in the Solid State. *Angewandte Chemie - International Edition*, **41**, 48–76. [https://doi.org/10.1002/1521-3773\(20020104\)41:1<48::AID-ANIE48>3.0.CO;2-U](https://doi.org/10.1002/1521-3773(20020104)41:1<48::AID-ANIE48>3.0.CO;2-U)
- Stephenson, C. J., McInnis, J. P., Chen, C., Weberski, M. P., Motta, A., Delferro, M., and Marks, T. J. (2014). Ni(II) Phenoxyminato Olefin Polymerization Catalysis: Striking Coordinative Modulation of Hyperbranched Polymer Microstructure and Stability by a Proximate Sulfonyl Group. *ACS Catalysis*, **4**(3), 999–1003. <https://doi.org/10.1021/cs500114b>
- Sujith, S., Joe, D. J., Na, S. J., Park, Y. W., Choi, C. H., and Lee, B. Y. (2005). Ethylene/Polar Norbornene Copolymerizations by Bimetallic Salicylaldimine-Nickel Catalysts. *Macromolecules*, **38**(24), 10027–10033. <https://doi.org/10.1021/ma051344i>
- Sun, J., Zhu, K., Gao, F., Wang, C., Liu, J., Peden, C. H. F., and Wang, Y. (2011). Direct Conversion of Bio-ethanol to Isobutene on Nanosized $Zn_xZr_yO_z$ Mixed Oxides with Balanced Acid - Base Sites. *Journal of the American Chemical Society*, **133**(29), 11096–11099. <https://doi.org/10.1021/ja204235v>
- Sun, W.-H., Yang, H., Li, Z., and Li, Y. (2003). Vinyl Polymerization of Norbornene with Neutral Salicylaldiminato Nickel(II) Complexes. *Organometallics*, **22**(18), 3678–3683. <https://doi.org/10.1021/om030018t>
- Suo, H., Solan, G. A., Ma, Y., and Sun, W. H. (2018). Developments in compartmentalized bimetallic transition metal ethylene polymerization catalysts. *Coordination Chemistry Reviews*, **372**, 101–116. <https://doi.org/10.1016/j.ccr.2018.06.006>
- Suzuki, N., Haraga, K., Shimamura, T., and Masuyama, Y. (2015). Synthesis and Structures of Ti-Pd Heterobimetallic Complexes. *European Journal of Inorganic Chemistry*, 5480–5487. <https://doi.org/10.1002/ejic.201501003>
- Svejda, S. A., and Brookhart, M. (1999). Ethylene Oligomerization and Propylene Dimerization using Cationic (α -Diimine)nickel(II) Catalysts. *Organometallics*, **18**(1), 65–74. <https://doi.org/10.1021/om980736t>
- Takemoto, S., Kuwata, S., Nishibayashi, Y., and Hidai, M. (1998). Synthesis of Heterobimetallic Fe-M (M = Ni, Pd, Pt) Complexes Containing the 1,1'-Ferrocenedithiolato Ligand and Their Conversion to Trinuclear Complexes. *Inorganic Chemistry*, **37**(25), 6428–6434. <https://doi.org/10.1021/ic9806129>
- Takeuchi, D., Chiba, Y., Takano, S., Kurihara, H., Kobayashi, M., and Osakada, K. (2017). Ethylene Polymerization Catalyzed by Dinickel Complexes with a Double-Decker Structure. *Polymer Chemistry*, **8**(34), 5112–5119. <https://doi.org/10.1039/c7py00333a>
- Tang, X., Huang, Y.-T., Liu, H., Liu, R.-Z., Shen, D.-S., Liu, N., and Liu, F.-S. (2013). α -Hydroxyimine palladium complexes: Synthesis, molecular structure, and their activities towards the Suzuki–Miyaura cross-coupling reaction. *Journal of Organometallic Chemistry*, **729**, 95–102. <https://doi.org/10.1016/j.jorganchem.2013.01.018>
- Tardiff, B. J., Smith, J. C., Duffy, S. J., Vogels, C. M., Decken, A., and Westcott, S. A. (2007). Synthesis, characterization, and reactivity of Pd(II) salicylaldimine complexes derived from aminophenols. *Canadian Journal of Chemistry*, **85**(5), 392–399.

<https://doi.org/10.1139/v07-036>

- Tas, E., Kilic, A., Durgun, M., Yilmaz, I., Ozdemir, I., and Gurbuz, N. (2009). Mono- and dinuclear Pd(II) complexes of different salicylaldimine ligands as catalysts of transfer hydrogenation of nitrobenzene with cyclohexene and Suzuki-Miyaura coupling reactions. *Journal of Organometallic Chemistry*, **694**(3), 446–454. <https://doi.org/10.1016/j.jorganchem.2008.11.021>
- Tas, Esref, Kilic, A., Konak, N., and Yilmaz, I. (2008). The sterically hindered salicylaldimine ligands with their copper(II) metal complexes: Synthesis, spectroscopy, electrochemical and thin-layer spectroelectrochemical features. *Polyhedron*, **27**(3), 1024–1032. <https://doi.org/10.1016/j.poly.2007.11.038>
- Tolstikov, A. G., Karpyshev, N. N., Tolstikova, O. V, Khlebnikova, T. B., Sal'nikov, G. E., Mamatyuk, V. I., Gatilov, Y. V., and Bagryanskaya, I. Y. (2001). Derivatives of L-Pimaric Acid in the Synthesis of Chiral Organophosphorus Ligands from Decahydrophenanthrene Series. *Russian Journal of Organic Chemistry*, **37**(8), 1134–1148.
- Tranchier, J.-P., Ratovelomanana-vidal, V., and Genet, J.-P. (1997). Asymmetric Hydrogenation of Phenylthio Ketones with Chiral Ru(II) Catalysts. *Tetrahedron Letters*, **38**(17), 2951–2954.
- Vaz, B., Alvarez, R., Nieto, M., Paniello, A. I., and Lera, A. R. De. (2001). Suzuki cross-coupling of meso -dibromoporphyrins for the synthesis of functionalized A2B2 porphyrins. *Tetrahedron Letters*, **42**, 7409–7412.
- Vigato, P. A., and Tamburini, S. (2004). The challenge of cyclic and acyclic schiff bases and related derivatives. *Coordination Chemistry Reviews*, **248**, 1717–2128. <https://doi.org/10.1016/j.cct.2003.09.003>
- Waltman, A. W., Younkin, T. R., and Grubbs, R. H. (2004). Insights into the Deactivation of Neutral Nickel Ethylene Polymerization Catalysts in the Presence of Functionalized Olefins. *Organometallics*, **23**(22), 5121–5123. <https://doi.org/10.1021/om049360b>
- Wang, C., Friedrich, S., Younkin, T. R., Li, R. T., Grubbs, R. H., Bansleben, D. A., and Day, M. W. (1998). Neutral nickel(II)-based catalysts for ethylene polymerization. *Organometallics*, **17**(15), 3149–3151. <https://doi.org/10.1021/om980176y>
- Wang, Leyong, Sun, W. H., Han, L., Li, Z., Hu, Y., He, C., and Yan, C. (2002). Cobalt and nickel complexes bearing 2,6-bis (imino) phenoxy ligands: Syntheses, structures and oligomerization studies. *Journal of Organometallic Chemistry*, **650**(1–2), 59–64. [https://doi.org/10.1016/S0022-328X\(02\)01149-X](https://doi.org/10.1016/S0022-328X(02)01149-X)
- Wang, Lincai, Zhang, C., and Wang, Z. (2007). Synthesis and Characterization of Iron, Cobalt, and Nickel Complexes Bearing Novel N,N -Chelate Ligands and Their Catalytic Properties in Ethylene Oligomerization. *European Journal of Inorganic Chemistry*, 2477–2487. <https://doi.org/10.1002/ejic.200700020>
- Wang, S., Sun, W. H., and Redshaw, C. (2014). Recent progress on nickel-based systems for ethylene oligo-/polymerization catalysis. *Journal of Organometallic Chemistry*, **751**, 717–741. <https://doi.org/10.1016/j.jorganchem.2013.08.021>

- Wang, W. H., and Jin, G. X. (2006). Binuclear neutral nickel complexes bearing bis(bidentate) salicylaldiminato ligands: Synthesis, structure and ethylene polymerization behavior. *Inorganic Chemistry Communications*, **9**(5), 548–550. <https://doi.org/10.1016/j.inoche.2006.02.015>
- Wang, Y., and Poirier, R. A. (1997). Factors that Influence the C=N Stretching Frequency in Imines. *Journal of Physical Chemistry A*, **101**(5), 907–912. <https://doi.org/10.1021/jp9617332>
- Weberski, M. P., Chen, C., Delferro, M., and Marks, T. J. (2012). Ligand Steric and Fluoroalkyl Substituent Effects on Enchainment Cooperativity and Stability in Bimetallic nickel(II) Polymerization Catalysts. *Chemistry - A European Journal*, **18**(34), 10715–10732. <https://doi.org/10.1002/chem.201200713>
- Weberski, M. P., Chen, C., Delferro, M., Zuccaccia, C., MacChioni, A., and Marks, T. J. (2012). Suppression of β -Hydride Chain Transfer in Nickel(II)-Catalyzed Ethylene Polymerization via Weak Fluorocarbon Ligand-Product Interactions. *Organometallics*, **31**(9), 3773–3789. <https://doi.org/10.1021/om3002735>
- Wehrmann, P., and Mecking, S. (2008). Highly Active Binuclear Neutral Nickel(II) Catalysts Affording High Molecular Weight Polyethylene. *Organometallics*, **27**(7), 1399–1408. <https://doi.org/10.1021/om700942z>
- Wiedemann, T., Gregor Voit, A., Tchernook, A., Roesle, P., Göttker-Schnetmann, and Mecking, S. (2014). Monofunctional Hyperbranched Ethylene Oligomers. *Journal of the American Chemical Society*, **136**(5), 2078–2085. <https://doi.org/10.1021/ja411945n>
- Xi, C., Wu, Y., and Yan, X. (2008). cis-Fashioned palladium (II) complexes of 2-phenylbenzimidazole ligands: Synthesis, characterization, and catalytic behavior towards Suzuki-Miyaura reaction. *Journal of Organometallic Chemistry*, **693**(26), 3842–3846. <https://doi.org/10.1016/j.jorganchem.2008.09.042>
- Xue, L. W., Li, X. W., Zhao, G. Q., and Yang, W. C. (2013). Synthesis, crystal structure, and thermal analysis of a dioxomolybdenum(VI) complex derived from N,N'-bis(5-methylsalicylidene)-1,3-diaminopropane. *Synthesis and Reactivity in Inorganic, Metal-Organic and Nano-Metal Chemistry*, **43**(10), 1514–1517. <https://doi.org/10.1080/15533174.2012.762793>
- Yang, Q., Kermagoret, A., Agostinho, M., Siri, O., and Braunstein, P. (2006). Nickel Complexes with Functional Zwitterionic N,O-Benzoquinoneminoimine-Type Ligands: Syntheses, Structures, and Catalytic Oligomerization of Ethylene. *Organometallics*, **25**(23), 5518–5527.
- Younkin, T. R., Connor, E. F., Henderson, J. I., Friedrich, S. K., Grubbs, R. H., and Bansleben, D. A. (2000). Neutral, Single-Component Nickel(II) Polyolefin Catalysts That Tolerate Heteroatoms. *Science*, **287**(5452), 460–462. <https://doi.org/10.1126/science.287.5452.460>
- Younkin, T. R., Connor, E. F., Henderson, J. I., Friedrich, S. K., Grubbs, R. H., and Bansleben, D. A. (2000b). Neutral, Single-Component Nickel (II) Polyolefin Catalysts That Tolerate Heteroatoms. *Science*, **287**, (5452), 460–462. <https://doi.org/10.1126/science.287.5452.460>
- Yu, S. M., Berkefeld, A., Göttker-Schnetmann, I., Müller, G., and Mecking, S. (2007). Synthesis

- of Aqueous Polyethylene Dispersions with Electron-Deficient Neutral Nickel(II) Catalysts with Enolatoimine Ligands. *Macromolecules*, **40**(3), 421–428.
<https://doi.org/10.1021/ma061804n>
- Yuan, J., Mei, T., Gomes, P. T., Marques, M. M., Wang, X., Liu, Y., Miao, C., and Xie, X. (2011). New octahedral bis- α -diimine nickel(II) complexes containing chloro-substituted aryl groups: Synthesis, characterization and testing as ethylene polymerisation catalysts. *Journal of Organometallic Chemistry*, **696**(20), 3251–3256.
<https://doi.org/10.1016/j.jorganchem.2011.07.009>
- Yundong, L., Yongwei, W., and Chanjuan, X. (2009). 2-Pyridylquinoxaline derivatives as N,N-ligands for palladium-catalyzed Suzuki-Miyaura reaction. *Applied Organometallic Chemistry*, **23**, 329–332. <https://doi.org/10.1002/aoc.1516>
- Zhang, D., and Jin, G. (2003). Novel , Highly Active Binuclear 2,5-Disubstituted Amino- p - benzoquinone - Nickel(II) Ethylene Polymerization Catalysts. *Organometallics*, **22**, 2851–2854.
- Zhang, D., and Jin, G. X. (2006). Bimetallic nickel complexes of trimethyl phenyl linked salicylaldimine ligands: Synthesis, structure and their ethylene polymerization behaviors. *Inorganic Chemistry Communications*, **9**(12), 1322–1325.
<https://doi.org/10.1016/j.inoche.2006.08.017>
- Zhang, D., Jin, G. X., and Hu, N. H. (2003). Ethylene Polymerization by Self-Immobilized Neutral Nickel Catalysts Bearing Allyl Groups. *European Journal of Inorganic Chemistry*, (8), 1570–1576. <https://doi.org/10.1002/ejic.200390205>
- Zhang, S., Shi, L., and Ding, Y. (2011). Theoretical analysis of the mechanism of palladium(II) acetate-catalyzed oxidative heck coupling of electron-deficient arenes with alkenes: Effects of the pyridine-type ancillary ligand and origins of the meta -regioselectivity. *Journal of the American Chemical Society*, **133**, 20218–20229. <https://doi.org/10.1021/ja205294y>
- Zhang, X. L. (2016). Copper(II) Complexes With Bis-Schiff Bases: Synthesis, Crystal Structures, and Antibacterial Activities. *Synthesis and Reactivity in Inorganic, Metal-Organic and Nano-Metal Chemistry*, **46**(12), 1848–1853.
<https://doi.org/10.1080/15533174.2015.1137069>
- Zhou, X., Wang, C., Chu, Y., Xu, J., Wang, Q., Qi, G., Zhao, X., Feng, N., and Deng, F. (2019). Observation of an oxonium ion intermediate in ethanol dehydration to ethene on zeolite. *Nature Communications*, **10**(1), 1–9. <https://doi.org/10.1038/s41467-019-09956-7>
- Zhou, Y., Liu, L., Yang, M., Lu, R., Jin, Y., and Chen, W. (2018). Synthesis, crystal structure and biological property of a novel phenolato-bridged trinuclear copper(II) complex derived from bis-Schiff base ligand. *Inorganic and Nano-Metal Chemistry*, **48**(6), 291–295.
<https://doi.org/10.1080/24701556.2018.1503682>
- Zhou, Y. M., Ye, X. R., Xin, F. B., and Xin, X. Q. (1999). Solid state self-assembly synthesis of cobalt(II), nickel(II), copper(II) and zinc(II) complexes with a bis-Schiff base. *Transition Metal Chemistry*, **24**(1), 118–120. <https://doi.org/10.1023/A:1006989707001>
- Zuideveld, M. A., Wehrmann, P., Röhr, C., and Mecking, S. (2004). Remote Substituents

Controlling Catalytic Polymerization by Very Active and Robust Neutral Nickel(II) Complexes. *Angewandte Chemie - International Edition*, **43**(7), 869–873.
<https://doi.org/10.1002/anie.200352062>

APPENDICES

Appendix A: FTIR Graphs for Ligands

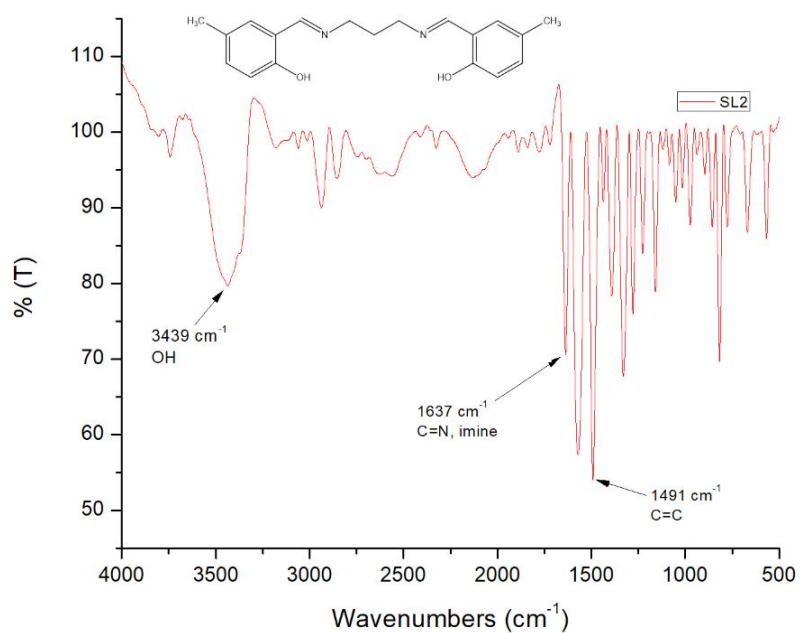


Figure A.1: FTIR spectrum for the ligand SL2

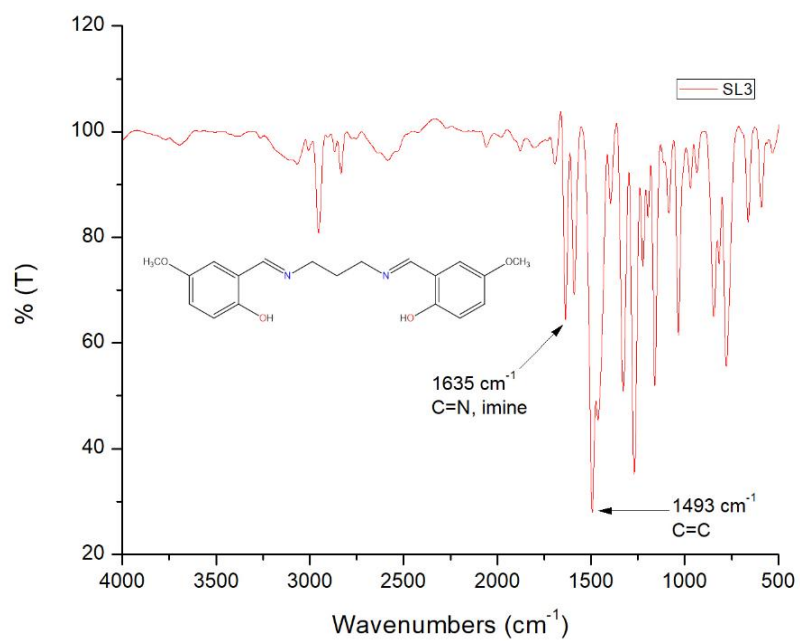


Figure A.2: FTIR spectrum for the ligand SL3

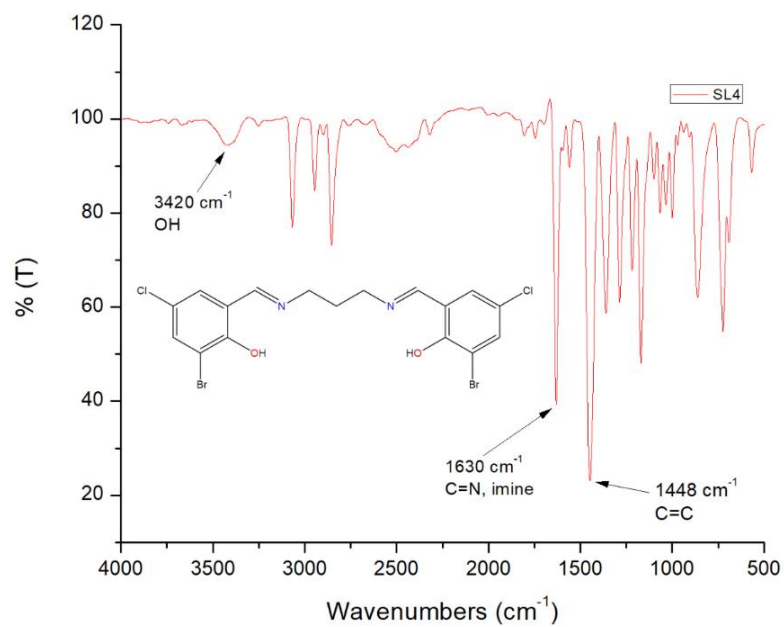


Figure A.3: FTIR spectrum for the ligand SL4

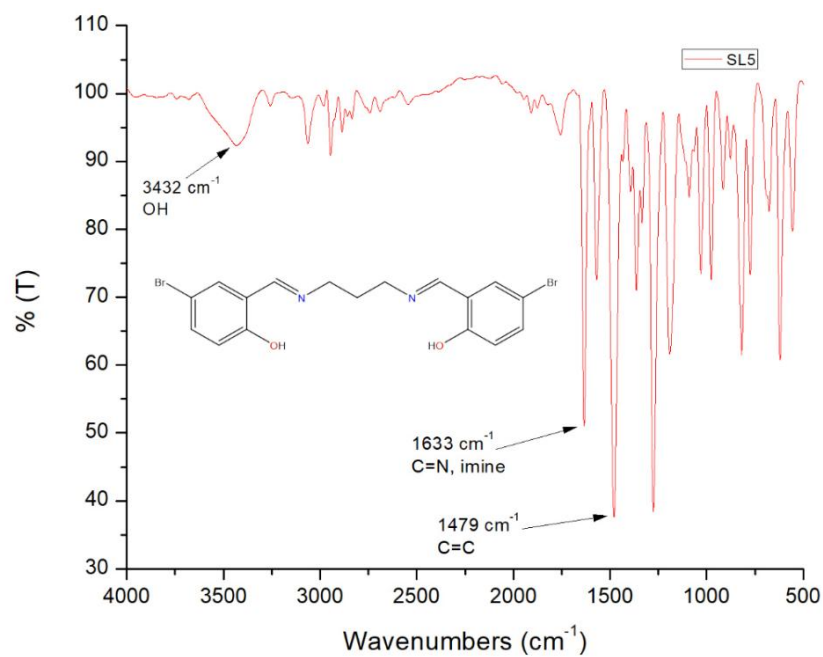


Figure A.4: FTIR spectrum for the ligand SL5

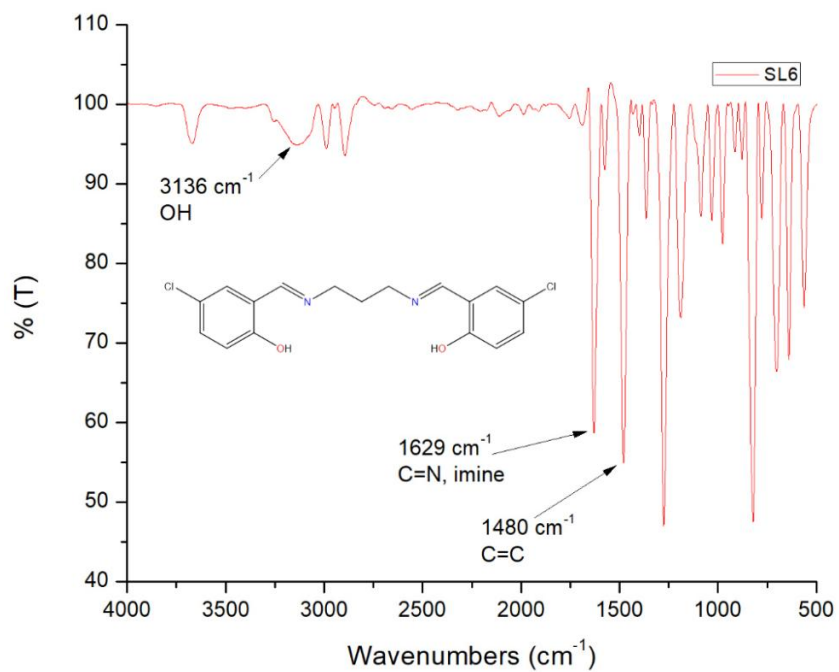


Figure A.5: FTIR spectrum for the ligand SL6

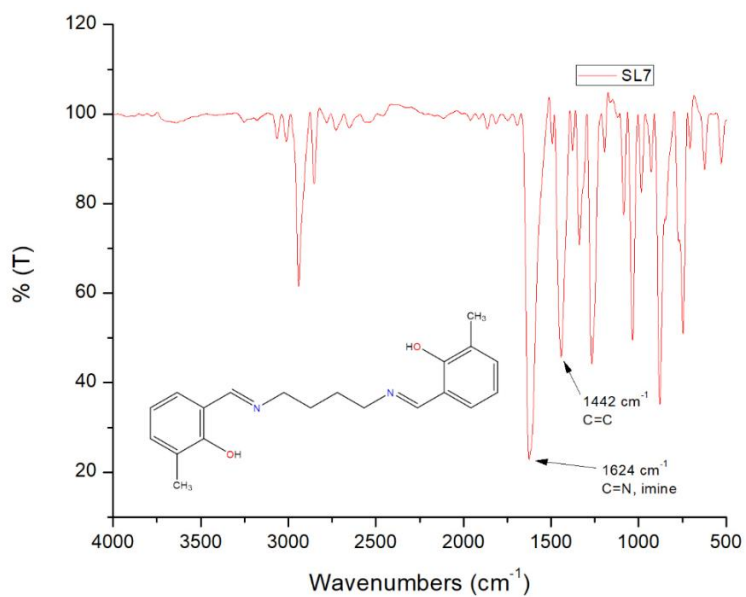


Figure A.6: FTIR spectrum for the ligand SL7

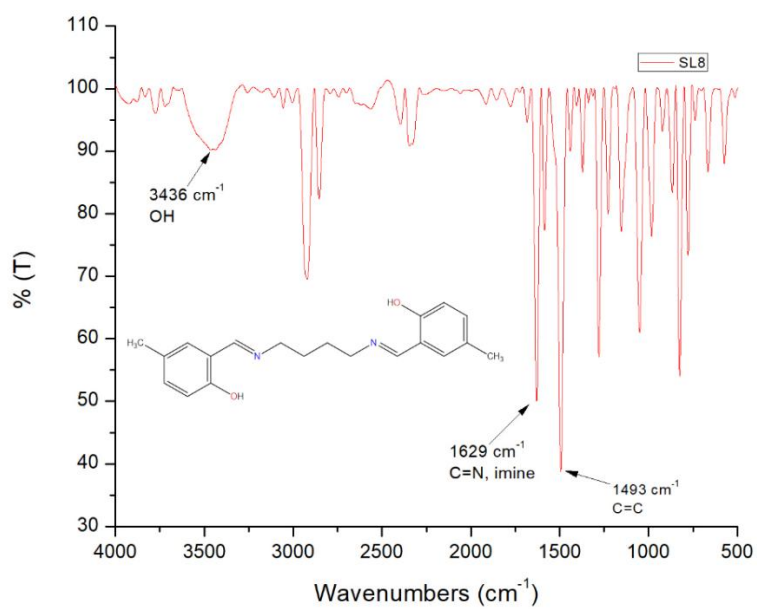


Figure A.7: FTIR spectrum for the ligand SL8

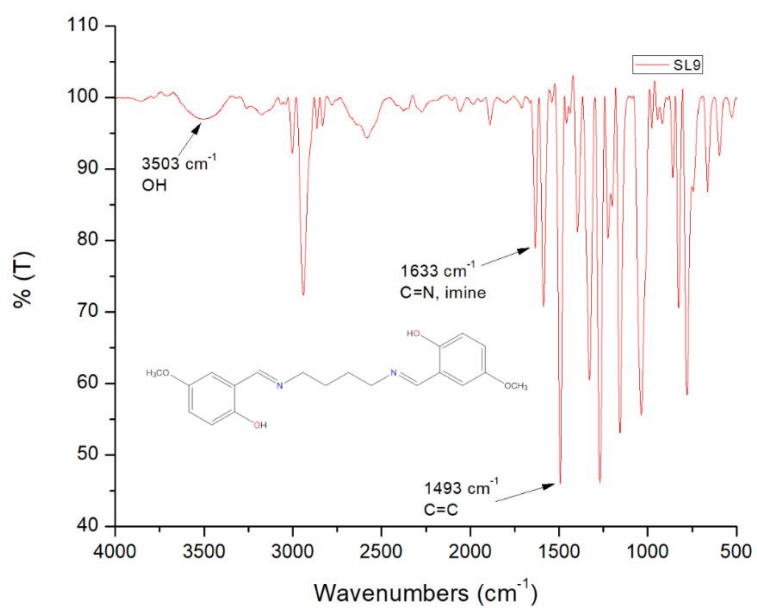


Figure A.8: FTIR spectrum for the ligand SL9

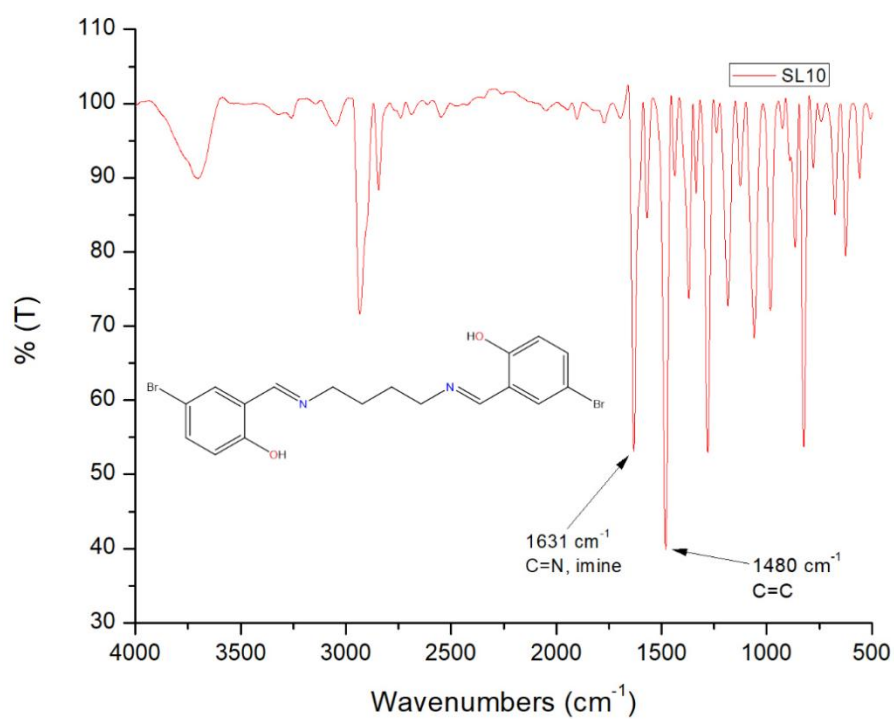


Figure A.9: FTIR spectrum for the ligand SL10

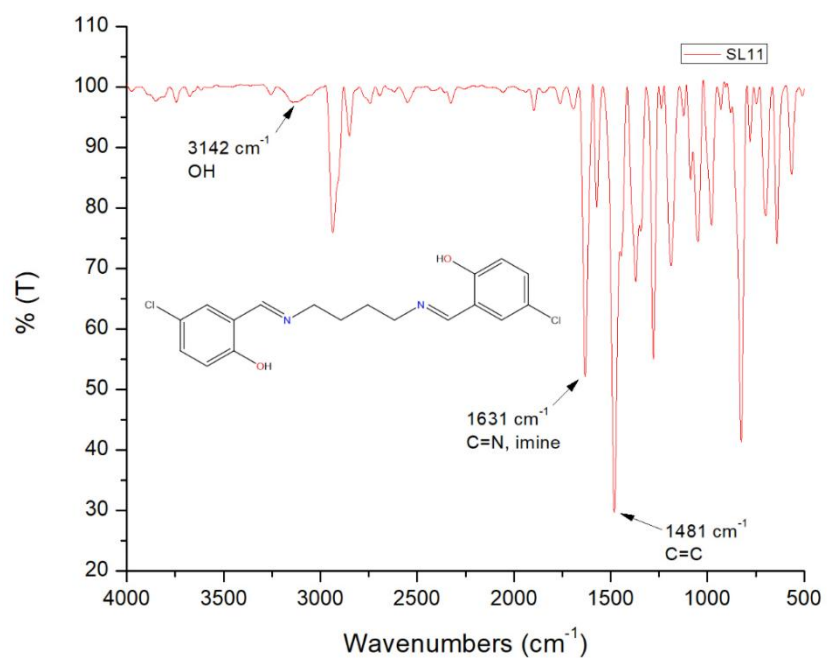


Figure A.10: FTIR spectrum for the ligand SL11

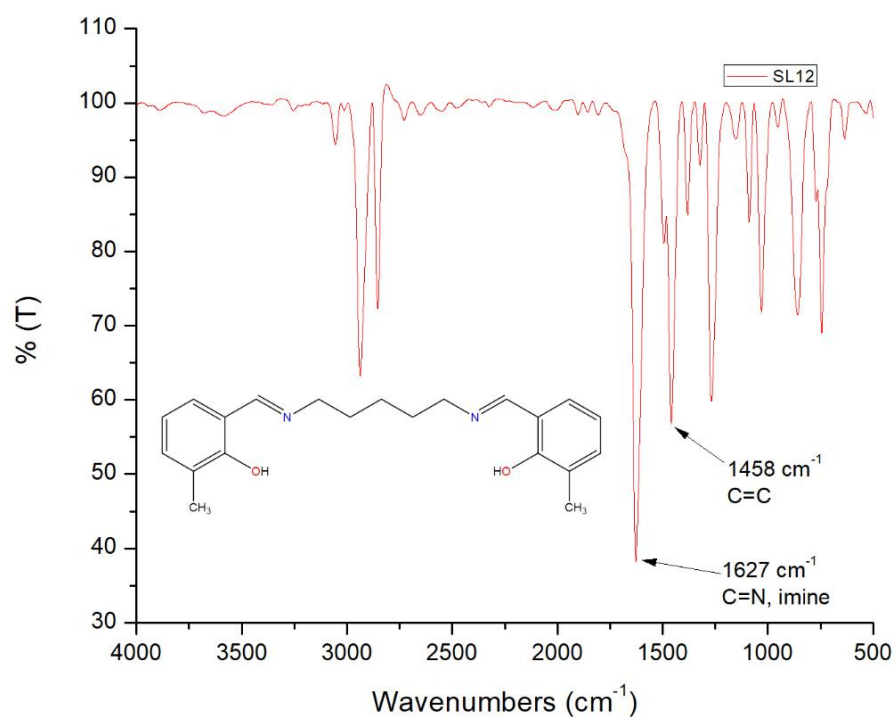


Figure A.11: FTIR spectrum for the ligand SL12

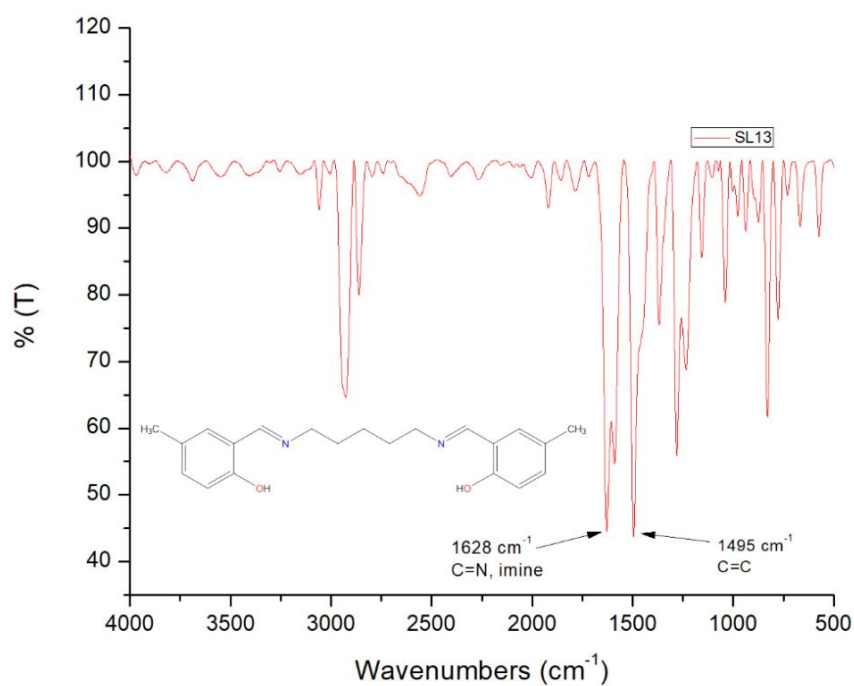


Figure A.12: FTIR spectrum for the ligand SL13

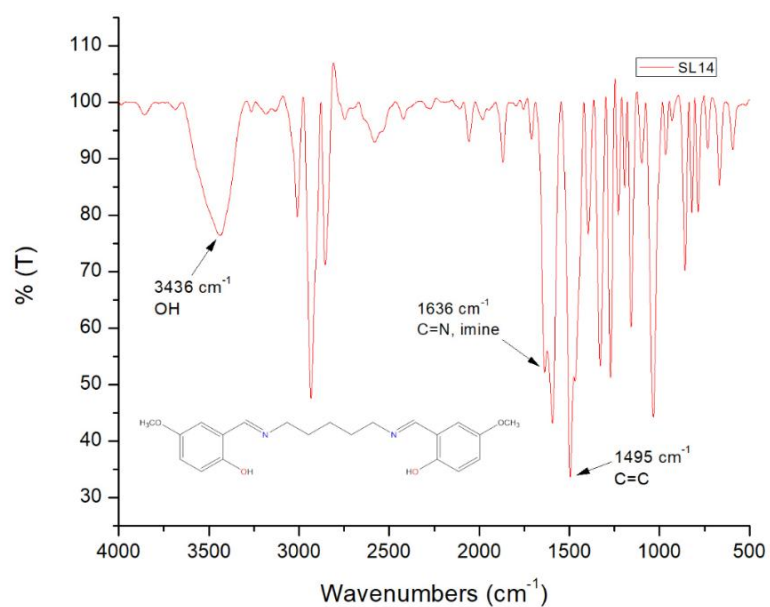


Figure A.13: FTIR spectrum for the ligand SL14

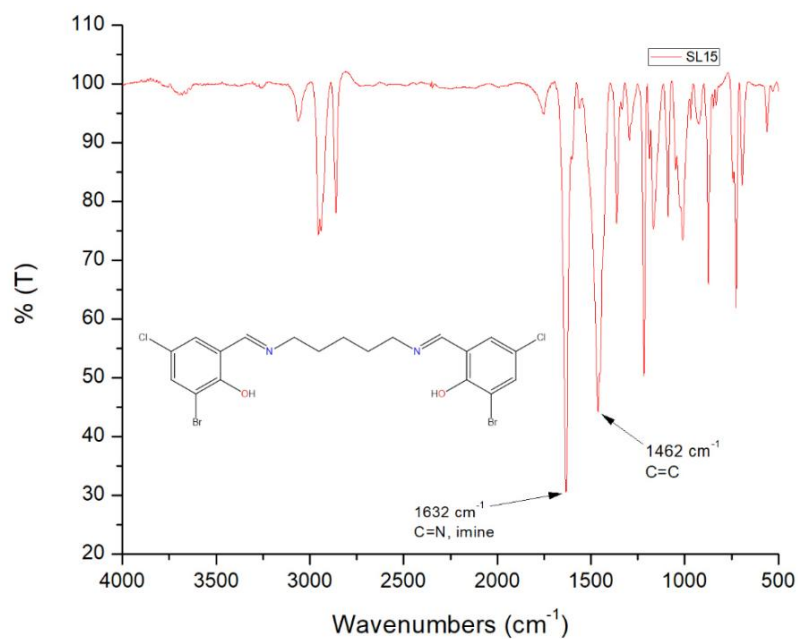


Figure A.14: FTIR spectrum for the ligand SL15

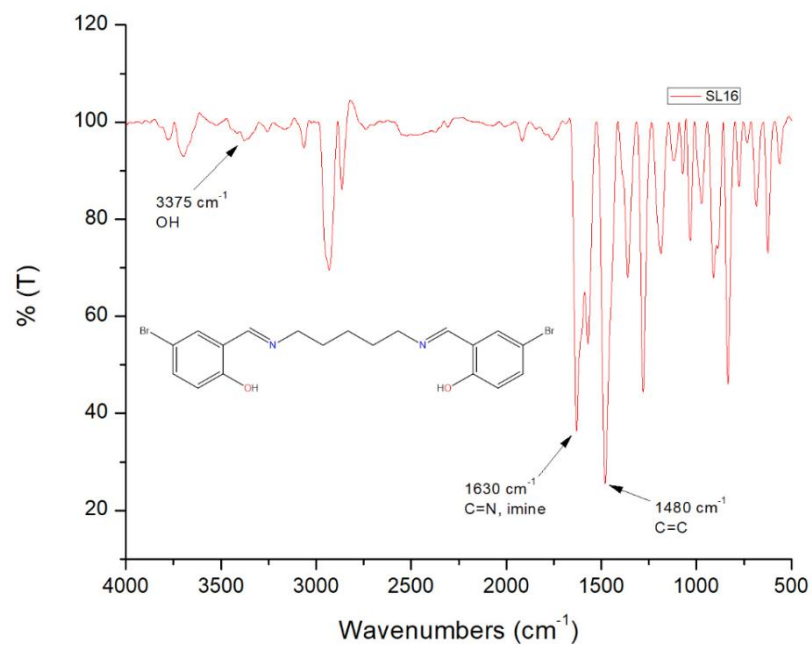


Figure A.15: FTIR spectrum for the ligand SL16

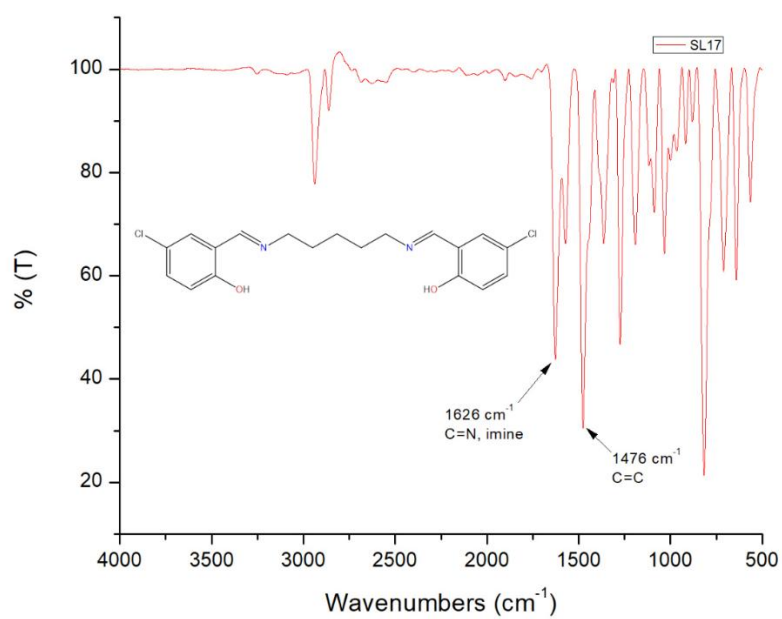
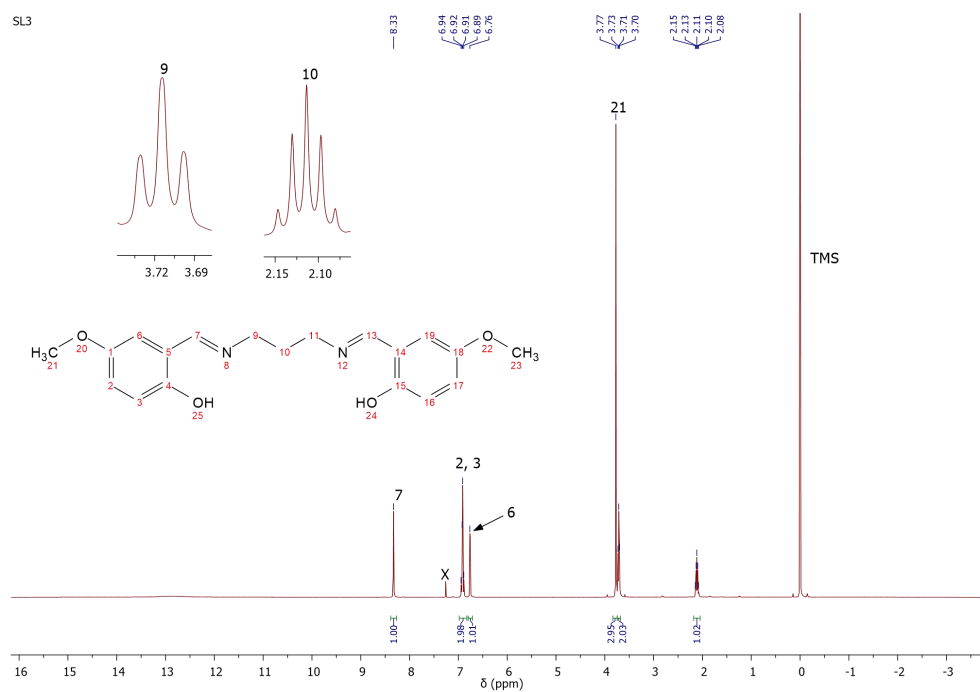
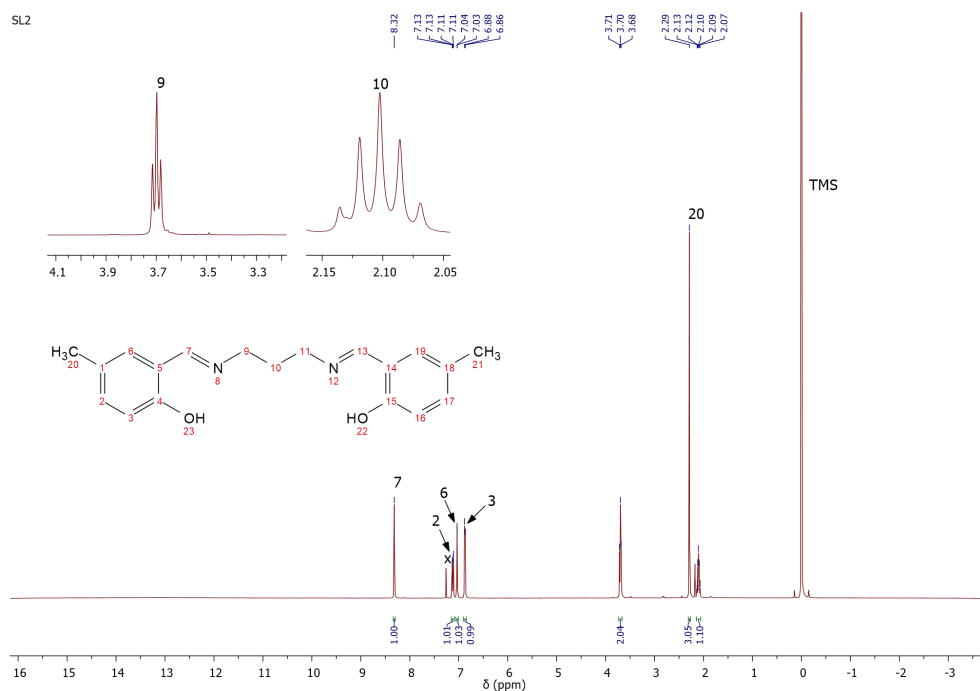
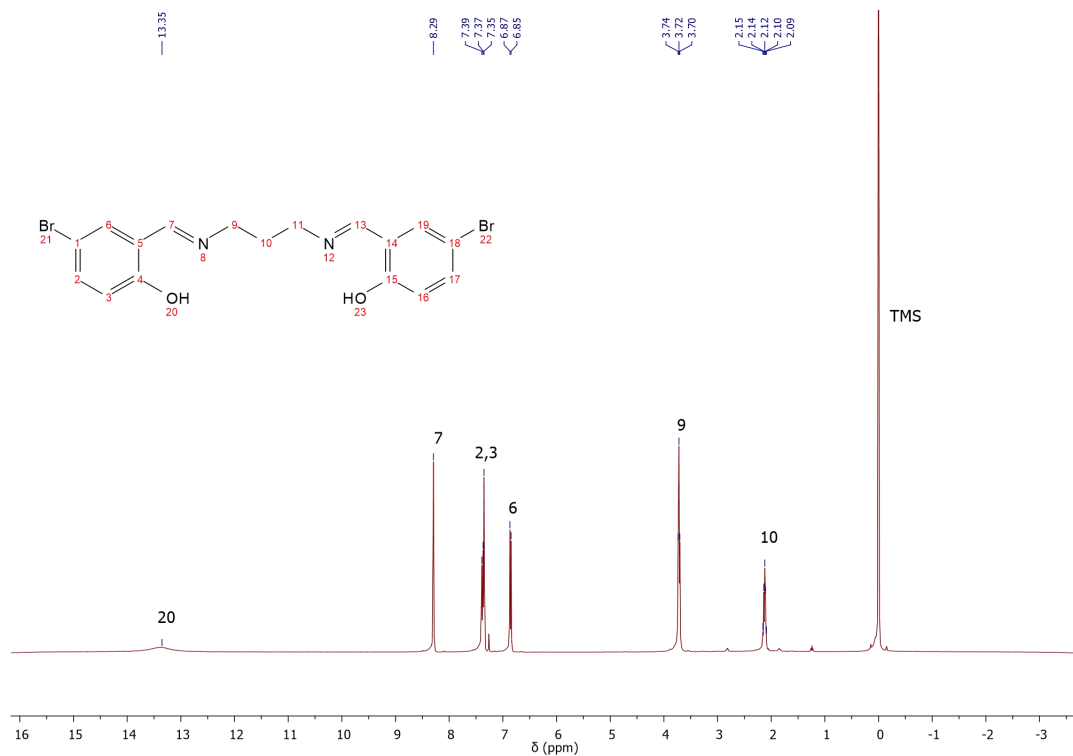
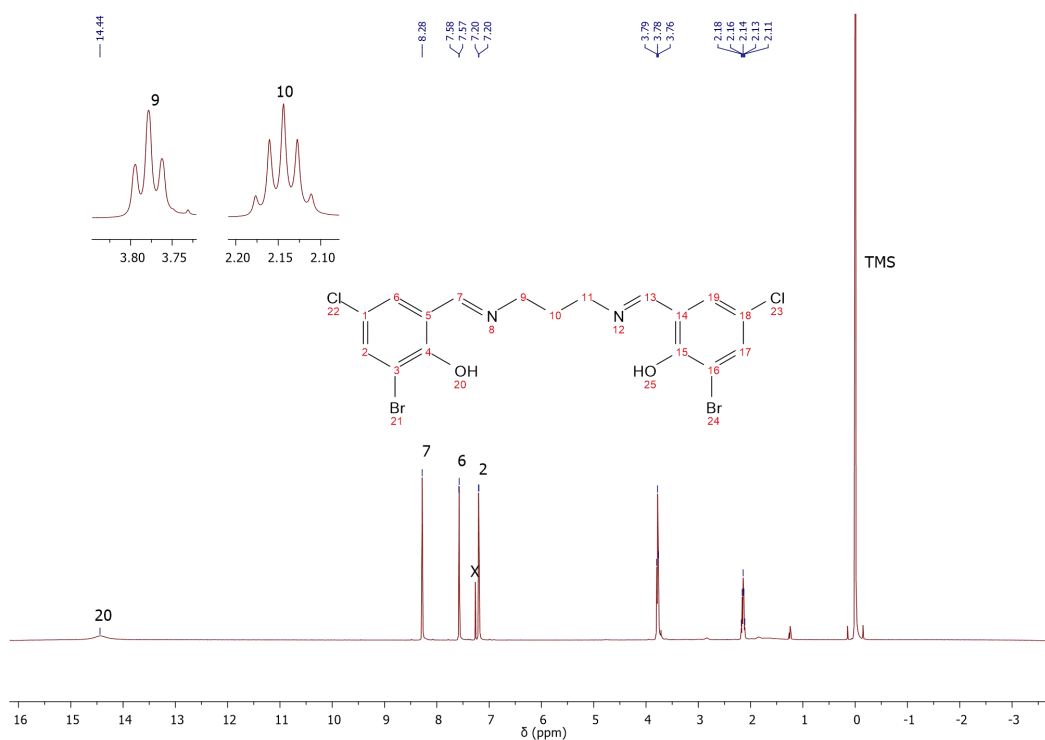


Figure A.16: FTIR spectrum for the ligand SL17

Appendix B: NMR Graphs for Ligands





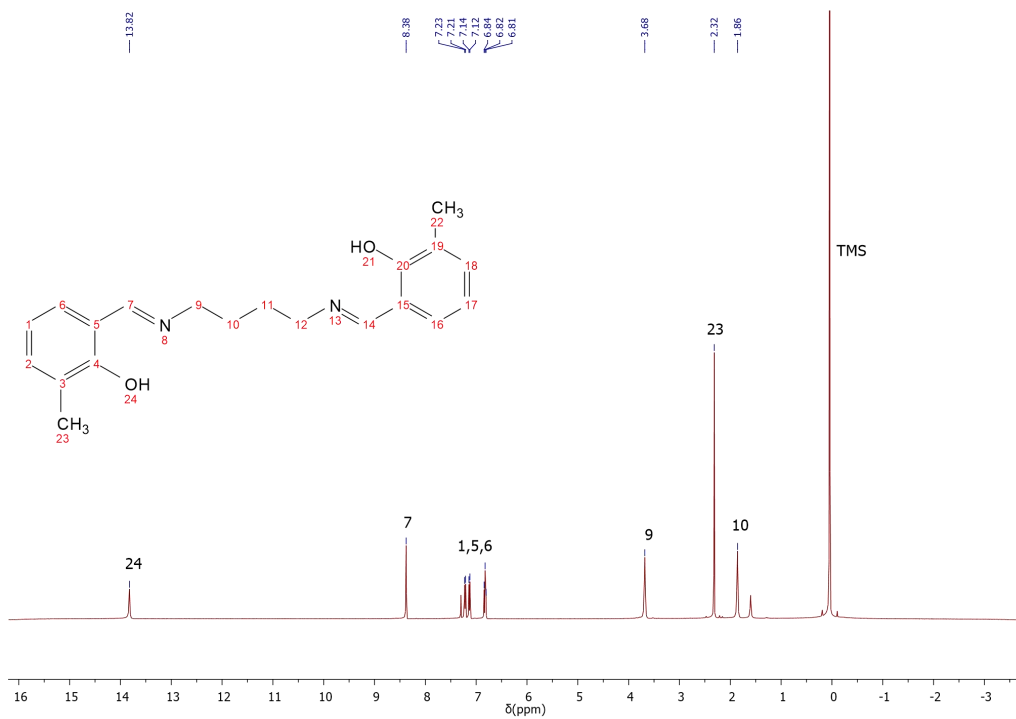
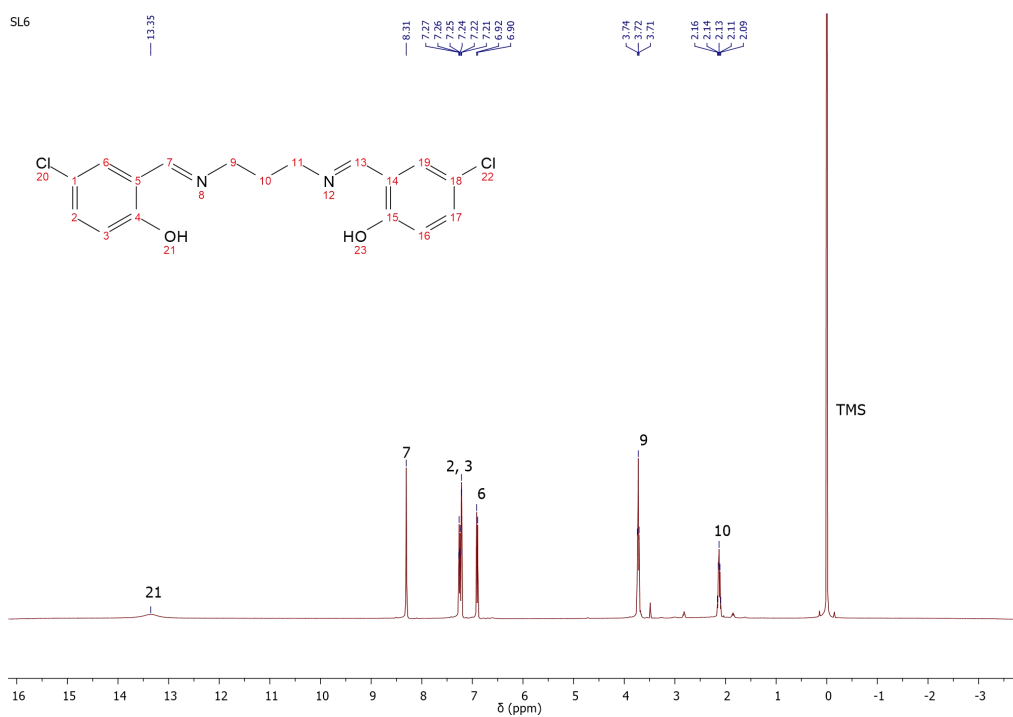




Figure B.7: $^1\text{H NMR}$ for SL8 (χ solvent CDCl₃-d₁)

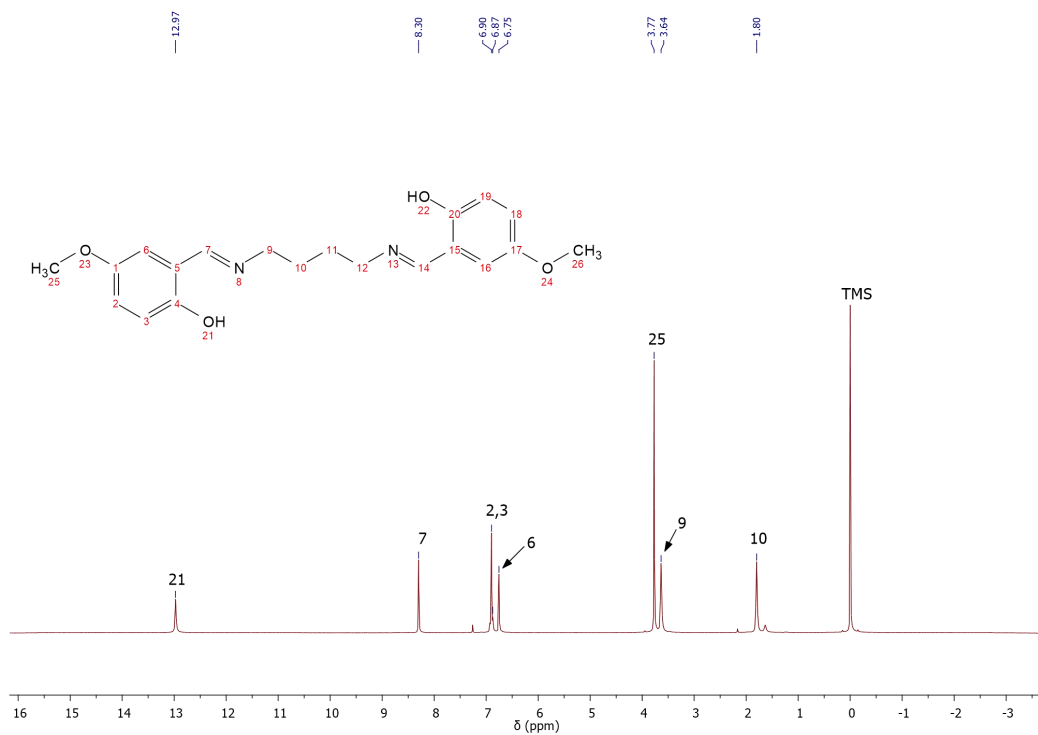


Figure B.8: $^1\text{H NMR}$ for SL9 (χ solvent CDCl₃-d₁)

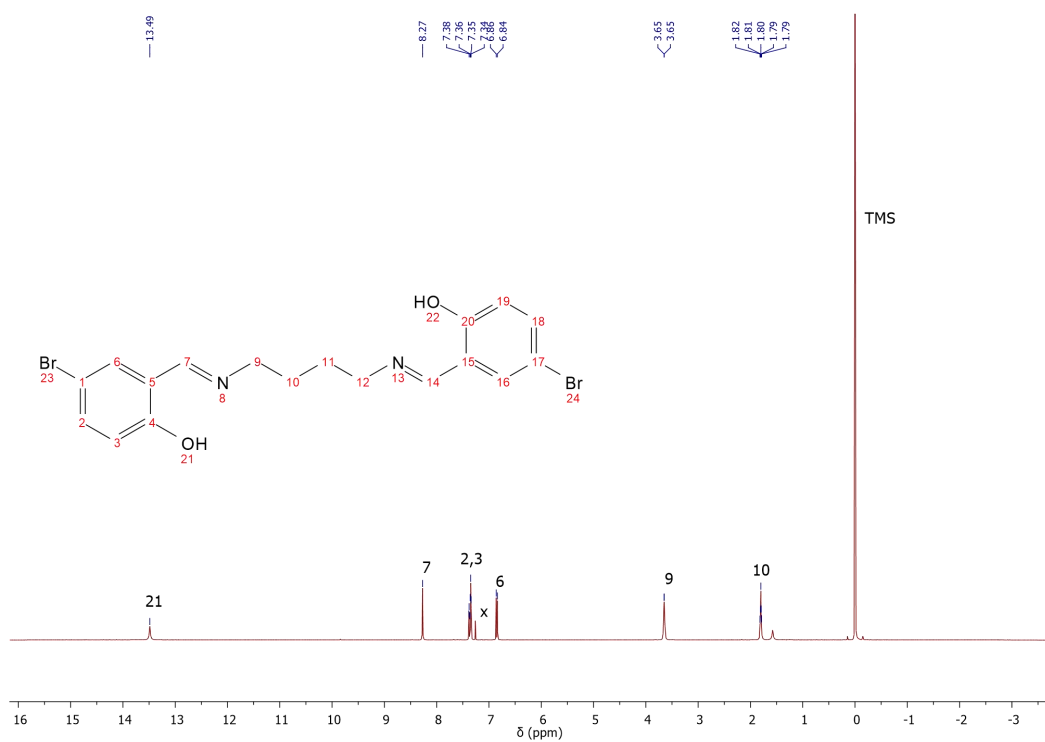


Figure B.9: ^1H NMR for SL10 (x solvent CDCl_3-d_1)

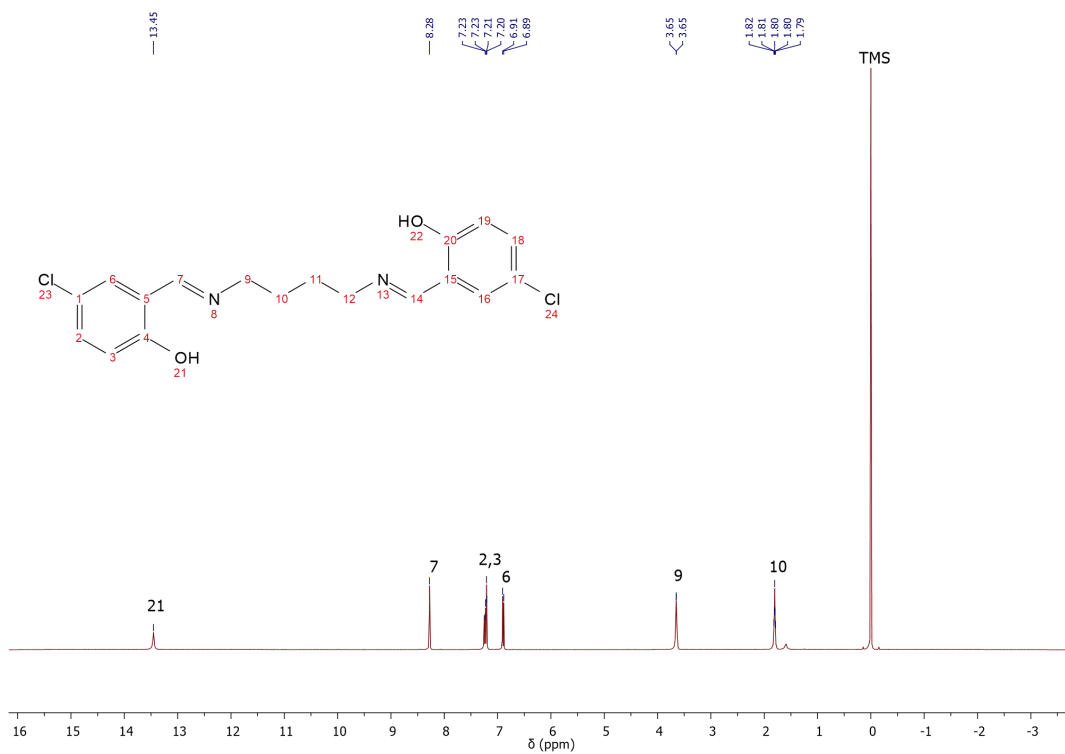


Figure B.10: ^1H NMR for SL11 (x solvent CDCl_3-d_1)

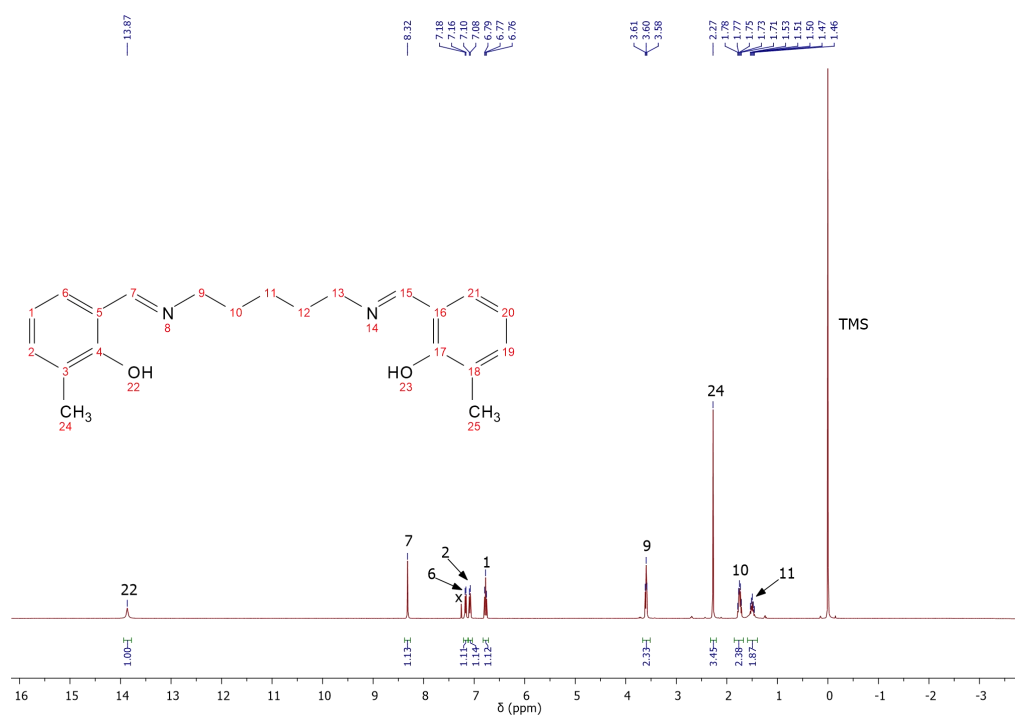


Figure B.11: ¹H NMR for SL12 (ⁿ solvent CDCl₃-d₁)

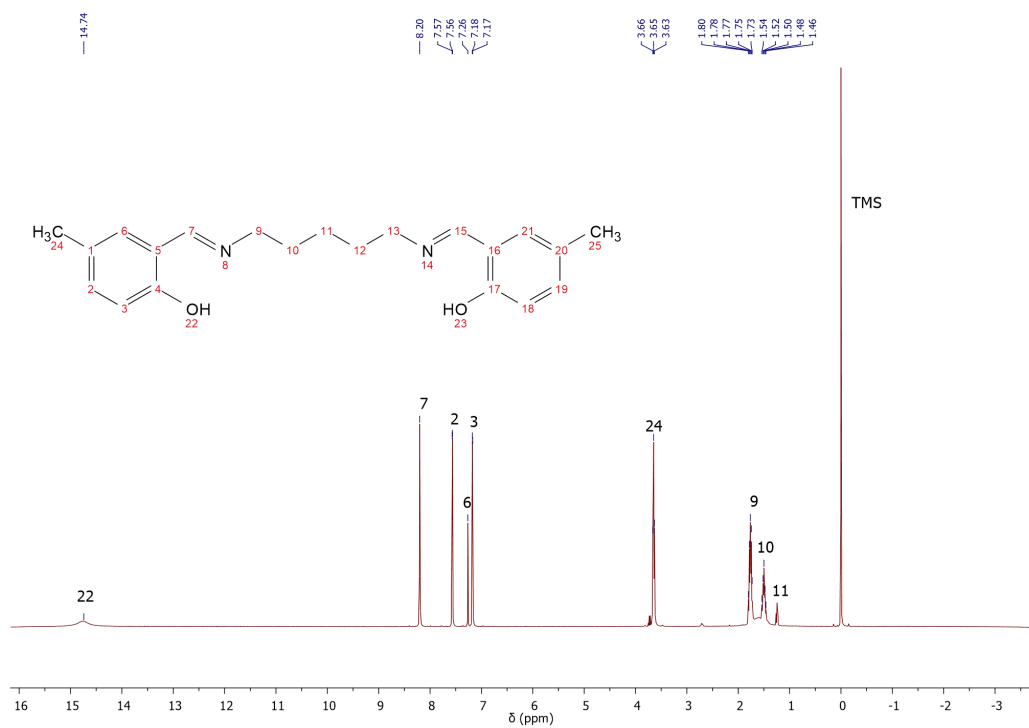


Figure B.12: ¹H NMR for SL13 (ⁿ solvent CDCl₃-d₁)

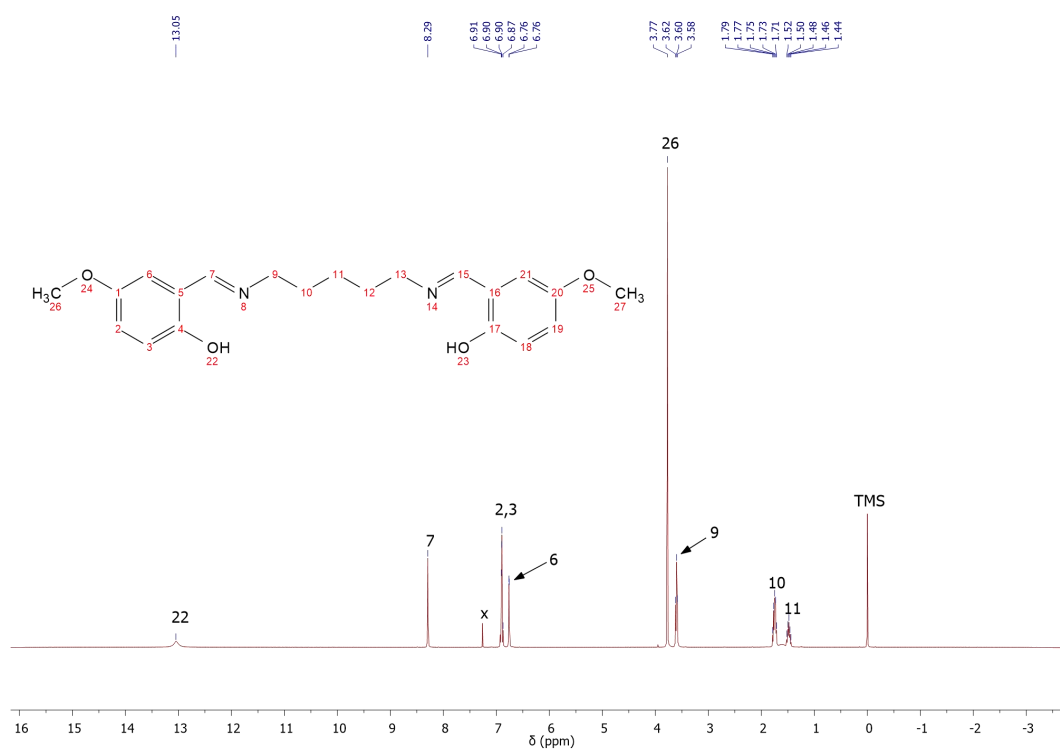


Figure B.13: ¹H NMR for SL14 (^x solvent CDCl₃-d₁)

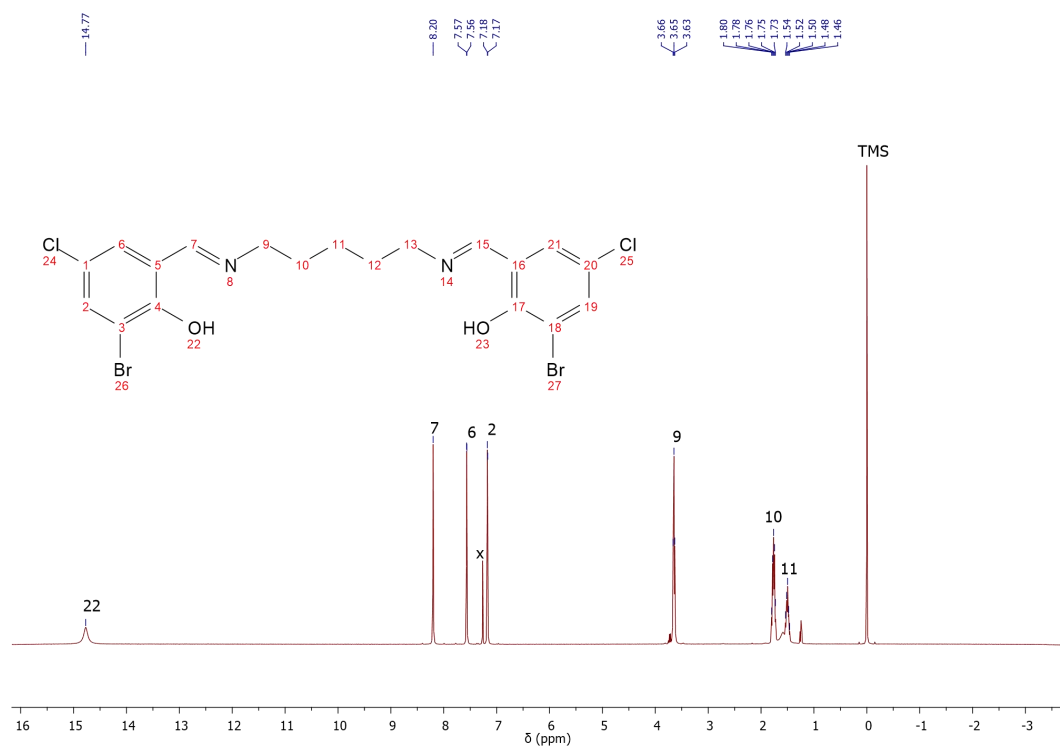


Figure B.14: ¹H NMR for SL15 (^x solvent CDCl₃-d₁)

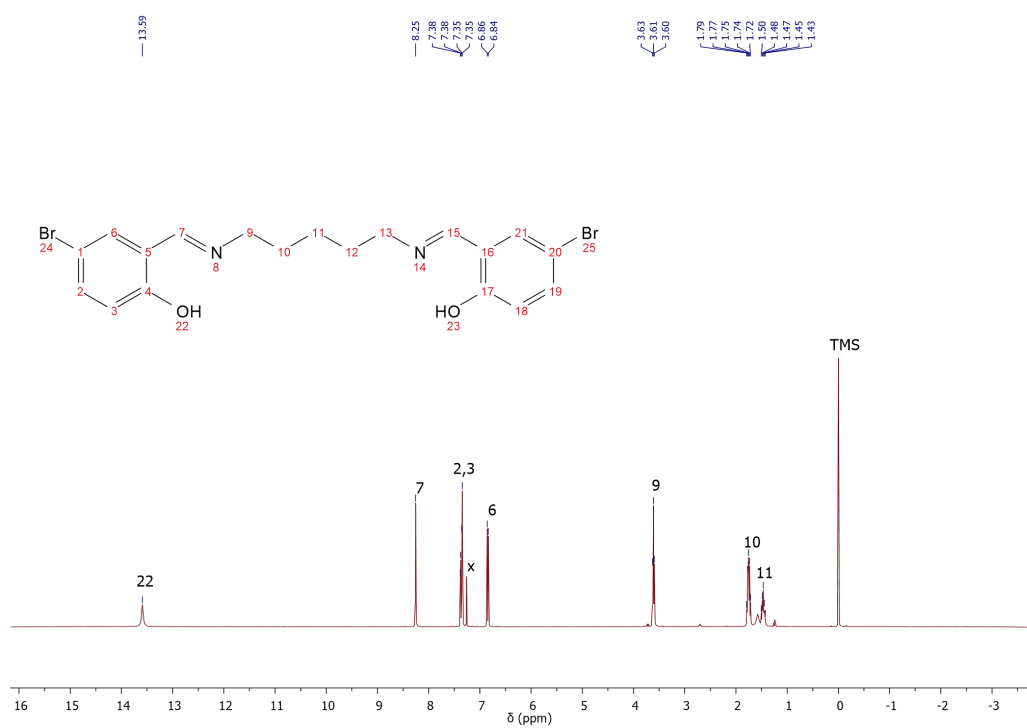


Figure B.15: ¹H NMR for SL16 (x solvent CDCl₃-d₁)

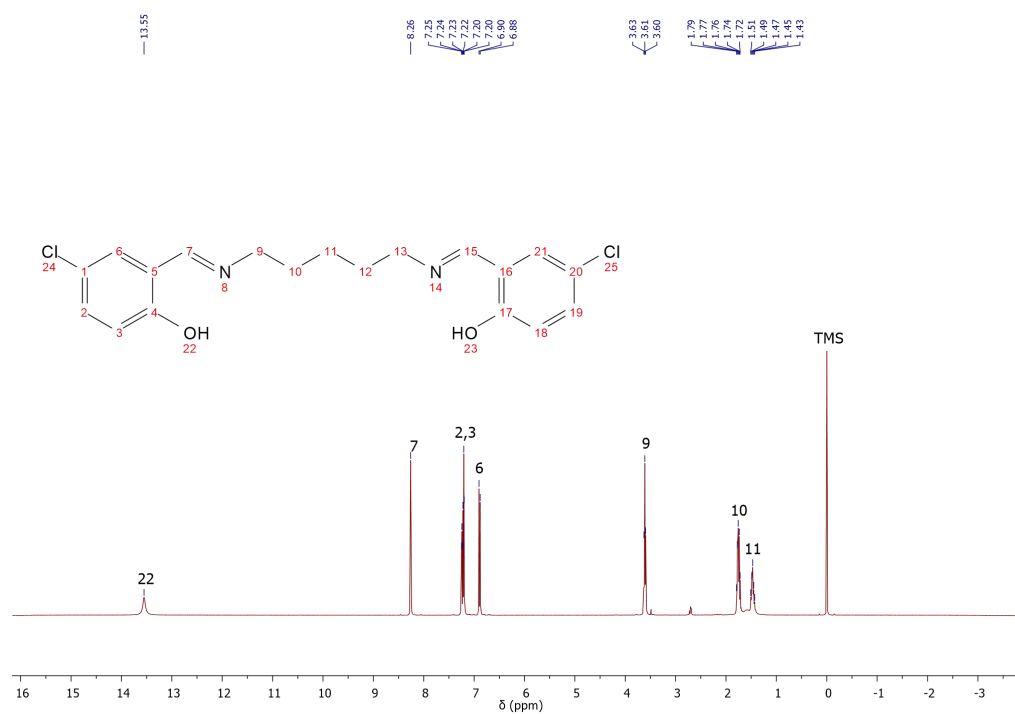
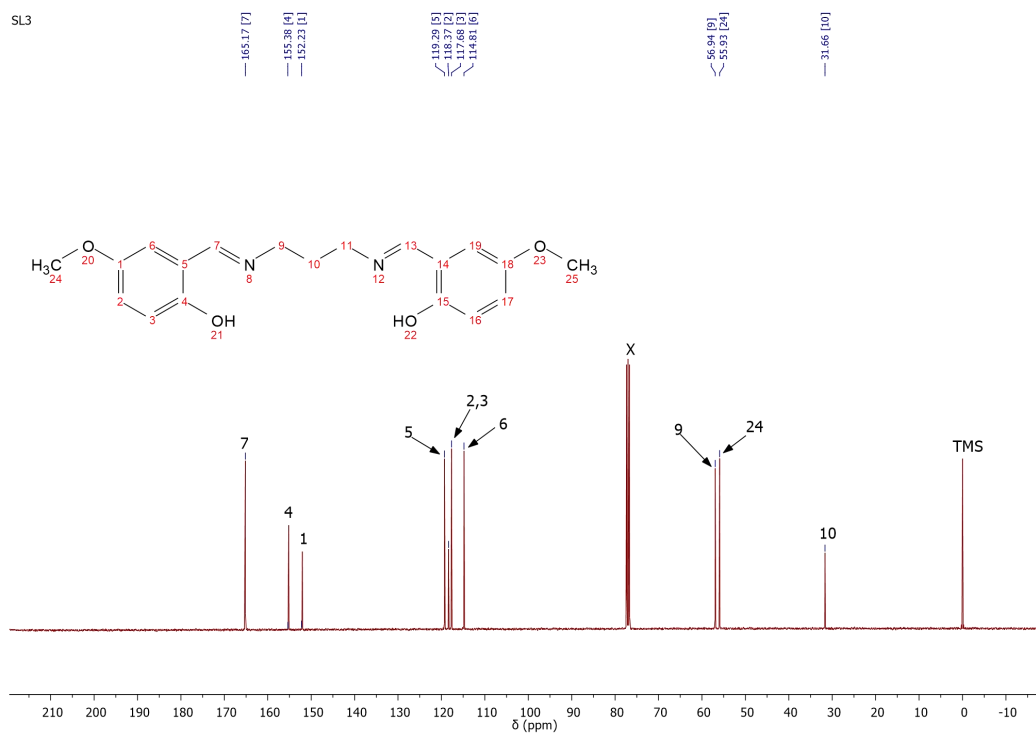
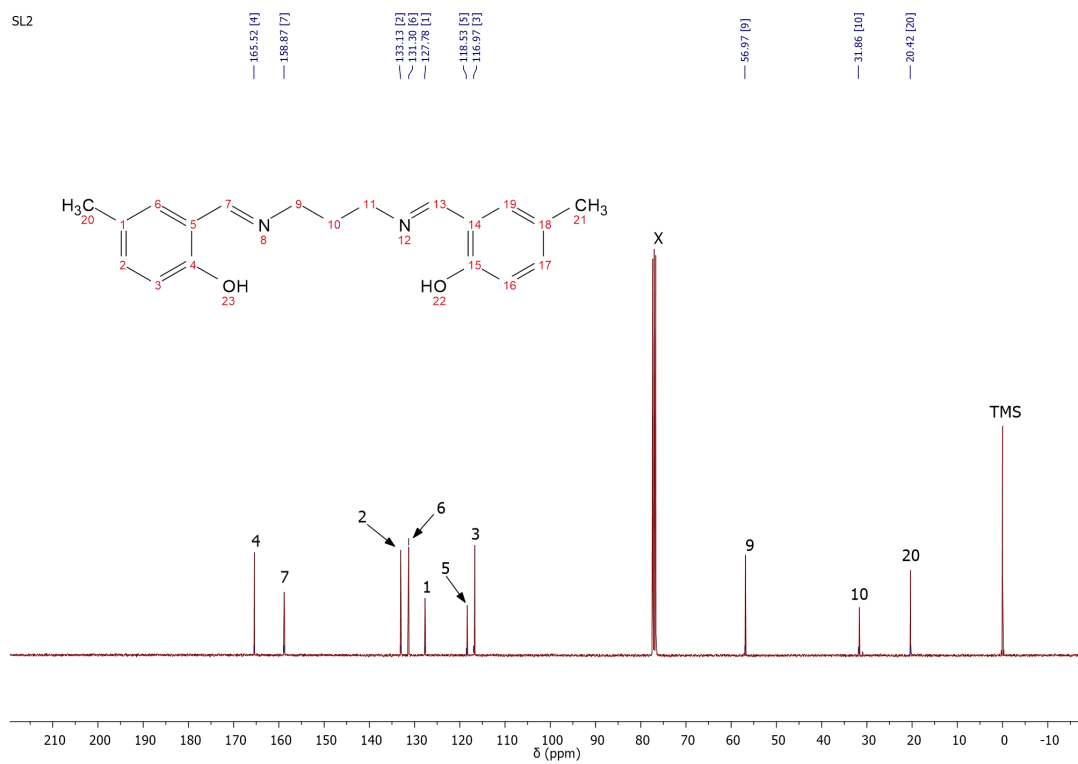
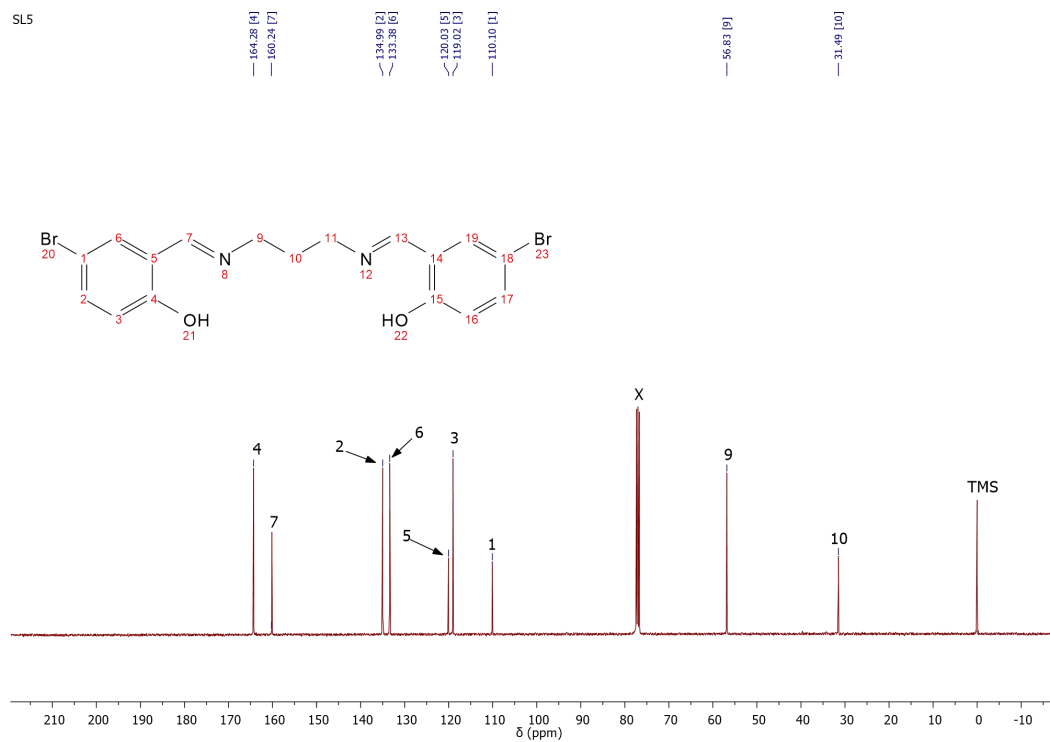
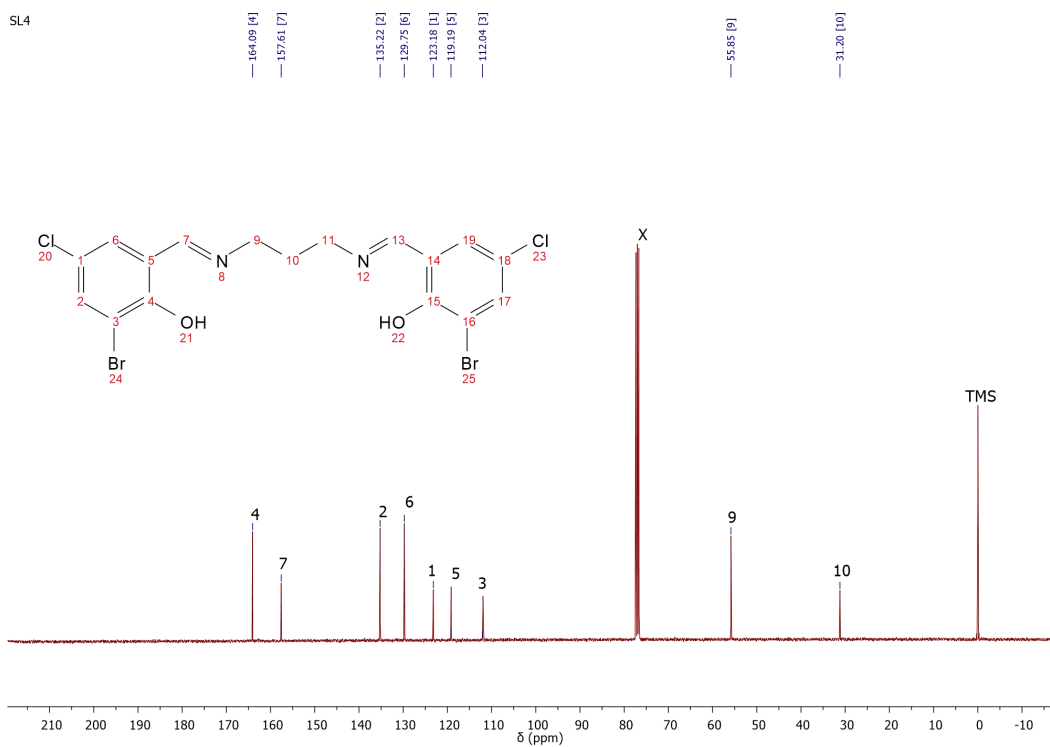


Figure B.16: ¹H NMR for SL17 (x solvent CDCl₃-d₁)





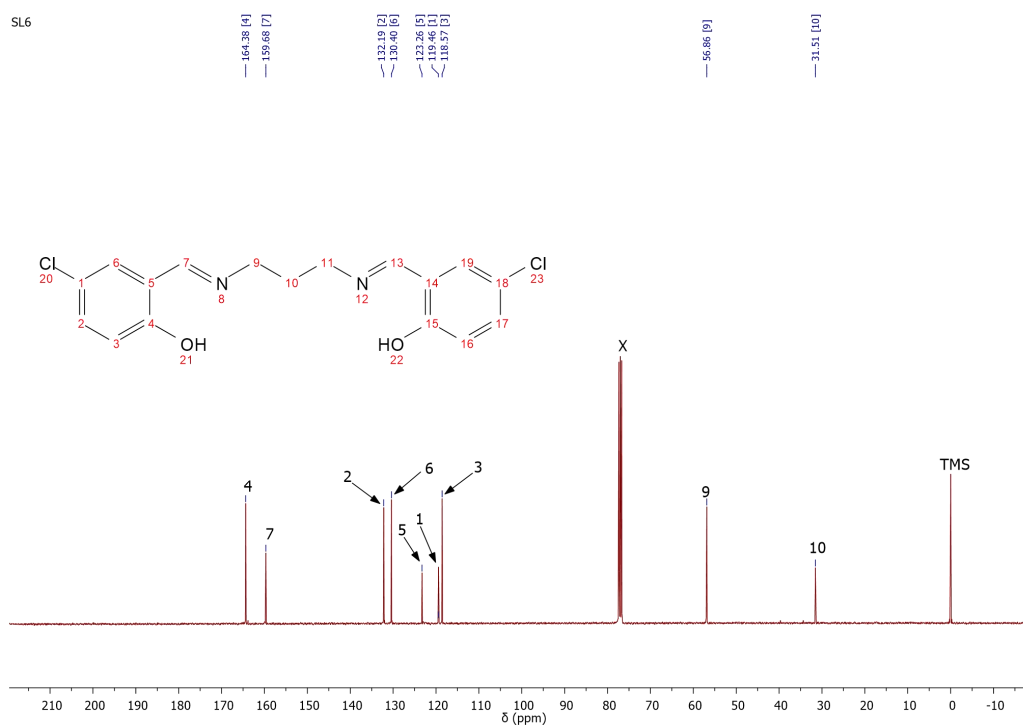


Figure B.21: ^{13}C NMR for SL6 (κ solvent CDCl_3-d_1)

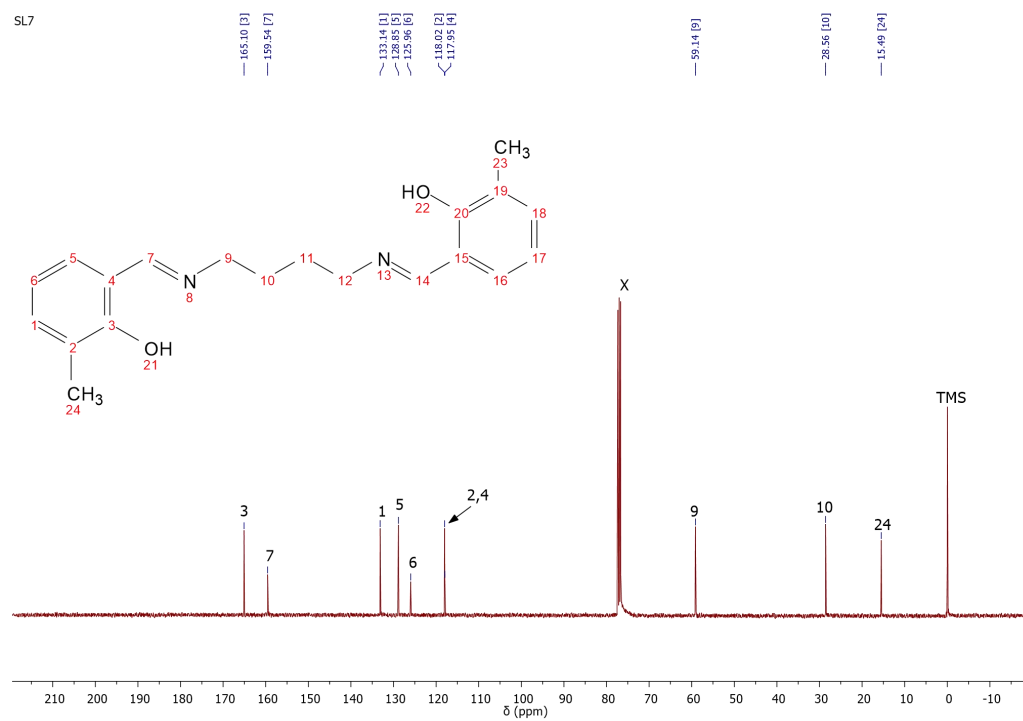


Figure B.22: ^{13}C NMR for SL7 (κ solvent CDCl_3-d_1)

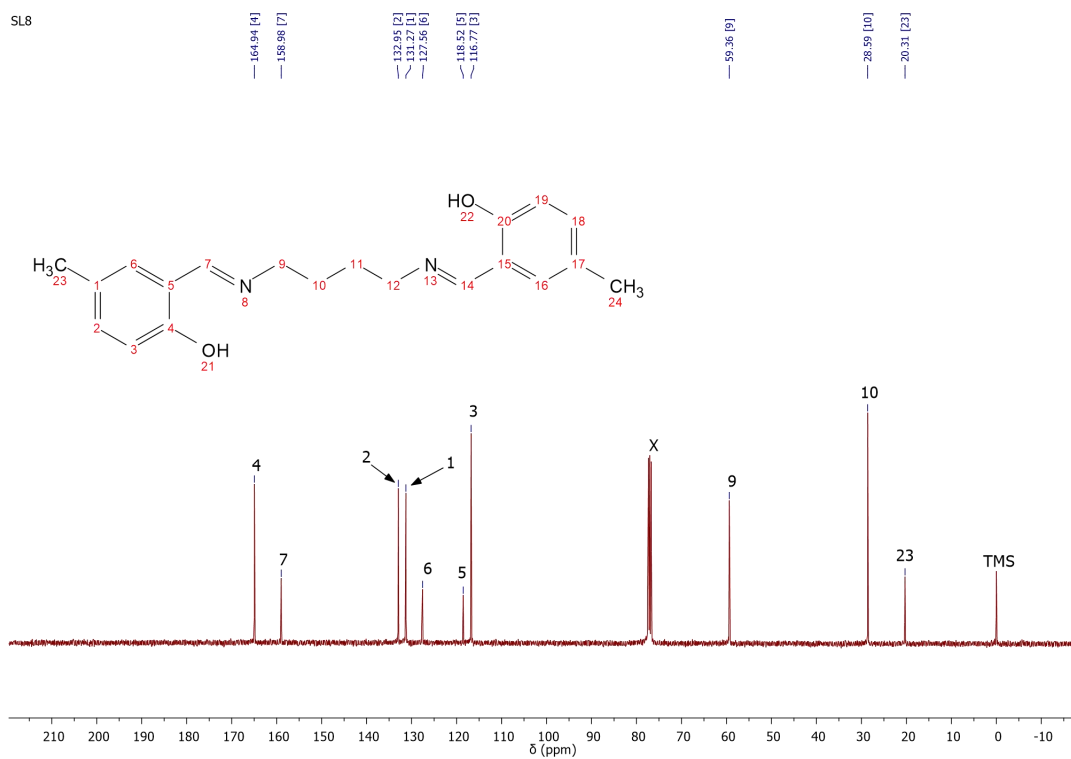


Figure B.23: ^{13}C NMR for SL8 (χ solvent CDCl_3-d_1)

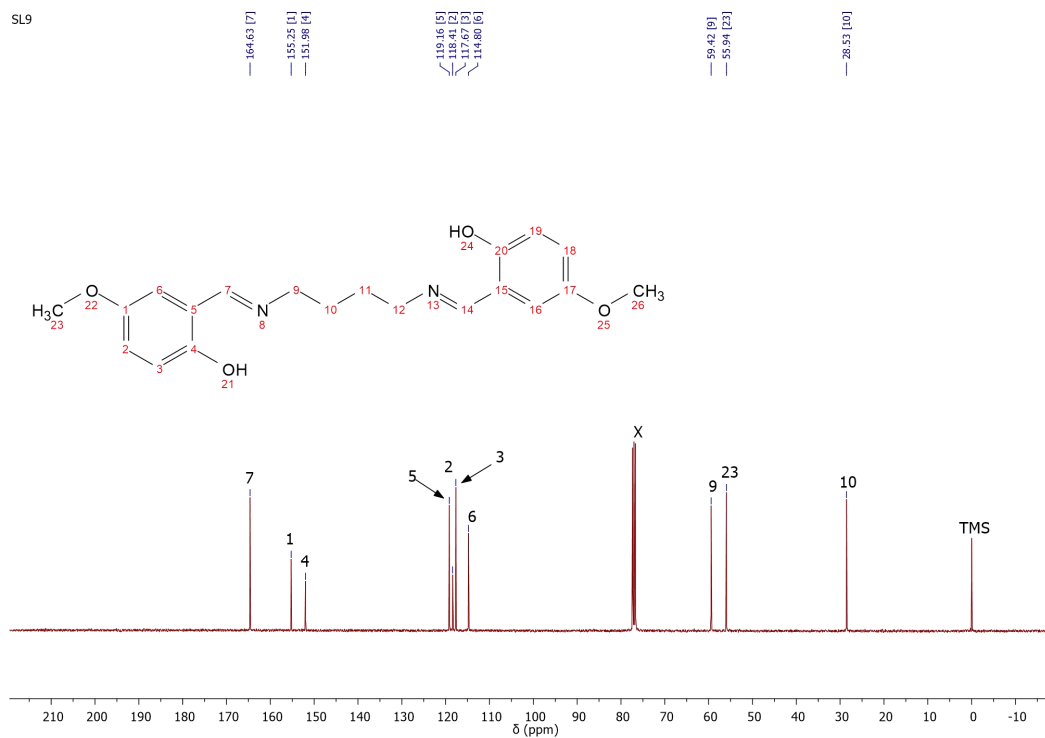
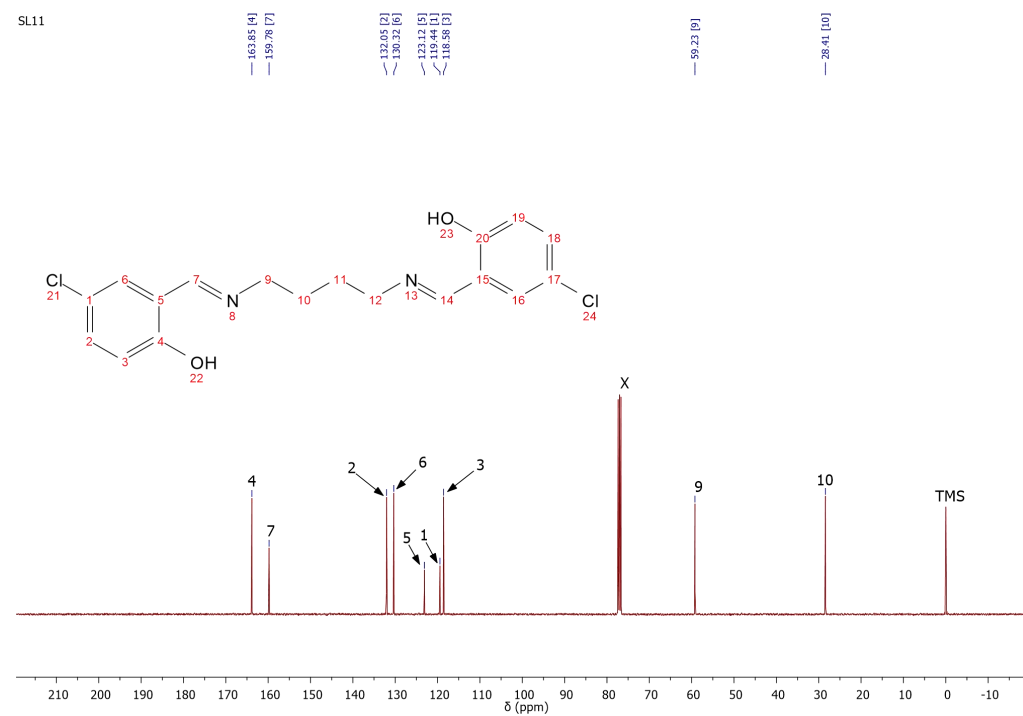
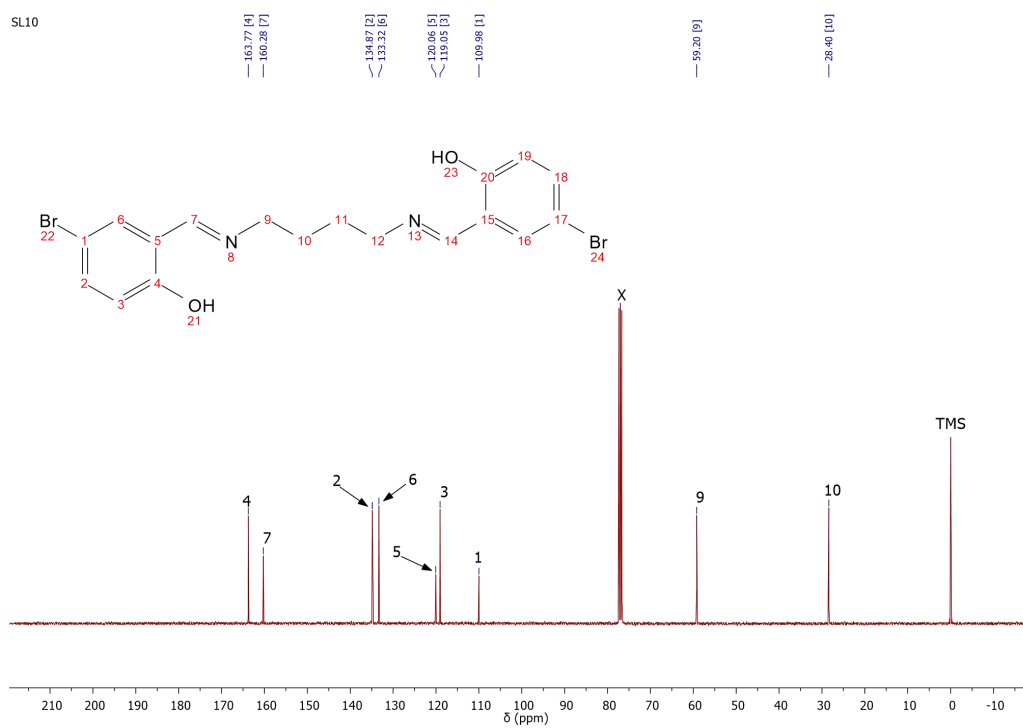
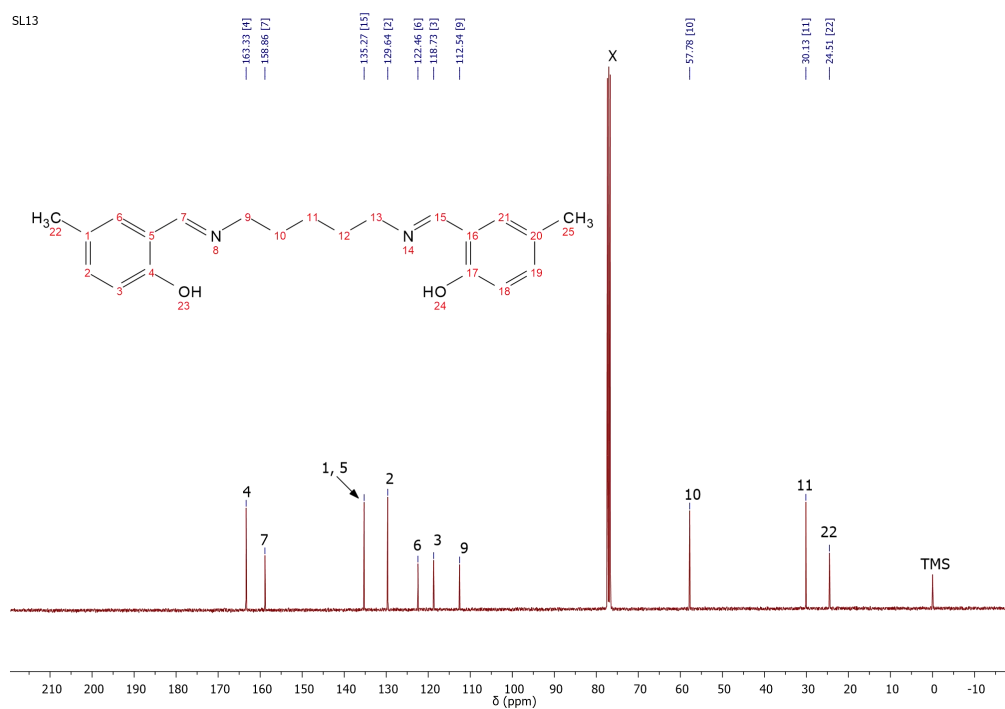
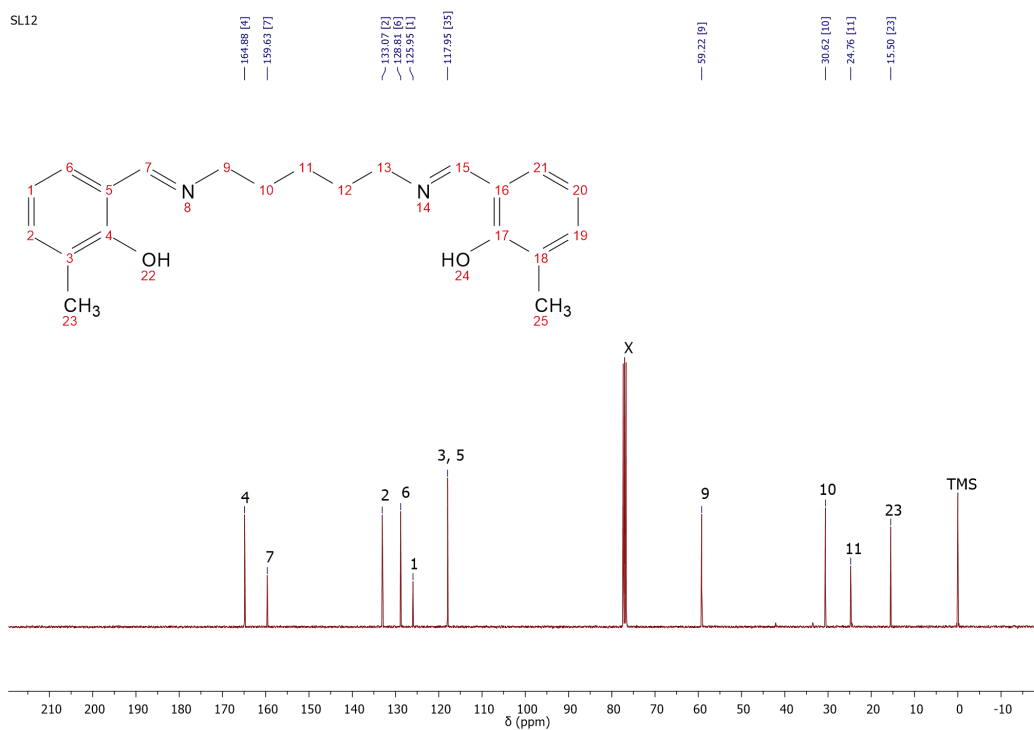


Figure B.24: ^{13}C NMR for SL9 (χ solvent CDCl_3-d_1)





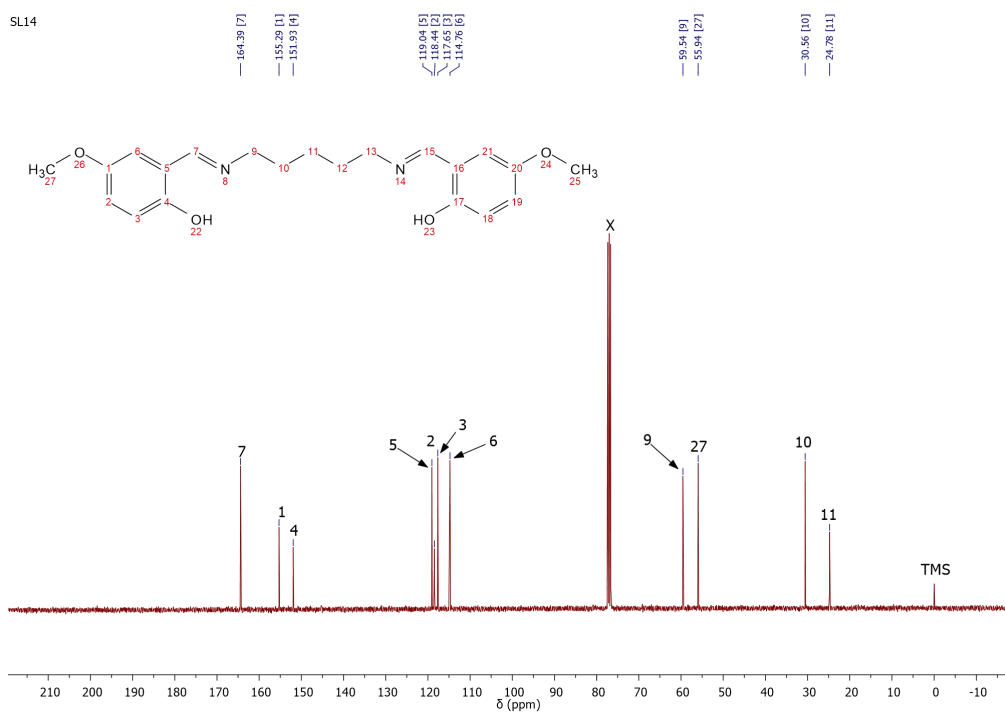


Figure B.29: ¹³C NMR for SL14 (^x solvent CDCl₃-d₁)

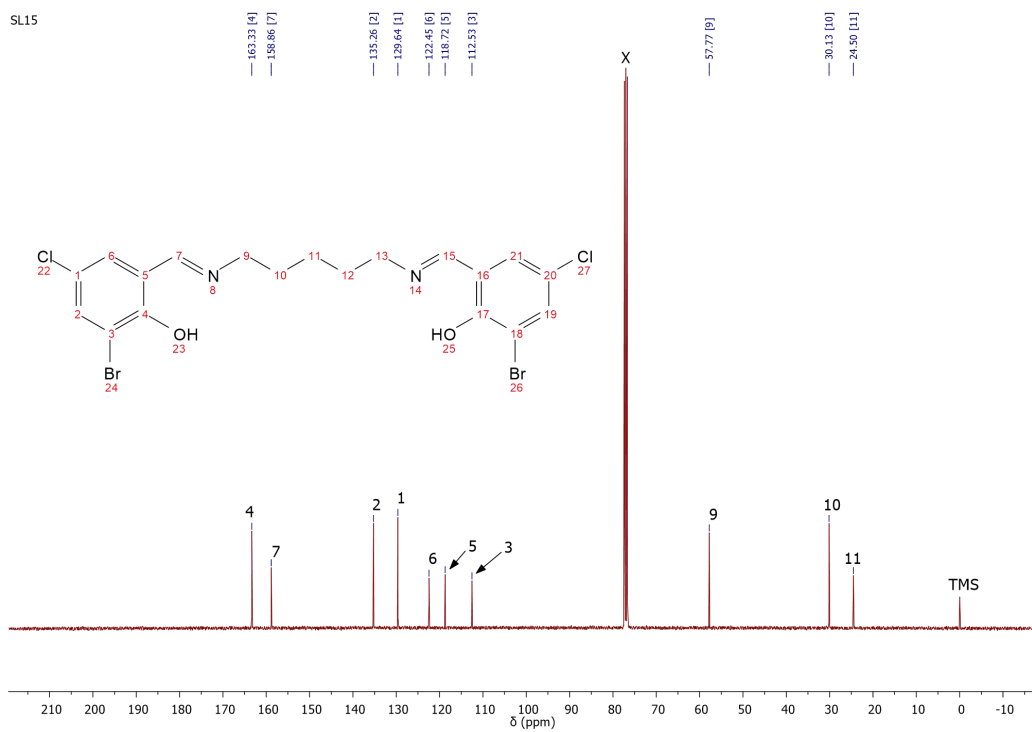


Figure B.30: ¹³C NMR for SL15 (^x solvent CDCl₃-d₁)

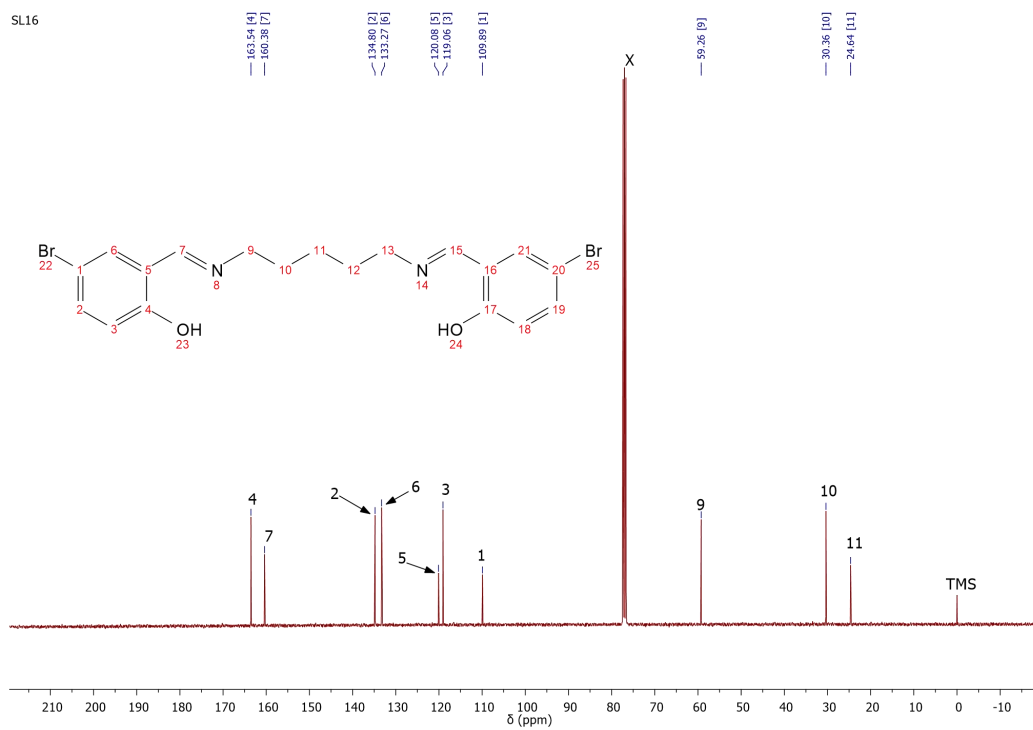


Figure B.31: ^{13}C NMR for SL16 (x solvent CDCl_3-d_1)

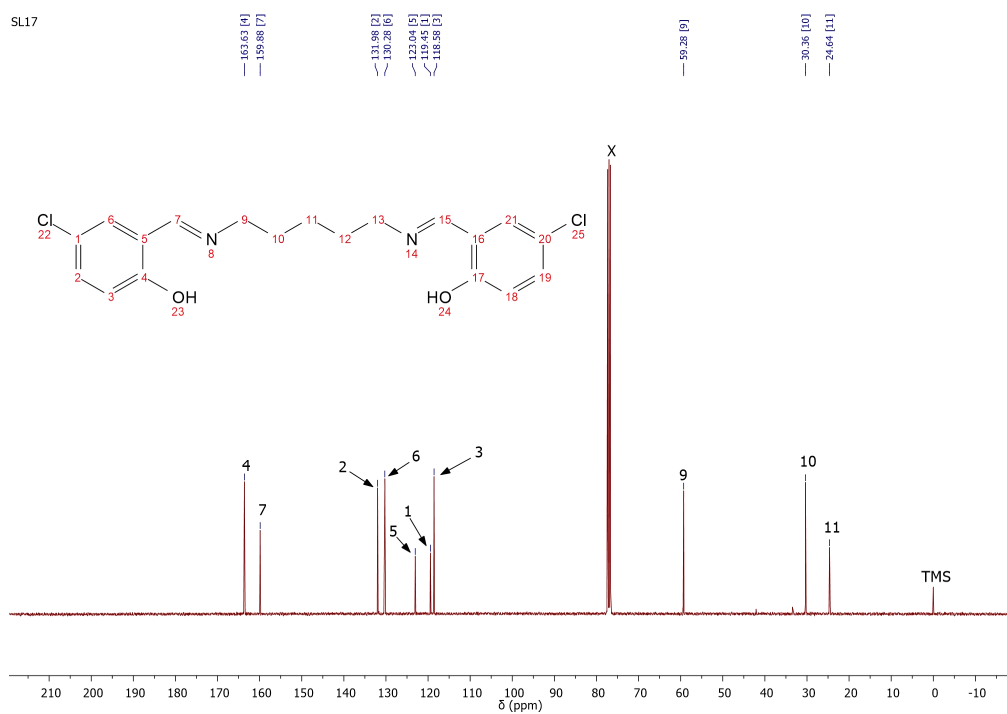


Figure B.32: ^{13}C NMR for SL17 (x solvent CDCl_3-d_1)

Appendix C: FTIR Graphs for Complexes

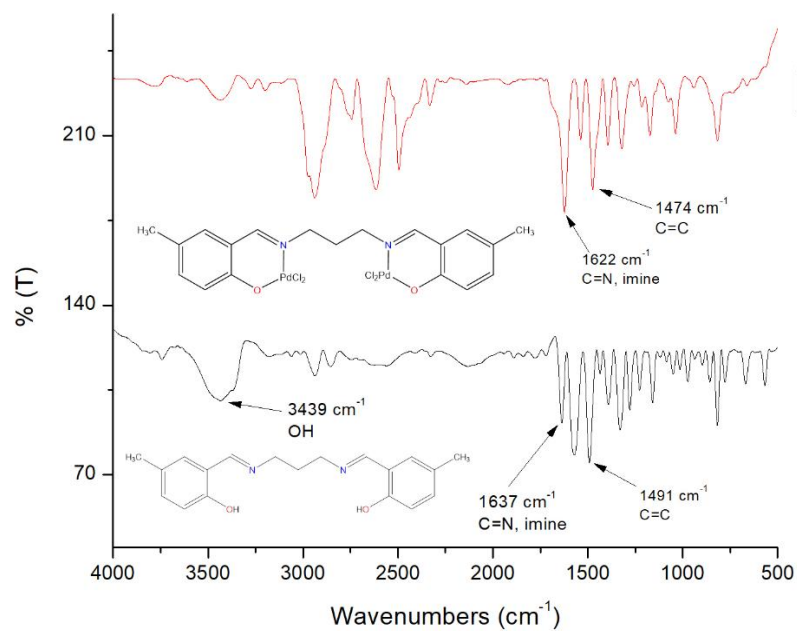


Figure C.1: FTIR spectra for C2 and SL2

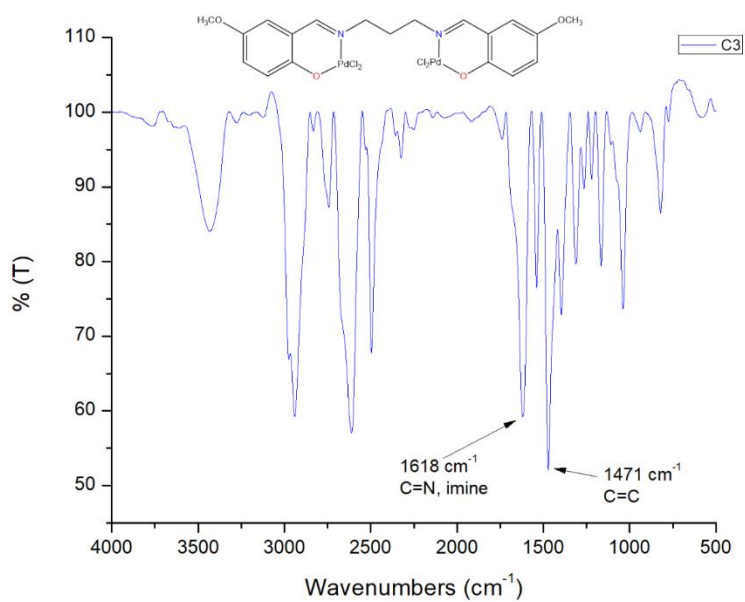


Figure C.2: FTIR spectrum for C3

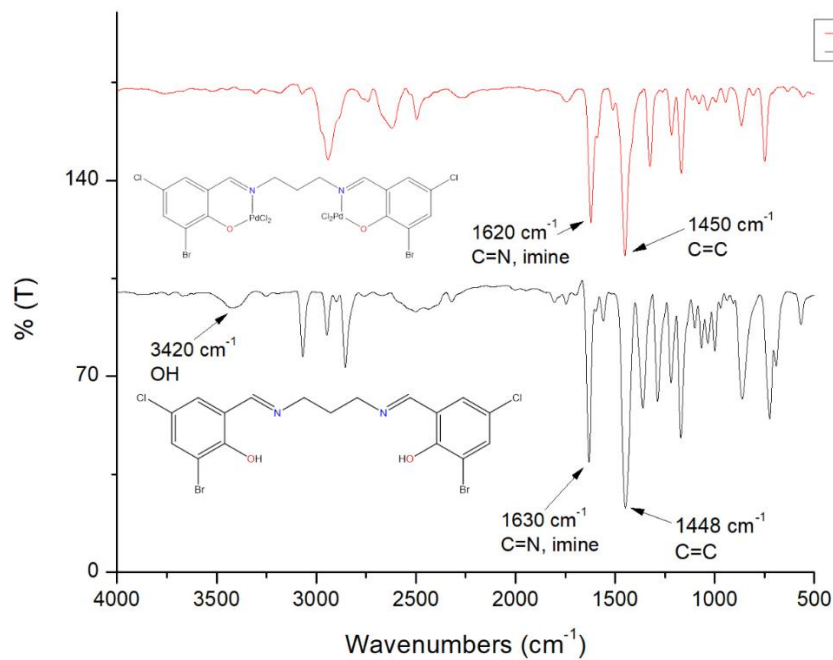


Figure C.3: FTIR spectra for C4 and SL4

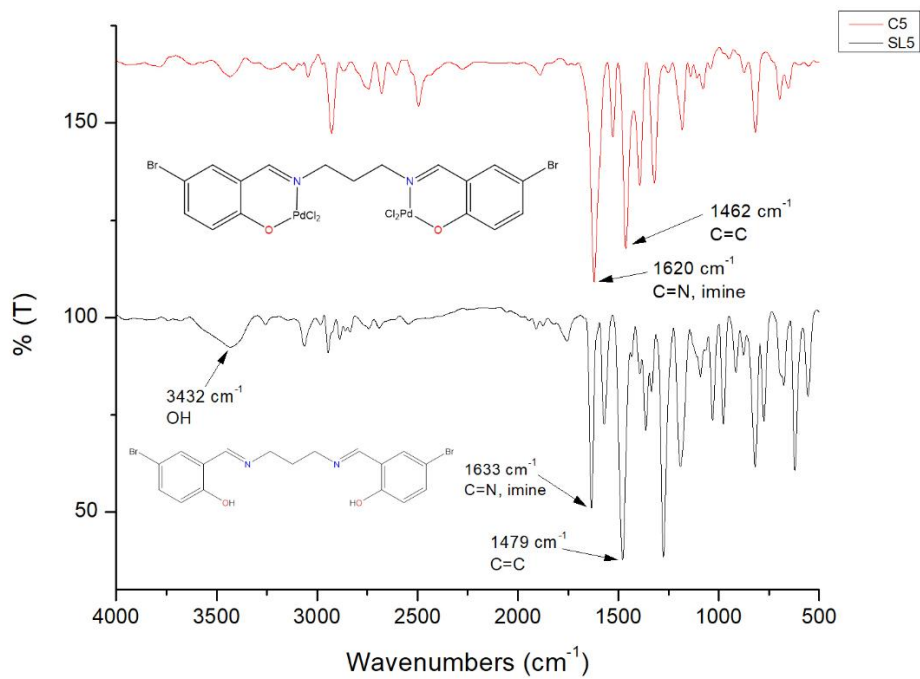


Figure C.4: FTIR spectra for C5 and SL5

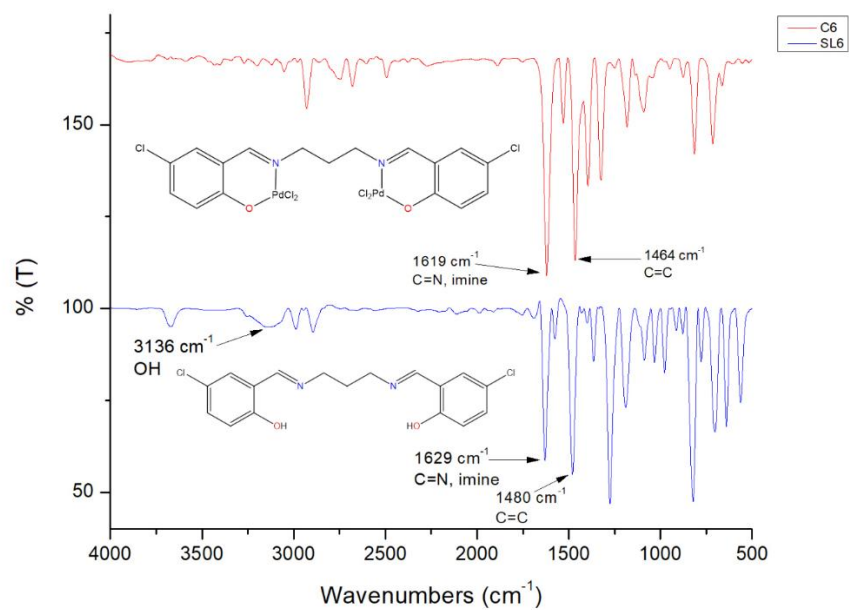


Figure C.5: FTIR spectra for C6 and SL6

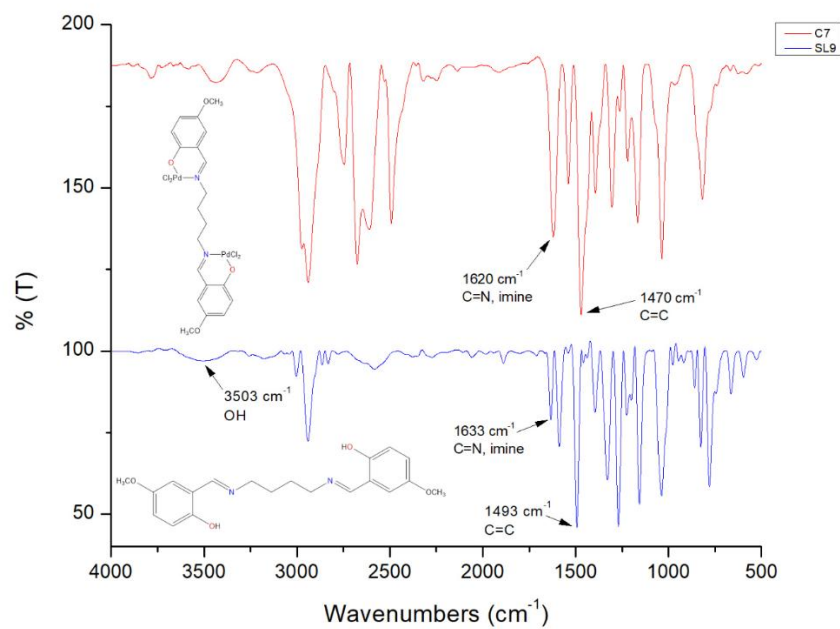


Figure C.6: FTIR spectra for C7 and SL9

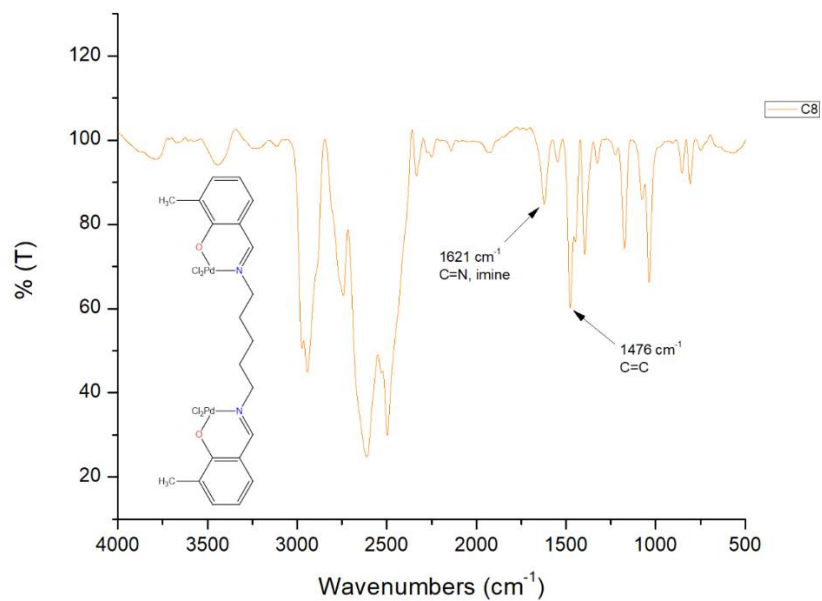


Figure C.7: FTIR spectrum for C8

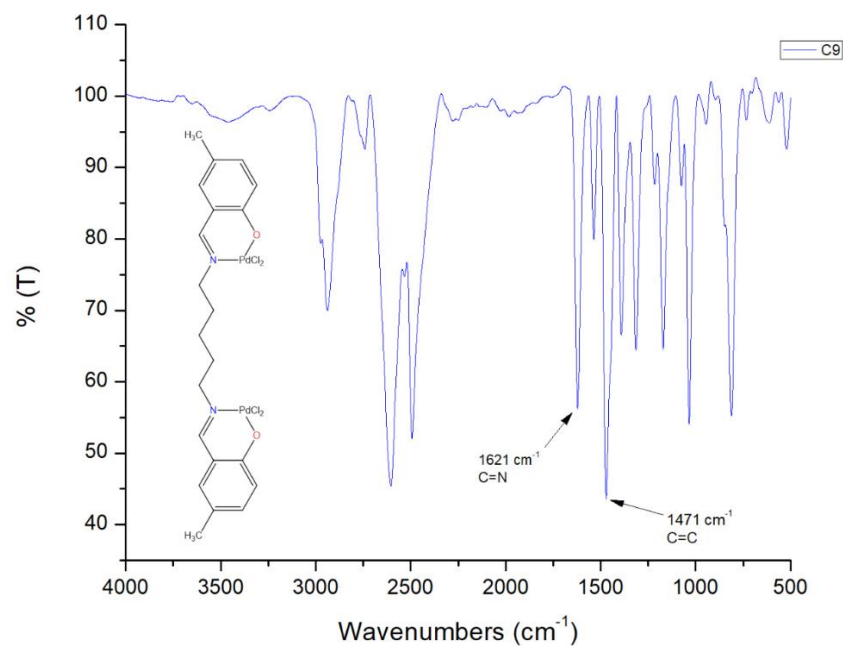


Figure C.8: FTIR spectrum for C9

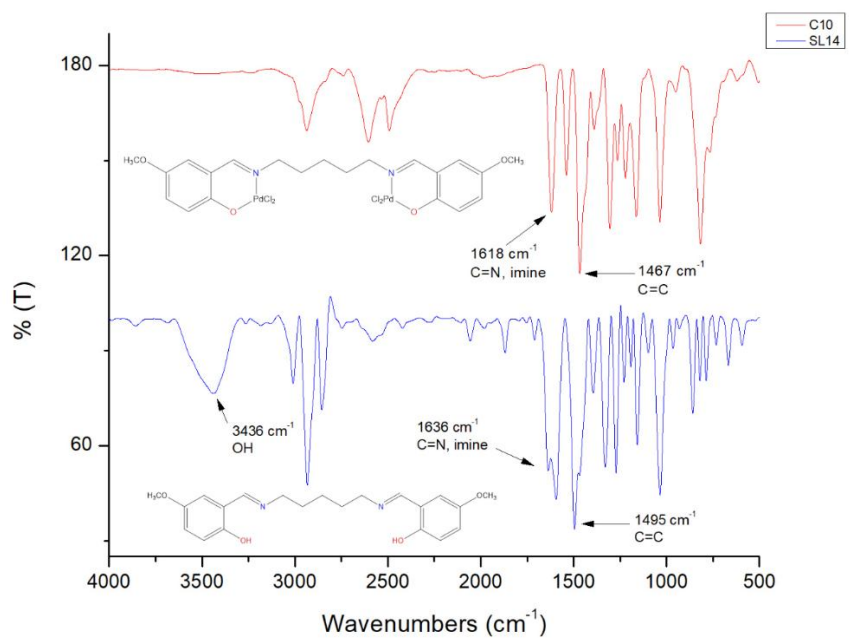


Figure C.9: FTIR spectra for C10 and SL14

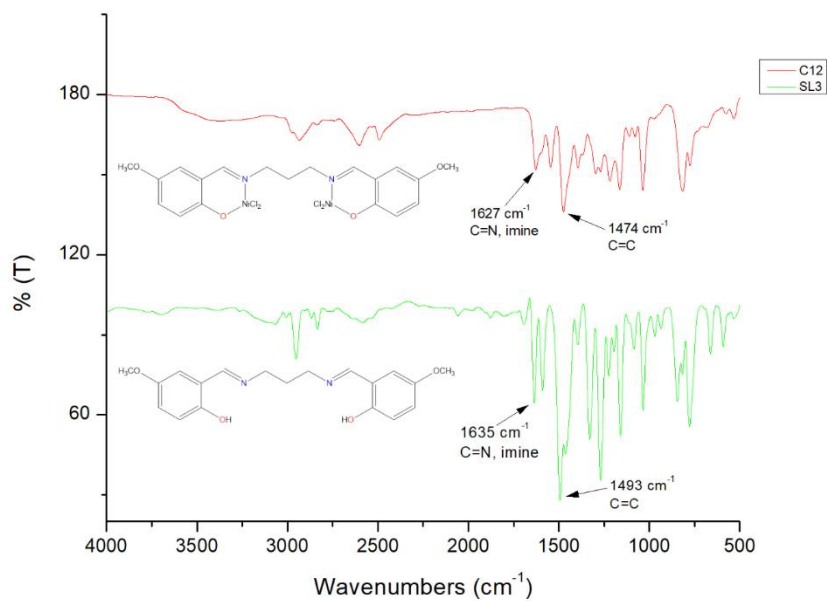


Figure C.10: FTIR spectra for C12 and SL3

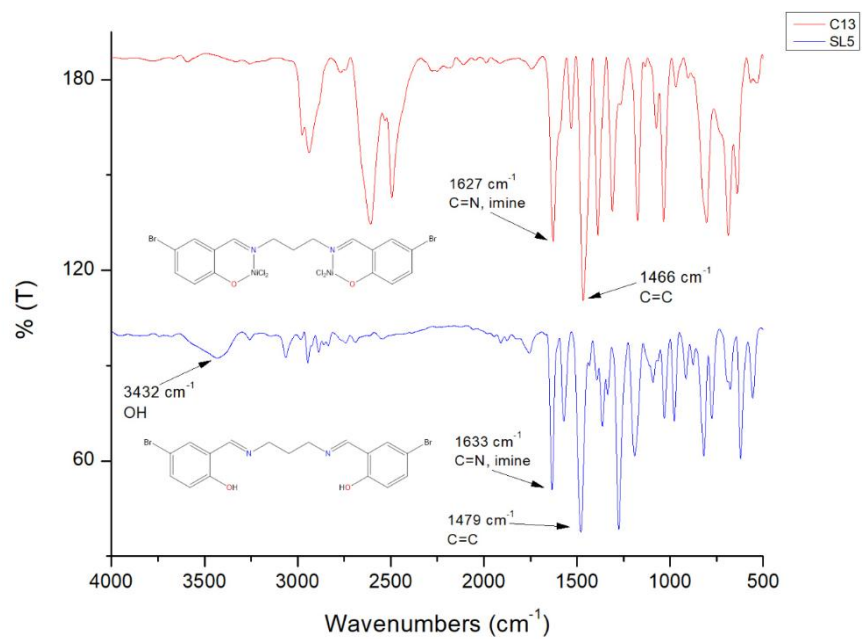


Figure C.11: FTIR spectra for C13 and SL5

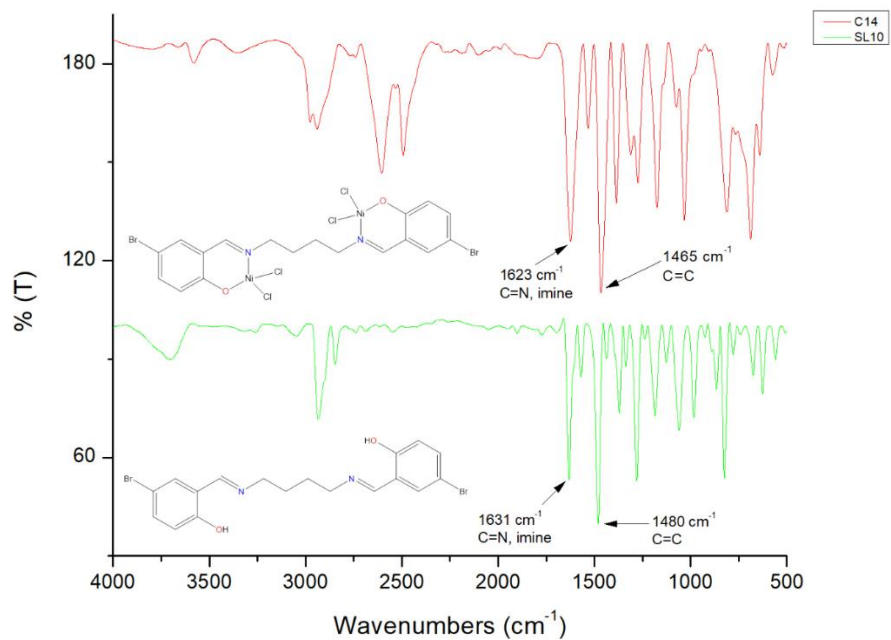
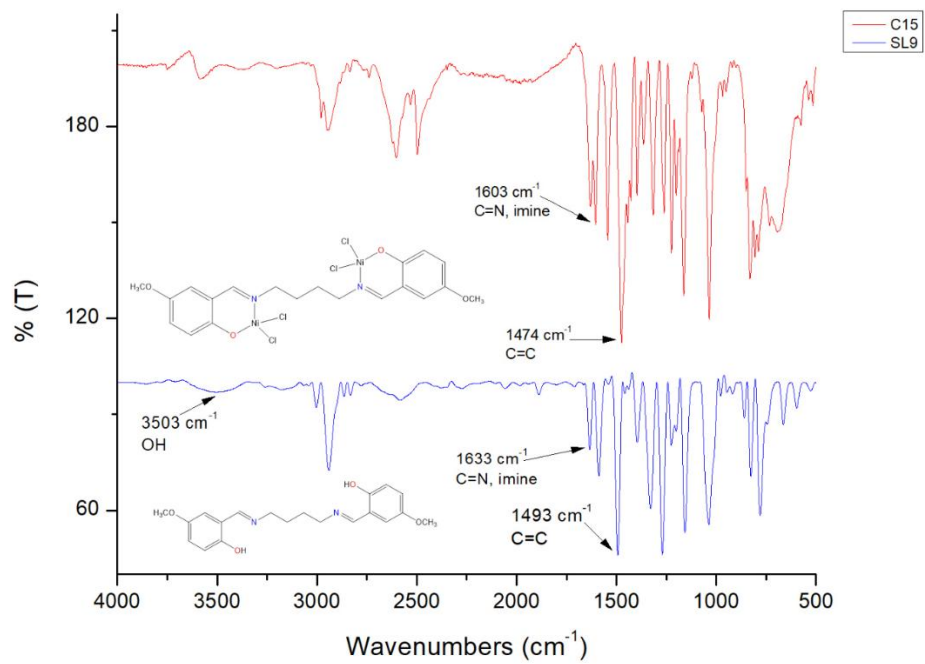
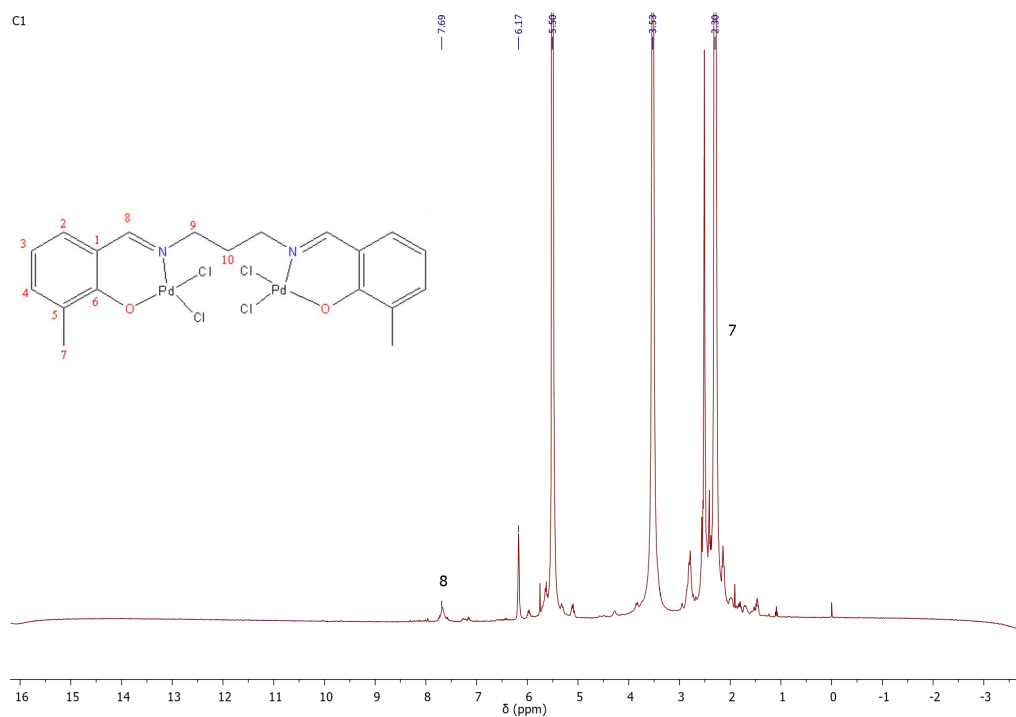
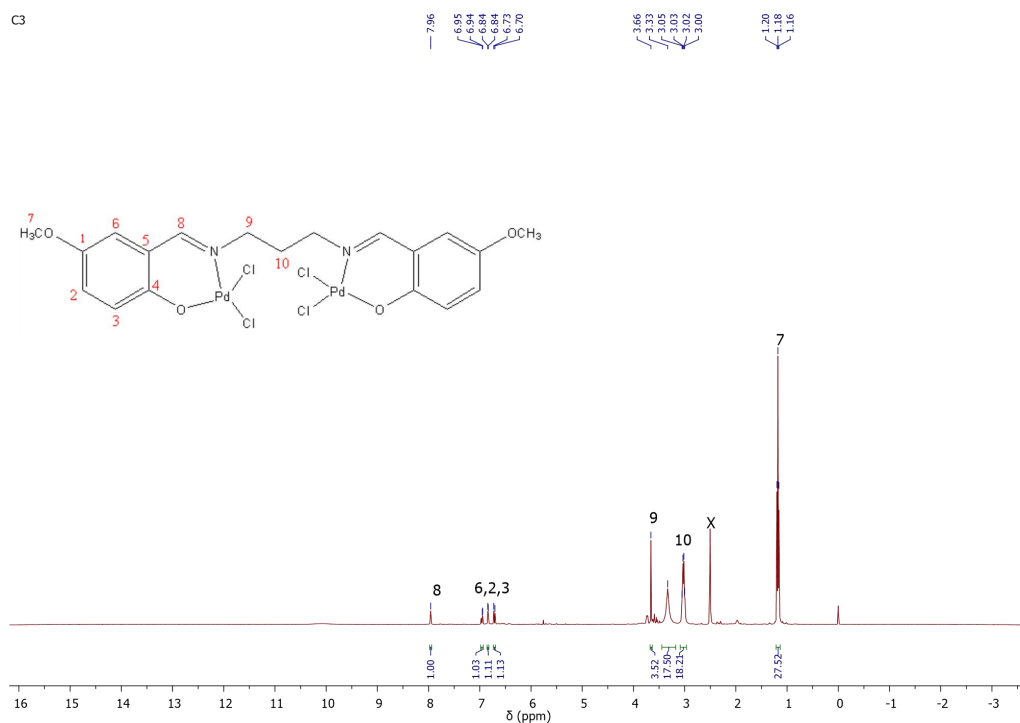


Figure C.12: FTIR spectra for C14 and SL10



Appendix D: NMR Graphs for Complexes

Figure D.1: ^1H NMR for C1 (\times solvent DMSO- d_6)Figure D.2: ^1H NMR for Complex C3 (\times solvent DMSO- d_6)

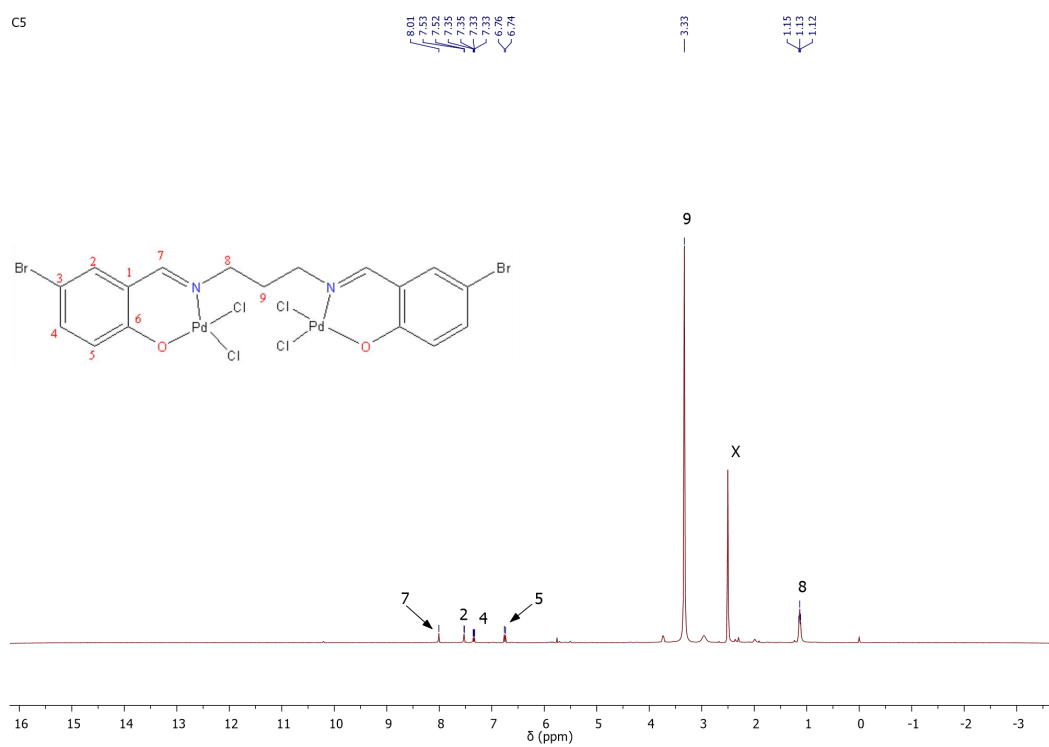


Figure D.3: ^1H NMR for C5 (α solvent DMSO- d_6)

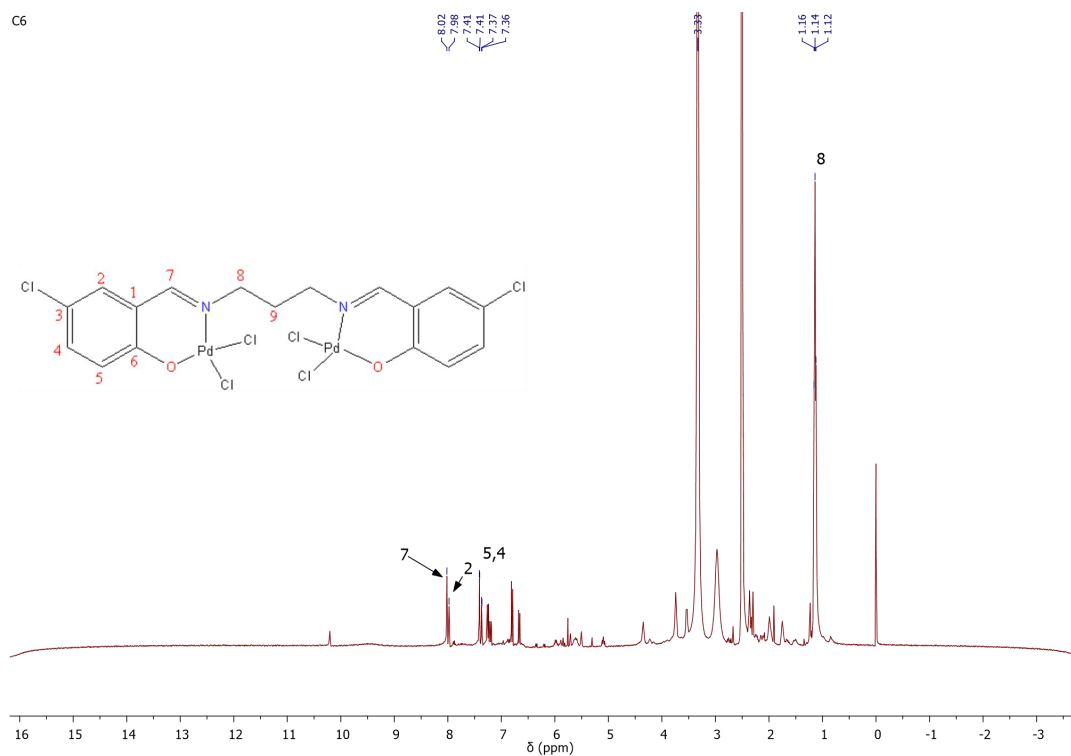
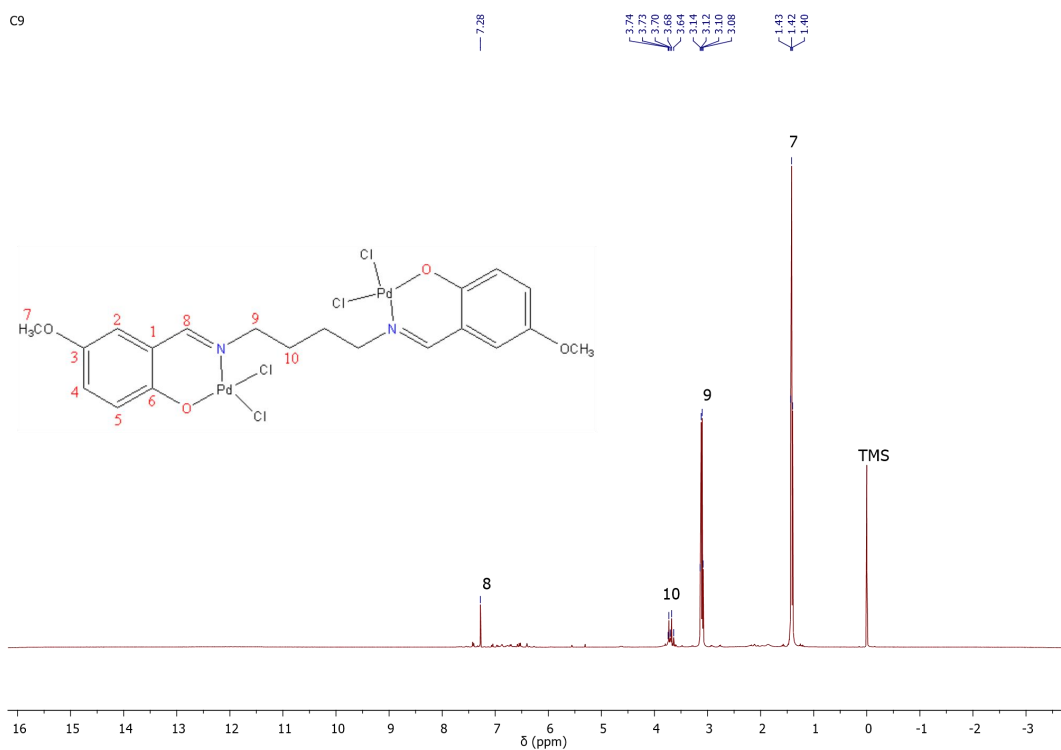
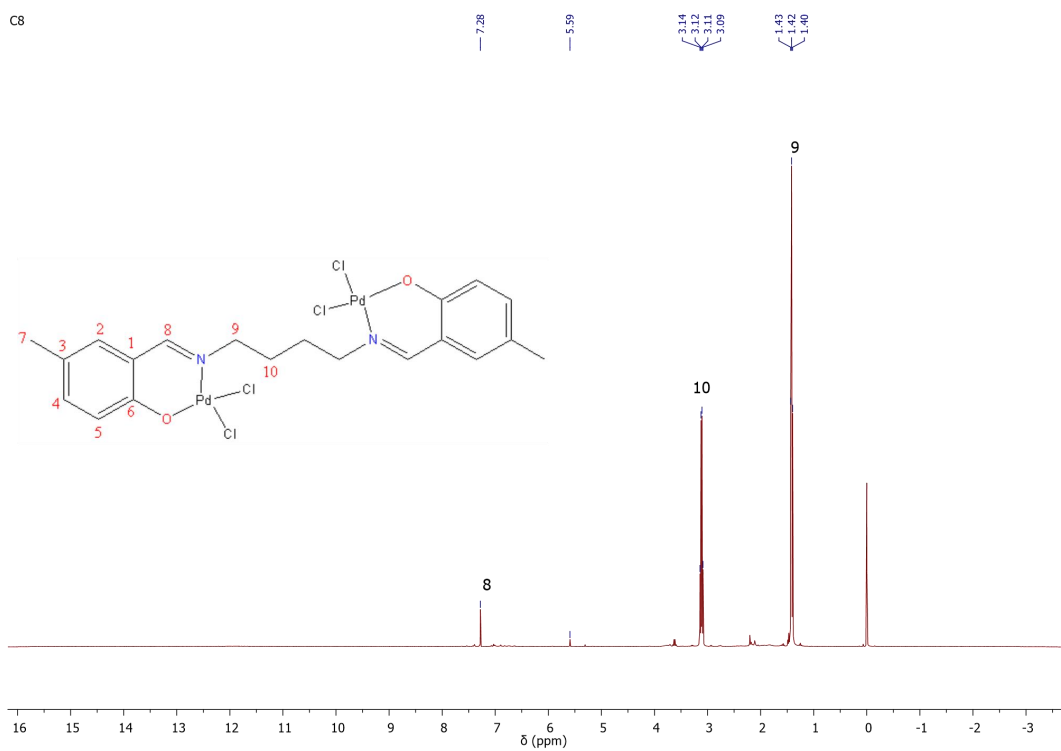
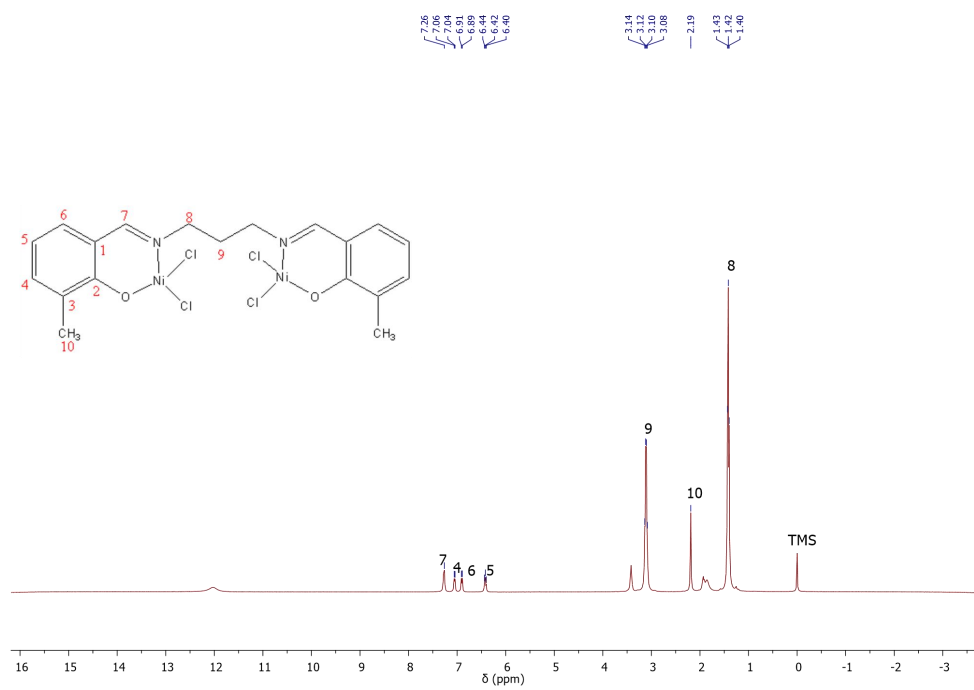
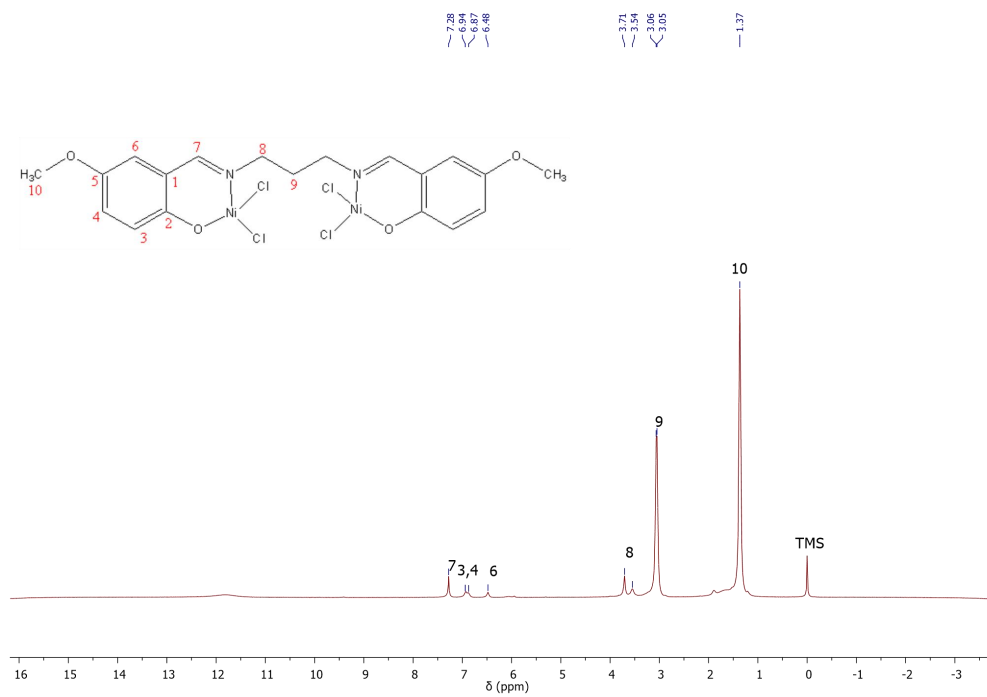
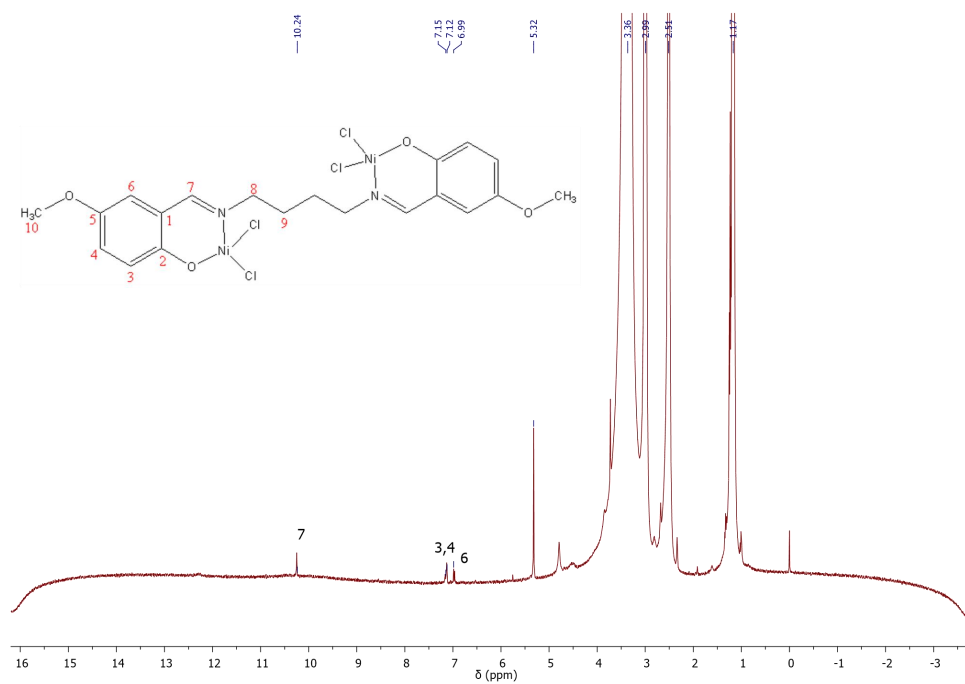
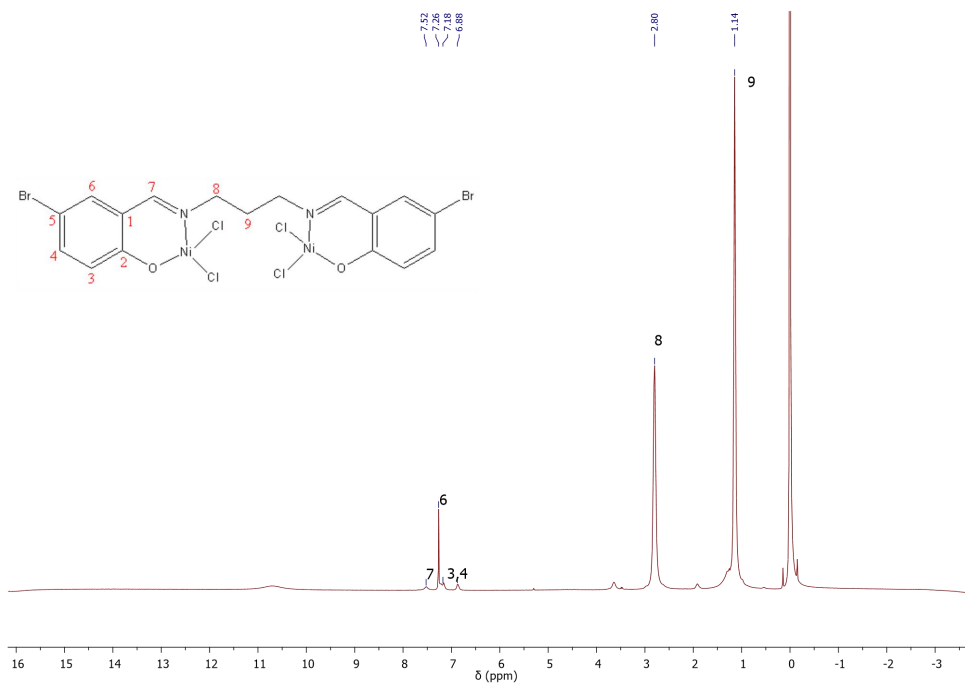
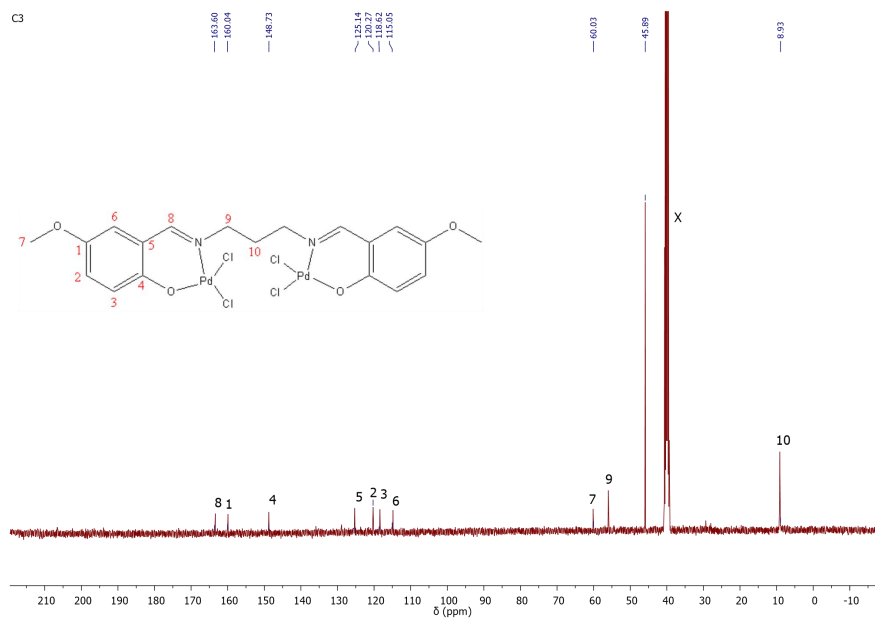
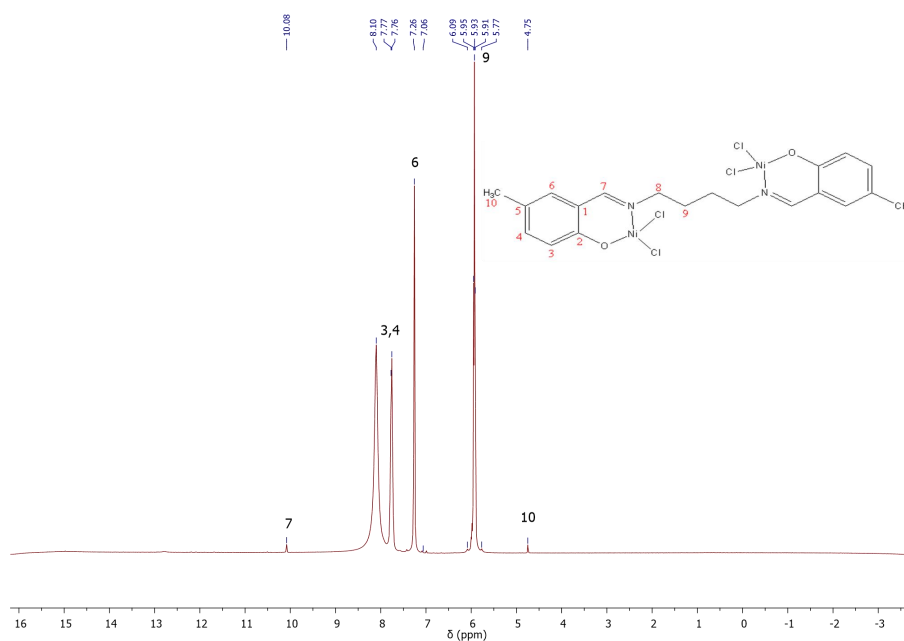


Figure D.4: ^1H NMR for C6 (α solvent DMSO- d_6)



Figure D.7: ¹H NMR for C11Figure D.8: ¹H NMR for C12

**Figure D.9: ¹H NMR for C13****Figure D.10: ¹H NMR for C14**



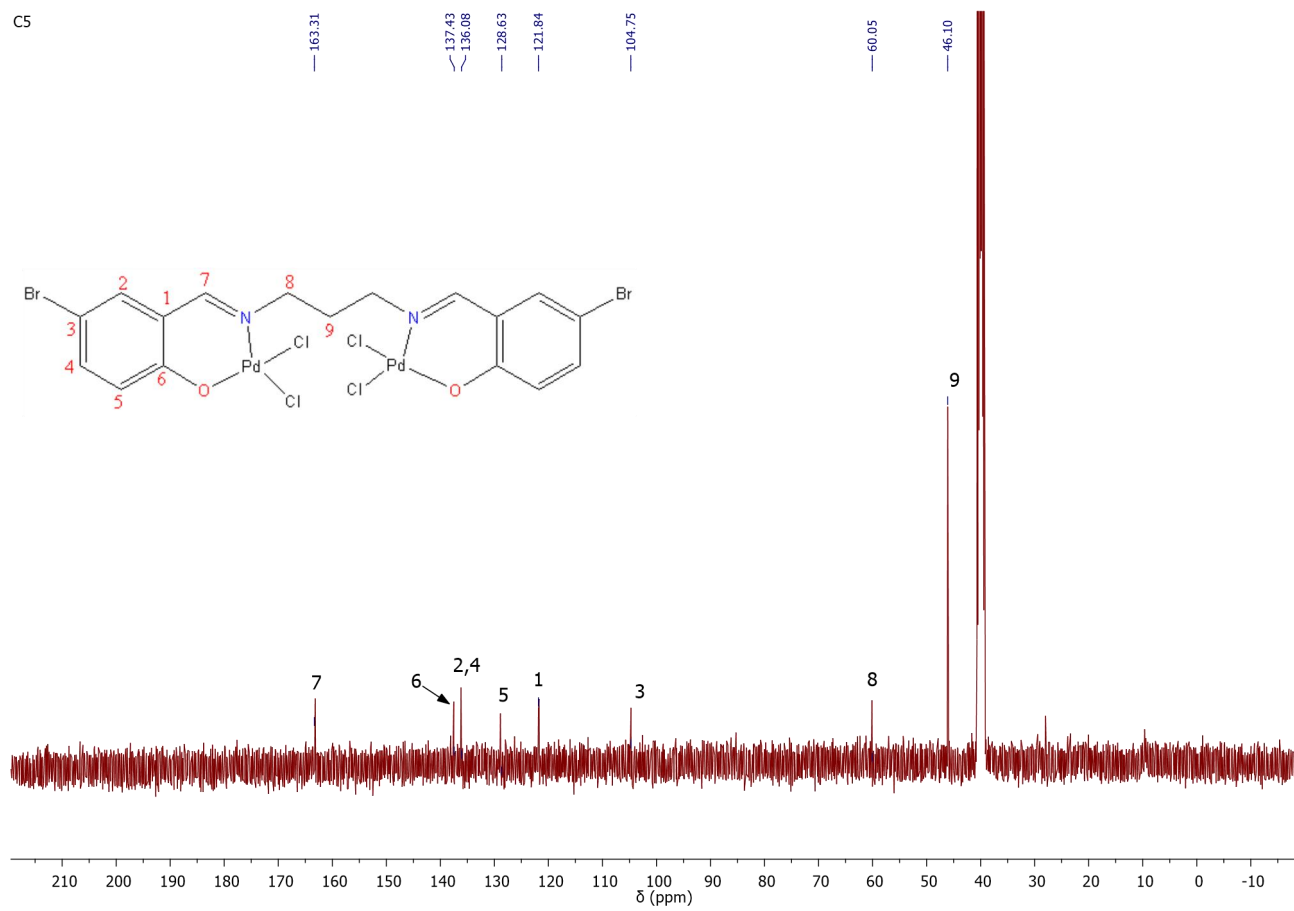


Figure D.13: ^{13}C NMR for C5 (κ solvent $\text{DMSO-}d_6$)

Appendix E: Tables

Table E.1: Bond angles for the ligand SL2

Number	Atom1	Atom2	Atom3	Angle
1	H1	O1	C1	109.5
2	H2	O2	C14	109.5
3	C12	N2	C11	119.0(1)
4	C8	N1	C9	118.8(1)
5	C12	C13	C19	119.9(1)
6	C12	C13	C14	121.1(1)
7	C19	C13	C14	119.0(1)
8	H6	C6	C4	118.7
9	H6	C6	C7	118.7
10	C4	C6	C7	122.6(1)
11	C6	C4	C3	117.1(1)
12	C6	C4	C5	121.6(1)
13	C3	C4	C5	121.3(1)
14	C6	C7	C8	120.1(1)
15	C6	C7	C1	118.8(1)
16	C8	C7	C1	121.1(1)
17	N2	C12	C13	121.9(1)
18	N2	C12	H12	119
19	C13	C12	H12	119
20	C13	C19	H19	118.9
21	C13	C19	C17	122.1(1)
22	H19	C19	C17	118.9
23	C19	C17	C16	117.5(1)
24	C19	C17	C18	120.6(1)
25	C16	C17	C18	121.8(1)
26	C4	C3	H3	119.1
27	C4	C3	C2	121.9(1)
28	H3	C3	C2	119.1
29	N1	C8	C7	121.5(1)
30	N1	C8	H8	119.3
31	C7	C8	H8	119.3
32	C3	C2	H2A	119.7
33	C3	C2	C1	120.6(1)
34	H2A	C2	C1	119.7
35	C17	C16	H16	119.2
36	C17	C16	C15	121.6(2)

37	H16	C16	C15	119.2
38	C17	C18	H18A	109.5
39	C17	C18	H18B	109.5
40	C17	C18	H18C	109.5
41	H18A	C18	H18B	109.5
42	H18A	C18	H18C	109.5
43	H18B	C18	H18C	109.5
44	O2	C14	C13	121.4(1)
45	O2	C14	C15	119.5(1)
46	C13	C14	C15	119.1(1)
47	O1	C1	C7	121.5(1)
48	O1	C1	C2	119.4(1)
49	C7	C1	C2	119.1(1)
50	H10A	C10	H10B	107.9
51	H10A	C10	C11	109.2
52	H10A	C10	C9	109.2
53	H10B	C10	C11	109.2
54	H10B	C10	C9	109.2
55	C11	C10	C9	112.2(1)
56	C4	C5	H5A	109.5
57	C4	C5	H5B	109.5
58	C4	C5	H5C	109.5
59	H5A	C5	H5B	109.5
60	H5A	C5	H5C	109.5
61	H5B	C5	H5C	109.5
62	N2	C11	C10	110.7(1)
63	N2	C11	H11A	109.5
64	N2	C11	H11B	109.5
65	C10	C11	H11A	109.5
66	C10	C11	H11B	109.5
67	H11A	C11	H11B	108.1
68	C16	C15	C14	120.6(2)
69	C16	C15	H15	119.7
70	C14	C15	H15	119.7
71	N1	C9	C10	111.1(1)
72	N1	C9	H9A	109.4
73	N1	C9	H9B	109.4
74	C10	C9	H9A	109.4
75	C10	C9	H9B	109.4
76	H9A	C9	H9B	108

Table E.2: Bond lengths for the ligand SL2

Atom1	Atom2	Type	Polymeric	Cyclic	Length	SybylType
O1	H1	Unknown	no	acyclic	0.84	1
O1	C1	Unknown	no	acyclic	1.348(2)	1
O2	H2	Unknown	no	acyclic	0.84	1
O2	C14	Unknown	no	acyclic	1.352(2)	1
N2	C12	Unknown	no	acyclic	1.274(2)	un
N2	C11	Unknown	no	acyclic	1.463(2)	1
N1	C8	Unknown	no	acyclic	1.278(2)	un
N1	C9	Unknown	no	acyclic	1.458(2)	1
C13	C12	Unknown	no	acyclic	1.458(2)	un
C13	C19	Unknown	no	cyclic	1.395(2)	un
C13	C14	Unknown	no	cyclic	1.407(2)	un
C6	H6	Unknown	no	acyclic	0.95	1
C6	C4	Unknown	no	cyclic	1.386(2)	un
C6	C7	Unknown	no	cyclic	1.396(2)	un
C4	C3	Unknown	no	cyclic	1.400(2)	un
C4	C5	Unknown	no	acyclic	1.506(2)	1
C7	C8	Unknown	no	acyclic	1.457(2)	un
C7	C1	Unknown	no	cyclic	1.412(2)	un
C12	H12	Unknown	no	acyclic	0.95	1
C19	H19	Unknown	no	acyclic	0.95	1
C19	C17	Unknown	no	cyclic	1.389(2)	un
C17	C16	Unknown	no	cyclic	1.392(2)	un
C17	C18	Unknown	no	acyclic	1.503(2)	1
C3	H3	Unknown	no	acyclic	0.95	1
C3	C2	Unknown	no	cyclic	1.377(2)	un
C8	H8	Unknown	no	acyclic	0.95	1
C2	H2A	Unknown	no	acyclic	0.95	1
C2	C1	Unknown	no	cyclic	1.389(2)	un
C16	H16	Unknown	no	acyclic	0.95	1
C16	C15	Unknown	no	cyclic	1.381(2)	un
C18	H18A	Unknown	no	acyclic	0.98	1
C18	H18B	Unknown	no	acyclic	0.98	1
C18	H18C	Unknown	no	acyclic	0.98	1
C14	C15	Unknown	no	cyclic	1.388(2)	un
C10	H10A	Unknown	no	acyclic	0.99	1
C10	H10B	Unknown	no	acyclic	0.99	1
C10	C11	Unknown	no	acyclic	1.516(2)	1
C10	C9	Unknown	no	acyclic	1.511(2)	1

C5	H5A	Unknown	no	acyclic	0.98	1
C5	H5B	Unknown	no	acyclic	0.98	1
C5	H5C	Unknown	no	acyclic	0.98	1
C11	H11A	Unknown	no	acyclic	0.99	1
C11	H11B	Unknown	no	acyclic	0.99	1
C15	H15	Unknown	no	acyclic	0.95	1
C9	H9A	Unknown	no	acyclic	0.99	1
C9	H9B	Unknown	no	acyclic	0.99	1

Table E.3: Atoms and symmetry operations for the ligand SL2

Number	Label	Charge	SybylType	Xfrac + ESD	Yfrac + ESD	Zfrac + ESD	Symm. op.
1	O1	0	O.3	0.75882(6)	0.8209(2)	0.27355(8)	x,y,z
2	H1	0	H	0.721521	0.747671	0.276516	x,y,z
3	O2	0	O.3	0.41009(6)	1.0089(2)	0.47933(10)	x,y,z
4	H2	0	H	0.43511	0.903102	0.460415	x,y,z
5	N2	0	N.2	0.43897(6)	0.6204(2)	0.40381(9)	x,y,z
6	N1	0	N.2	0.67781(7)	0.4894(2)	0.31845(9)	x,y,z
7	C13	0	C.2	0.32289(7)	0.7585(2)	0.41226(9)	x,y,z
8	C6	0	C.2	0.85811(7)	0.3428(2)	0.37430(9)	x,y,z
9	H6	0	H	0.850499	0.196294	0.400062	x,y,z
10	C4	0	C.2	0.92561(7)	0.4208(2)	0.36927(9)	x,y,z
11	C7	0	C.2	0.80083(7)	0.4712(2)	0.34299(9)	x,y,z
12	C12	0	C.2	0.37444(7)	0.5928(3)	0.38494(10)	x,y,z
13	H12	0	H	0.359468	0.460389	0.352108	x,y,z
14	C19	0	C.2	0.25266(7)	0.7184(2)	0.39178(9)	x,y,z
15	H19	0	H	0.239309	0.581013	0.361196	x,y,z
16	C17	0	C.2	0.20162(7)	0.8730(2)	0.41466(10)	x,y,z
17	C3	0	C.2	0.93485(8)	0.6371(3)	0.33055(10)	x,y,z
18	H3	0	H	0.98055	0.694931	0.325968	x,y,z
19	C8	0	C.2	0.73110(7)	0.3780(3)	0.34833(10)	x,y,z
20	H8	0	H	0.725134	0.231154	0.374611	x,y,z
21	C2	0	C.2	0.87955(8)	0.7683(2)	0.29892(10)	x,y,z
22	H2A	0	H	0.887618	0.914471	0.273133	x,y,z
23	C16	0	C.2	0.22283(8)	1.0720(3)	0.45988(11)	x,y,z
24	H16	0	H	0.188915	1.180246	0.47646	x,y,z
25	C18	0	C.3	0.12648(8)	0.8250(3)	0.39069(11)	x,y,z
26	H18A	0	H	0.117236	0.849437	0.325719	x,y,z
27	H18B	0	H	0.09743	0.928573	0.424766	x,y,z

28	H18C	0	H	0.115783	0.665793	0.405955	x,y,z
29	C14	0	C.2	0.34274(8)	0.9615(3)	0.45794(11)	x,y,z
30	C1	0	C.2	0.81206(8)	0.6886(3)	0.30440(10)	x,y,z
31	C10	0	C.3	0.55888(8)	0.5540(3)	0.36317(11)	x,y,z
32	H10A	0	H	0.554359	0.688536	0.322515	x,y,z
33	H10B	0	H	0.577304	0.608376	0.422955	x,y,z
34	C5	0	C.3	0.98661(8)	0.2776(3)	0.40219(11)	x,y,z
35	H5A	0	H	0.971548	0.118938	0.410774	x,y,z
36	H5B	0	H	1.00559	0.339013	0.459826	x,y,z
37	H5C	0	H	1.022393	0.281639	0.357412	x,y,z
38	C11	0	C.3	0.48792(8)	0.4486(3)	0.37346(12)	x,y,z
39	H11A	0	H	0.470656	0.384241	0.314726	x,y,z
40	H11B	0	H	0.491539	0.321829	0.417903	x,y,z
41	C15	0	C.2	0.29194(9)	1.1161(3)	0.48124(13)	x,y,z
42	H15	0	H	0.30483	1.253449	0.512165	x,y,z
43	C9	0	C.3	0.60952(8)	0.3859(3)	0.32523(13)	x,y,z
44	H9A	0	H	0.613306	0.249316	0.364905	x,y,z
45	H9B	0	H	0.592026	0.334995	0.264545	x,y,z

Table E.4: Torsions for the atoms of ligand SL2

Number	Atom1	Atom2	Atom3	Atom4	Torsion
1	H1	O1	C1	C7	-5.8
2	H1	O1	C1	C2	174.8
3	H2	O2	C14	C13	1.1
4	H2	O2	C14	C15	-178.8
5	C11	N2	C12	C13	-179.3(1)
6	C11	N2	C12	H12	0.7
7	C12	N2	C11	C10	154.3(1)
8	C12	N2	C11	H11A	33.5
9	C12	N2	C11	H11B	-84.9
10	C9	N1	C8	C7	179.6(1)
11	C9	N1	C8	H8	-0.4
12	C8	N1	C9	C10	132.5(2)
13	C8	N1	C9	H9A	11.6
14	C8	N1	C9	H9B	-106.6
15	C19	C13	C12	N2	-178.6(1)
16	C19	C13	C12	H12	1.4
17	C14	C13	C12	N2	2.5(2)
18	C14	C13	C12	H12	-177.5
19	C12	C13	C19	H19	1.3
20	C12	C13	C19	C17	-178.7(1)

21	C14	C13	C19	H19	-179.7
22	C14	C13	C19	C17	0.3(2)
23	C12	C13	C14	O2	-1.0(2)
24	C12	C13	C14	C15	178.9(1)
25	C19	C13	C14	O2	-179.9(1)
26	C19	C13	C14	C15	-0.1(2)
27	H6	C6	C4	C3	179.7
28	H6	C6	C4	C5	1
29	C7	C6	C4	C3	-0.3(2)
30	C7	C6	C4	C5	-179.0(1)
31	H6	C6	C7	C8	-1.3
32	H6	C6	C7	C1	-179.8
33	C4	C6	C7	C8	178.7(1)
34	C4	C6	C7	C1	0.2(2)
35	C6	C4	C3	H3	-179.8
36	C6	C4	C3	C2	0.2(2)
37	C5	C4	C3	H3	-1
38	C5	C4	C3	C2	179.0(1)
39	C6	C4	C5	H5A	14.7
40	C6	C4	C5	H5B	-105.3
41	C6	C4	C5	H5C	134.7
42	C3	C4	C5	H5A	-164.1
43	C3	C4	C5	H5B	75.9
44	C3	C4	C5	H5C	-44.1
45	C6	C7	C8	N1	-178.5(1)
46	C6	C7	C8	H8	1.5
47	C1	C7	C8	N1	-0.1(2)
48	C1	C7	C8	H8	179.9
49	C6	C7	C1	O1	-179.6(1)
50	C6	C7	C1	C2	-0.1(2)
51	C8	C7	C1	O1	2.0(2)
52	C8	C7	C1	C2	-178.6(1)
53	C13	C19	C17	C16	-0.4(2)
54	C13	C19	C17	C18	179.4(1)
55	H19	C19	C17	C16	179.6
56	H19	C19	C17	C18	-0.6
57	C19	C17	C16	H16	-179.8
58	C19	C17	C16	C15	0.2(2)
59	C18	C17	C16	H16	0.4
60	C18	C17	C16	C15	-179.6(2)
61	C19	C17	C18	H18A	-74.5
62	C19	C17	C18	H18B	165.5
63	C19	C17	C18	H18C	45.5
64	C16	C17	C18	H18A	105.2
65	C16	C17	C18	H18B	-14.7
66	C16	C17	C18	H18C	-134.7

67	C4	C3	C2	H2A	179.9
68	C4	C3	C2	C1	-0.1(2)
69	H3	C3	C2	H2A	-0.1
70	H3	C3	C2	C1	179.9
71	C3	C2	C1	O1	179.5(1)
72	C3	C2	C1	C7	0.1(2)
73	H2A	C2	C1	O1	-0.5
74	H2A	C2	C1	C7	-179.9
75	C17	C16	C15	C14	0.0(3)
76	C17	C16	C15	H15	-180
77	H16	C16	C15	C14	-180
78	H16	C16	C15	H15	0
79	O2	C14	C15	C16	179.8(2)
80	O2	C14	C15	H15	-0.2
81	C13	C14	C15	C16	-0.1(3)
82	C13	C14	C15	H15	179.9
83	H10A	C10	C11	N2	-54.6
84	H10A	C10	C11	H11A	66.2
85	H10A	C10	C11	H11B	-175.4
86	H10B	C10	C11	N2	63.1
87	H10B	C10	C11	H11A	-176.1
88	H10B	C10	C11	H11B	-57.7
89	C9	C10	C11	N2	-175.7(1)
90	C9	C10	C11	H11A	-54.9
91	C9	C10	C11	H11B	63.4
92	H10A	C10	C9	N1	60.5
93	H10A	C10	C9	H9A	-178.6
94	H10A	C10	C9	H9B	-60.5
95	H10B	C10	C9	N1	-57.2
96	H10B	C10	C9	H9A	63.7
97	H10B	C10	C9	H9B	-178.1
98	C11	C10	C9	N1	-178.4(1)
99	C11	C10	C9	H9A	-57.5
100	C11	C10	C9	H9B	60.7

Table E.5: Bond angles for the ligand SL3

Number	Atom1	Atom2	Atom3	Angle
1	C24	O6	C26	116.4(1)
2	H5	O5	C21	109.5
3	C36	O8	C38	116.7(1)
4	H7	O7	C33	109.5
5	C27	N3	C28	118.3(1)
6	C31	N4	C30	118.0(1)
7	O6	C24	C25	125.2(1)
8	O6	C24	C23	115.2(1)
9	C25	C24	C23	119.6(1)
10	C24	C25	H25	119.9
11	C24	C25	C20	120.3(1)
12	H25	C25	C20	119.8
13	C37	C32	C31	119.5(1)
14	C37	C32	C33	119.6(1)
15	C31	C32	C33	120.9(1)
16	O5	C21	C20	121.5(1)
17	O5	C21	C22	119.0(1)
18	C20	C21	C22	119.6(1)
19	C25	C20	C21	119.5(1)
20	C25	C20	C27	119.6(1)
21	C21	C20	C27	120.8(1)
22	C24	C23	H23	119.7
23	C24	C23	C22	120.7(1)
24	H23	C23	C22	119.7
25	N3	C27	C20	122.3(1)
26	N3	C27	H27	118.9
27	C20	C27	H27	118.9
28	C21	C22	C23	120.3(1)
29	C21	C22	H22	119.8
30	C23	C22	H22	119.8
31	C32	C37	H37	119.8
32	C32	C37	C36	120.4(1)
33	H37	C37	C36	119.8
34	N4	C31	C32	121.9(1)
35	N4	C31	H31	119
36	C32	C31	H31	119
37	H29A	C29	H29B	107.9
38	H29A	C29	C28	109.2

39	H29A	C29	C30	109.2
40	H29B	C29	C28	109.2
41	H29B	C29	C30	109.2
42	C28	C29	C30	112.0(1)
43	O7	C33	C32	122.0(1)
44	O7	C33	C34	118.7(1)
45	C32	C33	C34	119.3(1)
46	O8	C36	C37	125.1(1)
47	O8	C36	C35	115.5(1)
48	C37	C36	C35	119.4(1)
49	N3	C28	C29	111.1(1)
50	N3	C28	H28A	109.4
51	N3	C28	H28B	109.4
52	C29	C28	H28A	109.4
53	C29	C28	H28B	109.4
54	H28A	C28	H28B	108
55	N4	C30	C29	111.0(1)
56	N4	C30	H30A	109.4
57	N4	C30	H30B	109.4
58	C29	C30	H30A	109.4
59	C29	C30	H30B	109.4
60	H30A	C30	H30B	108
61	C33	C34	H34	119.7
62	C33	C34	C35	120.6(1)
63	H34	C34	C35	119.7
64	O6	C26	H26A	109.5
65	O6	C26	H26B	109.5
66	O6	C26	H26C	109.5
67	H26A	C26	H26B	109.5
68	H26A	C26	H26C	109.5
69	H26B	C26	H26C	109.5
70	C36	C35	C34	120.7(1)
71	C36	C35	H35	119.7
72	C34	C35	H35	119.6
73	O8	C38	H38A	109.5
74	O8	C38	H38B	109.5
75	O8	C38	H38C	109.5
76	H38A	C38	H38B	109.5
77	H38A	C38	H38C	109.5
78	H38B	C38	H38C	109.5
79	H1	O1	C2	109.5

80	C17	O4	C19	116.6(1)
81	C5	O2	C7	116.6(1)
82	H3	O3	C14	109.5
83	C12	N2	C11	118.7(1)
84	C8	N1	C9	119.6(1)
85	C6	C1	C8	119.6(1)
86	C6	C1	C2	119.6(1)
87	C8	C1	C2	120.8(1)
88	H18	C18	C17	119.8
89	H18	C18	C13	119.8
90	C17	C18	C13	120.4(1)
91	N2	C12	H12	119.2
92	N2	C12	C13	121.5(1)
93	H12	C12	C13	119.2
94	O2	C5	C4	115.2(1)
95	O2	C5	C6	125.2(1)
96	C4	C5	C6	119.7(1)
97	O4	C17	C18	124.9(1)
98	O4	C17	C16	115.5(1)
99	C18	C17	C16	119.6(1)
100	C5	C4	H4	119.7
101	C5	C4	C3	120.7(1)
102	H4	C4	C3	119.7
103	C1	C6	C5	120.2(1)
104	C1	C6	H6A	119.9
105	C5	C6	H6A	119.9
106	C18	C13	C12	119.4(1)
107	C18	C13	C14	119.5(1)
108	C12	C13	C14	121.1(1)
109	C4	C3	H3A	119.9
110	C4	C3	C2	120.3(1)
111	H3A	C3	C2	119.9
112	O3	C14	C13	121.9(1)
113	O3	C14	C15	118.8(1)
114	C13	C14	C15	119.3(1)
115	C17	C16	H16	119.7
116	C17	C16	C15	120.5(1)
117	H16	C16	C15	119.7
118	N1	C8	C1	121.5(1)
119	N1	C8	H8A	119.3
120	C1	C8	H8A	119.3

121	O1	C2	C1	121.6(1)
122	O1	C2	C3	118.9(1)
123	C1	C2	C3	119.5(1)
124	C14	C15	C16	120.6(1)
125	C14	C15	H15	119.7
126	C16	C15	H15	119.7
127	N2	C11	H11A	109.7
128	N2	C11	H11B	109.7
129	N2	C11	C10	109.8(1)
130	H11A	C11	H11B	108.2
131	H11A	C11	C10	109.7
132	H11B	C11	C10	109.7
133	N1	C9	H9A	109.7
134	N1	C9	H9B	109.7
135	N1	C9	C10	109.8(1)
136	H9A	C9	H9B	108.2
137	H9A	C9	C10	109.7
138	H9B	C9	C10	109.7
139	C11	C10	C9	112.5(1)
140	C11	C10	H10A	109.1
141	C11	C10	H10B	109.1
142	C9	C10	H10A	109.1
143	C9	C10	H10B	109.1
144	H10A	C10	H10B	107.8
145	O4	C19	H19A	109.5
146	O4	C19	H19B	109.5
147	O4	C19	H19C	109.5
148	H19A	C19	H19B	109.5
149	H19A	C19	H19C	109.5
150	H19B	C19	H19C	109.5
151	O2	C7	H7A	109.5
152	O2	C7	H7B	109.5
153	O2	C7	H7C	109.5
154	H7A	C7	H7B	109.5
155	H7A	C7	H7C	109.5
156	H7B	C7	H7C	109.5

Table E.6: Bond lengths for the ligand SL3

Number	Atom1	Atom2	Type	Polymeric	Cyclic	Length	SybylType
1	O6	C24	Unknown	no	acyclic	1.374(2)	1
2	O6	C26	Unknown	no	acyclic	1.428(2)	1
3	O5	H5	Unknown	no	acyclic	0.84	1
4	O5	C21	Unknown	no	acyclic	1.358(2)	1
5	O8	C36	Unknown	no	acyclic	1.374(2)	1
6	O8	C38	Unknown	no	acyclic	1.426(2)	1
7	O7	H7	Unknown	no	acyclic	0.84	1
8	O7	C33	Unknown	no	acyclic	1.357(2)	1
9	N3	C27	Unknown	no	acyclic	1.279(2)	un
10	N3	C28	Unknown	no	acyclic	1.462(2)	1
11	N4	C31	Unknown	no	acyclic	1.277(2)	un
12	N4	C30	Unknown	no	acyclic	1.462(1)	1
13	C24	C25	Unknown	no	cyclic	1.380(2)	un
14	C24	C23	Unknown	no	cyclic	1.400(2)	un
15	C25	H25	Unknown	no	acyclic	0.95	1
16	C25	C20	Unknown	no	cyclic	1.408(2)	un
17	C32	C37	Unknown	no	cyclic	1.407(2)	un
18	C32	C31	Unknown	no	acyclic	1.459(2)	un
19	C32	C33	Unknown	no	cyclic	1.404(2)	un
20	C21	C20	Unknown	no	cyclic	1.404(2)	un
21	C21	C22	Unknown	no	cyclic	1.392(2)	un
22	C20	C27	Unknown	no	acyclic	1.455(2)	un
23	C23	H23	Unknown	no	acyclic	0.95	1
24	C23	C22	Unknown	no	cyclic	1.380(2)	un
25	C27	H27	Unknown	no	acyclic	0.95	1
26	C22	H22	Unknown	no	acyclic	0.95	1
27	C37	H37	Unknown	no	acyclic	0.95	1
28	C37	C36	Unknown	no	cyclic	1.382(2)	un
29	C31	H31	Unknown	no	acyclic	0.95	1
30	C29	H29A	Unknown	no	acyclic	0.99	1
31	C29	H29B	Unknown	no	acyclic	0.99	1
32	C29	C28	Unknown	no	acyclic	1.525(2)	1
33	C29	C30	Unknown	no	acyclic	1.521(2)	1
34	C33	C34	Unknown	no	cyclic	1.394(2)	un
35	C36	C35	Unknown	no	cyclic	1.399(2)	un
36	C28	H28A	Unknown	no	acyclic	0.99	1
37	C28	H28B	Unknown	no	acyclic	0.99	1
38	C30	H30A	Unknown	no	acyclic	0.99	1

39	C30	H30B	Unknown	no	acyclic	0.99	1
40	C34	H34	Unknown	no	acyclic	0.95	1
41	C34	C35	Unknown	no	cyclic	1.375(2)	un
42	C26	H26A	Unknown	no	acyclic	0.98	1
43	C26	H26B	Unknown	no	acyclic	0.98	1
44	C26	H26C	Unknown	no	acyclic	0.98	1
45	C35	H35	Unknown	no	acyclic	0.95	1
46	C38	H38A	Unknown	no	acyclic	0.98	1
47	C38	H38B	Unknown	no	acyclic	0.98	1
48	C38	H38C	Unknown	no	acyclic	0.98	1
49	O1	H1	Unknown	no	acyclic	0.84	1
50	O1	C2	Unknown	no	acyclic	1.355(2)	1
51	O4	C17	Unknown	no	acyclic	1.376(2)	1
52	O4	C19	Unknown	no	acyclic	1.428(2)	1
53	O2	C5	Unknown	no	acyclic	1.376(2)	1
54	O2	C7	Unknown	no	acyclic	1.431(2)	1
55	O3	H3	Unknown	no	acyclic	0.84	1
56	O3	C14	Unknown	no	acyclic	1.353(2)	1
57	N2	C12	Unknown	no	acyclic	1.276(2)	un
58	N2	C11	Unknown	no	acyclic	1.461(1)	1
59	N1	C8	Unknown	no	acyclic	1.279(2)	un
60	N1	C9	Unknown	no	acyclic	1.456(2)	1
61	C1	C6	Unknown	no	cyclic	1.406(2)	un
62	C1	C8	Unknown	no	acyclic	1.458(2)	un
63	C1	C2	Unknown	no	cyclic	1.408(2)	un
64	C18	H18	Unknown	no	acyclic	0.95	1
65	C18	C17	Unknown	no	cyclic	1.383(2)	un
66	C18	C13	Unknown	no	cyclic	1.404(2)	un
67	C12	H12	Unknown	no	acyclic	0.95	1
68	C12	C13	Unknown	no	acyclic	1.460(2)	un
69	C5	C4	Unknown	no	cyclic	1.402(2)	un
70	C5	C6	Unknown	no	cyclic	1.381(2)	un
71	C17	C16	Unknown	no	cyclic	1.398(2)	un
72	C4	H4	Unknown	no	acyclic	0.95	1
73	C4	C3	Unknown	no	cyclic	1.379(2)	un
74	C6	H6A	Unknown	no	acyclic	0.95	1
75	C13	C14	Unknown	no	cyclic	1.407(2)	un
76	C3	H3A	Unknown	no	acyclic	0.95	1
77	C3	C2	Unknown	no	cyclic	1.393(2)	un
78	C14	C15	Unknown	no	cyclic	1.394(2)	un
79	C16	H16	Unknown	no	acyclic	0.95	1

80	C16	C15	Unknown	no	cyclic	1.379(2)	un
81	C8	H8A	Unknown	no	acyclic	0.95	1
82	C15	H15	Unknown	no	acyclic	0.95	1
83	C11	H11A	Unknown	no	acyclic	0.99	1
84	C11	H11B	Unknown	no	acyclic	0.99	1
85	C11	C10	Unknown	no	acyclic	1.517(2)	1
86	C9	H9A	Unknown	no	acyclic	0.99	1
87	C9	H9B	Unknown	no	acyclic	0.99	1
88	C9	C10	Unknown	no	acyclic	1.519(2)	1
89	C10	H10A	Unknown	no	acyclic	0.99	1
90	C10	H10B	Unknown	no	acyclic	0.99	1
91	C19	H19A	Unknown	no	acyclic	0.98	1
92	C19	H19B	Unknown	no	acyclic	0.98	1
93	C19	H19C	Unknown	no	acyclic	0.98	1
94	C7	H7A	Unknown	no	acyclic	0.98	1
95	C7	H7B	Unknown	no	acyclic	0.98	1
96	C7	H7C	Unknown	no	acyclic	0.98	1

Table E.7: Atoms and symmetry operations for SL3

Number	Label	Charge	SybylType	Xfrac + ESD	Yfrac + ESD	Zfrac + ESD	Symm. op.
1	O6	0	O.3	1.55754(9)	0.33937(9)	0.31279(5)	x,y,z
2	O5	0	O.3	1.31448(10)	0.50156(10)	0.04248(5)	x,y,z
3	H5	0	H	1.237988	0.543286	0.045283	x,y,z
4	O8	0	O.3	0.33143(11)	1.11795(9)	-0.21311(5)	x,y,z
5	O7	0	O.3	0.83858(10)	1.00789(10)	-0.07485(6)	x,y,z
6	H7	0	H	0.830515	0.94269	-0.03657	x,y,z
7	N3	0	N.2	1.10852(11)	0.61038(11)	0.10395(6)	x,y,z
8	N4	0	N.2	0.71366(12)	0.80493(11)	0.02206(6)	x,y,z
9	C24	0	C.2	1.48744(13)	0.38222(12)	0.24849(7)	x,y,z
10	C25	0	C.2	1.35979(13)	0.45058(12)	0.24175(7)	x,y,z
11	H25	0	H	1.312962	0.470175	0.28396	x,y,z
12	C32	0	C.2	0.59164(14)	0.94654(12)	-0.07808(7)	x,y,z
13	C21	0	C.2	1.36807(13)	0.46151(12)	0.11052(7)	x,y,z
14	C20	0	C.2	1.29862(13)	0.49141(12)	0.17260(7)	x,y,z
15	C23	0	C.2	1.55486(13)	0.35183(12)	0.18638(7)	x,y,z
16	H23	0	H	1.642188	0.303881	0.191095	x,y,z
17	C27	0	C.2	1.16592(13)	0.56640(12)	0.16597(7)	x,y,z
18	H27	0	H	1.120292	0.583301	0.209186	x,y,z
19	C22	0	C.2	1.49573(14)	0.39083(13)	0.11833(7)	x,y,z
20	H22	0	H	1.542399	0.369332	0.076634	x,y,z
21	C37	0	C.2	0.46205(14)	0.97414(12)	-0.11295(7)	x,y,z

22	H37	0	H	0.380184	0.919552	-0.0931	x,y,z
23	C31	0	C.2	0.59903(14)	0.83349(12)	-0.01199(7)	x,y,z
24	H31	0	H	0.516101	0.779522	0.006248	x,y,z
25	C29	0	C.3	0.84936(14)	0.61013(13)	0.08893(7)	x,y,z
26	H29A	0	H	0.867342	0.588435	0.040979	x,y,z
27	H29B	0	H	0.838673	0.524779	0.128716	x,y,z
28	C33	0	C.2	0.71203(14)	1.02807(13)	-0.10728(7)	x,y,z
29	C36	0	C.2	0.45320(15)	1.08025(13)	-0.17593(7)	x,y,z
30	C28	0	C.3	0.97714(14)	0.68794(13)	0.10245(7)	x,y,z
31	H28A	0	H	0.988506	0.77312	0.062576	x,y,z
32	H28B	0	H	0.95955	0.70973	0.150392	x,y,z
33	C30	0	C.3	0.71120(14)	0.68880(13)	0.08734(7)	x,y,z
34	H30A	0	H	0.629171	0.630021	0.086542	x,y,z
35	H30B	0	H	0.698256	0.719104	0.132918	x,y,z
36	C34	0	C.2	0.70240(16)	1.13219(13)	-0.17212(8)	x,y,z
37	H34	0	H	0.784447	1.185617	-0.19324	x,y,z
38	C26	0	C.3	1.48568(14)	0.35928(14)	0.37840(7)	x,y,z
39	H26A	0	H	1.47032	0.455186	0.371662	x,y,z
40	H26B	0	H	1.544258	0.323917	0.420753	x,y,z
41	H26C	0	H	1.393147	0.312406	0.387818	x,y,z
42	C35	0	C.2	0.57518(16)	1.15822(13)	-0.20576(7)	x,y,z
43	H35	0	H	0.570062	1.229888	-0.24972	x,y,z
44	C38	0	C.3	0.20563(16)	1.03975(14)	-0.18412(8)	x,y,z
45	H38A	0	H	0.221552	0.947494	-0.18617	x,y,z
46	H38B	0	H	0.125309	1.077613	-0.21382	x,y,z
47	H38C	0	H	0.183609	1.040429	-0.13243	x,y,z
48	O1	0	O.3	0.82827(10)	-0.04750(9)	0.55293(5)	x,y,z
49	H1	0	H	0.741873	-0.0292	0.560078	x,y,z
50	O4	0	O.3	-0.09778(10)	0.65984(9)	0.29364(5)	x,y,z
51	O2	0	O.3	1.08066(9)	-0.26643(9)	0.81671(5)	x,y,z
52	O3	0	O.3	0.32536(10)	0.57513(9)	0.49242(5)	x,y,z
53	H3	0	H	0.327646	0.494988	0.518086	x,y,z
54	N2	0	N.2	0.25208(11)	0.32361(10)	0.53692(6)	x,y,z
55	N1	0	N.2	0.58958(11)	-0.03456(10)	0.62779(6)	x,y,z
56	C1	0	C.2	0.80376(13)	-0.11505(11)	0.68697(7)	x,y,z
57	C18	0	C.2	0.03139(13)	0.50149(12)	0.38875(6)	x,y,z
58	H18	0	H	-0.02377	0.427796	0.384914	x,y,z
59	C12	0	C.2	0.15773(13)	0.34682(12)	0.48904(6)	x,y,z
60	H12	0	H	0.098819	0.275347	0.485404	x,y,z
61	C5	0	C.2	1.00870(13)	-0.20881(12)	0.75430(7)	x,y,z
62	C17	0	C.2	0.00597(13)	0.62857(12)	0.34410(6)	x,y,z
63	C4	0	C.2	1.08933(13)	-0.19136(12)	0.68659(7)	x,y,z
64	H4	0	H	1.186717	-0.21778	0.686534	x,y,z
65	C6	0	C.2	0.86740(13)	-0.16964(12)	0.75443(7)	x,y,z
66	H6A	0	H	0.813028	-0.17963	0.800238	x,y,z
67	C13	0	C.2	0.13824(13)	0.48064(12)	0.43972(6)	x,y,z

68	C3	0	C.2	1.02872(14)	-0.13623(12)	0.62004(7)	x,y,z
69	H3A	0	H	1.084817	-0.12396	0.574548	x,y,z
70	C14	0	C.2	0.22085(13)	0.58987(13)	0.44443(7)	x,y,z
71	C16	0	C.2	0.08789(13)	0.73660(12)	0.34964(7)	x,y,z
72	H16	0	H	0.070388	0.82403	0.319122	x,y,z
73	C8	0	C.2	0.65313(13)	-0.07827(12)	0.68792(7)	x,y,z
74	H8A	0	H	0.601071	-0.08698	0.734248	x,y,z
75	C2	0	C.2	0.88559(14)	-0.09846(12)	0.61926(7)	x,y,z
76	C15	0	C.2	0.19393(14)	0.71731(13)	0.39903(7)	x,y,z
77	H15	0	H	0.249088	0.791527	0.402139	x,y,z
78	C11	0	C.3	0.26454(14)	0.18768(12)	0.58530(7)	x,y,z
79	H11A	0	H	0.20263	0.126079	0.568978	x,y,z
80	H11B	0	H	0.232374	0.185364	0.636981	x,y,z
81	C9	0	C.3	0.43912(13)	0.00131(13)	0.63129(7)	x,y,z
82	H9A	0	H	0.406034	-0.00418	0.683274	x,y,z
83	H9B	0	H	0.381299	-0.06229	0.614258	x,y,z
84	C10	0	C.3	0.41888(14)	0.14261(13)	0.58241(7)	x,y,z
85	H10A	0	H	0.479949	0.204969	0.598633	x,y,z
86	H10B	0	H	0.450539	0.14667	0.530434	x,y,z
87	C19	0	C.3	-0.19903(15)	0.55669(14)	0.29607(7)	x,y,z
88	H19A	0	H	-0.15153	0.485879	0.278293	x,y,z
89	H19B	0	H	-0.27668	0.594162	0.26427	x,y,z
90	H19C	0	H	-0.23837	0.519227	0.347302	x,y,z
91	C7	0	C.3	1.00718(15)	-0.27163(14)	0.88683(7)	x,y,z
92	H7A	0	H	0.979169	-0.18105	0.887868	x,y,z
93	H7B	0	H	1.070513	-0.30911	0.926831	x,y,z
94	H7C	0	H	0.921539	-0.32828	0.893787	x,y,z

Table E.8: Torsions for the atoms of ligand SL3

Number	Atom1	Atom2	Atom3	Atom4	Torsion
1	C26	O6	C24	C25	4.9(2)
2	C26	O6	C24	C23	-175.1(1)
3	C24	O6	C26	H26A	-60.9
4	C24	O6	C26	H26B	179.1
5	C24	O6	C26	H26C	59.1
6	H5	O5	C21	C20	-0.5
7	H5	O5	C21	C22	-179.6
8	C38	O8	C36	C37	-0.6(2)
9	C38	O8	C36	C35	179.7(1)
10	C36	O8	C38	H38A	-62
11	C36	O8	C38	H38B	178

12	C36	O8	C38	H38C	58
13	H7	O7	C33	C32	-0.7
14	H7	O7	C33	C34	-179.9
15	C28	N3	C27	C20	-178.3(1)
16	C28	N3	C27	H27	1.7
17	C27	N3	C28	C29	-110.7(1)
18	C27	N3	C28	H28A	128.4
19	C27	N3	C28	H28B	10.2
20	C30	N4	C31	C32	-179.3(1)
21	C30	N4	C31	H31	0.7
22	C31	N4	C30	C29	139.8(1)
23	C31	N4	C30	H30A	18.9
24	C31	N4	C30	H30B	-99.3
25	O6	C24	C25	H25	-1
26	O6	C24	C25	C20	179.1(1)
27	C23	C24	C25	H25	179
28	C23	C24	C25	C20	-1.0(2)
29	O6	C24	C23	H23	0.7
30	O6	C24	C23	C22	-179.3(1)
31	C25	C24	C23	H23	-179.3
32	C25	C24	C23	C22	0.7(2)
33	C24	C25	C20	C21	0.3(2)
34	C24	C25	C20	C27	-178.4(1)
35	H25	C25	C20	C21	-179.7
36	H25	C25	C20	C27	1.6
37	C31	C32	C37	H37	0.5
38	C31	C32	C37	C36	-179.5(1)
39	C33	C32	C37	H37	-179.5
40	C33	C32	C37	C36	0.5(2)
41	C37	C32	C31	N4	-179.4(1)
42	C37	C32	C31	H31	0.6
43	C33	C32	C31	N4	0.6(2)
44	C33	C32	C31	H31	-179.4
45	C37	C32	C33	O7	178.4(1)
46	C37	C32	C33	C34	-2.4(2)
47	C31	C32	C33	O7	-1.6(2)
48	C31	C32	C33	C34	177.6(1)
49	O5	C21	C20	C25	-178.5(1)
50	O5	C21	C20	C27	0.2(2)
51	C22	C21	C20	C25	0.6(2)
52	C22	C21	C20	C27	179.3(1)

53	O5	C21	C22	C23	178.3(1)
54	O5	C21	C22	H22	-1.7
55	C20	C21	C22	C23	-0.9(2)
56	C20	C21	C22	H22	179.1
57	C25	C20	C27	N3	177.3(1)
58	C25	C20	C27	H27	-2.7
59	C21	C20	C27	N3	-1.4(2)
60	C21	C20	C27	H27	178.6
61	C24	C23	C22	C21	0.2(2)
62	C24	C23	C22	H22	-179.8
63	H23	C23	C22	C21	-179.8
64	H23	C23	C22	H22	0.2
65	C32	C37	C36	O8	-178.3(1)
66	C32	C37	C36	C35	1.5(2)
67	H37	C37	C36	O8	1.7
68	H37	C37	C36	C35	-178.5
69	H29A	C29	C28	N3	-59
70	H29A	C29	C28	H28A	61.9
71	H29A	C29	C28	H28B	-179.9
72	H29B	C29	C28	N3	58.7
73	H29B	C29	C28	H28A	179.6
74	H29B	C29	C28	H28B	-62.2
75	C30	C29	C28	N3	179.9(1)
76	C30	C29	C28	H28A	-59.2
77	C30	C29	C28	H28B	59
78	H29A	C29	C30	N4	-53
79	H29A	C29	C30	H30A	67.9
80	H29A	C29	C30	H30B	-173.9
81	H29B	C29	C30	N4	-170.8
82	H29B	C29	C30	H30A	-49.9
83	H29B	C29	C30	H30B	68.3
84	C28	C29	C30	N4	68.1(1)
85	C28	C29	C30	H30A	-171
86	C28	C29	C30	H30B	-52.8
87	O7	C33	C34	H34	1.6
88	O7	C33	C34	C35	-178.4(1)
89	C32	C33	C34	H34	-177.6
90	C32	C33	C34	C35	2.4(2)
91	O8	C36	C35	C34	178.3(1)
92	O8	C36	C35	H35	-1.8
93	C37	C36	C35	C34	-1.5(2)

94	C37	C36	C35	H35	178.5
95	C33	C34	C35	C36	-0.4(2)
96	C33	C34	C35	H35	179.6
97	H34	C34	C35	C36	179.6
98	H34	C34	C35	H35	-0.4
99	H1	O1	C2	C1	0.3
100	H1	O1	C2	C3	179.7
101	C19	O4	C17	C18	9.7(2)
102	C19	O4	C17	C16	-169.3(1)
103	C17	O4	C19	H19A	-69.8
104	C17	O4	C19	H19B	170.2
105	C17	O4	C19	H19C	50.2
106	C7	O2	C5	C4	173.0(1)
107	C7	O2	C5	C6	-7.5(2)
108	C5	O2	C7	H7A	-56.4
109	C5	O2	C7	H7B	-176.4
110	C5	O2	C7	H7C	63.6
111	H3	O3	C14	C13	-2.7
112	H3	O3	C14	C15	176.7
113	C11	N2	C12	H12	-0.9
114	C11	N2	C12	C13	179.1(1)
115	C12	N2	C11	H11A	7.6
116	C12	N2	C11	H11B	-111.1
117	C12	N2	C11	C10	128.3(1)
118	C9	N1	C8	C1	-179.9(1)
119	C9	N1	C8	H8A	0.1
120	C8	N1	C9	H9A	6.4
121	C8	N1	C9	H9B	-112.3
122	C8	N1	C9	C10	127.1(1)
123	C8	C1	C6	C5	178.0(1)
124	C8	C1	C6	H6A	-2
125	C2	C1	C6	C5	-1.1(2)
126	C2	C1	C6	H6A	179
127	C6	C1	C8	N1	-176.5(1)
128	C6	C1	C8	H8A	3.5
129	C2	C1	C8	N1	2.5(2)
130	C2	C1	C8	H8A	-177.5
131	C6	C1	C2	O1	179.3(1)
132	C6	C1	C2	C3	-0.1(2)
133	C8	C1	C2	O1	0.3(2)
134	C8	C1	C2	C3	-179.1(1)

135	H18	C18	C17	O4	1.4
136	H18	C18	C17	C16	-179.7
137	C13	C18	C17	O4	-178.6(1)
138	C13	C18	C17	C16	0.3(2)
139	H18	C18	C13	C12	-3.3
140	H18	C18	C13	C14	179.1
141	C17	C18	C13	C12	176.7(1)
142	C17	C18	C13	C14	-0.8(2)
143	N2	C12	C13	C18	-179.0(1)
144	N2	C12	C13	C14	-1.5(2)
145	H12	C12	C13	C18	1
146	H12	C12	C13	C14	178.5
147	O2	C5	C4	H4	-0.8
148	O2	C5	C4	C3	179.2(1)
149	C6	C5	C4	H4	179.6
150	C6	C5	C4	C3	-0.4(2)
151	O2	C5	C6	C1	-178.2(1)
152	O2	C5	C6	H6A	1.8
153	C4	C5	C6	C1	1.3(2)
154	C4	C5	C6	H6A	-178.7
155	O4	C17	C16	H16	-0.7
156	O4	C17	C16	C15	179.3(1)
157	C18	C17	C16	H16	-179.8
158	C18	C17	C16	C15	0.2(2)
159	C5	C4	C3	H3A	179.3
160	C5	C4	C3	C2	-0.7(2)
161	H4	C4	C3	H3A	-0.8
162	H4	C4	C3	C2	179.3
163	C18	C13	C14	O3	-179.8(1)
164	C18	C13	C14	C15	0.8(2)
165	C12	C13	C14	O3	2.7(2)
166	C12	C13	C14	C15	-176.7(1)
167	C4	C3	C2	O1	-178.5(1)
168	C4	C3	C2	C1	1.0(2)
169	H3A	C3	C2	O1	1.5
170	H3A	C3	C2	C1	-179
171	O3	C14	C15	C16	-179.7(1)
172	O3	C14	C15	H15	0.3
173	C13	C14	C15	C16	-0.3(2)
174	C13	C14	C15	H15	179.7
175	C17	C16	C15	C14	-0.2(2)

176	C17	C16	C15	H15	179.8
177	H16	C16	C15	C14	179.8
178	H16	C16	C15	H15	-0.2
179	N2	C11	C10	C9	-179.7(1)
180	N2	C11	C10	H10A	59.1
181	N2	C11	C10	H10B	-58.5
182	H11A	C11	C10	C9	-59
183	H11A	C11	C10	H10A	179.8
184	H11A	C11	C10	H10B	62.2
185	H11B	C11	C10	C9	59.7
186	H11B	C11	C10	H10A	-61.5
187	H11B	C11	C10	H10B	-179.1
188	N1	C9	C10	C11	-178.4(1)
189	N1	C9	C10	H10A	-57.2
190	N1	C9	C10	H10B	60.4
191	H9A	C9	C10	C11	-57.7
192	H9A	C9	C10	H10A	63.5
193	H9A	C9	C10	H10B	-178.9
194	H9B	C9	C10	C11	61
195	H9B	C9	C10	H10A	-177.8
196	H9B	C9	C10	H10B	-60.2

Table E.9: Bond angles for the ligand SL6

Number	Atom1	Atom2	Atom3	Angle
1	H2	O2	C12	109.5
2	H1	O1	C2	109.5
3	C10	N2	C9	119.2(2)
4	C6	N1	C7	118.4(2)
5	C6	C1	C2	120.7(2)
6	C6	C1	C5	120.0(2)
7	C2	C1	C5	119.3(2)
8	C12	C11	C16	119.2(2)
9	C12	C11	C10	120.4(2)
10	C16	C11	C10	120.4(2)
11	N1	C6	C1	122.0(2)
12	N1	C6	H6	119
13	C1	C6	H6	119
14	O2	C12	C11	120.7(2)
15	O2	C12	C13	119.3(2)
16	C11	C12	C13	120.0(2)

17	C11	C16	H16	120.1
18	C11	C16	C15	119.9(2)
19	H16	C16	C15	120.1
20	H14	C14	C13	120.1
21	H14	C14	C15	120.1
22	C13	C14	C15	119.8(2)
23	O1	C2	C1	121.5(2)
24	O1	C2	C3	118.9(2)
25	C1	C2	C3	119.5(2)
26	N2	C10	C11	121.1(2)
27	N2	C10	H10	119.4
28	C11	C10	H10	119.4
29	C12	C13	C14	120.0(2)
30	C12	C13	H13	120
31	C14	C13	H13	120
32	C1	C5	H5	119.9
33	C1	C5	C00N	120.2(2)
34	H5	C5	C00N	119.9
35	N1	C7	H7A	109.4
36	N1	C7	H7B	109.4
37	N1	C7	C8	111.0(2)
38	H7A	C7	H7B	108
39	H7A	C7	C8	109.4
40	H7B	C7	C8	109.4
41	N2	C9	H9A	109.6
42	N2	C9	H9B	109.6
43	N2	C9	C8	110.2(1)
44	H9A	C9	H9B	108.1
45	H9A	C9	C8	109.6
46	H9B	C9	C8	109.6
47	C2	C3	H3	119.6
48	C2	C3	C4	120.8(2)
49	H3	C3	C4	119.6
50	C12	C15	C16	119.7(1)
51	C12	C15	C14	119.1(1)
52	C16	C15	C14	121.1(2)
53	C3	C4	H4	120.3
54	C3	C4	C00N	119.4(2)
55	H4	C4	C00N	120.3
56	C7	C8	C9	112.3(2)
57	C7	C8	H8A	109.1

58	C7	C8	H8B	109.2
59	C9	C8	H8A	109.1
60	C9	C8	H8B	109.2
61	H8A	C8	H8B	107.9
62	Cl1	C00N	C5	119.5(1)
63	Cl1	C00N	C4	119.6(1)
64	C5	C00N	C4	120.8(2)

Table E.10: Bond lengths for the ligand SL6

Number	Atom1	Atom2	Type	Polymeric	Cyclic	Length	SybylType
1	Cl2	C15	Unknown	no	acyclic	1.747(2)	1
2	Cl1	C00N	Unknown	no	acyclic	1.747(2)	1
3	O2	H2	Unknown	no	acyclic	0.84	1
4	O2	C12	Unknown	no	acyclic	1.352(2)	1
5	O1	H1	Unknown	no	acyclic	0.84	1
6	O1	C2	Unknown	no	acyclic	1.347(2)	1
7	N2	C10	Unknown	no	acyclic	1.277(2)	un
8	N2	C9	Unknown	no	acyclic	1.458(2)	1
9	N1	C6	Unknown	no	acyclic	1.270(2)	un
10	N1	C7	Unknown	no	acyclic	1.465(2)	1
11	C1	C6	Unknown	no	acyclic	1.461(2)	un
12	C1	C2	Unknown	no	cyclic	1.408(3)	un
13	C1	C5	Unknown	no	cyclic	1.394(3)	un
14	C11	C12	Unknown	no	cyclic	1.411(3)	un
15	C11	C16	Unknown	no	cyclic	1.395(3)	un
16	C11	C10	Unknown	no	acyclic	1.459(2)	un
17	C6	H6	Unknown	no	acyclic	0.95	1
18	C12	C13	Unknown	no	cyclic	1.389(2)	un
19	C16	H16	Unknown	no	acyclic	0.95	1
20	C16	C15	Unknown	no	cyclic	1.378(2)	1
21	C14	H14	Unknown	no	acyclic	0.95	1
22	C14	C13	Unknown	no	cyclic	1.385(3)	un
23	C14	C15	Unknown	no	cyclic	1.387(3)	1
24	C2	C3	Unknown	no	cyclic	1.392(3)	un
25	C10	H10	Unknown	no	acyclic	0.95	1
26	C13	H13	Unknown	no	acyclic	0.95	1
27	C5	H5	Unknown	no	acyclic	0.95	1
28	C5	C00N	Unknown	no	cyclic	1.381(3)	1

29	C7	H7A	Unknown	no	acyclic	0.99	1
30	C7	H7B	Unknown	no	acyclic	0.99	1
31	C7	C8	Unknown	no	acyclic	1.518(3)	1
32	C9	H9A	Unknown	no	acyclic	0.99	1
33	C9	H9B	Unknown	no	acyclic	0.99	1
34	C9	C8	Unknown	no	acyclic	1.527(3)	1
35	C3	H3	Unknown	no	acyclic	0.95	1
36	C3	C4	Unknown	no	cyclic	1.382(3)	un
37	C4	H4	Unknown	no	acyclic	0.95	1
38	C4	C00N	Unknown	no	cyclic	1.390(3)	1
39	C8	H8A	Unknown	no	acyclic	0.99	1
40	C8	H8B	Unknown	no	acyclic	0.99	1

Table E.11: Atoms and symmetry operations for SL6

Number	Label	Charge	SybylType	Xfrac + ESD	Yfrac + ESD	Zfrac + ESD	Symm. op.
1	Cl2	0	Cl	1.10363(4)	0.40682(5)	0.85677(3)	x,y,z
2	Cl1	0	Cl	-0.34202(4)	0.62663(5)	0.54789(3)	x,y,z
3	O2	0	O.3	0.62213(11)	0.65443(14)	0.87003(8)	x,y,z
4	H2	0	H	0.5747	0.61433	0.834375	x,y,z
5	O1	0	O.3	0.17783(11)	0.70772(14)	0.58508(8)	x,y,z
6	H1	0	H	0.211985	0.627309	0.600642	x,y,z
7	N2	0	N.2	0.55323(13)	0.49458(17)	0.74761(9)	x,y,z
8	N1	0	N.2	0.19619(14)	0.43361(16)	0.63859(9)	x,y,z
9	C1	0	C.2	0.00772(16)	0.54926(19)	0.59980(10)	x,y,z
10	C11	0	C.2	0.75538(16)	0.49264(19)	0.80485(11)	x,y,z
11	C6	0	C.2	0.08309(16)	0.42382(19)	0.63017(11)	x,y,z
12	H6	0	H	0.046383	0.332113	0.644051	x,y,z
13	C12	0	C.2	0.73300(16)	0.59819(18)	0.86524(11)	x,y,z
14	C16	0	C.2	0.87032(17)	0.4348(2)	0.80260(11)	x,y,z
15	H16	0	H	0.886258	0.362084	0.762992	x,y,z
16	C14	0	C.2	0.93943(17)	0.58905(19)	0.91654(11)	x,y,z
17	H14	0	H	1.002926	0.622583	0.953782	x,y,z
18	C2	0	C.2	0.05877(17)	0.6870(2)	0.57858(11)	x,y,z
19	C10	0	C.2	0.65921(16)	0.4437(2)	0.74586(11)	x,y,z
20	H10	0	H	0.675716	0.372844	0.705461	x,y,z
21	C13	0	C.2	0.82529(17)	0.64544(19)	0.92057(11)	x,y,z
22	H13	0	H	0.810133	0.716487	0.961201	x,y,z
23	C5	0	C.2	-0.11593(17)	0.53221(19)	0.58972(11)	x,y,z

24	H5	0	H	-0.15111	0.438904	0.602579	x,y,z
25	C7	0	C.3	0.26498(17)	0.3011(2)	0.66755(12)	x,y,z
26	H7A	0	H	0.294839	0.247799	0.621022	x,y,z
27	H7B	0	H	0.212519	0.231075	0.694411	x,y,z
28	C9	0	C.3	0.46016(16)	0.4434(2)	0.68711(12)	x,y,z
29	H9A	0	H	0.4964	0.384245	0.645068	x,y,z
30	H9B	0	H	0.419232	0.531609	0.660744	x,y,z
31	C3	0	C.2	-0.01511(18)	0.8051(2)	0.55049(12)	x,y,z
32	H3	0	H	0.019129	0.898769	0.537172	x,y,z
33	C15	0	C.3	0.96071(16)	0.4834(2)	0.85794(11)	x,y,z
34	C4	0	C.2	-0.13765(18)	0.7879(2)	0.54172(11)	x,y,z
35	H4	0	H	-0.18748	0.869098	0.522622	x,y,z
36	C8	0	C.3	0.36970(16)	0.3461(2)	0.72666(12)	x,y,z
37	H8A	0	H	0.409941	0.253985	0.749008	x,y,z
38	H8B	0	H	0.33966	0.40249	0.772098	x,y,z
39	C00N	0	C.3	-0.18738(17)	0.6506(2)	0.56110(11)	x,y,z

Table E.12: Torsions for the atoms of ligand SL6

Number	Atom1	Atom2	Atom3	Atom4	Torsion
1	H2	O2	C12	C11	2.1
2	H2	O2	C12	C13	-177.9
3	H1	O1	C2	C1	2.7
4	H1	O1	C2	C3	-177.5
5	C9	N2	C10	C11	179.5(2)
6	C9	N2	C10	H10	-0.4
7	C10	N2	C9	H9A	-9.2
8	C10	N2	C9	H9B	-127.8
9	C10	N2	C9	C8	111.5(2)
10	C7	N1	C6	C1	-178.5(2)
11	C7	N1	C6	H6	1.5
12	C6	N1	C7	H7A	99
13	C6	N1	C7	H7B	-19.3
14	C6	N1	C7	C8	-140.1(2)
15	C2	C1	C6	N1	0.0(3)
16	C2	C1	C6	H6	-180
17	C5	C1	C6	N1	178.5(2)
18	C5	C1	C6	H6	-1.5
19	C6	C1	C2	O1	0.3(3)
20	C6	C1	C2	C3	-179.4(2)
21	C5	C1	C2	O1	-178.2(2)
22	C5	C1	C2	C3	2.1(3)
23	C6	C1	C5	H5	-0.1

24	C6	C1	C5	COON	179.9(2)
25	C2	C1	C5	H5	178.4
26	C2	C1	C5	COON	-1.6(3)
27	C16	C11	C12	O2	-178.8(2)
28	C16	C11	C12	C13	1.2(3)
29	C10	C11	C12	O2	0.7(3)
30	C10	C11	C12	C13	-179.3(2)
31	C12	C11	C16	H16	178.7
32	C12	C11	C16	C15	-1.4(3)
33	C10	C11	C16	H16	-0.9
34	C10	C11	C16	C15	179.1(2)
35	C12	C11	C10	N2	-0.2(3)
36	C12	C11	C10	H10	179.8
37	C16	C11	C10	N2	179.3(2)
38	C16	C11	C10	H10	-0.7
39	O2	C12	C13	C14	-180.0(2)
40	O2	C12	C13	H13	0
41	C11	C12	C13	C14	0.0(3)
42	C11	C12	C13	H13	-180
43	C11	C16	C15	Cl2	178.2(1)
44	C11	C16	C15	C14	0.3(3)
45	H16	C16	C15	Cl2	-1.8
46	H16	C16	C15	C14	-179.7
47	H14	C14	C13	C12	178.9
48	H14	C14	C13	H13	-1.1
49	C15	C14	C13	C12	-1.1(3)
50	C15	C14	C13	H13	178.9
51	H14	C14	C15	Cl2	3
52	H14	C14	C15	C16	-179.1
53	C13	C14	C15	Cl2	-177.0(1)
54	C13	C14	C15	C16	1.0(3)
55	O1	C2	C3	H3	-1
56	O1	C2	C3	C4	179.0(2)
57	C1	C2	C3	H3	178.7
58	C1	C2	C3	C4	-1.2(3)
59	C1	C5	COON	Cl1	179.4(1)
60	C1	C5	COON	C4	0.2(3)
61	H5	C5	COON	Cl1	-0.6
62	H5	C5	COON	C4	-179.8
63	N1	C7	C8	C9	-64.1(2)
64	N1	C7	C8	H8A	174.8
65	N1	C7	C8	H8B	57.1
66	H7A	C7	C8	C9	56.8
67	H7A	C7	C8	H8A	-64.3
68	H7A	C7	C8	H8B	178
69	H7B	C7	C8	C9	175

70	H7B	C7	C8	H8A	53.9
71	H7B	C7	C8	H8B	-63.8
72	N2	C9	C8	C7	175.0(1)
73	N2	C9	C8	H8A	-63.9
74	N2	C9	C8	H8B	53.8
75	H9A	C9	C8	C7	-64.3
76	H9A	C9	C8	H8A	56.9
77	H9A	C9	C8	H8B	174.5
78	H9B	C9	C8	C7	54.3
79	H9B	C9	C8	H8A	175.4
80	H9B	C9	C8	H8B	-66.9
81	C2	C3	C4	H4	179.9
82	C2	C3	C4	COON	-0.1(3)
83	H3	C3	C4	H4	-0.1
84	H3	C3	C4	COON	179.9
85	C3	C4	COON	Cl1	-178.5(1)
86	C3	C4	COON	C5	0.7(3)
87	H4	C4	COON	Cl1	1.5
88	H4	C4	COON	C5	-179.3

Table E.13: Bond angles for the ligand SL9

Number	Atom1	Atom2	Atom3	Angle
1	C18	O4	C20	117.2(2)
2	H3	O3	C15	109.4
3	H1	O1	C2	109.5
4	C5	O2	C7	117.1(2)
5	C8	N1	C9	118.2(2)
6	C13	N2	C12	117.6(2)
7	O1	C2	C1	121.9(2)
8	O1	C2	C3	118.7(2)
9	C1	C2	C3	119.4(2)
10	O3	C15	C16	118.2(2)
11	O3	C15	C14	122.3(2)
12	C16	C15	C14	119.4(2)
13	C15	C16	H16	119.9
14	C15	C16	C17	120.2(2)
15	H16	C16	C17	119.9
16	C15	C14	C19	119.9(2)
17	C15	C14	C13	120.7(2)
18	C19	C14	C13	119.3(2)
19	H10A	C10	H10B	107.9
20	H10A	C10	C9	109.3

21	H10A	C10	C11	109.3
22	H10B	C10	C9	109.3
23	H10B	C10	C11	109.3
24	C9	C10	C11	111.7(2)
25	O4	C18	C17	115.2(2)
26	O4	C18	C19	125.1(2)
27	C17	C18	C19	119.7(2)
28	H6	C6	C1	119.9
29	H6	C6	C5	119.9
30	C1	C6	C5	120.2(2)
31	N1	C8	H8	119.3
32	N1	C8	C1	121.3(2)
33	H8	C8	C1	119.3
34	C16	C17	C18	120.9(2)
35	C16	C17	H17	119.5
36	C18	C17	H17	119.6
37	N1	C9	C10	111.0(2)
38	N1	C9	H9A	109.4
39	N1	C9	H9B	109.4
40	C10	C9	H9A	109.4
41	C10	C9	H9B	109.5
42	H9A	C9	H9B	108
43	H4	C4	C5	119.5
44	H4	C4	C3	119.5
45	C5	C4	C3	121.0(2)
46	C14	C19	C18	119.9(2)
47	C14	C19	H19	120.1
48	C18	C19	H19	120.1
49	C2	C1	C6	119.8(2)
50	C2	C1	C8	120.9(2)
51	C6	C1	C8	119.4(2)
52	O2	C5	C6	125.0(2)
53	O2	C5	C4	115.7(2)
54	C6	C5	C4	119.3(2)
55	N2	C13	C14	121.7(2)
56	N2	C13	H13	119.2
57	C14	C13	H13	119.2
58	C10	C11	H11A	109.3
59	C10	C11	H11B	109.3
60	C10	C11	C12	111.6(2)
61	H11A	C11	H11B	108

62	H11A	C11	C12	109.3
63	H11B	C11	C12	109.3
64	N2	C12	C11	110.8(2)
65	N2	C12	H12A	109.5
66	N2	C12	H12B	109.5
67	C11	C12	H12A	109.5
68	C11	C12	H12B	109.5
69	H12A	C12	H12B	108.1
70	O4	C20	H20A	109.5
71	O4	C20	H20B	109.5
72	O4	C20	H20C	109.5
73	H20A	C20	H20B	109.5
74	H20A	C20	H20C	109.5
75	H20B	C20	H20C	109.5
76	C2	C3	C4	120.2(2)
77	C2	C3	H3A	119.9
78	C4	C3	H3A	119.9
79	O2	C7	H7A	109.5
80	O2	C7	H7B	109.5
81	O2	C7	H7C	109.5
82	H7A	C7	H7B	109.4
83	H7A	C7	H7C	109.5
84	H7B	C7	H7C	109.5

Table E.14: Bond lengths for the ligand SL9

Number	Atom1	Atom2	Type	Polymeric	Cyclic	Length	SybylType
1	O4	C18	Unknown	no	acyclic	1.377(3)	1
2	O4	C20	Unknown	no	acyclic	1.428(3)	1
3	O3	H3	Unknown	no	acyclic	0.84	1
4	O3	C15	Unknown	no	acyclic	1.357(3)	1
5	O1	H1	Unknown	no	acyclic	0.84	1
6	O1	C2	Unknown	no	acyclic	1.356(3)	1
7	O2	C5	Unknown	no	acyclic	1.374(3)	1
8	O2	C7	Unknown	no	acyclic	1.425(3)	1
9	N1	C8	Unknown	no	acyclic	1.283(3)	un
10	N1	C9	Unknown	no	acyclic	1.463(3)	1
11	N2	C13	Unknown	no	acyclic	1.283(3)	un
12	N2	C12	Unknown	no	acyclic	1.461(3)	1

13	C2	C1	Unknown	no	cyclic	1.403(3)	un
14	C2	C3	Unknown	no	cyclic	1.393(3)	un
15	C15	C16	Unknown	no	cyclic	1.396(3)	un
16	C15	C14	Unknown	no	cyclic	1.401(3)	un
17	C16	H16	Unknown	no	acyclic	0.95	1
18	C16	C17	Unknown	no	cyclic	1.380(3)	un
19	C14	C19	Unknown	no	cyclic	1.407(3)	un
20	C14	C13	Unknown	no	acyclic	1.456(3)	un
21	C10	H10A	Unknown	no	acyclic	0.99	1
22	C10	H10B	Unknown	no	acyclic	0.99	1
23	C10	C9	Unknown	no	acyclic	1.515(3)	1
24	C10	C11	Unknown	no	acyclic	1.519(3)	1
25	C18	C17	Unknown	no	cyclic	1.391(3)	un
26	C18	C19	Unknown	no	cyclic	1.388(3)	un
27	C6	H6	Unknown	no	acyclic	0.95	1
28	C6	C1	Unknown	no	cyclic	1.405(3)	un
29	C6	C5	Unknown	no	cyclic	1.384(3)	un
30	C8	H8	Unknown	no	acyclic	0.95	1
31	C8	C1	Unknown	no	acyclic	1.459(3)	un
32	C17	H17	Unknown	no	acyclic	0.95	1
33	C9	H9A	Unknown	no	acyclic	0.99	1
34	C9	H9B	Unknown	no	acyclic	0.99	1
35	C4	H4	Unknown	no	acyclic	0.95	1
36	C4	C5	Unknown	no	cyclic	1.396(3)	un
37	C4	C3	Unknown	no	cyclic	1.378(3)	un
38	C19	H19	Unknown	no	acyclic	0.95	1
39	C13	H13	Unknown	no	acyclic	0.95	1
40	C11	H11A	Unknown	no	acyclic	0.99	1
41	C11	H11B	Unknown	no	acyclic	0.99	1
42	C11	C12	Unknown	no	acyclic	1.521(3)	1
43	C12	H12A	Unknown	no	acyclic	0.99	1
44	C12	H12B	Unknown	no	acyclic	0.99	1
45	C20	H20A	Unknown	no	acyclic	0.98	1
46	C20	H20B	Unknown	no	acyclic	0.98	1
47	C20	H20C	Unknown	no	acyclic	0.98	1
48	C3	H3A	Unknown	no	acyclic	0.95	1
49	C7	H7A	Unknown	no	acyclic	0.98	1
50	C7	H7B	Unknown	no	acyclic	0.98	1
51	C7	H7C	Unknown	no	acyclic	0.98	1

Table E.15: Atoms and symmetry operations for SL9

Number	Label	Charge	SybylType	Xfrac + ESD	Yfrac + ESD	Zfrac + ESD	Symm. op.
1	O4	0	O.3	0.00990(12)	0.0797(3)	0.79304(9)	x,y,z
2	O3	0	O.3	0.24919(12)	-0.2351(3)	0.51775(10)	x,y,z
3	H3	0	H	0.250824	-0.14261	0.473486	x,y,z
4	O1	0	O.3	0.49423(13)	1.1699(3)	0.18013(10)	x,y,z
5	H1	0	H	0.490835	1.066749	0.219273	x,y,z
6	O2	0	O.3	0.82349(13)	0.9927(3)	-0.04984(10)	x,y,z
7	N1	0	N.2	0.54579(14)	0.7912(3)	0.26385(11)	x,y,z
8	N2	0	N.2	0.21211(14)	0.1411(3)	0.42787(11)	x,y,z
9	C2	0	C.2	0.57652(17)	1.1180(4)	0.12601(13)	x,y,z
10	C15	0	C.2	0.18869(17)	-0.1481(4)	0.58234(14)	x,y,z
11	C16	0	C.2	0.18253(17)	-0.2721(4)	0.66495(13)	x,y,z
12	H16	0	H	0.218728	-0.41461	0.673975	x,y,z
13	C14	0	C.2	0.13610(16)	0.0626(4)	0.57031(13)	x,y,z
14	C10	0	C.3	0.39022(17)	0.5529(4)	0.31019(14)	x,y,z
15	H10A	0	H	0.361685	0.500406	0.2413	x,y,z
16	H10B	0	H	0.340043	0.683755	0.317511	x,y,z
17	C18	0	C.2	0.06823(17)	0.0180(4)	0.72087(14)	x,y,z
18	C6	0	C.2	0.72360(17)	0.8693(4)	0.07859(14)	x,y,z
19	H6	0	H	0.766908	0.733038	0.086129	x,y,z
20	C8	0	C.2	0.61923(16)	0.7529(4)	0.20764(13)	x,y,z
21	H8	0	H	0.660896	0.61534	0.212042	x,y,z
22	C17	0	C.2	0.12403(17)	-0.1884(4)	0.73355(14)	x,y,z
23	H17	0	H	0.121833	-0.27287	0.79021	x,y,z
24	C9	0	C.3	0.52678(18)	0.6169(4)	0.33066(14)	x,y,z
25	H9A	0	H	0.555757	0.668091	0.399719	x,y,z
26	H9B	0	H	0.577009	0.486792	0.322409	x,y,z
27	C4	0	C.2	0.67834(18)	1.2199(4)	-0.00069(14)	x,y,z
28	H4	0	H	0.690968	1.323512	-0.04809	x,y,z
29	C19	0	C.2	0.07448(16)	0.1445(4)	0.63968(13)	x,y,z
30	H19	0	H	0.03721	0.286095	0.630955	x,y,z
31	C1	0	C.2	0.64008(17)	0.9164(4)	0.13709(13)	x,y,z
32	C5	0	C.2	0.74297(18)	1.0207(4)	0.01003(14)	x,y,z
33	C13	0	C.2	0.15127(16)	0.2041(4)	0.49011(14)	x,y,z
34	H13	0	H	0.115172	0.346666	0.483727	x,y,z
35	C11	0	C.3	0.36864(17)	0.3739(4)	0.37980(14)	x,y,z
36	H11A	0	H	0.393288	0.428976	0.448467	x,y,z

37	H11B	0	H	0.421949	0.245724	0.374869	x,y,z
38	C12	0	C.3	0.23267(17)	0.3020(4)	0.35600(14)	x,y,z
39	H12A	0	H	0.178671	0.43163	0.35644	x,y,z
40	H12B	0	H	0.209525	0.236696	0.289134	x,y,z
41	C20	0	C.3	-0.05252(18)	0.2871(4)	0.78128(15)	x,y,z
42	H20A	0	H	0.009102	0.405346	0.787026	x,y,z
43	H20B	0	H	-0.09828	0.304663	0.832568	x,y,z
44	H20C	0	H	-0.11122	0.293736	0.71617	x,y,z
45	C3	0	C.2	0.59650(18)	1.2685(4)	0.05643(14)	x,y,z
46	H3A	0	H	0.553564	1.405081	0.048317	x,y,z
47	C7	0	C.3	0.8705(2)	0.7766(4)	-0.05657(15)	x,y,z
48	H7A	0	H	0.920348	0.730496	0.008381	x,y,z
49	H7B	0	H	0.92301	0.776058	-0.10376	x,y,z
50	H7C	0	H	0.800605	0.674657	-0.07895	x,y,z

Table E.16: Torsions for the atoms of ligand SL9

Number	Atom1	Atom2	Atom3	Atom4	Torsion
1	C20	O4	C18	C17	-177.8(2)
2	C20	O4	C18	C19	2.2(3)
3	C18	O4	C20	H20A	-66.6
4	C18	O4	C20	H20B	173.4
5	C18	O4	C20	H20C	53.4
6	H3	O3	C15	C16	-176.3
7	H3	O3	C15	C14	1.8
8	H1	O1	C2	C1	1.3
9	H1	O1	C2	C3	-179.7
10	C7	O2	C5	C6	13.6(3)
11	C7	O2	C5	C4	-167.0(2)
12	C5	O2	C7	H7A	-63
13	C5	O2	C7	H7B	177.1
14	C5	O2	C7	H7C	57
15	C9	N1	C8	H8	-1.8
16	C9	N1	C8	C1	178.2(2)
17	C8	N1	C9	C10	-120.6(2)
18	C8	N1	C9	H9A	118.5
19	C8	N1	C9	H9B	0.3
20	C12	N2	C13	C14	-174.1(2)
21	C12	N2	C13	H13	5.9
22	C13	N2	C12	C11	108.0(2)
23	C13	N2	C12	H12A	-12.9
24	C13	N2	C12	H12B	-131.2
25	O1	C2	C1	C6	179.4(2)

26	O1	C2	C1	C8	0.3(3)
27	C3	C2	C1	C6	0.5(3)
28	C3	C2	C1	C8	-178.6(2)
29	O1	C2	C3	C4	-179.2(2)
30	O1	C2	C3	H3A	0.8
31	C1	C2	C3	C4	-0.2(3)
32	C1	C2	C3	H3A	179.8
33	O3	C15	C16	H16	-1.3
34	O3	C15	C16	C17	178.8(2)
35	C14	C15	C16	H16	-179.4
36	C14	C15	C16	C17	0.6(3)
37	O3	C15	C14	C19	-180.0(2)
38	O3	C15	C14	C13	-3.9(3)
39	C16	C15	C14	C19	-1.9(3)
40	C16	C15	C14	C13	174.1(2)
41	C15	C16	C17	C18	1.3(3)
42	C15	C16	C17	H17	-178.7
43	H16	C16	C17	C18	-178.7
44	H16	C16	C17	H17	1.3
45	C15	C14	C19	C18	1.3(3)
46	C15	C14	C19	H19	-178.7
47	C13	C14	C19	C18	-174.8(2)
48	C13	C14	C19	H19	5.2
49	C15	C14	C13	N2	0.4(3)
50	C15	C14	C13	H13	-179.6
51	C19	C14	C13	N2	176.5(2)
52	C19	C14	C13	H13	-3.5
53	H10A	C10	C9	N1	59.7
54	H10A	C10	C9	H9A	-179.5
55	H10A	C10	C9	H9B	-61.2
56	H10B	C10	C9	N1	-58.3
57	H10B	C10	C9	H9A	62.6
58	H10B	C10	C9	H9B	-179.2
59	C11	C10	C9	N1	-179.3(2)
60	C11	C10	C9	H9A	-58.4
61	C11	C10	C9	H9B	59.8
62	H10A	C10	C11	H11A	-177.2
63	H10A	C10	C11	H11B	64.8
64	H10A	C10	C11	C12	-56.2
65	H10B	C10	C11	H11A	-59.3
66	H10B	C10	C11	H11B	-177.3
67	H10B	C10	C11	C12	61.7
68	C9	C10	C11	H11A	61.7
69	C9	C10	C11	H11B	-56.2
70	C9	C10	C11	C12	-177.2(2)
71	O4	C18	C17	C16	178.2(2)

72	O4	C18	C17	H17	-1.8
73	C19	C18	C17	C16	-1.9(3)
74	C19	C18	C17	H17	178.1
75	O4	C18	C19	C14	-179.5(2)
76	O4	C18	C19	H19	0.5
77	C17	C18	C19	C14	0.6(3)
78	C17	C18	C19	H19	-179.4
79	H6	C6	C1	C2	179.8
80	H6	C6	C1	C8	-1.1
81	C5	C6	C1	C2	-0.2(3)
82	C5	C6	C1	C8	178.9(2)
83	H6	C6	C5	O2	-0.9
84	H6	C6	C5	C4	179.7
85	C1	C6	C5	O2	179.1(2)
86	C1	C6	C5	C4	-0.3(3)
87	N1	C8	C1	C2	-2.4(3)
88	N1	C8	C1	C6	178.5(2)
89	H8	C8	C1	C2	177.6
90	H8	C8	C1	C6	-1.5
91	H4	C4	C5	O2	1.1
92	H4	C4	C5	C6	-179.5
93	C3	C4	C5	O2	-178.9(2)
94	C3	C4	C5	C6	0.5(3)
95	H4	C4	C3	C2	179.7
96	H4	C4	C3	H3A	-0.3
97	C5	C4	C3	C2	-0.3(3)
98	C5	C4	C3	H3A	179.8
99	C10	C11	C12	N2	-176.0(2)
100	C10	C11	C12	H12A	-55.2
101	C10	C11	C12	H12B	63.1
102	H11A	C11	C12	N2	-55
103	H11A	C11	C12	H12A	65.9
104	H11A	C11	C12	H12B	-175.9
105	H11B	C11	C12	N2	62.9
106	H11B	C11	C12	H12A	-176.2
107	H11B	C11	C12	H12B	-57.9


Appendix F: Turnitin Originality Report

Turnitin Originality Report

Processed on: 28-Feb-2022 08:25 EAT
ID: 1772627092
Word Count: 45521
Submitted: 1

SC/PhD/07/13 By Mochere
Orang'o Daniel

Document Viewer



<p style="text-align: center;">Similarity Index</p> <p style="font-size: 24px; font-weight: bold; text-align: center;">19%</p>	<p style="text-align: center; font-weight: bold;">Similarity by Source</p> <table style="width: 100%; border-collapse: collapse;"> <tr> <td style="padding: 2px 5px;">Internet Sources:</td> <td style="text-align: right; padding: 2px 5px;">15%</td> </tr> <tr> <td style="padding: 2px 5px;">Publications:</td> <td style="text-align: right; padding: 2px 5px;">6%</td> </tr> <tr> <td style="padding: 2px 5px;">Student Papers:</td> <td style="text-align: right; padding: 2px 5px;">4%</td> </tr> </table>	Internet Sources:	15%	Publications:	6%	Student Papers:	4%
Internet Sources:	15%						
Publications:	6%						
Student Papers:	4%						

include quoted
 include bibliography
 excluding matches < 4 words
 mode:

1% match () http://theochem.weizmann.ac.il	✖
1% match (Internet from 06-Oct-2010) http://www.britannica.com	✖
1% match (student papers from 21-Jan-2021) Submitted to University of Lincoln on 2021-01-21	✖
1% match (Internet from 04-Jan-2022) https://cpk-front-devel.mzk.cz/EDS/Search?filter%5B%5D=ContentProvider%3A%22Academic+Search+Index%22&filter%5B%5D=Publisher%3A%22de+gruyter%22&lookfor=%22O.%22&type=AU	✖
<1% match (Internet from 26-Nov-2020) https://www.britannica.com/science/organometallic-compound/Metal-clusters	✖
<1% match (student papers from 03-Nov-2016) Submitted to University of Lincoln on 2016-11-03	✖
<1% match (Internet from 17-May-2015) http://en.wikipedia.org	✖
<1% match (Internet from 13-Dec-2020) https://en.wikipedia.org/wiki/Schiff_base	✖
<1% match (Internet from 01-Jan-2022) "Oxophilicity", Wikipedia, en, 2022	✖
<1% match (Internet from 17-Jan-2022) http://lib.buet.ac.bd:8080	✖